



**SYNTHETIC DAMAGE CURVES FOR CONCRETE GIRDER  
BRIDGE DECKS UNDER FLOOD HAZARD**

A thesis submitted in fulfilment of the requirements for the degree

of

**Doctor of Philosophy**

by

**Farook Kalendher**

BSc (Eng.)(Hons.)(University of Moratuwa, Sri Lanka)

MSc (Space Studies) (International Space University, France)

College of Science, Engineering and Health

School of Engineering

RMIT University

Melbourne, Australia.

October 2017

## DECLARATION

---

I certify that except where due acknowledgement has been made, the work is that of the author alone; the work has not been submitted previously, in whole or in part, to qualify for any other academic award; the content of the thesis is the result of work which has been carried out since the official commencement date of the approved research program; any editorial work, paid or unpaid, carried out by a third party is acknowledged; and, ethics procedures and guidelines have been followed.

I acknowledge the support I have received for my research through the provision of an Australian Government Research Training Program Scholarship.

Farook Kalendher

6<sup>th</sup> October 2017

## ACKNOWLEDGEMENT

---

I would like to take this opportunity to thank and acknowledge all those who have offered their invaluable wisdom and support during the course of this research.

First and foremost, my sincere thanks and gratitude goes to Professor Sujeeva Setunge for her uninterrupted and generous support as my principal supervisor. She is a great soul with the biggest heart who not only helped me understand and progress in the research but also showed me a valuable academic attitude, which beyond doubt is a lesson of a lifetime.

I would like to express my appreciation to my associate supervisors Associate Professor Kevin Zhang and Dr. Hessam Mohseni for their thoughtful feedback and helpful assistance. I would also like to tender my sincere gratitude to Dr. Dilan Robert for his extra hand to learn necessary software competency required for this research. Dr. Nirdosha Gamage, my undergraduate batch mate, must also be gratefully remembered at this juncture who was the first point of contact to get me enrolled to this research programme at RMIT University.

I would like to acknowledge the Civil and Infrastructure Engineering, School of Engineering, RMIT University for providing me the post graduate research scholarship to conduct this postgraduate research. I wish to appreciate the assistance of the administrative staff at the School of Engineering of RMIT University.

I would also like to thank Bushfire & Natural Hazard Cooperative Research Centres of Australia (BNHCRC) for providing me an opportunity to actively take part in their funded research programme - “Enhancing resilience of critical road infrastructure under natural hazards” - under which my research programme was formed of and granting me a top up scholarship.

Sincere thanks should also go to Lockyer Valley Regional Council (LVRC) in Queensland for providing data to initiate this research in the form of bridge inspection reports that was specifically compiled aftermath of 2013 severe flood events in Queensland.

I am indebted to my beloved parents, for their continuous encouragement and support throughout my years of education. I sincerely dedicate this thesis to them. My deepest

gratitude is for my wife, Zafaya, for her unconditional love, support, patience, encouragement and understanding. Our kids, Inousha, Iflal and Ifaz, have been a great source of inspiration, light and love in brightening my days of research over this period and beyond. I would also like to express my gratitude to all my teachers, from primary school up to post graduate level, for their contribution and support.

Last, but not the least, I would like to thank all my colleagues and friends for their continuous support and understanding.

## ABSTRACT

---

In recent years, frequencies of flood events in Australia have increased. It is noted that flood events cause the most damage to infrastructure compared to any other natural hazards in the world. Road bridges are lifeline structures with a pre and post disaster critical functionality. Failure or damage of bridges during an extreme flood event can have severe consequences to the community as well as road authorities and emergency services. Currently a major gap in knowledge is the ability to evaluate the vulnerability of bridge structures using a methodology which captures the variability of the event intensities and the variability of the structural capacity. The research presented here addresses this knowledge gap.

Research commenced with a comprehensive literature review covering review of major bridge design codes in the world, literature on flood loading, vulnerability modelling of bridges and numerical modelling approaches to simulate bridges under natural hazards. Damage indices proposed by researchers to depict the levels of damage to structures are also noted.

A comprehensive analysis of case studies of failure of bridges under flood loading under the 2011 and 2013 floods in Queensland and Victoria was undertaken to establish the major failure mode of bridges under flood loading. This identified that failure of girder and deck of concrete girder bridges, which constitute more than 60% of the bridge network, is a common case study to investigate. Two bridges were selected for analysis and the outcome was used to establish the vulnerability modelling methodology.

A deterministic analysis of the selected structures was undertaken under variable flood loading to establish the analysis methodology using ABAQUS software. The loading configuration considered covered flood, log impact and debris impact. This analysis demonstrated that Kapernicks Bridge would fail at a flood velocity of 3.71m/s which closely agrees with the recorded flood velocity as well.

Understanding the limitations of the deterministic analysis where the variability of flood loading and the variability of structural capacity cannot be accounted for, a probabilistic fragility analysis was undertaken to establish the probability of failure of the bridges.

Probability distribution was established for flood velocity as well as the structural section capacity. Fragility curves were derived for concrete girder bridges using the developed methodology.

The methodology developed is applicable for any bridge structure when the flood loading distribution for the location of the bridge can be established.

Contribution to the existing knowledge from this research has been the methodology developed to quantify vulnerability of road infrastructure exposed to flood hazard that would assist evaluate damage state for bridge structures. Emergency Management could use this damage state to assess evacuation routes while Road Authority could make decisions on strengthening the bridge structure.

A sensitivity analysis was undertaken to explore the effect of span of the bridge and also increase in flood frequency on the probability of failure.

A method to derive damage indices which can be used by bridge engineers for decision making has been demonstrated.

## LIST OF PUBLICATIONS

---

The research outcomes from this Ph.D study have been published in peer reviewed conferences and journals. The complete list of the publications is provided as follows:

### Peer Reviewed Conferences:

1. **Farook Kalendher**, Sujeeva Setunge, and Hessam Mohseni, 'Failure Mechanisms of Bridge Infrastructure in an Extreme Flood Event', in Proceedings of the 1st International Conference on Infrastructure Failures and Consequences (ICFC 2014) (RMIT Publishing, 2014), pp. 124-132.
2. **Farook Kalendher**, Sujeeva Setunge, and Hessam Mohseni, ' Deriving Damage Indices for Concrete Girder Bridges subjected to Flood Loading', in Proceedings of the 6th International Conference on Structural Engineering and Construction Management 2015 (ICSECM 2015), Kandy, Sri Lanka December 11-14, 2015, pp. 29-35
3. **Farook Kalendher**, Sujeeva Setunge, and Hessam Mohseni, ' Analysis of Flood Impact on Reinforced Concrete (Prestressed) Girder Bridges – a Case Study', in Proceedings of the 8th International Conference on Bridge Maintenance, Safety and Management 2016 (IABMAS 2016), Foz do Iguacu, Brazil June 26 - 30, 2016, pp 200-209
4. **Farook Kalendher**, Sujeeva Setunge, Dilan Robert, and Hessam Mohseni, ' Fragility Curves for concrete girder bridges under flood hazard ', in Proceedings of the 9th

International Conference on Bridge Maintenance, Safety and Management 2018 (IABMAS 2018), Melbourne, Australia July 09 - 13, 2018 (Submitted)

**Peer Reviewed Journals:**

5. **Farook Kalendher**, Sujeeva Setunge, Dilan Robert, and Hessam Mohseni (2017). 'Application of fragility curves to estimate concrete girder bridge damage under flood hazard: a case study of Lockyer valley Region, Queensland, Australia.' Journal of the International Society for the Prevention and Mitigation of Natural Hazards (In peer-review process)
6. **Farook Kalendher**, Sujeeva Setunge, Dilan Robert, and Hessam Mohseni (2017). 'Methodology for the development of probabilistic fragility curves for concrete girder bridges under flood hazard.' Journal of the International Association for Earthquake Engineering (In peer-review process)



## TABLE OF CONTENTS

---

|  |           |
|--|-----------|
| DECLARATION.....   | i         |
| ACKNOWLEDGEMENT.....   | ii        |
| ABSTRACT.....  | iv        |
| LIST OF PUBLICATIONS.....  | vi        |
| TABLE OF CONTENTS.....   | viii      |
| LIST OF FIGURES.....   | xiii      |
| LIST OF TABLES.....  | xvi       |
| LIST OF EQUATIONS.....   | xviii     |
| <b>1 Introduction .....</b>  | <b>1</b>  |
| 1.1 Research Background.....   | 1         |
| 1.2 Research Significance .....  | 3         |
| 1.3 Research Aim and Objectives .....  | 7         |
| 1.4 Contribution to the existing knowledge / Research gap.....                           | 7         |
| 1.5 Research Scope .....   | 8         |
| 1.6 Outline of the Chapters .....  | 8         |
| <b>2 Literature Review .....</b>   | <b>10</b> |
| 2.1 Introduction .....   | 10        |
| 2.2 Understanding floods .....   | 10        |
| 2.2.1 Estimating the chance of a flood occurring.....                                    | 11        |
| 2.3 Review of current bridge design standards .....                                      | 13        |
| 2.3.1 AS 5100 .....  | 13        |
| 2.3.2 Euro code .....  | 14        |
| 2.3.3 American standards.....  | 16        |
| 2.4 Design process of bridges for flood loading according to the current standards ..... | 16        |
| 2.4.1 Design loads & load combinations .....   | 16        |
| 2.4.1.1 AS 5100 .....  | 16        |
| 2.4.1.2 Euro codes.....  | 19        |
| 2.4.1.3 American Standards .....   | 21        |
| 2.4.2 Structural analysis of bridges .....   | 26        |
| 2.4.2.1 Bridges .....  | 26        |
| 2.4.2.2 Types of bridges and usage in Australia .....                                    | 26        |
| 2.4.2.3 Concrete bridges .....   | 26        |
| 2.4.2.4 U-slab bridge.....   | 29        |
| 2.4.2.5 Steel bridges.....   | 30        |
| 2.4.2.6 Timber bridges .....   | 32        |
| 2.4.3 Design procedure .....   | 33        |

|          |  |           |
|----------|--|-----------|
| 2.4.3.1  | Bridges .....  | 33        |
| 2.5      | A review of previous research on design of bridges for flood loading ..... | 34        |
| 2.6      | Bridge collapse under natural hazards .....                                | 42        |
| 2.6.1    | Natural factors .....  | 43        |
| 2.6.1.1  | Flood .....  | 43        |
| 2.6.1.2  | Scour .....  | 44        |
| 2.6.1.3  | Earthquake .....   | 44        |
| 2.6.1.4  | Landslide.....   | 44        |
| 2.6.1.5  | Debris flow.....   | 45        |
| 2.6.1.6  | Hurricane and typhoon.....   | 45        |
| 2.7      | Collapse mechanisms of bridges/failure modes .....                         | 46        |
| 2.7.1    | Flood and scour.....   | 46        |
| 2.7.2    | Earthquake .....   | 47        |
| 2.7.3    | Hurricane.....   | 48        |
| 2.7.4    | Summary of failure mechanism .....   | 48        |
| 2.8      | Australian bridges subjected to extreme flood events.....                  | 49        |
| 2.9      | Vulnerability modelling of bridges .....                                   | 53        |
| 2.9.1    | Definition of Resilience/Vulnerability .....                               | 53        |
| 2.9.2    | Vulnerability Assessment .....   | 54        |
| 2.10     | Quantifying damage to bridges under flood for decision making.....         | 56        |
| 2.11     | Fragility analysis of bridges .....  | 58        |
| 2.12     | Chapter summary .....  | 59        |
| <b>3</b> | <b>Research Methodology .....</b>  | <b>61</b> |
| 3.1      | Research questions .....   | 62        |
| 3.2      | Analysis of case studies.....  | 62        |
| 3.3      | Numerical modeling of the selected structures. (Deterministic).....        | 65        |
| 3.3.1    | As built Structural Drawing of the Tenthill Creek Bridge .....             | 66        |
| 3.3.2    | Concrete and Steel Material Properties.....                                | 66        |
| 3.3.3    | Flood Loading as per AS 5100 bridge design standard .....                  | 71        |
| 3.3.4    | Flood Intensity Measure.....   | 71        |
| 3.3.5    | Method of analysis:.....   | 72        |
| 3.3.5.1  | Simple Linear Analysis:.....   | 73        |
| 3.3.5.2  | Nonlinear Analysis:.....   | 73        |
| 3.3.5.3  | Calculation of Bending Moment from ABAQUS Elemental Stress output .....    | 74        |
| 3.4      | Numerical modeling of the selected structures. (Probabilistic) .....       | 75        |
| 3.5      | Fragility curves.....  | 75        |
| 3.6      | Chapter Summary.....   | 76        |
| <b>4</b> | <b>Analysis of Case Studies.....</b>                                       | <b>77</b> |
| 4.1      | Introduction .....   | 77        |

|          |  |           |
|----------|--|-----------|
| 4.2      | Overview of case study analysis .....  | 78        |
| 4.3      | Inspection data for damaged bridges.....   | 79        |
| 4.4      | Major failure modes/mechanism.....   | 93        |
| 4.5      | Focus on concrete girder bridges .....   | 93        |
| 4.6      | Chapter summary .....  | 94        |
| <b>5</b> | <b>Numerical modelling of the case study bridge – Deterministic analysis .....</b> | <b>95</b> |
| 5.1      | Introduction .....   | 95        |
| 5.2      | ABAQUS Finite Element Software .....   | 95        |
| 5.2.1    | ABAQUS/CAE.....  | 96        |
| 5.2.2    | ABAQUS/Standard.....   | 96        |
| 5.2.3    | ABAQUS/Explicit .....  | 96        |
| 5.2.4    | ABAQUS/ CFD .....  | 97        |
| 5.2.5    | ABAQUS/Multiphysics .....  | 97        |
| 5.2.6    | User developed subroutines .....   | 97        |
| 5.3      | Description of the case study bridges.....   | 97        |
| 5.3.1    | Tenthill Creek Bridge.....   | 97        |
| 5.3.1.1  | Location of the bridge .....   | 97        |
| 5.3.1.2  | Details of the Bridge .....  | 98        |
| 5.3.2    | Kapernicks bridge .....  | 101       |
| 5.3.2.1  | Location of the bridge .....   | 101       |
| 5.3.2.2  | Detail of the bridge .....   | 101       |
| 5.4      | Deriving Flood Induced Bending Moment on the Girder.....                           | 102       |
| 5.4.1    | Method 1: Modelling of Bridge Girder using beam elements. ....                     | 103       |
| 5.4.2    | Method 2: Modelling of Bridge Girder using solid elements .....                    | 103       |
| 5.5      | Model Validation.....  | 104       |
| 5.5.1    | Method validation when the bridge girder was modelled using beam elements.....     | 104       |
| 5.5.2    | Method validation when the bridge girder was modelled using solid elements .....   | 105       |
| 5.6      | Development of Vulnerability Curves. ....  | 107       |
| 5.6.1    | Definition of Vulnerability/Resilience.....  | 108       |
| 5.6.2    | Forces on bridge resulting from flood event.....                                   | 109       |
| 5.6.2.1  | Forces on superstructure due to water flow.....                                    | 109       |
| 5.6.2.2  | Forces due to Debris .....   | 109       |
| 5.6.2.3  | Forces due to Log Impact.....  | 110       |
| 5.6.3    | Characterization of Damage / measure of the structural damage.....                 | 110       |
| 5.6.4    | Deriving Damage Index .....  | 113       |
| 5.6.5    | Calculation of the existing moment capacity of the girder ( $\phi M_u$ ).....      | 113       |
| 5.6.6    | Estimating flood induced bending moment ( $M^*$ ) .....                            | 115       |
| 5.6.7    | Deriving Deterministic Vulnerability Curves .....                                  | 119       |
| 5.6.8    | Severity of Damage.....  | 121       |
| 5.6.8.1  | Complete Damage.....   | 122       |
| 5.6.8.2  | Extreme Damage.....  | 122       |
| 5.6.8.3  | Major Damage .....   | 122       |
| 5.6.8.4  | Moderate Damage.....   | 122       |

|          |  |            |
|----------|--|------------|
| 5.6.8.5  | Minor Damage .....   | 122        |
| 5.6.9    | Results and discussion .....   | 123        |
| 5.7      | Validation of this research.....   | 125        |
| 5.8      | Conclusions of Chapter 5 .....   | 125        |
| <b>6</b> | <b>Numerical Modelling of the case study bridge – Probabilistic Analysis .....</b>       | <b>127</b> |
| 6.1      | Introduction .....   | 127        |
| 6.2      | Effect of Flood Intensity (Demand Model).....  | 131        |
| 6.2.1    | Analysis of flood data .....   | 132        |
| 6.2.2    | Analysis of Actual Flood Velocity Distribution .....                                     | 134        |
| 6.3      | Parametric Study in ABAQUS.....  | 137        |
| 6.3.1    | Log Impact Analysis on the bridge girder.....  | 141        |
| 6.4      | Effect of Compressive Strength for Concrete (Capacity Model).....                        | 142        |
| 6.4.1    | Resistance Statistics .....  | 142        |
| 6.5      | Determination of Failure Probability of the bridge.....                                  | 146        |
| 6.5.1    | Fragility curves for Tenthill Creek Bridge.....  | 147        |
| 6.5.2    | Fragility curves for Kapernicks Bridge.....  | 149        |
| 6.6      | Parametric study for fragility curves .....  | 151        |
| 6.6.1    | Effect of different bridge span .....  | 151        |
| 6.6.2    | Effect of different flood velocity distribution .....                                    | 156        |
| 6.7      | Summary of the Chapter .....   | 159        |
| <b>7</b> | <b>Damage Indices for Practical Application.....</b>                                     | <b>161</b> |
| 7.1      | Introduction .....   | 161        |
| 7.2      | Types of damage indices.....   | 161        |
| 7.2.1    | Structural Capacity based Damage Index .....   | 161        |
| 7.2.2    | Cost based Damage Index.....   | 162        |
| 7.3      | Damage Interpretation.....   | 168        |
| 7.3.1    | Concrete Plastic Damage Model.....   | 169        |
| 7.4      | Damage Measurement.....  | 170        |
| 7.4.1    | Calculating the damage parameters (dc & dt) for damaged plasticity model in ABAQUS ..... | 171        |
| 7.4.2    | Classification of damage state to the bridge girder .....                                | 171        |
| 7.5      | Interpretation of Damage Curves .....  | 174        |
| 7.6      | Application of fragility curves for end users and decision makers .....                  | 180        |
| 7.7      | Chapter summary .....  | 181        |
| <b>8</b> | <b>Summary, conclusions and recommendation .....</b>                                     | <b>183</b> |
| 8.1      | Summary .....  | 183        |

|                        |   |            |
|------------------------|---|------------|
| 8.2                    | Conclusions .....   | 183        |
| 8.2.1                  | Findings from the review of literature .....  | 185        |
| 8.2.2                  | Findings from the analysis of the case studies .....                                    | 185        |
| 8.2.3                  | Findings from the numerical modelling of the case study bridge – Deterministic approach | 185        |
| 8.2.4                  | Findings from the numerical modelling of the case study bridge – Probabilistic approach | 186        |
| 8.2.5                  | Findings from damage indices for practical application .....                            | 187        |
| 8.3                    | Recommendations for future research: .....  | 188        |
| <b>REFERENCES.....</b> |   | <b>189</b> |
| <b>APPENDICES.....</b> |   | <b>203</b> |

## LIST OF FIGURES

---

|   |    |
|---|----|
| FIGURE 1.1: DAMAGED BRIDGES IN LOCKYER VALLEY REGION IN QUEENSLAND (THE LOCKYER CREEK FLOOD OF JANUARY 2011) .....                        | 5  |
| FIGURE 2.1: FLOOD PEAKS IN EASTERN AUSTRALIA OVER THE PERIOD 26 NOVEMBER 2010 – 29 JANUARY 2011[VAN DEN HONERT AND MCANENEY (2011B)]..... | 11 |
| FIGURE 2.2: THE CHANCES OF A FLOOD IN ANY GIVEN YEAR (BUREAU OF METEOROLOGY, 2003).....   | 12 |
| FIGURE 2.3: ULTIMATE LOAD FACTOR ( $\gamma MF$ ).....   | 14 |
| FIGURE 2.4: TYPICAL TIME CHARACTERISTICS OF (A) ACCIDENTAL AND (B) VARIABLE LOAD. EUROCODE (2005) 15                                      | 15 |
| FIGURE 2.5: TYPICAL PROBABILITY DISTRIBUTION OF (A) ACCIDENTAL AND (B) VARIABLE LOADS (EUROCODE, 2005).....                               | 15 |
| FIGURE 2.6: PRESSURE AND FORCE DUE TO CURRENTS ON BRIDGE PIERS (ALAMPALLI ET AL., 1997) .....   | 20 |
| FIGURE 2.7: PRESSURE AND FORCE DUE TO CURRENTS (CHEN AND LUI, 2005).....  | 20 |
| FIGURE 2.8: PLAN VIEW OF PIER (AASHTO, 2012).....   | 23 |
| FIGURE 2.9: DESIGN FLOOD VELOCITY .....   | 24 |
| FIGURE 2.10: TYPES OF BEAM BRIDGES (DEPARTMENT OF MAIN ROADS, 2006).....  | 27 |
| FIGURE 2.11: GIRDER (I BEAM) CAST IN-SITU WITH DECK (DEPARTMENT OF MAIN ROADS, 2006) .....  | 27 |
| FIGURE 2.12: GIRDER (T BEAM) CAST IN-SITU WITH DECK (DEPARTMENT OF MAIN ROADS, 2006) .....  | 28 |
| FIGURE 2.13: BOX GIRDER BRIDGE UNDER CONSTRUCTION (DEPARTMENT OF MAIN ROADS, 2006).....   | 28 |
| FIGURE 2.14: EXAMPLE OF A CABLE STAYED BRIDGE (LEVY, 2011).....   | 29 |
| FIGURE 2.15: A TYPICAL U-SLAB BRIDGE SECTION CONSTRUCTED IN VICTORIA (NASIM ET AL., 2017) .....   | 30 |
| FIGURE 2.16: TYPES OF STEEL GIRDER BRIDGES (AUSTROAD'92, 1992) .....  | 31 |
| FIGURE 2.17: TRUSS CONFIGURATIONS. (AUSTROAD'92, 1992) .....  | 31 |
| FIGURE 2.18: BURDEKIN RIVER BRIDGE, AYR, QUEENSLAND (BURDEKIN SHIRE COUNCIL, 2012).....   | 32 |
| FIGURE 2.19: NEW COUNTRY CREEK BRIDGE NEAR KILCOY, TIMBER GIRDER BRIDGE (EYRE ET AL., 2012) .....   | 33 |
| FIGURE 2.20: DISTRIBUTION OF CAUSES OF THE 503 REPORTED BRIDGE COLLAPSES IN US (WARDHANA AND HADIPRIONO, 2003).....                       | 42 |
| FIGURE 2.21: COLLAPSE OF THE SCHOHARIE CREEK BRIDGE DUE TO FLOOD IN 1987 (REPRINTED FROM USGS 2012).....                                  | 43 |
| FIGURE 2.22: COLLAPSE OF A BRIDGE DUE TO LANDSLIDE (IMAGE COURTESY OF (ZHONG ET AL., 2013)).....  | 45 |
| FIGURE 2.23: BRIDGE COLLAPSED UNDER TYPHOON.....  | 46 |
| FIGURE 2.24: SCOURING AROUND A BRIDGE FOUNDATION (LIN ET AL., 2010) .....   | 47 |
| FIGURE 2.25: KAPERNICKS BRIDGE BEFORE WATER RISE (MURRAY AND KEMP, 2011) .....  | 49 |
| FIGURE 2.26: KAPERNICKS BRIDGE AFTER WATER RISE (MURRAY AND KEMP, 2011) .....   | 50 |
| FIGURE 2.27: DAMAGE TO KAPERNICKS BRIDGE (APPROACH WASHED AWAY) (MURRAY AND KEMP, 2011) .....   | 50 |
| FIGURE 2.28: DAMAGE TO KAPERNICKS BRIDGE (CRACKING IN GIRDER) (MURRAY AND KEMP, 2011) .....   | 51 |
| FIGURE 2.29: ABUTMENT WASHED AWAY ON GATTON-ESK ROAD BRIDGE (EZEJUGH, 2014).....  | 51 |
| FIGURE 2.30: SCOUR AROUND PIER AND EXPOSED PILES ON GEOFF FISHER BRIDGE (EZEJUGH, 2014).....  | 52 |
| FIGURE 2.31: REPRESENTATION OF RESILIENCE AND VULNERABILITY .....   | 53 |
| FIGURE 3.1: RESEARCH METHODOLOGY .....  | 64 |
| FIGURE 3.2: RESPONSE OF CONCRETE TO UNIAXIAL LOADING IN TENSION (A) AND COMPRESSION (B). (HANIF ET AL., 2016).....                        | 67 |
| FIGURE 3.3: COMPRESSIVE YIELD STRESS VS INELASTIC STRAIN (HANIF ET AL., 2016) .....   | 67 |
| FIGURE 3.4: CONCRETE TENSILE SOFTENING MODEL, YIELD STRESS VS CRACKING STRAIN (HANIF ET AL., 2016). 67                                    | 67 |
| FIGURE 3.5: DAMAGE PARAMETER VS INELASTIC STRAIN (HANIF ET AL., 2016) .....   | 68 |
| FIGURE 3.6: DAMAGE PARAMETER VS CRACKING STRAIN (HANIF ET AL., 2016) .....  | 68 |
| FIGURE 3.7: EIGHT-NODE ELEMENT WITH REDUCED INTEGRATION (C3D8R AND F3D8R)(ABAQUS 6.14) .....  | 69 |
| FIGURE 3.8: FOUR-NODE TETRAHEDRAL ELEMENT (C3D4 AND F3D4)(ABAQUS 6.14).....   | 69 |
| FIGURE 3.9: 2-NODE LINEAR BEAM ELEMENT (B31) (ABAQUS 6.14).....   | 70 |
| FIGURE 3.10: NEWTON-RAPHSON ITERATION IN 2 LOAD INCREMENTS (ABAQUS 6.14).....   | 71 |
| FIGURE 3.11: RIVER PROFILE OF LOCKYER CREEK AT HELIDON NUMBER 3.....  | 72 |

|  |     |
|--|-----|
| FIGURE 3.12: DIRECT BENDING MOMENT OUTPUT FROM ABAQUS .....  | 73  |
| FIGURE 3.13: BEAM SECTION STRESS DISTRIBUTION .....  | 74  |
| FIGURE 3.14: MODEL DEVELOPMENT OF BRIDGE AND DECK IN ABAQUS .....  | 75  |
| FIGURE 4.1: SOME OF THE SNAP SHOTS OF THE AFFECTED BRIDGES.....  | 79  |
| FIGURE 4.2: ILLUSTRATIVE PAGE FROM BRIDGE INSPECTION REPORT.....   | 81  |
| FIGURE 4.3: EXTRACT FROM BRIDGE INSPECTION REPORT.....   | 82  |
| FIGURE 4.4: TYPES OF BRIDGES INCLUDED IN THE BRIDGE INSPECTION REPORT .....  | 84  |
| FIGURE 5.1: SOLUTION SEQUENCE IN ABAQUS .....  | 95  |
| FIGURE 5.2 LOCATION OF TENTHILL BRIDGE .....   | 98  |
| FIGURE 5.3 PHOTOS OF THE TENTHILL BRIDGE .....   | 99  |
| FIGURE 5.4 PHOTOS OF THE TENTHILL BRIDGE .....   | 99  |
| FIGURE 5.5 SCHEMATIC DETAILS OF THE HEADSTOCK AND SUPERSTRUCTURE.....  | 100 |
| FIGURE 5.6: KAPERNICKS BRIDGE PHOTO #1 .....   | 101 |
| FIGURE 5.7: KAPERNICKS BRIDGE PHOTO #2 .....   | 102 |
| FIGURE 5.8: KAPERNICKS BRIDGE SECTIONAL VIEW.....  | 102 |
| FIGURE 5.9: RENDERED VIEW OF THE I GIRDER BEAM PROFILE.....  | 103 |
| FIGURE 5.10 ILLUSTRATION OF BEAM SUPPORT CONDITIONS.....   | 104 |
| FIGURE 5.11: FIXED SUPPORTED GIRDER .....  | 105 |
| FIGURE 5.12: SIMPLY SUPPORTED BRIDGE GIRDER .....  | 105 |
| FIGURE 5.13: CONSIDERED MID-SPAN ELEMENTS .....  | 106 |
| FIGURE 5.14: REPRESENTATION OF RESILIENCE .....  | 108 |
| FIGURE 5.15: BRIDGE GIRDER SECTION .....   | 114 |
| FIGURE 5.16: ABAQUS BRIDGE DECK MODEL.....   | 116 |
| FIGURE 5.17: VULNERABILITY CURVES FOR KAPERNICKS BRIDGE .....  | 120 |
| FIGURE 5.18: VULNERABILITY CURVES FOR TENTHILL CREEK BRIDGE .....  | 121 |
| FIGURE 6.1: EXAMPLE FRAGILITIES FOR ILLUSTRATION .....   | 128 |
| FIGURE 6.2: TENTHILL CREEK BRIDGE CONFIGURATION.....   | 130 |
| FIGURE 6.3: SECTION DETAIL OF THE BRIDGE DECK AND GIRDER .....   | 131 |
| FIGURE 6.4: ABAQUS BRIDGE DECK MODEL .....   | 131 |
| FIGURE 6.5: EXTRACTION OF AS GIVEN DATA FROM WATER MONITORING COMMITTEE OF QLD GOVERNMENT<br>(STATION: HELIDON No.3) ..... | 133 |
| FIGURE 6.6: RIVER PROFILE OF LOCKYER CREEK AT HELIDON NUMBER 3.....  | 133 |
| FIGURE 6.7: SIMPLIFIED RIVER PROFILE (EXAGGERATED FIGURE).....   | 134 |
| FIGURE 6.8: FLOOD VELOCITY DISTRIBUTION (DEC.2010 – JAN 2011).....   | 135 |
| FIGURE 6.9: FLOOD VELOCITY DISTRIBUTION (JAN 7-10, 2011) .....   | 135 |
| FIGURE 6.10: FLOOD VELOCITY DISTRIBUTION (1987-2016).....  | 136 |
| FIGURE 6.11: ABAQUS SCRIPT FOR PARAMETRIC STUDY .....  | 139 |
| FIGURE 6.12: PARAMETRIC STUDY REPORT FOR STRESS OUTPUT.....  | 140 |
| FIGURE 6.13: URBAN DEBRIS (TOOWOOMBA); CARS AND FOUR-WHEEL DRIVES.....   | 141 |
| FIGURE 6.14: COMMERCIAL CONTAINER .....  | 142 |
| FIGURE 6.15: GEOMETRY OF THE I GIRDER WITH REINFORCEMENTS .....  | 143 |
| FIGURE 6.16: @RISK SOFTWARE INTERFACE.....   | 145 |
| FIGURE 6.17: FRAGILITY CURVE FOR TENTHILL CREEK BRIDGE UNDER FLOOD ONLY IMPACT.....  | 147 |
| FIGURE 6.18: FRAGILITY CURVE FOR TENTHILL CREEK BRIDGE UNDER FLOOD AND LOG IMPACT .....                                    | 148 |
| FIGURE 6.19: FRAGILITY CURVE FOR KAPERNICKS BRIDGE UNDER FLOOD ONLY IMPACT.....  | 149 |
| FIGURE 6.20: FRAGILITY CURVE FOR KAPERNICKS BRIDGE UNDER FLOOD AND LOG IMPACT .....  | 150 |
| FIGURE 6.21: FRAGILITY CURVE FOR 15M SPAN BRIDGE UNDER FLOOD ONLY IMPACT .....   | 152 |
| FIGURE 6.22: FRAGILITY CURVE FOR 15M SPAN BRIDGE UNDER FLOOD AND LOG IMPACT.....   | 153 |
| FIGURE 6.23: FRAGILITY CURVE FOR 45M SPAN BRIDGE UNDER FLOOD ONLY IMPACT .....   | 154 |
| FIGURE 6.24: FRAGILITY CURVE FOR 45M SPAN BRIDGE UNDER FLOOD AND LOG IMPACT.....   | 155 |
| FIGURE 6.25: RIVER PROFILE OF BRISBANE RIVER AT LINVILLE (143007A) .....   | 156 |
| FIGURE 6.26: FLOOD VELOCITY DISTRIBUTION FOR BRISBANE RIVER AT LINVILLE (143007A).....                                     | 157 |

|   |     |
|---|-----|
| FIGURE 6.27: FRAGILITY CURVE FOR VELOCITY DISTRIBUTION # 2 (FLOOD ONLY IMPACT FOR TENTHILL CREEK BRIDGE) .....                                  | 158 |
| FIGURE 6.28: FRAGILITY CURVE FOR VELOCITY DISTRIBUTION # 2 (FLOOD AND LOG IMPACT FOR TENTHILL CREEK BRIDGE) .....                               | 159 |
| FIGURE 7.1: COMPARISON OF ACTUAL DI AND ESTIMATED DI .....  | 168 |
| FIGURE 7.2: UNIAXIAL STRESS – STRAIN PLOT (ABAQUS 6.14).....  | 170 |
| FIGURE 7.3: CONCRETE TENSION DAMAGE PARAMETER (DT).....   | 170 |
| FIGURE 7.4: CONCRETE COMPRESSION DAMAGE PARAMETER (DC).....   | 171 |
| FIGURE 7.5: FRAGILITY CURVE COMPARISONS FOR TENTHILL CREEK BRIDGE UNDER FLOOD AND LOG IMPACT .  | 174 |
| FIGURE 7.6: FRAGILITY CURVE COMPARISON FOR KAPERINICKS BRIDGE UNDER FLOOD AND LOG IMPACT .....  | 175 |
| FIGURE 7.7: FRAGILITY CURVE COMPARISON FOR DIFFERENT SPAN OF BRIDGES UNDER FLOOD ONLY IMPACT....  | 176 |
| FIGURE 7.8: FRAGILITY CURVE COMPARISON FOR DIFFERENT SPAN OF BRIDGES UNDER FLOOD AND LOG IMPACT .....   | 177 |
| FIGURE 7.9: FRAGILITY CURVE COMPARISON FOR DIFFERENT TYPES OF FLOOD VELOCITY DISTRIBUTION FOR TENTHILL BRIDGE UNDER FLOOD ONLY IMPACT .....     | 178 |
| FIGURE 7.10: FRAGILITY CURVE COMPARISON FOR DIFFERENT TYPES OF FLOOD VELOCITY DISTRIBUTION FOR TENTHILL BRIDGE UNDER FLOOD AND LOG IMPACT ..... | 179 |

## LIST OF TABLES

---

|   |     |
|---|-----|
| TABLE 1-1: COST OF DISASTERS (EMERGENCY MANAGEMENT AUSTRALIA – WWW.EMA.GOV.AU).....   | 2   |
| TABLE 1-2: LOCKYER VALLEY REGIONAL COUNCIL BRIDGE DATA [(LOKUGE AND SETUNGE, 2013)].....  | 6   |
| TABLE 2-1: DRAG COEFFICIENTS (AASHTO, 2012).....  | 22  |
| TABLE 2-2: LATERAL DRAG COEFFICIENT (AASHTO, 2012) .....  | 23  |
| TABLE 2-3: COMPARISONS OF THE DESIGN LOADS OF THE THREE STANDARDS .....   | 25  |
| TABLE 2-4: MOST COMMON CAUSE FOR COLLAPSE OF DIFFERENT TYPES OF BRIDGES .....   | 48  |
| TABLE 3-1: SUMMARY OF CASE STUDY BRIDGE DETAILS .....   | 65  |
| TABLE 3-2: MECHANICAL PROPERTIES OF CONCRETE (HANIF ET AL., 2016) .....   | 67  |
| TABLE 4-1: AUSTRALIAN BRIDGE DESIGN STANDARDS.....  | 83  |
| TABLE 4-2: DETAILS OF DAMAGED BRIDGES .....   | 85  |
| TABLE 4-3: FAILURE MECHANISMS OF SELECTED BRIDGES.....  | 89  |
| TABLE 5-1: COMPARISONS OF BENDING MOMENTS (BEAM ELEMENTS).....  | 104 |
| TABLE 5-2: MOMENT CALCULATION TABLE FOR SIMPLY SUPPORTED CONDITION .....  | 106 |
| TABLE 5-3: MOMENT CALCULATION TABLE FOR FIXED SUPPORTED CONDITION .....   | 107 |
| TABLE 5-4: COMPARISONS OF BENDING MOMENTS (SOLID ELEMENTS) .....  | 107 |
| TABLE 5-5: DAMAGE INDICES .....   | 112 |
| TABLE 5-6: EXCEL SHEET FOR MOMENT CAPACITY CALCULATION .....  | 115 |
| TABLE 5-7: SUPPORT REACTIONS AT GIRDERS .....   | 116 |
| TABLE 5-8: DAMAGE INDICES FOR KAPERNICKS BRIDGE.....  | 117 |
| TABLE 5-9: DAMAGE INDICES FOR TENTHILL CREEK BRIDGE.....  | 117 |
| TABLE 5-10: DAMAGE INDICES FOR DIFFERENT TYPES OF FLOOD IMPACT FOR KAPERNICKS BRIDGE .....  | 118 |
| TABLE 5-11: DAMAGE INDICES FOR DIFFERENT TYPES OF FLOOD IMPACT FOR TENT HILL CREEK BRIDGE.....  | 119 |
| TABLE 5-12: TABLE OF DAMAGE SEVERITY CLASSIFICATION .....   | 123 |
| TABLE 5-13: THRESHOLD HAZARD INTENSITY MEASURE FOR KAPERNICKS BRIDGE (DI=1).....  | 124 |
| TABLE 5-14: THRESHOLD HAZARD INTENSITY MEASURE FOR TENTHILL CREEK BRIDGE (DI=1) .....   | 124 |
| TABLE 5-15: HAZARD INTENSITY MEASURE FOR KAPERNICKS BRIDGE.....   | 124 |
| TABLE 5-16: HAZARD INTENSITY MEASURE FOR TENTHILL CREEK BRIDGE.....   | 125 |
| TABLE 6-1: SUMMARY OF THE FLOOD VELOCITY DATA ANALYSIS .....  | 136 |
| TABLE 6-2: FLOOD VELOCITY VALUES USED IN THE PARAMETRIC STUDY .....   | 137 |
| TABLE 6-3: TYPICAL M* CALCULATION.....  | 140 |
| TABLE 6-4: RANDOM VARIABLE PARAMETERS (ADOPTED FROM TAVARES (2011)) .....   | 144 |
| TABLE 6-5: FAILURE PROBABILITY FOR CASE STUDY BRIDGES .....   | 150 |
| TABLE 6-6: FAILURE PROBABILITY FOR HYPOTHETICAL BRIDGES OF TWO DIFFERENT SPANS. ....  | 155 |
| TABLE 6-7: FAILURE PROBABILITY OF BRIDGES WHEN THE FLOOD VELOCITY CHANGED.....  | 159 |
| TABLE 7-1: MAXIMUM CONTRIBUTION FACTORS FOR ITEMS 1-10 .....  | 165 |
| TABLE 7-2: ACTUAL DAMAGE INDEX FOR THE BRIDGES .....  | 166 |
| TABLE 7-3: ESTIMATION OF DI FOR BELFORD BRIDGE .....  | 167 |
| TABLE 7-4: CLASSIFICATION OF DAMAGE SEVERITY ((RAMESH, 2009)).....  | 172 |
| TABLE 7-5: DAMAGE INTERPRETATION TABLE.....   | 173 |
| TABLE 7-6: COMPARISON OF FAILURE PROBABILITY FOR DIFFERENT TYPES OF FLOOD IMPACT (TENTHILL CREEK BRIDGE).....                                     | 174 |
| TABLE 7-7: COMPARISON OF FAILURE PROBABILITY FOR DIFFERENT TYPES OF FLOOD IMPACT (KAPERNICKS BRIDGE).....   | 175 |
| TABLE 7-8: COMPARISONS OF FAILURE PROBABILITY FOR DIFFERENT SPAN LENGTH OF THE BRIDGE (FLOOD ONLY IMPACT).....                                    | 176 |
| TABLE 7-9: COMPARISONS OF FAILURE PROBABILITY FOR DIFFERENT SPAN LENGTH OF THE BRIDGE (FLOOD WITH LOG IMPACT).....                                | 177 |
| TABLE 7-10: COMPARISONS OF PROBABILITY OF FAILURE FOR DIFFERENT FLOOD VELOCITY DISTRIBUTION (TENTHILL CREEK BRIDGE UNDER FLOOD ONLY IMPACT) ..... | 178 |

|   |     |
|---|-----|
| TABLE 7-11: COMPARISONS OF PROBABILITY OF FAILURE FOR DIFFERENT FLOOD VELOCITY DISTRIBUTION<br>(TENTHILL CREEK BRIDGE UNDER FLOOD WITH LOG IMPACT)..... | 179 |
| TABLE 7-12: PROBABILITY OF FAILURE FOR DIFFERENT SCENARIOS (DI=1.0).....  | 180 |
| TABLE 7-13: PROBABILITY OF FAILURE FOR DIFFERENT SCENARIOS (DIFFERENT DAMAGE SEVERITY) .....  | 181 |

## LIST OF EQUATIONS

---

|                     |     |
|---------------------|-----|
| EQUATION 2-1 .....  | 17  |
| EQUATION 2-2 .....  | 17  |
| EQUATION 2-3 .....  | 18  |
| EQUATION 2-4 .....  | 18  |
| EQUATION 2-5 .....  | 19  |
| EQUATION 2-6 .....  | 19  |
| EQUATION 2-7 .....  | 20  |
| EQUATION 2-8 .....  | 21  |
| EQUATION 2-9 .....  | 22  |
| EQUATION 2-10 ..... | 22  |
| EQUATION 2-11 ..... | 23  |
| EQUATION 2-12 ..... | 25  |
| EQUATION 2-13 ..... | 34  |
| EQUATION 2-14 ..... | 35  |
| EQUATION 2-15 ..... | 35  |
| EQUATION 2-16 ..... | 36  |
| EQUATION 2-17 ..... | 36  |
| EQUATION 2-18 ..... | 37  |
| EQUATION 2-19 ..... | 37  |
| EQUATION 2-20 ..... | 38  |
| EQUATION 2-21 ..... | 38  |
| EQUATION 2-22 ..... | 38  |
| EQUATION 2-23 ..... | 39  |
| EQUATION 2-24 ..... | 39  |
| EQUATION 2-25 ..... | 40  |
| EQUATION 2-26 ..... | 40  |
| EQUATION 2-27 ..... | 40  |
| EQUATION 2-28 ..... | 41  |
| EQUATION 3-1 .....  | 72  |
| EQUATION 3-2 .....  | 74  |
| EQUATION 5-1 .....  | 109 |
| EQUATION 5-2 .....  | 109 |
| EQUATION 5-3 .....  | 109 |
| EQUATION 5-4 .....  | 110 |
| EQUATION 5-5 .....  | 110 |
| EQUATION 5-6 .....  | 111 |
| EQUATION 5-7 .....  | 111 |
| EQUATION 5-8 .....  | 111 |
| EQUATION 5-9 .....  | 111 |
| EQUATION 5-10 ..... | 112 |
| EQUATION 5-11 ..... | 113 |
| EQUATION 5-12 ..... | 113 |
| EQUATION 5-13 ..... | 122 |
| EQUATION 6-1 .....  | 127 |
| EQUATION 6-2 .....  | 128 |
| EQUATION 6-3 .....  | 129 |
| EQUATION 6-4 .....  | 129 |
| EQUATION 6-5 .....  | 132 |
| EQUATION 6-6 .....  | 143 |

|                    |     |
|--------------------|-----|
| EQUATION 7-1 ..... | 161 |
| EQUATION 7-2 ..... | 162 |
| EQUATION 7-3 ..... | 163 |
| EQUATION 7-4 ..... | 163 |
| EQUATION 7-5 ..... | 164 |
| EQUATION 7-6 ..... | 168 |
| EQUATION 7-7 ..... | 169 |
| EQUATION 7-8 ..... | 169 |

# **1 Introduction**

## **1.1 Research Background**

Every year in Australia, floods cause millions of dollars damage to buildings and critical infrastructure, such as roads and railways as well as to agricultural land and crops. They also disrupt business and can affect the health of communities. Between 1967 and 2005, the average direct annual cost of flooding has been estimated at A\$377 million (Department of Infrastructure and Regional Development, 2008).

Australia's variable climate has always been a factor in natural disasters that have had significant impact on an evolving road infrastructure and on the communities that rely on the roads. Table 1-1(below) shows the average annual cost of natural disasters by state and territory between 1967 and 2005. From these data it can be seen that during this period severe storms and cyclones inflicted the most economic damage, followed by flooding. The data are strongly influenced by three extreme events - Cyclone Tracy in NT (1974), the Newcastle earthquake in NSW (1989) and the Sydney hailstorm also NSW (1999), as well as three flood events in Queensland (South East Qld, 2001; Western Qld, 2004; and the Sunshine Coast, 2005). Climate change has increased the risk from extreme events and the update of this table that includes data for the years 2007 to 2013 - during which there were extreme climate events in Qld, Vic, SA and NSW – will be of great interest to this research.

Table 1-1: Cost of disasters (Emergency Management Australia – www.ema.gov.au)

| <b>State and territory</b>                                      | <b>Flood</b> | <b>Severe storms</b> | <b>Cyclones</b> | <b>Earthquakes</b> | <b>Bushfires</b> | <b>Total</b>  |
|---|--------------|----------------------|-----------------|--------------------|------------------|---------------|
| <i>Cost (\$ million in 2005 Australian dollars)<sup>a</sup></i> |              |                      |                 |                    |                  |               |
| <b>NSW</b>  | 172.3        | 217.1                | 0.6             | 145.7              | 23.9             | 559.6         |
| <b>VIC</b>  | 40.2         | 23.8                 | 0.0             | 0.0                | 36.7             | 100.6         |
| <b>QLD</b>  | 124.5        | 46.7                 | 99.3            | 0.0                | 0.7              | 271.2         |
| <b>SA</b>   | 19.3         | 16.7                 | 0.0             | 0.0                | 13.0             | 49.0          |
| <b>WA</b>   | 4.7          | 13.0                 | 43.3            | 3.1                | 4.6              | 68.7          |
| <b>TAS</b>  | 6.9          | 1.2                  | 0.0             | 0.0                | 11.5             | 19.5          |
| <b>NT</b>   | 9.1          | 0.4                  | 138.5           | 0.3                | 0.0              | 148.3         |
| <b>ACT</b>  | 0.0          | 0.5                  | 0.0             | 0.0                | 9.7              | 10.2          |
| <b>Australia</b>  | <b>376.9</b> | <b>325.2</b>         | <b>281.6</b>    | <b>149.1</b>       | <b>100.1</b>     | <b>1232.9</b> |
| <b>Share of total<br/>(per cent)<sup>c</sup></b>                | <b>30.9</b>  | <b>26.7</b>          | <b>23.1</b>     | <b>12.2</b>        | <b>8.2</b>       | <b>100.0</b>  |

a. These figures exclude the cost of death and injury

b. Figure includes costs associated with a storm involving several eastern states (\$216.7million) which has not been allocated to any individual state data in the table.

c. Figures may not add to totals due to rounding.

Source: BITRE analysis of Emergency Management Australia database <www.ema.gov.au>

Bridge collapse has tremendous consequences in every nation's transportation system. The recent flood events in Queensland, Australia between April 2010 and January 2013 had adverse effects on the bridge network of Queensland. Queensland state controlled road network included 3337km of roads and 6500 bridges and culverts (IBISWORLD, 2011).

It's reported in the recent literature that due to climate change, frequency of flood events has increased as well as they have become more intense. Queensland local governments are planning for with 5% increase in rainfall intensity per degree of global warming as the climate change factor to be incorporated in the flood studies (QueenslandGovernment, 2010). Climate change will not have a huge impact on the infrastructure as the effect due to short-term impact loads are built into the safety factors in the design process (Kong et al., 2013). However, extreme natural disasters will have an impact on the vulnerability as the infrastructure may not be designed for such a long-term intense event.

## **1.2 Research Significance**

In 2009 March flood in North West Queensland covered 62% of the state with water leading to \$234 Million damage to infrastructure (QueenslandGovernment, 2010). Theodore in Queensland was flooded 3 times within 12 months in 2010 and it was the first town, which had to be completely evacuated in Queensland. 2010-2011 floods in Queensland had a huge impact particularly on central and southern Queensland resulting in the state owned properties such as 9170 road network, 4748 rail network, 89 severely damaged bridges and culverts, 411 schools and 138 national parks (QueenslandGovernment, 2012). Approximately 18000 residential and commercial properties were significantly affected in Brisbane and Ipswich during this time (IBISWORLD, 2011). More than \$42 million was paid for individuals, families and households while more than \$121million in grants has been paid to small businesses, primary producers and non-profit organizations and more than \$12 million in concessional loans to small businesses and primary produces (QueenslandGovernment, 2012). The Australian and Queensland governments have committed \$6.8 billion rebuilding the state. The damage to the road work network alone has been estimated to more than \$ 7 billion (Pritchard, 2013). After 2011/2012 extreme flood events in Queensland, the helicopters were required for post disaster operations as well as rigorous inspection of bridges prior to re-opening for recovery operation (Pritchard, 2013).

From December 2010 to January 2011, Western Australia, Victoria, New South Wales and Queensland experienced widespread flooding. There was extensive damage to both public and private property, towns were evacuated and 37 lives were lost, 35 of those in Queensland. Three quarters of Queensland was declared a disaster zone, an area greater than France and Germany combined, and the total cost to the Australian economy has been estimated at more than \$30 billion (UnderstandingFloods, 2011).

Bridge infrastructure plays a pivotal role in post disaster recovery such as evacuation and search and rescue operations because bridges are critical transportation infrastructure without which the access to the affected areas would be hindered. Lockyer Valley Regional Council in Queensland has compiled a comprehensive bridge inspection report for about 47 bridges in the region before they opened the bridges for traffic after the flood has receded. The study on this report indicated that the damage to bridge structures are complex and requires a detailed knowledge of underlying design principals, current classification of roads/bridges as well as

construction methods adopted during different periods of design and construction. Critical observation of this bridge inspection data that included the photos of the affected bridges reveals that the failure of the bridges was primarily due to the impacts on the components of bridge such as bridge approaches, relieving slabs, abutments, wing walls and misalignment of piers. The report also reveals that some of the bridges were inundated as long as 96 hours and the fill under the relieving slab had undermined. The impact load of the huge rocks, shipping containers, vehicles and the other unexpected debris that were carried along the flood water with high velocity was the primary cause of damage to bridge deck, abutments, wing walls and piers.

Typically bridges are designed for a 100 year service life and more recent structures such as Gateway bridges has been designed for a 200 year design life. However, with the increase in frequency of extreme events, the probability of failure would increase, resulting in a reduction in expected design life. Furthermore the damage to structures will affect the service provided to the community.

Reported literature mostly discusses either a frame work or a computational method to assist in the decision making process on interventions after an extreme event so that the decision makers can prioritise the rehabilitation process[(Bocchini and Frangopol, 2012), Bertero and Bresler (1977), Chen et al. (2009a), Choi et al. (2004)]. A major gap in research is the lack of assessment techniques and tools to reduce the vulnerability of road infrastructure to enhance both community and structural resilience.

The research presented here examined the process for quantifying vulnerability of bridges and strategies to enhance resilience of bridges to flood hazard. It also aims to understand the factors influencing the resilience and vulnerability of bridge structures when exposed to an extreme flood event with the longer term goal of feeding in to design specifications of new bridge structures and maintenance and management decisions taken on existing structures. The outcome of this research will also facilitate predicting the failure of the bridge structure under flood hazard which would eventually help road authorities to strengthen the bridge structures considering the risk and likelihood.

A Bridge could be damaged in many ways when it is under an extreme flood event. If the bridge is completely inundated during the flood, the damage to the bridge depends on the

length of time it was submerged as well as the types of debris collected around or passing the bridge components. Extra care should be taken to inspect the supports of the bridges, even after the flood water recedes. Approaches of a bridge could be damaged due to debris impact, settlement or depressions. Debris against substructure and superstructure, bank erosion and damage to scour protection will damage the waterways. Bridge substructure could fail due to movement of abutments, wing walls, piers, rotation of piers and missing, damaged dislodged or poorly seating of the bearings while the superstructure could fail due to the debris on deck, rotation of deck, dipping of deck over piers or damage of girders. Pritchard (2013) identified that urban debris such as cars; containers etc. and the insufficient bridge span to through that debris were the main cause for damaging bridges during the aftermath of 2011/2012 extreme flood events in Queensland. Figure 1.1 (below) depicts some the damaged bridges from Lockyer Valley Region in Queensland.



Figure 1.1: Damaged Bridges in Lockyer Valley Region in Queensland (The Lockyer Creek Flood of January 2011)

Analysis of the performance of bridges under 2011/2013 flood in Lockyer Valley Region, Queensland indicates that the bridge deck is the most commonly affected component followed by the bridge approach, pier/abutment scouring, cracks in the abutment wing walls and misalignment of abutment headstock connections to piles. Reinforced or pre-stressed concrete girder bridges are a common design configuration used in Australia. During the Lockyer Valley floods in 2013, vulnerability of girder bridges was observed by significant damage to these structures. The details of some of the bridges obtained from the Lockyer Valley Regional Council Bridge Inspection Data report are given in Table 1-2(below). Concrete girder bridges are the most recurrent types of bridge in Australia and 25 out of 47 bridges in the case study region (Lockyer Valley Region) are concrete girder bridges. Hence

concrete girder bridges have been selected for case studies in this research to derive structural vulnerability models and determine vulnerable structures in the road network.

Table 1-2: Lockyer Valley Regional Council Bridge Data (Lokuge and Setunge, 2013)

| Lockyer Valley Regional Council Bridge Data (2013 Event) |                        |                  |             |              |                                   |      |           |          |                        |                   |
|--|------------------------|------------------|-------------|--------------|-----------------------------------|------|-----------|----------|------------------------|-------------------|
| Bridge Name  | Bridge Fully Submersed | Location X and Y |             | Elevation(m) | Bridge Material & Bridge Material | Span | Length(m) | Age      | Roadway Classification | Avg Daily Traffic |
| Magarrigals Bridge                                       | Yes                    | 152.3643857      | -27.6932327 | 128          | Concrete pre cast                 | 2    | 22m       | 1 Year   | Rural Access           | NA                |
| Peters Bridge  | Yes                    | 152.36971        | -27.775738  | 185          | Concrete                          | 4    | 54.1      | 1 Year   | Rural Access           | NA                |
| Middletons Bridge  | Yes                    | 152.459445       | -27.469041  | 69           | Timber                            |      | 20.9m     | 49 Years | Rural Collector        | 309vpd (2010)     |
| Davey's Bridge   | Yes                    | 152.276383       | -27.552483  | 99           | Concrete                          | 2    | 21.6m     | 41 Years | Rural Collector        | 1444vpd (2009)    |
| Belford Bridge   | Yes                    | 152.283218       | -27.544789  | 98           | Concrete                          | 2    | 17m       | 24 Years | Urban Arterial         | 1453vpd (2010)    |
| Logan Bridge   | Yes                    | 152.214551       | -27.633273  | 132          |                                   | 4    | 64.2m     | 9 Years  | Rural Arterial         | 1161vpd (2004)    |
| Frankie Steinhardt's Bridge                              | Yes                    | 152.237605       | -27.591714  | 114          | Concrete                          | 3    | 42m       | 3 Years  | Rural Access           | 247vpd (2002)     |
| Hoger Bridge   |                        | 152.259173       | -27.657696  | 161          | Concrete                          | 1    |           | 1 Year   | Rural Access           | 24vpd (2008)      |
| Sheep Station Bridge                                     |                        | 152.122427       | -27.548562  | 139          | Concrete                          | 1    | 22m       | 1 Year   | Urban Collector        | 230vpd (2010)     |
| Duncan's Bridge  | Yes                    | 152.122427       | -27.620055  | 168          | Concrete                          | 3    | 36.9      | 48 Years | Rural Arterial         | 294vpd (2009)     |
| Murphy Bridge  | Yes                    | 152.12269        | -27.563122  | 129          | Concrete                          |      | 36.6      | 23 Years | Rural Collector        | 191vpd (2002)     |
| The Willows Bridge                                       | Yes                    | 152.081029       | -27.507247  | 162          | Concrete                          | 1    | 15        | 3 Years  | Rural Collector        | 121vpd (2008)     |
| The Dairy Bridge   | Yes                    | 152.073296       | -27.464339  | 228          | Concrete. Timber Girders          | 2    | 22.1      | 8 Years  | Rural Arterial         | 77vpd (2002)      |
| Greer Bridge   | No                     | 152.096362       | -27.545896  | 155          | Concrete. Timber Girders          | 4    | 36.8      | 6 Years  | Rural Arterial         | 1193vpd (2008)    |
| McGrath Bridge   | Yes                    | 152.363778       | -27.729337  | 140          | Concrete                          | 3    | 40        | 4 Years  | Rural Collector        | 290vpd (2006)     |
| Clarke Bridge (Thorton)                                  | Yes                    | 152.373109       | -27.798447  | 109          | Timber                            |      | 6.1       | 49 Years | Rural Access           | 100vpd (?)        |
| vpd = Vehicles Per Day                                   |                        |                  |             |              |                                   |      |           |          |                        |                   |

Bridge structures have a major impact on resilience of road infrastructure and the damage to bridges could increase the vulnerability of the community served by the road infrastructure significantly. A systematic method of quantifying vulnerability of bridge structures under varying flood loading is currently a significant gap in knowledge.

Internationally vulnerability of bridge structures has been well examined under earth quake loading. Only a few studies [(Greg Rogencamp, 2012) , (Durmus, 2012)] covered the failure or damage to bridge structure under flood loading.

The extensive literature review in this research shows that significant research have been carried out on studying the vulnerability of building infrastructure under the influence of certain natural hazards such as earthquake, hurricane etc. However, little or no literature have been reported on quantifying vulnerability of road infrastructure under flood hazard Furthermore, it is noted that no comprehensive approach for structural integrity assessment of bridge structures subjected to lateral floodwater forces, were carried out.

### **1.3 Research Aim and Objectives**

Proposed research aims to understand the factors influencing vulnerability and resilience of bridges when exposed to extreme flood events so that decisions on maintenance or strengthening can be undertaken to enhance the resilience of vulnerable structures. In achieving the major aim, the following objectives will be focussed on.

1. Identify major failure mechanisms of bridge structures under flood loading.
2. Understand provisions of current bridge design codes.
3. Numerical modelling of girder bridges to simulate flood loading.
4. Development of vulnerability models which provide relationship between exposure and damage

### **1.4 Research gap**

1/ Literature review indicated that there are many publications on vulnerability modelling of bridges under seismic loading, yet, the research into understanding of vulnerability modelling of bridges under flood loading is limited.

2/ Road authorities do not have a well-developed method to understand the probability of failure of bridges under variable flood loading.

3/ A method for decision making to enhance resilience of bridges under flood loading is not available.

## 1.5 Research Scope

The scope of the work proposed here focus on understanding vulnerability of concrete girder bridge decks under flood and log impact. This is a very common and major failure mode identified through the analysis of case studies. Other failure modes are excluded from this analysis.

The contribution to knowledge comes from the understanding of the vulnerability of concrete girder bridges as well as the methodology developed for vulnerability modelling of bridges under flood.

## 1.6 Outline of the Chapters

The presented thesis consists of eight chapters as outlined below:

**Chapter 1** introduces the background of the research followed by the significance of the study and its contribution to the body of knowledge of the discipline. The aims and objectives of the research as well as the research scope have been covered in this chapter.

**Chapter 2** presents a critical review of the literature aimed at gathering information and state of-the-art knowledge and methods for conducting the research project and interpreting the outcomes. This stage begins with reviewing design process of bridges for flood loading in accordance with existing bridge design standards and previous research work in published literatures. Collapse mechanisms/failure modes and the vulnerability modelling of the bridges are then reviewed. Furthermore, the literature review includes quantifying damage to bridges under flood for decision making and fragility analysis of bridges.

**Chapter 3** introduces the research methodology adopted in this research. The research questions as well as the approach used to address the questions are explained in this chapter. Brief introduction about the analysis of case studies in this research is presented here. Numerical modelling of the selected case study structures deterministically and as well as probabilistically are outlined in this chapter. These are then elaborated in the Chapters 4, 5 and 6

**Chapter 4** discusses the Analysis of the case studies in this research. An in depth analysis of Lockyer Valley Regional Council Bridge Inspection Report is presented here. Focus on Concrete Girder bridges and the major failure modes/mechanisms of the affected bridges are also presented in this chapter.

**Chapter 5** presents the numerical modelling of the case study bridge deterministically using ABAQUS Finite Element software. It includes detailed descriptions of the case study bridge with its geometry and the reinforcement to model the bridge using ABAQUS software. Deriving Flood induced minor axis bending moment on the bridge girder and model validation are finally discussed.

**Chapter 6** illustrates the probabilistic modelling of the same case study bridge described in chapter 5. The effect of flood intensity and the concrete material are considered here to capture their uncertainties. The actual flood velocity distribution to the case study geographical location is discussed. Finally using @Risk adds in with MS Excel, failure probabilities of the bridges under flood hazard are derived. A parametric study is carried out for different span length of the bridge girder with and without log impact and the results are finally presented for decision making.

**Chapter 7** presents the damage indices for practical application. It further explains the interpretation of these curves and their use for end users and decision makers.

**Chapter 8** summarises the general conclusions drawn from the research, explores possible further research in the area and recommends further research.



## **2 Literature Review**

### **2.1 Introduction**

This Chapter presents a review of flood loading on bridge structures and a detailed review of current literature on vulnerability of bridges under flood loading. This included a review of bridge design standards to understand the philosophy of design of bridges for resilience to flood loading, current published work on vulnerability modelling of bridges, methods of quantifying the damages to bridges under flood loading, numerical modelling of bridge structures, fragility analysis and the gaps in knowledge base.

### **2.2 Understanding floods**

When water inundates land that is normally dry, this is called a flood. Floods can be caused by a number of processes, but the dominant cause in Australia is rainfall. Floods are a natural process, but mankind's activities affect flooding. Floods occur at irregular intervals and vary in size, area of extent, and duration (QueenslandGovernment, 2013)

Since the beginning of 2011, floods have led to major devastation and personal tragedy around the world. At the same time as the Australian floods, more than 800 people died in floodwaters and mudslides in Brazil and South Africa recorded 70 flood related deaths. Many lives have also been lost due to flooding in the Philippines, Pakistan and Sri Lanka (UnderstandingFloods, 2011). Figure 2.1(below) indicates flood peaks in Eastern Australia over the period 26 November 2010 – 29 January 2011.

Floods impact on both individuals and communities, and have social, economic, and environmental consequences. The consequences of floods, both negative and positive, vary greatly depending on the location and extent of flooding, and the vulnerability and value of the natural and constructed environments they affect.

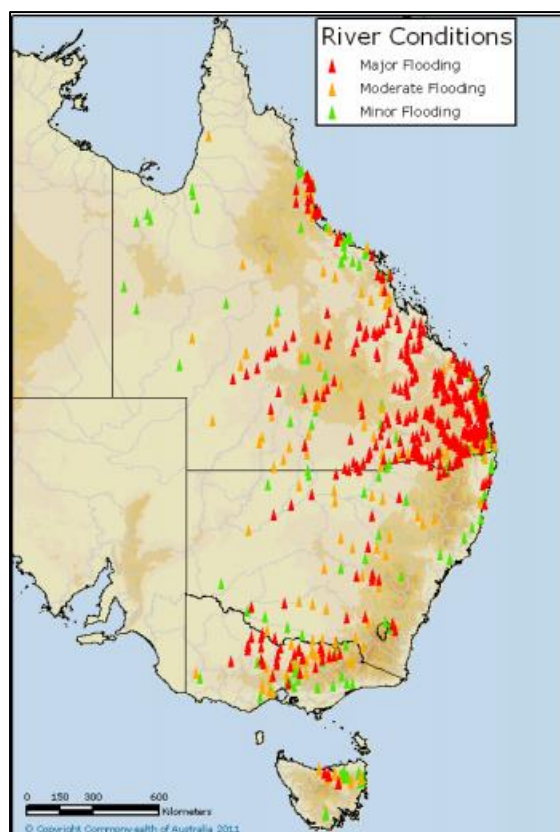


Figure 2.1: Flood peaks in Eastern Australia over the period 26 November 2010 – 29 January 2011[van den Honert and McAneney (2011a)]

### 2.2.1 Estimating the chance of a flood occurring

Understanding the likelihood and intensity of floods is important for managing flood risk. The chance of a flood event can be described using a variety of terms, but the preferred method is the Annual Exceedance Probability (AEP). A flood with a one per cent AEP has a one in a hundred chance of being exceeded in any year. Currently, the one per cent AEP event is designated as having an ‘acceptable’ risk for planning purposes nearly everywhere in Australia. However, good planning needs to consider more than just the one per cent AEP flood.

Floods are often defined according to their likelihood of occurring in any given year. The most commonly used definition in planning is the ‘1 in 100-year flood’. This refers to a flood level or a peak that has a one in a hundred, or one per cent, chance of being equalled or exceeded in any year. Similarly, a ‘1 in 200-year flood’ has a one in two hundred, or 0.5 per cent, chance of being equalled or exceeded in any one year.

The best method for calculating the chance of different sized floods occurring is statistical analysis of long-term flood records from stream gauging stations. Where a long-term flood

record exists, and no significant changes have occurred to the catchment, a statistical technique known as flood frequency analysis can be used to determine the likelihood of floods of different sizes occurring at a specific site in the future (Figure 2.2 (below)). However, Australia's flood records do not extend far into the past, and flood events are highly variable, meaning there is still a level of uncertainty in defining such flood estimates. Climate change may also affect the flood frequency and intensity.

Where sufficient flood records do not exist, or a very rare flood needs to be estimated, rainfall based techniques are used. These use statistical analyses of rainfall records, together with computer models based on the geographical characteristics (for example, catchment area, waterway length) of the region being studied, to determine the chance of different sized floods occurring. These models can be set up to take account of changes that affect runoff, such as new dams and urbanisation. However the computer models used to convert rainfall to runoff are not perfect, making rainfall techniques generally less reliable than the use of long-term flood records.

Both of these techniques result in predictions for peak water flows at key locations in rivers. These predictions are translated into flood levels at any point of interest in the floodplain, through the use of further computer models known as floodplain hydraulic models.

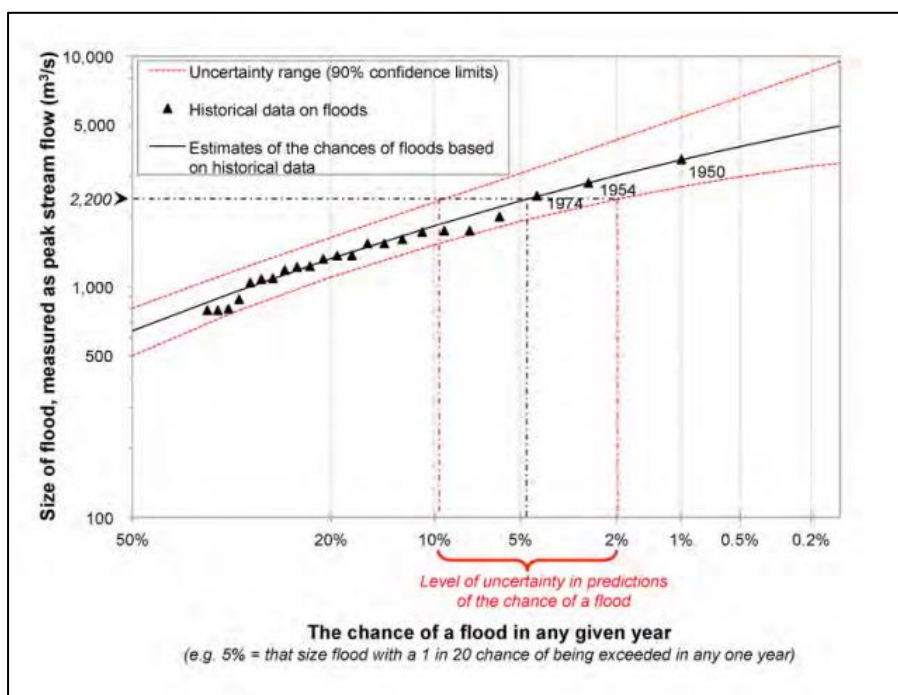


Figure 2.2: The chances of a flood in any given year (BureauOfMeteorology, 2003)

Figure 2.2 (above) presents the chance of floods of different intensities based on flood frequency analysis of historical flood records at Bellingen, NSW. There is always a level of uncertainty inherent in such analyses. For example, the chance of a flood with a stream flow of 2,200 m<sup>3</sup> /s (as arrowed, left hand axis) in any year is estimated to be between 1 in 50 (2%) and 1 in 10 (10%). This is said to be ‘within 90% confidence limits’, i.e. we are 90% sure that it will be in this range – with a 10% chance we will be wrong, and it will be outside this range, higher or lower. The more confidence there is in the data the closer the confidence limits (red dashed lines) will be to the estimate (black line).

## 2.3 Review of current bridge design standards

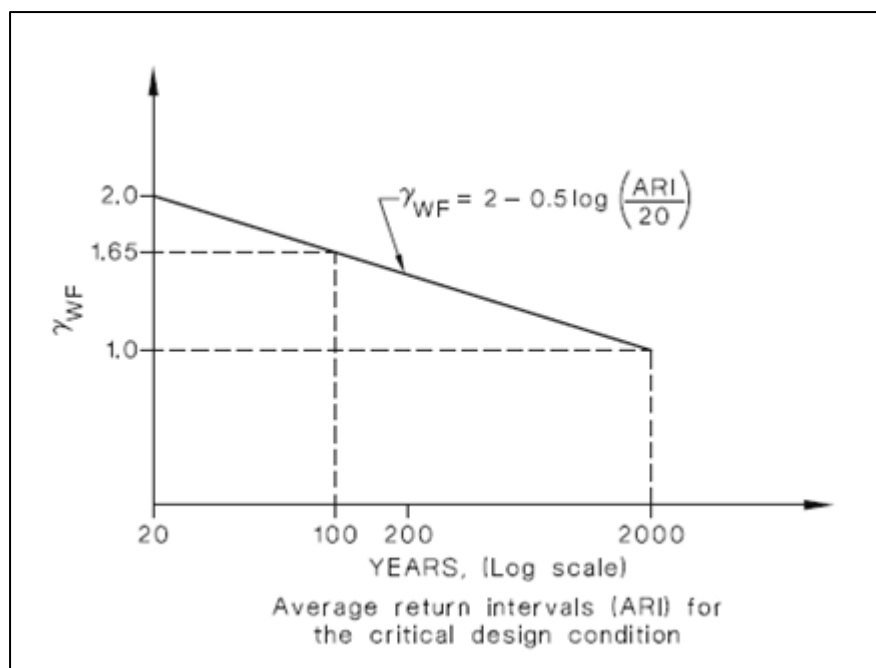
The review of literature commenced with an analysis of the current design standards in the globe to understand the design philosophy of bridge structures. These included the Australian Standard (AS 5100, 2004), the European standard (Euro code) and the American standard (AASHTO).

### 2.3.1 AS 5100

#### Ultimate Limit state

AS 5100 Australia (2004) states that *“The ultimate limit states define the capability of a bridge to withstand, without collapse, any flood of a magnitude up to and including that with a 2000 year average return interval, whichever produces the most severe effect. It can be accepted that scour of the stream bed and considerable damage to approaches and embankments may take place, provided that the structural integrity of the bridge is maintained.”*

*“As the critical design condition may occur at the flood level which just causes overtopping of the superstructure, an estimate of the return interval of such a flood shall be made and, if appropriate, this condition shall be considered in the design. Where the critical design condition occurs at an average return interval of less than **2000 years**, the ultimate load factor ( $\gamma_{WF}$ ) shall be obtained from the following figure (Figure 2.3(below)), but shall be not greater than 2.0”(Australia, 2004).*

Figure 2.3: Ultimate Load Factor ( $\gamma_{WF}$ )

### Serviceability limit states

*The serviceability limit states define the capability of the road and bridge systems to remain open during a serviceability design flood or to sustain an overtopping flood without damage to bridges, culverts, floodways or embankments within the system. The serviceability design flood shall be that with a **20 year** average return interval.*

### **2.3.2 Euro code**

Euro code 1, Part 1.7 Eurocode (2005) considers flood, fire and earthquake as accidental effects and has suggested a risk analysis to be undertaken for such events. It states that accidental load will most probably not occur during the working life of the structure. Even if the load is present, it normally will take only a short time, varying from a few seconds in the case of an explosive accident to some days in the case of a flood accident. Figure 2.4 Eurocode (2005) shows the typical difference between a variable and an accidental load verses time. Figure 2.5 Eurocode (2005) shows a typical probability distribution for the one year maximum of the loads. Accidental loads have a probability of 98% per year or more to be zero.

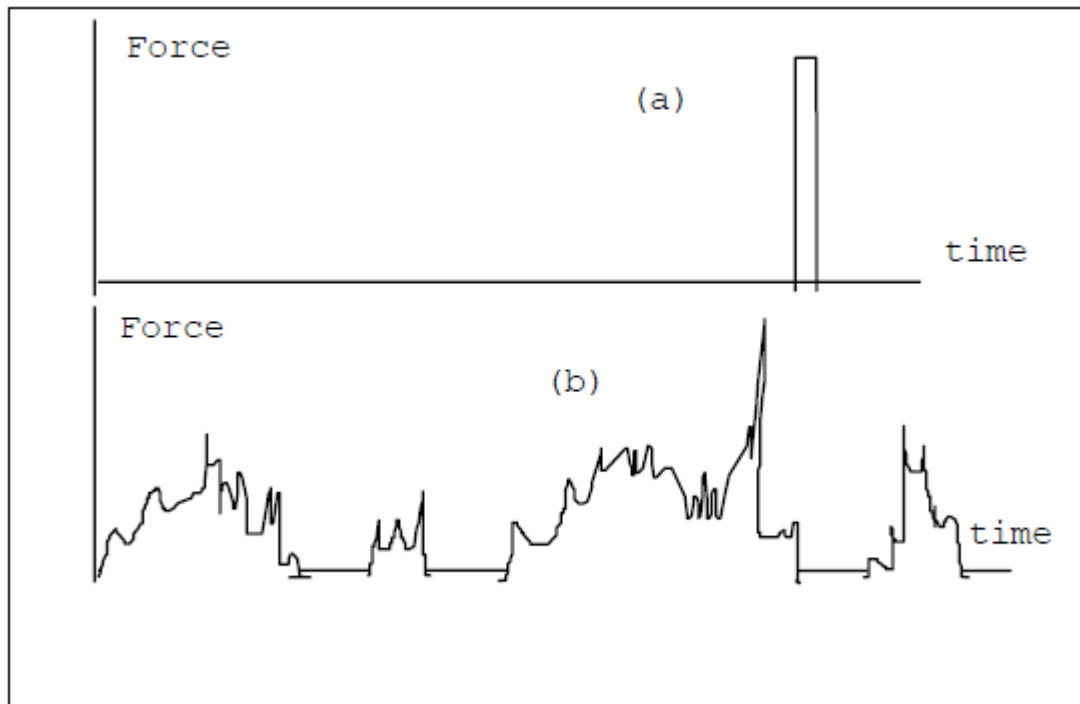


Figure 2.4: Typical time characteristics of (a) accidental and (b) variable load. Eurocode (2005)

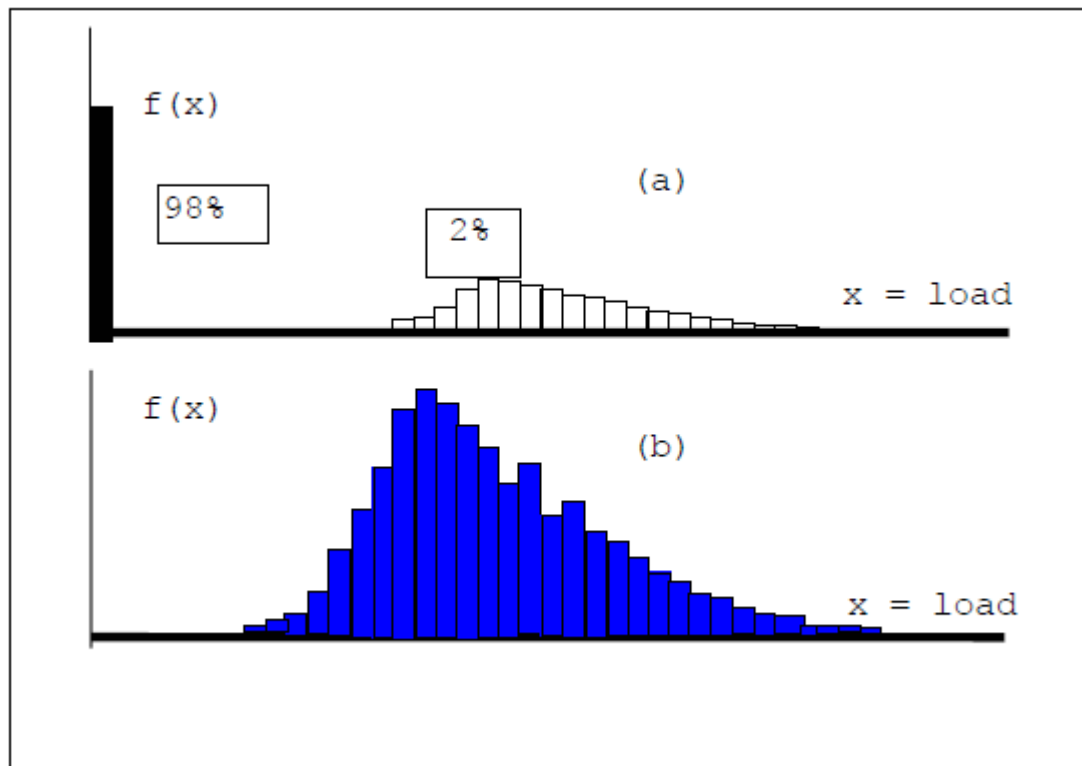


Figure 2.5: Typical probability distribution of (a) accidental and (b) variable loads (Eurocode, 2005).

Accidental actions on structures, that are in general more complex, are usually represented as static loads and structural response is usually performed using linear elastic analysis.

### **2.3.3 American standards**

(AASHTO, 2012) states that the extreme event limit state shall be taken to ensure the structural survival of a bridge during a major flood, or when collided by a vessel, vehicle, or ice flow, possibly under scoured conditions.

Gosain et al. (1977) asserts that “*the design flood should at least be equivalent to the flood having a 1 percent chance of being equaled or exceeded in any given year (i.e., the base flood or 100-year flood, which served as the load basis in ASCE 7-95). In some instances, the design flood may exceed the base flood in elevation or spatial extent; this excess will occur where a community has designated a greater flood (lower frequency, higher return period) as the flood to which the community will regulate new construction.*”

## **2.4 Design process of bridges for flood loading according to the current standards**

Jempson (2000) conducted an extensive experimental study to investigate the forces and moments coefficients on bridge superstructures. The effect of debris on the coefficients was also studied. The main aim of the study was to establish a more reliable design methodologies and coefficients than those proposed in Austroad'92 (1992). The research by Denson (1982) introduced the lift forces and moments to the hydrodynamic effect on the bridge structure. The study made a clear distinction between the buoyancy and lift forces in the vertical hydrodynamic action. The plots of the drag, lift and moment coefficients were developed at different velocity and inundation depth values. The authors stated that moment was not significant. The drag coefficients obtained for the AASHTO bridges were compared with a previous study.

### **2.4.1 Design loads & load combinations**

#### **2.4.1.1 AS 5100**

AS 5100 Bridge Design code (Section 15 of AS 5100.2-2004) Australia (2004) requires that bridges over waterways be designed for flood loadings. Equations are provided for determining the drag and lift forces on the superstructure for a serviceability limit state and an ultimate limit state. The serviceability design flood is to be associated with a 20 year return interval. The ultimate limit state design flood is to be associated with a 2000 year return interval.

The code recommends Equation 2-1 and Equation 2-2 for calculating the drag force and lift force on the superstructure respectively.

In the absence of more exact analysis, the code recommends a drag coefficient of 2.2. This is based on the research undertaken up to the time of publication of the code. The previous code, the 1976 NAASRA Bridge Design Specification, recommended a  $C_d$  of 1.4.

The current code suggests that lift force may act on the superstructure when the flood stage height is significantly higher than the superstructure and the deck is inclined by super elevation.

$C_d$  is provided as a function of the aspect ratio  $b/d$ , where  $b$  is the overall width of bridge between outer faces of the parapets, and  $d$  is the depth of solid superstructure.

$$F_d^* = 0.5C_dV^2A_s$$

Equation 2-1

where:

$C_d$  is the drag coefficient read from the chart given in the code;

$V$  is the mean velocity of water flow (flood);

$A_s$  is the wetted area of the superstructure, including any railings or parapets, projected on a plane normal to the water flow.

$$F_L^* = 0.5C_LV^2A_L$$

Equation 2-2

where:

$C_L$  is the lift coefficient read from the chart given in the code;

$V$  is the mean velocity of water flow (flood);

$A_L$  is the Plan deck area of the superstructure.

### Moment on superstructure

According to AS 5100 (Australia, 2004), drag and lift forces generate a moment about the longitudinal axis of the superstructure. The resulting moment at the soffit level at the centre line of the superstructure shall be calculated as follows:

$$M_g = 0.5C_m V^2 A_s d_{sp} \quad \text{Equation 2-3}$$

where:

$C_m$  is the moment coefficient and varies from 1.5 to 5 depending on the relative submergence of the superstructure.

$d_{sp}$  = *wetted depth of the superstructure projected on a plane normal to the water flow*

### Forces due to debris

Debris load acting on superstructures is given by the code as,

$$F_{deb} = 0.5C_d V^2 A_{deb} \quad \text{Equation 2-4}$$

where:

$C_d$  is the drag coefficient read from the chart given in the code;

$V$  is the mean velocity of water flow (flood);

$A_{deb}$  is the projected area of the debris mat described in the code.

### Forces due to moving objects

According to AS 5100 Australia (2004), where floating logs or large objects are a possible hazard, the drag forces exerted by such logs directly hitting bridge girder (superstructure) shall be calculated on the assumptions that a log with a minimum mass of 2 tons will be stopped in a distance of 75 millimetres for such solid girder (superstructure). A draft revision of the AS 5100 Australia (2004) suggests consideration of the “large item impact” in urban areas, where large floating items such as pontoons, pleasure craft, shipping containers etc. can impact the bridge structure. However, the code suggests that forces due to log impact or large item impact debris shall not be applied concurrently on the structure.

$F_{log}$  shall thus be given by the following equation.

$$F_{\log} = \frac{mV^2}{2d} \quad \text{Equation 2-5}$$

where:

m is the mass of the log or the impacting object;

d is the stopping distance specified by the code (eg. 0.075m for solid concrete piers);

V is the velocity of the water (m/s).

#### 2.4.1.2 Euro codes

Euro code 1 , Part 1.7 Eurocode (2005) considers flood, fire and earthquake as accidental effects and has suggested a risk analysis to be undertaken for such events. Following introduces some forces affecting bridges due to an event of flood.

Forces due to water flow

Euro code 1, Part 2.6 Alampalli et al. (1997) considers actions due to water during execution into two categories: static pressures and hydrodynamic effects. The magnitude of lateral water force to bridges is given by Equation 2-6 (Figure 2.6(below))

$$F_{wa} = k\rho_{wa}hbv_{wa}^2 \quad \text{Equation 2-6}$$

where:

$v_{wa}$  is the mean speed of the water, averaged over the depth, in m/s;

$\rho_{wa}$  is the density of water in kg/m<sup>3</sup> ;

h is the water depth, but not including, where relevant, local scour depth in meters;

b is the width of the object in meters;

k is the shape factor:

k = 0.72 for an object of square or rectangular horizontal cross-section,

k = 0.35 for an object of circular horizontal cross-section.

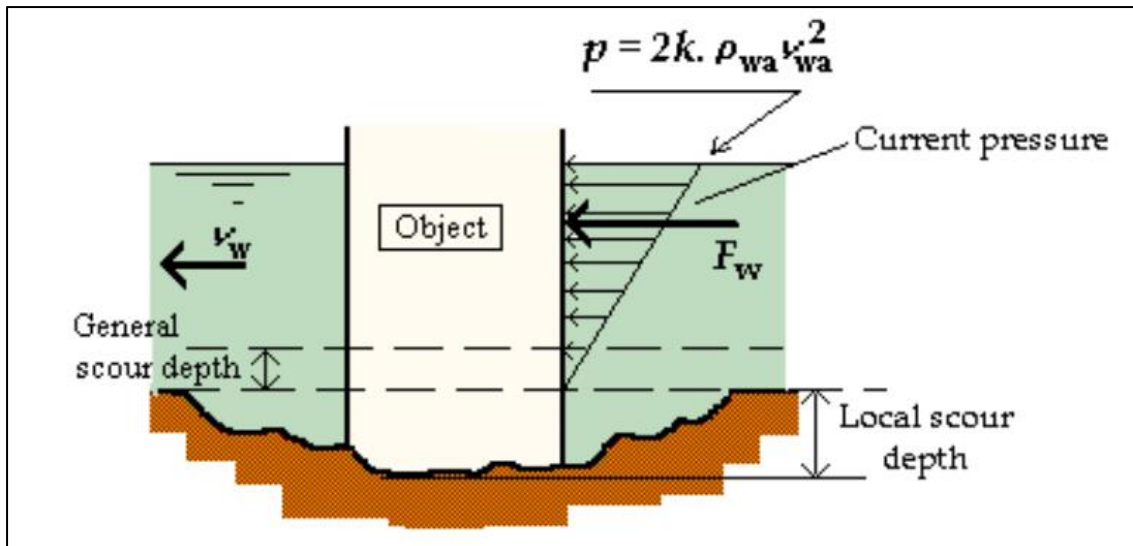


Figure 2.6: Pressure and Force due to currents on bridge piers (Alampalli et al., 1997)

Interestingly, Euro code 1, Part 1.6 Chen and Lui (2005) introduces the above formula with a minor difference, multiplying 0.5 to the formula, as follows (Equation 2-7) (Figure 2.7(below)):

$$F_{wa} = 0.5k\rho_{wa}hbv_{wa}^2$$

Equation 2-7

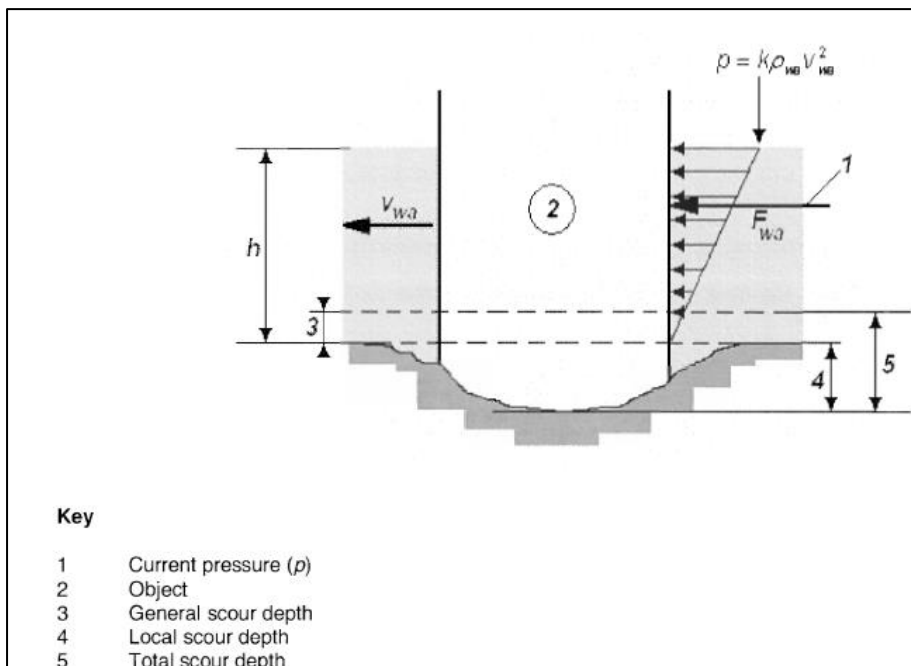


Figure 2.7: Pressure and Force due to currents (Chen and Lui, 2005)

However, the values of shape factor ( $k$ ) have been doubled accordingly, which will result the same water force, as follows:

$k = 1.44$  for an object of square or rectangular horizontal cross-section,

$k = 0.7$  for an object of circular horizontal cross-section.

Euro code 1 Chen and Lui (2005) also notes that a more refined formulation can be used to determine the water force for individual projects.

Forces due to debris

According to Euro code 1 Chen and Lui (2005), debris force  $F_{deb}$  should be calculated using the following formula (Equation 2-8):

$$F_{deb} = k_{deb} A_{deb} v_{wa}^2 \quad \text{Equation 2-8}$$

where:

$k_{deb}$  is a debris density parameter, in  $\text{kg/m}^3$  (recommended value is  $666 \text{ kg/m}^3$ );

$v_{wa}$  is the mean speed of the water average over the depth, in  $\text{m/s}$ ;

$A_{deb}$  is the area of obstruction presented by the trapped debris and false work, in  $\text{m}^2$ .

#### 2.4.1.3 American Standards

AASHTO (2012) categorises the water loads ( $W_A$ ) into 4 categories: static pressure, buoyancy, stream pressure and wave load. Similarly, Gosain et al. (1977) categorises the water loads into hydrostatic and hydrodynamic loads in where, wave loads are categorised as a special type of hydrodynamic loads. ASCE also mentions the Impact loads result from objects transported by floodwaters striking against structures and their components. The stream pressure has been further categorised into: longitudinal and lateral in (AASHTO, 2012).

##### 1. Hydrostatic loads

ASCE defines hydrostatic loads as the ones caused by water either above or below the ground level, which is either still or moves at velocities less than  $1.52 \text{ m/s}$ . These loads are equal to the product of the water pressure multiplied by the surface area on which the pressure acts (Gosain et al., 1977). These loads are further divided into vertical downward, upward and

lateral loads depending on the geometry of the surfaces and the distribution of hydrostatic pressure.

Longitudinal forces

The longitudinal forces on substructures which are similar to the drag forces mentioned in Australian standards are calculated as follows (Equation 2-9):

$$p = \frac{C_D V^2}{1,000} \quad \text{Equation 2-9}$$

where,

p is the pressure of flowing water (ksf);

C<sub>D</sub> is the drag coefficient for piers, which can be read from Table 2-1(below)

V is the design velocity for the design flood in strength and service limit states and for the check flood in the extreme event limit state (ft. /s).

Table 2-1: Drag coefficients (AASHTO, 2012)

| Type  | C <sub>D</sub> |
|---|----------------|
| Semicircular-nosed pier                             | 0.7            |
| Square-ended pier                                   | 1.4            |
| Debris lodged against the pier                      | 1.4            |
| Wedge-nosed pier with nose angle 90 degrees or less | 0.8            |

However, AASHTO (2012) also refers to the theoretically correct formulation for calculation of the drag force as follows (Equation 2-10):

$$p = \frac{C_D w V^2}{2g} \quad \text{Equation 2-10}$$

where,

w is the specific weight of water (kcf);

$C_D$  is the gravitational acceleration constant 32.2 (ft. /s<sup>2</sup>);

V is the velocity of water (ft. /s).

AASHTO (2012) asserts that the floating logs, roots, and other debris which may accumulate at piers and, by blocking parts of the waterway, need to be considered and provides a New Zealand Highway Bridge Design Specification provision as a design guidance.

Lateral forces

(AASHTO, 2012) also introduces the lateral forces which are uniformly distributed pressure on substructures due to water flowing at an angle,  $\theta$ , to the longitudinal axis of the pier Figure 2.8(below) (Equation 2-11)

$$p = \frac{C_L V^2}{1,000} \quad \text{Equation 2-11}$$

where,

p is the lateral pressure (ksf);

$C_L$  is the lateral drag coefficient, which depends on the angle  $\theta$  as shown in Figure 2.8(below) and Table 2-2(below).

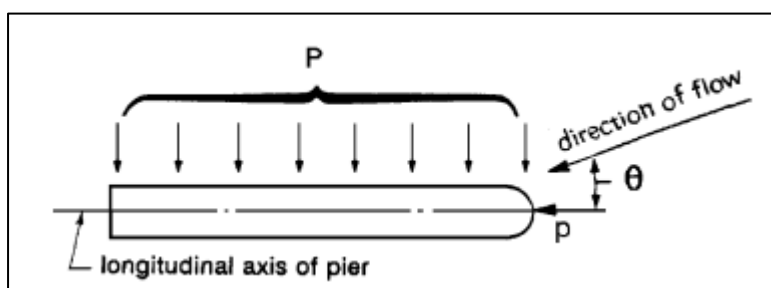


Figure 2.8: Plan View of Pier (AASHTO, 2012)

Table 2-2: Lateral Drag Coefficient (AASHTO, 2012)

| Angle, $\theta$ , between direction of flow and longitudinal axis of the pier | $C_L$ |
|---|-------|
| 0 degrees   | 0.0   |
| 5 degrees   | 0.5   |
| 10 degrees  | 0.7   |

|             |     |
|-------------|-----|
| 15 degrees  | 0.9 |
| ≥30 degrees | 1.0 |

### Flood velocity

As estimation of flood velocities includes a variety of epistemic uncertainties, FEMA Gosain et al. (1977) suggests a lower and upper bound for the estimation of flood velocities in design in coastal areas (Figure 2.9(below)), which are given as follows:

$$V = \frac{d_s}{t} \quad \text{Lower bound}$$

$$V = (gd_s)^{0.5} \quad \text{Upper bound}$$

where,

V is the flood velocity (m/s)

$d_s$  is the Stillwater flood depth (m)

t is 1 second

g is the gravitational constant ( $9.81 \text{ m/s}^2$ )

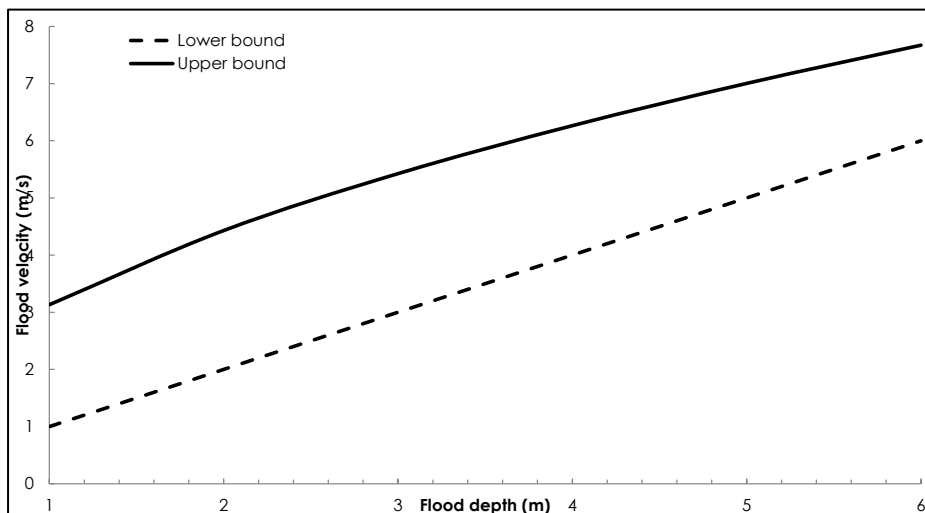


Figure 2.9: Design Flood Velocity

### Impact loads

Gosain et al. (1977) categorizes the impact loads into 3 categories: normal impact loads, special impact loads and extreme impact loads which are depending on the frequency and the

size of the object impacting the structure. ASCE suggests that “given the short-duration, impulsive loads generated by flood-borne debris, a dynamic analysis of the affected building or structure may be appropriate. However, in some cases (e.g., when the natural period of the building is much greater than 0.03 s), design professionals may wish to treat the impact load as a static load applied to the building or structure.”(Gosain et al., 1977).

Therefore, the following formula has been suggested by (Gosain et al., 1977) for estimation of the force.

$$F = \frac{\pi W V_b C_i C_o C_D C_B R_{max}}{2g\Delta_t} \quad \text{Equation 2-12}$$

Where,

F= Impact force, in lb. (N)

W= Debris weight in lb. (N)

V<sub>b</sub>= Velocity of object (assume equal to velocity of water, V) in ft/s (m/s)

g= Acceleration due to gravity, = 32.2ft/s<sup>2</sup> (9.81m/s<sup>2</sup>)

Δ<sub>t</sub> = Impact duration (time to reduce object velocity to zero), in s

C<sub>i</sub>= Importance coefficient

C<sub>o</sub>= Orientation coefficient

C<sub>D</sub>= Depth coefficient, = 0.8

C<sub>B</sub>= Blockage coefficient

R<sub>max</sub>= Maximum response ratio for impulsive load

Table 2-3(below) summarizes comparisons for the design loads of the three standards discussed above.

Table 2-3: Comparisons of the design loads of the three standards

| Design standards | Formulae for design flood load |                             |                                 |
|------------------|--------------------------------|-----------------------------|---------------------------------|
|                  | F <sub>d</sub> (Drag force)    | F <sub>L</sub> (Lift force) | F <sub>deb</sub> (Debris force) |
|                  |                                |                             |                                 |

|           |                                    |                            |  |
|-----------|------------------------------------|----------------------------|--|
|           |                                    |                            |  |
| AS5100    | $F_d^* = 0.5C_dV^2A_s$             | $F_L^* = 0.5C_LV^2A_L$     | $F_{deb} = 0.5C_dV^2A_{deb}$                           |
| Euro code | $F_{wa} = 0.5k\rho_{wa}hbv_{wa}^2$ | -                          | $F_{deb} = k_{deb}A_{deb}v_{wa}^2$                     |
| AASHTO    | $p = \frac{C_DwV^2}{2g}$           | $p = \frac{C_LV^2}{1,000}$ | $F = \frac{\pi WV_bC_iC_oC_D C_B R_{max}}{2g\Delta_t}$ |

## 2.4.2 Structural analysis of bridges

### 2.4.2.1 Bridges

Australia (2004) states that “analysis for all limit states shall be based on linear elastic assumptions except where nonlinear methods are specifically implied elsewhere in the standard or approved by the relevant authority”.

AASHTO (2012) accepts any method of analysis which can satisfy the requirements of equilibrium and compatibility and utilizes stress-strain relationships for the proposed materials.

### 2.4.2.2 Types of bridges and usage in Australia

There are many different types of bridges which are usually constructed of concrete, steel or timber. The main types of bridges are beam bridges, truss bridges, arch bridges, cable stayed and suspension bridges.

### 2.4.2.3 Concrete bridges

Beam bridges are the most common type of bridge built throughout Queensland and Australia. These bridges can be built out of timber, steel and concrete, but concrete is the most commonly used material. Beam bridges are usually the most cost effective bridge structure hence why they are used most often. A beam bridge can be; simply supported where the deck is supported only between two columns; a cantilever beam; and a continuous beam where the deck is one continuous unit. These types are illustrated in Figure 2.10(below).

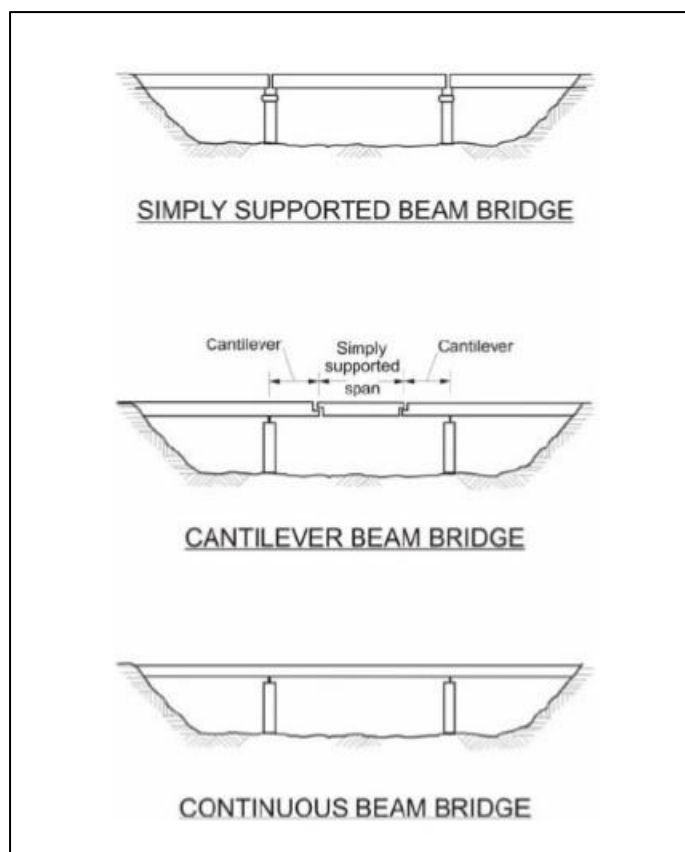


Figure 2.10: Types of Beam Bridges (DepartmentOfMainRoads, 2006)

For a concrete beam bridge, the beams that run along the length of the bridge are I or T shaped and can be hollow with circular or rectangular (box) voids (Department of Main Roads, 2006). Pre-stressed concrete deck units are used on small span bridges in Queensland usually around 8 to 22 m. For larger span bridges, pre-stressed concrete girders in the form of an I beam are used. These are used for 26 to 32 m spans. The deck is cast in-situ with the girders as shown in Figure 2.11(below).

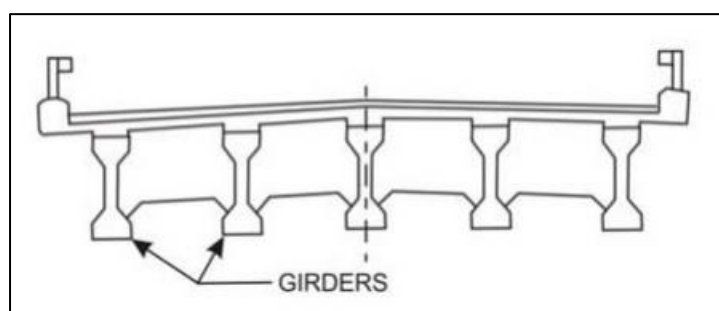


Figure 2.11: Girder (I beam) cast in-situ with deck (DepartmentOfMainRoads, 2006)

Super tee girders are also used for longer spans from 26 to 35 m. The T girders have a void in the centre to reduce weight and are also cast in-situ with the deck as shown in Figure 2.12(below). Pre-stressed concrete box girders are used for even longer spans for up to 260m

in Queensland. The girder usually features one or two rectangular voids. A box girder bridge being constructed is illustrated in Figure 2.13(below).

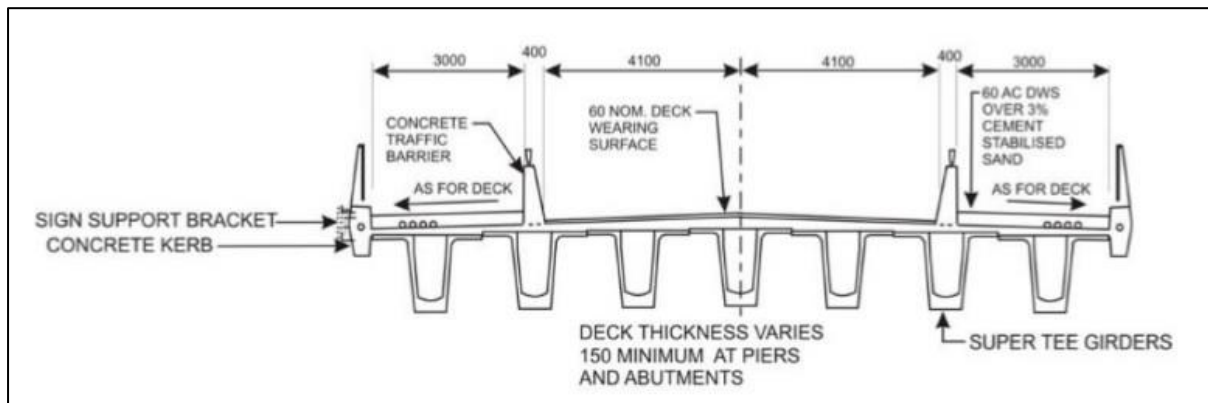


Figure 2.12: Girder (T beam) cast in-situ with deck (DepartmentOfMainRoads, 2006)

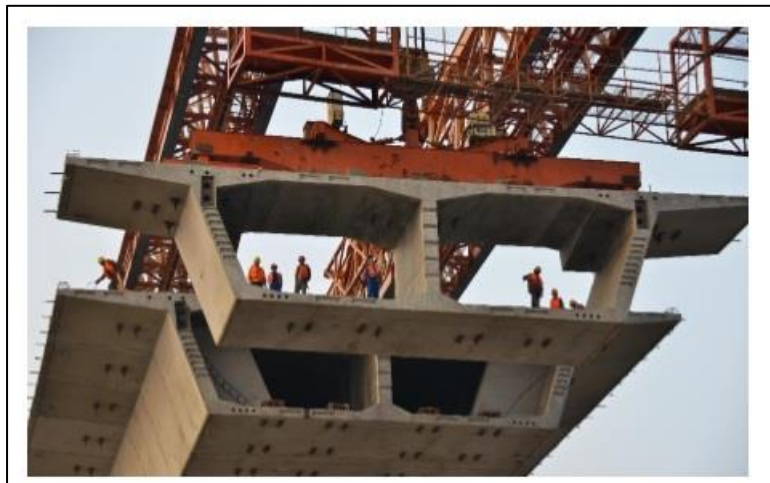


Figure 2.13: Box Girder Bridge under construction (DepartmentOfMainRoads, 2006)

An arch bridge is another form of bridge that can be constructed with concrete. An arch transmits its load to the supports by compression. This makes it ideal for concrete as it is weak in tension (Austroad'92, 1992). Pre-cast segments are usually used for the construction of an arch and during construction they must be supported by false work. False work is used to temporarily support a structure, such as an arch, until the structure is able to support itself.

The last form of concrete bridge is a cable stayed bridge. This type of bridge involves cables supporting the bridge deck from the top of one or two piers as shown in Figure 2.14(below). A cable stayed bridge offers a reduced superstructure depth and mass and has a good level of redundancy due to the ease of replacing a damaged cable. For a single plane of cables, where

the deck is supported by one line of cables down the centre, a pre-stressed concrete box girder is used. If two planes are used, where the cables hold the deck on both sides, then two girders are used to support the deck (Austroad'92, 1992). A cable stayed bridge can have spans up to 600m or more.



Figure 2.14: Example of a cable stayed bridge (Levy, 2011)

#### 2.4.2.4 U-slab bridge

Roads Corporation of Victoria (VicRoads) has identified U-slab bridges as the old and most vulnerable structure during flood loading. This kind of bridges is under maintenance but because of its vulnerability, it is not recommended to be constructed. Figure 2.15(below) shows a typical U-slab bridge section constructed in Victoria

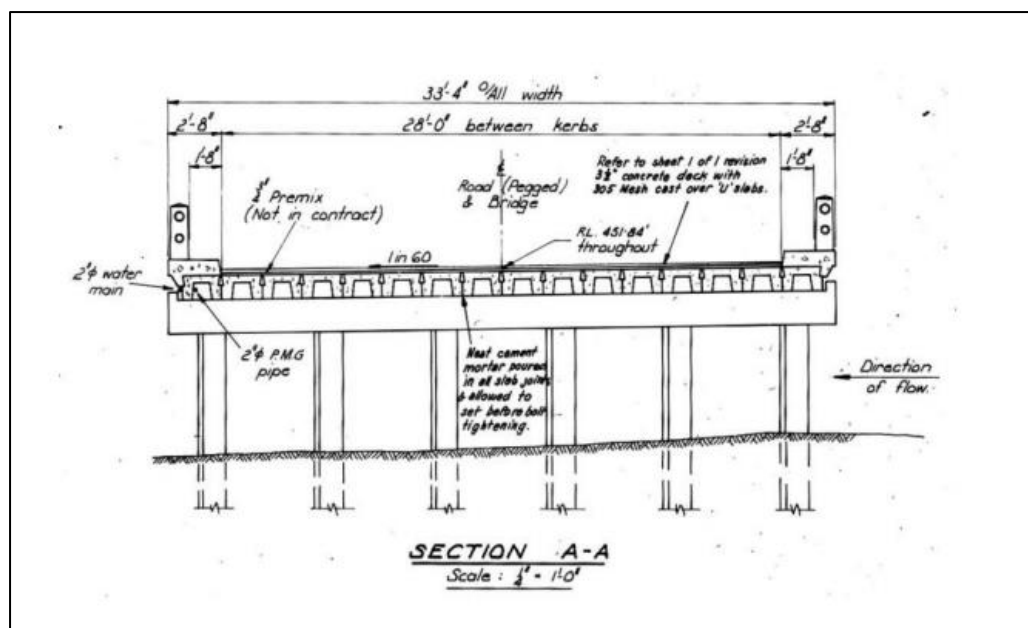


Figure 2.15: A typical U-slab bridge section constructed in Victoria (Nasim et al., 2017)

#### 2.4.2.5 Steel bridges

The common form of a steel bridge is the beam and girder type. Figure 2.16(below) depicts the type of steel girder bridges. The through girder features two girders with the deck supported by cross beams aligned with the bottom of the flange. The deck girder type is similar to the through girder except the cross beams are aligned with the top of the flange on the main girders. The I-beam bridge type consists of several girders that support the bridge deck. They can handle spans up to 20 m. The plate girders are similar to I-beam, although they are larger and can handle spans up to 50m. The trough girders have an open top section and can have spans up to 60 m. Finally the steel box girders are similar to the pre-stressed concrete ones and can have spans up to 80m. All of these girder type bridges have reinforced concrete decks.

Steel bridges can also come in the form of a truss. The earliest type of metallic truss bridge used in Australia was made from wrought iron and the members were manufactured in England and imported to Australia. During the 20th Century steel truss bridges came into construction. A truss was used if a longer span steel bridge was needed. The common

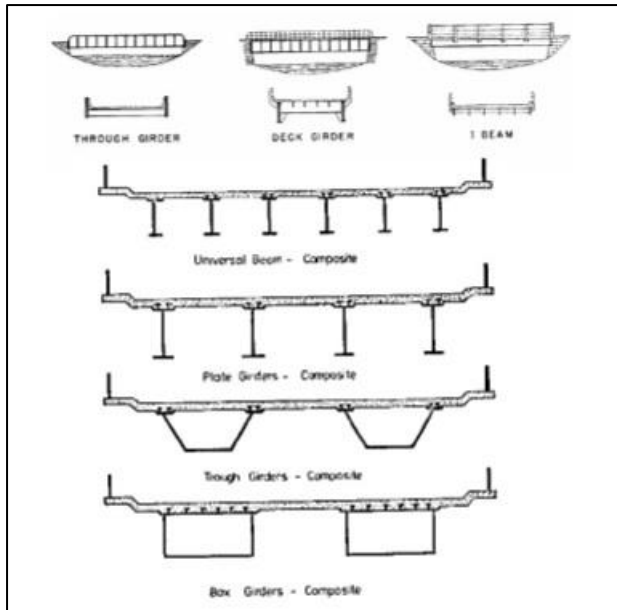


Figure 2.16: Types of steel girder bridges (Austroad'92, 1992)

configurations of a truss bridge are shown in Figure 2.17(below). The members steel members of a truss bridge are connected by pins. In an idealised truss the members are only subjected to axial forces, either compression or tension. A truss bridge doesn't have any member redundancy as the whole structure relies on each member performing. If a member fails then the triangulation of forces is lost (Austroad'92, 1992). Some notable steel truss bridges in Queensland are the Story Bridge in Brisbane and the Burdekin River Bridge pictured in (Figure 2.18(below)) located near Ayr. Steel truss bridges are no longer used in Queensland as there are more economical solutions available (Department of Main Roads, 2006)

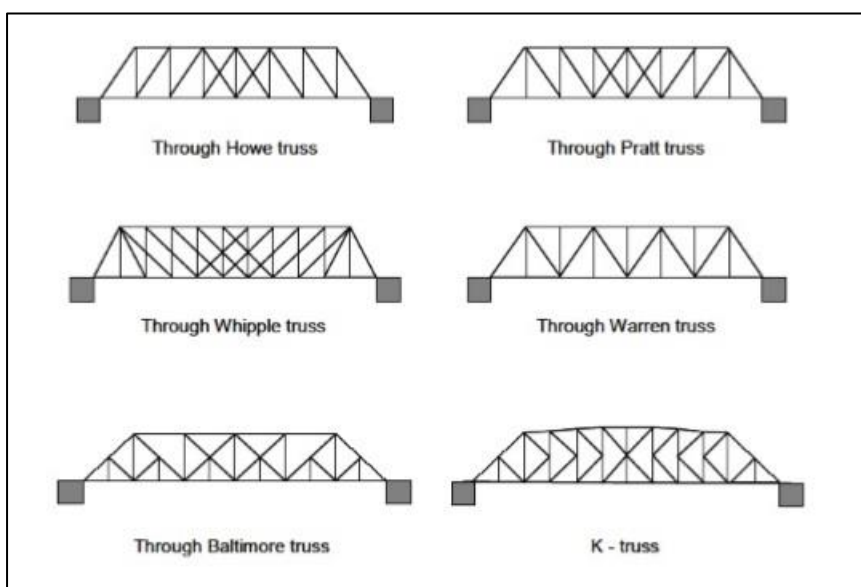


Figure 2.17: Truss Configurations. (Austroad'92, 1992)



Figure 2.18: Burdekin River Bridge, Ayr, Queensland (Burdekin Shire Council, 2012)

A suspension bridge is the last main type of steel bridge. They are not common in Australia as they are only economical for very large spans up to a maximum of 2 km (Department of Main Roads, 2006). The suspension bridge features elements that are only in tension. A suspension bridge works by having two cables suspended between two pylons in a curved shape. The bridge deck is supported by the two cables by vertical hangers that are vertically attached to the main two cables. The main cables are usually anchored to ground at both ends of the bridge (Corus Construction Services & Development, 2007). Westgate is a cable stayed bridge in Melbourne, Australia.

#### **2.4.2.6 Timber bridges**

Timber bridges were the first type of bridge used throughout Australia since early settlements in the middle of the twentieth century. Between 1926 and 1975 Main Roads Queensland built approximately 1300 timber bridges (Eyre et al., 2012). There is only less than 450 timber bridges still in service and have an average age of 60 years. As vehicular loads get higher and the timber bridges start to age they will have to be gradually replaced, except for those that are heritage listed. The most common type of timber bridges in Australia was the girder bridge. Similar to the other types of girder bridges it features longitudinal round timber girders that support the deck. The girders are supported by timber piles or piers. A simple girder bridge used throughout Queensland is shown in Figure 2.19(below). A timber bridge can also be in the form of a truss. This was used when longer spans were required as the girder type was unsuitable as many had been washed away in floods (Austroad'92, 1992). The timber truss was popular in New South Wales in the late 1800s to early 1900s.



Figure 2.19: New Country Creek bridge near Kilcoy, timber girder bridge (Eyre et al., 2012)

### 2.4.3 Design procedure

#### 2.4.3.1 Bridges

Australian standard Australia (2004) measures a 100 year design life for bridges. Therefore, the bridge structure and its elements shall satisfy all limit states during the design life. Limit states are categorised in two categories: 1. Ultimate limit state and 2. Serviceability limit state.

According to Australian standard Australia (2004) the ultimate limit states include the following:

*“(a) Stability limit state, which is the loss of static equilibrium by sliding, overturning or uplift of a part, or the whole of the structure.*

*(b) Strength limit state, which is an elastic, inelastic or buckling state in which the collapse condition is reached at one or more sections of the structure. Plastic or buckling redistribution of actions and resistance shall only be considered if data on the associated deformation characteristics of the structure from theory and tests is available.*

*(c) Failure or deformation of any foundation material causing excessive movement in the structure or failure of significant parts of the structure.*

*(d) Deterioration of strength occurring as a result of corrosion or fatigue, or both, such that the collapse strength of the damaged section is reached. Consideration shall be given to the implications of damage or any other local failure in relation to the available load paths.*

*(e) Brittle fracture failure of one or more sections of the structure of sufficient magnitude such that the structure is unfit for use.”*

Australian standard Australia (2004) defines the **serviceability limit states** to include the following:

*“(a) Deformation of foundation material or a major load-carrying element of sufficient magnitude that the structure has limitation on its use, or is of public concern.*

*(b) Permanent damage due to corrosion, cracking or fatigue, which significantly reduces the structural strength or useful service life of the structure.*

*(c) Vibration leading to structural damage or justifiable public concern.*

*(d) Flooding of the road or railway network, surrounding land and scour damage to the channel bed, banks and embankments.”*

## **2.5 A review of previous research on design of bridges for flood loading**

Apelt (1986) presented a thorough literature review for flood forces on bridges, which essentially pointed out the lack of studies on the subject. Experiments were carried out on two models of a 5-girder bridge with the scales of 1:100 and 1:25. Results of those experiments agreed with previous works, and average drag coefficients of 1.94 and 1.99 were measured when the water surface levels were at the bottom of the girders and on top of the bridge models, respectively.

Wellwood and Fenwick (1990) proposed a drag coefficient of 2.2 as a measure for a safer design of multi-girder bridge structures. Furthermore, a floodwater velocity higher than 2 m/s (6.56 ft. /s) was considered “medium to high.” The authors recommended further research for confirmation of the drag coefficient.

Jempson and Apelt (1992) continued their research with experiments using a 1:25 bridge superstructure model consisting of five Type IV girder, a deck and edge curbs. They recommended a drag coefficient of 2.0 for Type III and Type IV girder bridges and deck unit bridges. Equation 2-13 presents the formula that was used to evaluate the drag coefficient:

$$C_d = \frac{F_d}{0.5\rho V^2 A} \quad \text{Equation 2-13}$$

where,

$C_d$  = Drag coefficient

$F_d$  = Drag force in the direction of flow

$\rho$  Fluid Density

$V$  = Fluid Velocity

$A$  = Projected superstructure area normal to the flow

In 1995, FHWA recommended the use of Equation 2-14 for the calculation of lateral hydrodynamic drag forces for fully or partially submerged bridge superstructures. Recommended drag coefficient values were between 2.0 and 2.2.

$$F_d = c_d \rho H \frac{V^2}{2} \quad \text{Equation 2-14}$$

Where,

$F_d$  = Drag force per unit length of bridge, N/m

$c_d$  = Drag coefficient

$\rho$  = Density of water, 1000kg/m<sup>3</sup>

$H$  = Depth of submerge, m

$V$  = Velocity of flow, m/s

Jempson (2000) did further experiments with six different scaled bridge superstructure models. This yielded design recommendations for loadings on bridge superstructures with improved charts for drag and moment coefficients. The formula expressed in Equation 2-15 was recommended for calculation of moment acting on bridge superstructures, allowing for eccentricity of drag and lift forces. The maximum velocity condition for bridge superstructures was 1.201 m/s.

$$M_{PF} = M_{GS} + F_D \times L_F \quad \text{Equation 2-15}$$

Where,

$M_{PF}$  = Moment generated at the point of fixity, kNm

$M_{GS}$  = Moment generated at the girder soffit, kNm

$F_D$  = Usual drag force, kN

$L_F$  = Length of the lever arm from the point of fixity to the girder soffit, m

Plate experiments were done by NCHRP Parola (2000). A rational model for calculation of forces for complete range of blockage ratios was presented. Using “average contracted flow as reference velocity,” Equation 2-16 was recommended for the calculation of drag force. In this approach, the drag force was the difference between “hydrostatic force” and “water pressure force.”

$$F_D = F_X - F_{hX} \quad \text{Equation 2-16}$$

Where,

$F_D$  = Drag Force, kN

$F_X$  = Water pressure force on the plate in the stream wise direction that is due to stream flow, N

$F_{hX}$  = Hydrostatic force attributed to average stream wise pressure gradients, N

Malavasi and Guadagnini (2003) performed laboratory experiments to quantify hydrodynamic loads on a bridge deck with a rectangular cross-section. They argued that a drag coefficient of 3.40 would be the upper bound limit for bridges where the bridge length (l) to bridge thickness (s) ratio was greater than three. The l/s ratio certainly represented a “minimum” for real scale cases. However, they also concluded that FHWA’s recommended formula (Equation 2-14) generally overestimated the drag forces.

FHWA Kerényi et al. (2009) developed “fitting equations” and design charts for different types of bridges, which were outcomes of physical experimentation and CFD simulation models. The drag coefficient ( $C_D$ ) fitting equation for three and six-girder bridges, lift coefficient ( $C_L$ ) fitting equation for three and six-girder bridges and moment coefficient (CM) fitting equation for all bridge types are provided in Equation 2-17, Equation 2-18 and Equation 2-19:

$$C_D = Ae^{-2(h^*)^2} - Be^{-2(h^*)^2} + a \quad \text{Equation 2-17}$$

$$C_L = b(e^{-2(h^*)^2} - e^{-c(h^*)^{1.7}}) \quad \text{Equation 2-18}$$

$$C_M = d(h^*)^\alpha e^{-f(h^*)^2} + g \quad \text{Equation 2-19}$$

Coefficients A, B, a, b, c, d, f, g and  $\alpha$  for 6-girder and 3-girder bridges were provided as well as the corresponding  $h_{crit}^*$  for each  $C_D, C_L$ , and  $C_M$  value. The report also included the same variables for streamlined bridges “designed to reduce the force load during inundation.”

Results of 6-girder bridge deck analysis showed that a major drop in the drag coefficient for an inundation ratio ( $h^*$ ) of 0.5-0.8. However, as the bridge became more inundated ( $h^* > 1.5$ ), the drag coefficient values were levelled off to around 2. It was also observed that the lift coefficients were all negative, which meant a pull-down force, and they rapidly became more negative as  $h^*$  roughly equalled 0.65. The peak moment coefficient was observed when the bridge was roughly halfway inundated. Results of the 3-girder bridge deck analysis were somehow similar to the 6-girder bridge deck analysis results. However, the approach velocities ranged from 0.25 m/s to 0.50 m/s. Critical drag coefficients 2.15, 1.95 and  $\sim 1.1$  were recommended for 6-girder, 3-girder and streamlined bridges, respectively (Kerenyi et al., 2009). The 6-girder bridge model developed in this study was used by Azadbakht and Yim (2014).

Chen et al. (2009a) made a hydrodynamic investigation of a bridge collapse during Hurricane Katrina by two numerical models for US-90 Highway bridge across Biloxi Bay, Mississippi. It was concluded that “the bridge failure was caused by the wind waves accompanied by the storm surge generated by Hurricane Katrina.” It was also found that bridge decks with lower low chord elevation (i.e. bottom of girder elevation) than the critical elevation were subjected to “fatal wave impact.” This study demonstrated the importance of the height of a bridge with respect to acting hydrodynamic effects during a weather related event.

Guo (2010) investigated hydraulic forces on bridge decks. A well-written literature review was also a part of their report and significance of hydrodynamic loading generated by floodwater flow was emphasized, mentioning that it might cause overturning of the bridge deck and a possible failure of the superstructure. Their study was concerned with CFD and

reduced scale experiments. The minimum drag coefficient (found to be 0.5-0.8) was found to occur “perhaps” as the water reached the top of girders which was a transition to overtopping of the bridge deck.

FEMA Jones (2001) recommended the use of Equation 2-20 for the calculation of lateral hydrodynamic drag forces for all flow velocities:

$$F_{\text{dyn}} = \frac{1}{2} C_d \rho V^2 A \quad \text{Equation 2-20}$$

Where,

$F_{\text{dyn}}$  = Horizontal drag force (lb) acting at the still water mid-depth (halfway between the still water elevation and the eroded ground surface)

$C_d$  = Drag Coefficient

$\rho$  = Mass density of fluid

$V$  = Velocity of water

$A$  = Surface area of obstruction normal to flow ( $ft^2$ )

For Equation 2-20, mass density was assumed as 1.94 slugs/ft<sup>3</sup> for fresh water and 1.99 slugs/ft<sup>3</sup> for saltwater. Recommended values for drag coefficient were 2.0 for square/rectangular piles and 1.2 for round piles. For other types of piles or “obstructions,” FEMA recommended a range of drag coefficients (Jones, 2001)

Lwin et al. (2013) demonstrated how the performance of observed bridges was affected due to storm surge, wind, and debris and barges. The study looked into wave forces on bridge decks, followed by a recommendation for estimation method and countermeasures to restore the functionality of transportation systems. They recommended estimated wave-induced vertical and horizontal load components, as given in Equation 2-21 through Equation 2-24:

$$F_v = C_{v-va} F_v^* \quad \text{Equation 2-21}$$

$$F_h = [1 + C_r(N - 1)] c_{h-va} F_h^* \quad \text{Equation 2-22}$$

$$F_v^* = \gamma(\Delta Z_h)A_h \quad \text{Equation 2-23}$$

$$F_h^* = \gamma(\Delta Z_h)A_h \quad \text{Equation 2-24}$$

Where,

$F_v$  = Estimated vertical wave-induced load component (uplift)

$C_{v-va}$  = Empirical coefficient for the vertical varying load

$F_v^*$  = Reference vertical load

$F_h$  = Estimated horizontal wave-induced load component (lateral)

$C_r$  = Reduction coefficient for horizontal load from the blockage by the leading external girders.

$N$  = Number of girders supporting the bridge span deck

$c_{h-va}$  = Empirical coefficient for horizontal varying load

$F_h^*$  = Reference horizontal load

$\gamma$  = Unit weight of water (10078 N/m<sup>3</sup> for salt water)

$\Delta Z_v$  = Difference between the elevation of the crest of the maximum wave and the elevation of the underside of the bridge deck

$A_v$  = Area of the bridge contributing to vertical uplift, i.e., the projection of the bridge deck onto horizontal plane

$\Delta Z_h$  = Difference between the elevation of the crest of the maximum wave and the elevation of the centroid of  $A_h$

$A_h$  = Area of the projection of the bridge deck onto the vertical plane

Based on their study, Lwin et al. (2013) recommended a  $C_r$  value of 0.4. Despite the fact that their study is conservative and simple to apply, their approach was recommended for the estimation of wave loads on elevated bridges decks as “interim guidance.”

Yim et al. (2014) pointed out that even though many bridges survived the 2011 Great East Japan Earthquake, many of them were completely destroyed by the tsunami. According to Yim et al. (2014) this was purely an indicator of the fact that seismic design codes do not necessarily embrace the loads generated by tsunami waves. They further concluded that even though it is normally not applicable to tsunamis due to their “much longer time and length scales,” they were still able to compare their study results (i.e. horizontal drag force) with the American Association of State Highway and Transportation Officials (AASHTO, 2012) formula (Equation 2-25), since their tsunami model was relatively steady:

$$F_{HC} = C_d A \left( \frac{\rho_w}{2} \right) \frac{U_c^2}{1000} \quad \text{Equation 2-25}$$

Where,

$F_{HC}$  = Horizontal drag force

$C_d$  = Drag coefficient (taken as 2.5)

$A$  = Projected area of superstructure per unit length

$U_c$  = Current speed

Azadbakht and Yim (2014) thoroughly reviewed the literature and estimated tsunami loads on bridges. They conducted experimental and numerical techniques for five bridges in two different scenarios: (i) initial impact and overtopping, and (ii) full inundation. They used a 6-girder bridge model to assess wave impacts. They developed formulas for maximum horizontal force, downward maximum force and maximum uplift force, as given in Equation 2-26, Equation 2-27 and Equation 2-28:

$$\begin{aligned} F_{H_{max}} &= F_{h_{hs}} + F_d \\ &= 0.5\rho g(2h_0 - L_h)L_h + 0.5C_d\rho V^2L_h \end{aligned} \quad \text{Equation 2-26}$$

$$\begin{aligned} F_{DV_{max}} &= C_{DV} (F_{v_{hs}} + F_{v_s}) \\ &= C_{DV} [\rho g(h_0 - L_g - T_d)L_v + 0.5C_{v_s}\rho V^2L_{sb}] \end{aligned} \quad \text{Equation 2-27}$$

$$\begin{aligned} F_{UP} &= C_{UP}(F_b + F_l) \\ &= C_{UP}(\rho g V + 0.5 C_1 \rho V^2 L_v) \end{aligned} \quad \text{Equation 2-28}$$

Where,

$F_{H_{max}}$  = Maximum horizontal force

$F_{h_{hs}}$  = Hydrostatic horizontal force

$F_d$  = Drag force

$\rho$  = Density of water

$g$  = Acceleration of gravity

$h_0$  = Difference between the tsunami water free-surface elevation and low chord of the bridge

$L_h$  = Height of the bridge superstructure

$C_d$  = Drag coefficient

$V$  = Tsunami flow velocity

$F_{DV_{max}}$  = Downward vertical force

$C_{DV}$  = Empirical downward vertical force coefficient

$F_{v_{hs}}$  = Hydrostatic downward vertical force

$F_{v_s}$  = Slamming vertical force

$L_g$  = Height of the bridge girder

$T_d$  = Thickness of the bridge deck

$L_v$  = Width of the bridge superstructure

$C_{v_s}$  = Slamming coefficient in the vertical direction

$L_{sb}$  = Effective length of the bridge deck for a vertical slamming;  $4.L_b$

$F_{UP_{max}}$  = Maximum uplift force

$C_{UP}$  = Empirical uplift force

$F_b$  = Buoyancy force

$F_l$  = Lift force

$V$  = Volume of the bridge per unit length

$C_l$  = Lift coefficient

## 2.6 Bridge collapse under natural hazards

Throughout history, bridge collapses due to various reasons are reported. This section classifies the main reasons for bridge collapse into two broad categories, namely, natural factors and human factors. Since this research assesses bridge failure under flood which is a natural hazard, only the literatures pertaining to natural factors are described in detail. According to an investigation by Wardhana and Hadipriono (2003) during the period between 1989 and 2000, a total of 503 bridge collapses were reported in the United States with the distribution of causes of these bridge collapses shown in Figure 2.20(below). From Figure 2.20, it can be observed that flood and scour together account for nearly half of the bridge collapses.

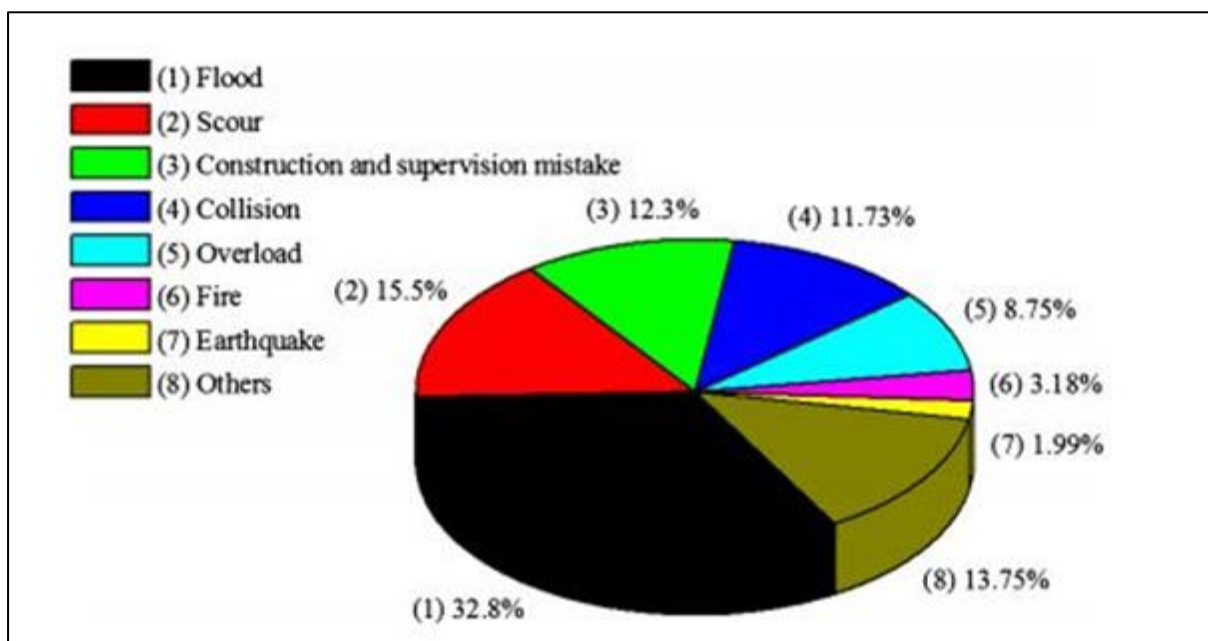


Figure 2.20: Distribution of causes of the 503 reported bridge collapses in US (Wardhana and Hadipriono, 2003)

### 2.6.1 Natural factors

Natural disasters, e.g., flood, scour, earthquake, landslide, debris flow, hurricane, and typhoon, are often unavoidable and can cause serious damages to bridges. The mechanisms of action on bridge structures by different natural factors vary significantly and are summarized in the following sections.

#### 2.6.1.1 Flood

Heavy precipitation usually leads to flooding, which may induce phenomena such as scour, erosion, river convergence, insufficient embedment depth, protection works-induced overfall or hydraulic jump, softened bedrock, sand mining, debris impact or abrasion on bridge foundations, etc. [(Witzany et al., 2008);(Hong et al., 2011);(Wang et al., 2014)]. One or a combination of these causes can result in dramatic reductions in the strength and stability of bridge key components and can even cause bridge failures, as shown in Figure 2.21(below).



Figure 2.21: Collapse of the Schoharie Creek Bridge due to flood in 1987 (reprinted from USGS 2012)

#### **2.6.1.2 Scour**

Scour is a phenomenon in which the level of the riverbed becomes lower under the effect of water erosion, leading to the exposure of bridge foundations (AASHTO, 1998). With an increase in scour depth, the lateral resistance of the soil supporting the foundation is significantly reduced, thus increasing the lateral deflection of the foundation head (Daniels et al., 2007);(Lin et al., 2010). Furthermore, when the critical scour depth is reached, bending buckling of the foundation may occur under the combined effect of the dead load of bridge superstructures and the traffic load (Walton et al., 1982); (Hughes et al., 2007).

#### **2.6.1.3 Earthquake**

Earthquakes lead to vertical and horizontal ground motions that can result in the failure of bridge substructures (Yang et al., 2015); (Wang et al., 2014). The vertical ground motion causes significant fluctuating axial forces in bridge columns or piers, which may induce outward buckling or crushing of the columns or piers (Kunnath et al., 2008);(Kim et al., 2010). Moreover, the vertical ground motion can result in significant amplification of the bending moment at the bridge mid-span, which may lead to the bending failure of the bridge deck (Veletzos et al., 2006); (Kunnath et al., 2008). Unlike the vertical ground motion, the horizontal ground motion mainly contributes to the shear failure of bridge columns or piers Priestley et al. (1994); Sun et al. (2012). In addition, both the vertical and horizontal ground motions may cause the liquefaction of the soil at the bridge foundations, which can greatly reduce the load-carrying capacity of the foundations and even directly lead to bridge collapse (Hashimoto and Chouw, 2003); (Wang et al., 2014).

#### **2.6.1.4 Landslide**

The occurrence of a landslide is mainly due to water saturation, earthquake, or volcanic eruption, and it may result in the downward and outward movement of slope-forming materials including rock, soil, artificial fill, or a combination of these materials (Iverson, 2000);(Varnes, 1984). These moving slope-forming materials, when hitting the bridge, will lead to severe damage or even collapse of the bridge, as shown in Figure 2.22(below).



Figure 2.22: Collapse of a bridge due to landslide (image courtesy of (Zhong et al., 2013))

#### **2.6.1.5 Debris flow**

A debris flow is usually translated from a landslide when water is incorporated into the landslide debris as it is jostled and remoulded during the downslope movement. Remoulding and incorporation of water reduce the strength of the debris and make it behave like a fluid, causing it to flow rather than slide (Hampton, 1972); (Takahashi, 1978). A debris flow exerts tremendous impact forces on the obstacles in its way, especially when large stones are transported. Moreover, a growing debris flow has severely erosive effects. Therefore, when a large-scale debris flow passes the site of a bridge, the damage to the bridge could be devastating (Takahashi, 1978).

#### **2.6.1.6 Hurricane and typhoon**

Hurricanes and typhoons are tropical cyclones that refer to low pressure systems that generally form in the tropics. They travel with wind waves accompanied by storm surges, which raise the water level to an elevation that is able to strike the superstructure of bridges along the coast. Bridge decks may be knocked off the pile caps by the impulsive vertical and horizontal forces generated by the storm waves riding on high surges (Robertson et al., 2007);

(Chen et al., 2009b), as illustrated in Figure 2.23(below). Moreover, after making their landfall, hurricanes usually lead to heavy rainfalls and cause a series of subsequent disasters such as flood, landside, and debris flow (Hong et al., 2011); (Wang et al., 2014).



Figure 2.23: Bridge collapsed under Typhoon

## **2.7 Collapse mechanisms of bridges/failure modes**

In this section, the collapse mechanisms of a few common bridge types, namely, beam bridges, arch bridges, steel truss bridges, and flexible long-span bridges are reviewed. Failure modes are presented under different hazard types which included them.

### **2.7.1 Flood and scour**

Flood and scour account for nearly half of all bridge failures (Wardhana and Hadipriono, 2003). Bridge scour generally includes four main types, namely, local scour, contraction scour, general scour, and channel migration, and can be seriously exacerbated by flood. Based on a review of the failure of 36 bridges, Lin et al. (2010) observed that the failure modes of bridges caused by bridge scour can be categorized into four main types: vertical failure, lateral failure, torsional failure, and bridge deck failure. Vertical failure of bridges caused by scour could be attributed to a combination of factors such as inadequate soil support and pile instability and can be generalized into four categories: inadequate bearing capacity of shallow foundations, penetration of friction piles, undermining of pile toes, and pile buckling, as illustrated in Figure 2.24(below) (Lin et al., 2010). Lateral failure usually

occurs in one of the following forms: pushover failure of piers, formation of structural hinges in piles, kick out failure of foundations, and excessive lateral movement of piers or foundations. Torsional failure refers to the failure of structures or structural components attacked by skewed flows. Bridge deck failure, usually in the form of deck unseating, may occur when the flood-induced external force is sufficiently large to overcome the gravity force of the bridge deck and the restraint forces from the support.



Figure 2.24: Scouring around a bridge foundation (Lin et al., 2010)

### 2.7.2 Earthquake

Ground shaking and rupture, which are the main effects created by earthquakes, can have significant impacts on the stability and safety of infrastructure, including bridges. Much research has been conducted to investigate the seismic-induced failures of beam bridges and the results showed that bridge decks, bearings, and supports (including abutments, piles, and columns) are the most vulnerable parts of bridges under the effect of earthquakes. The decks of simply-supported bridges, either single-span or multi-span, can fall off or slide away from the abutments or columns due to large horizontal ground movements [(Siddharthan et al., 1997); (Saadeghvaziri and Yazdani-Motlagh, 2008); (He et al., 2012)]. The horizontal ground movement can also lead to impact between adjacent spans and between the end-span and the abutment, which may result in the following problems for simply-supported bridges: failure of rocker bearings in the form of toppling (Nielson and DesRoches, 2006), shear failure of the steel bearings (Pan et al., 2010), and failure of abutment back walls [(DesRoches et al., 2004); (Saadeghvaziri and Yazdani-Motlagh, 2008)].

### 2.7.3 Hurricane

Coastal bridges are prone to attack by hurricanes (Okeil and Cai, 2008). The performance of coastal bridges under hurricanes has drawn increasing attention after the collapse of a large number of bridges during the last decades. Deck unseating (Fig. 5) has been found to be the predominant failure mode for simply-supported multi-span coastal bridges without supplemental restraints (such as shear keys) during hurricane events (Padgett et al., 2008); (Chen et al., 2009b); (Ataei and Padgett, 2012). Deck unseating could result once the uplift force from the wave and air trapped underneath the bridge deck overcomes the gravity load of the bridge deck and the restraint forces from the supports are not sufficient to resist the lateral wave forces. Padgett et al. (2008) also pointed out that the impact of barges, oil drilling platforms, tug boats, and other types of debris could also result in damage in the form of span misalignment and damages in fascia girders, fenders, and piles. Another failure mode for bridges during hurricanes is scour damage, including scour and erosion of abutments, slope failure, and undermining of approach spans.

Based on the observed failure modes of bridges due to hurricanes, it is obvious that the connections between the bridge deck and piles or abutments play an important role in standing hurricane induced wave loads, and that they should therefore be reinforced for bridges built in hurricane-prone zones (Xu and Cai, 2014).

Table 2-4: Most Common Cause for Collapse of Different Types of Bridges.

| <b>Types of bridge</b>    | <b>Most vulnerable causes</b>                    |
|---------------------------|--|
| Beam bridge               | Flood, scour, earthquake, collision, overloading |
| Masonry arch bridge       | Flood, scour, overloading, earthquake            |
| Steel arch bridge         | Overloading, wind                                |
| Steel truss bridge        | Overloading, fatigue                             |
| Flexible long-span bridge | Wind   |

### 2.7.4 Summary of failure mechanism

Different types of bridges are vulnerable and sensitive to different causes, which have been summarized in Table 2-4(above) (Deng et al., 2015).

The failure modes of beam bridges mainly include (1) bridge deck misalignment and falling off the abutments or columns due to inadequate support length of bridge decks or weak connections with supports; (2) bridge deck failure in the form of shear, crushing, and flexural failures; (3) bearings dysfunction in the form of shear failure or toppling; (4) pier and column failures in the form of shear, crushing, and erosion; and (5) progressive collapse due to unbalanced forces resulting from the loss of supports.

## 2.8 Australian bridges subjected to extreme flood events

In the latest extreme flood events, in 2013 and 2011, a significant number of bridges were harmed because of flood hazard. Bridge infrastructure in Lockyer Valley suffered significant damage from these flooding. One particular bridge that sustained damage in 2011 is Kapernicks Bridge which is located on Flagstone Creek Road near Helidon. The bridge has 3 × 20m spans which consist of four I-girders cast in-situ with the deck (Murray and Kemp, 2011). The bridge is illustrated in Figure 2.25(below) where the water level of Lockyer Creek is rising. Half an hour later the bridge is fully submerged by floodwaters as shown in Figure 2.26(below)



Figure 2.25: Kapernicks Bridge before water rise (Murray and Kemp, 2011)



Figure 2.26: Kapernicks Bridge after water rise (Murray and Kemp, 2011)

According to Murray and Kemp (2011) this bridge was overtopped by 2 m of water and had a debris mat along the full length of the bridge to a depth of 3 m. The bridge suffered scour to the abutments and lost the approach embankment on one side, and it also had significant cracking on two girders on the superstructure due to log impact. The washed away approach is shown in Figure 2.27(below) and the cracking in the girder is shown in Figure 2.28(below).



Figure 2.27: Damage to Kapernicks Bridge (Approach washed away) (Murray and Kemp, 2011)



Figure 2.28: Damage to Kapernicks Bridge (Cracking in girder) (Murray and Kemp, 2011)

Several other bridges were damaged in the Lockyer Valley in these flood events. A washed away abutment on the Gatton-Esk Road Bridge over the Lockyer Creek is shown in Figure 2.29(below). The Geoff Fisher Bridge, located near Fernvale and crosses the Brisbane River, was subjected to scour around its piers and the foundation piles were exposed as illustrated in Figure 2.30(below). Two timber bridges also required replacement after these flood events (Pritchard, 2013).



Figure 2.29: Abutment washed away on Gatton-Esk Road bridge (Ezeajugh, 2014)



Figure 2.30: Scour around pier and exposed piles on Geoff Fisher Bridge (Ezeajugh, 2014)

## 2.9 Vulnerability modelling of bridges

### 2.9.1 Definition of Resilience/Vulnerability

There are many definitions reported in the literature for resilience. It can be defined as the ability to return to normal functionality following an extreme event making sure that the damage is tolerable and affordable [(Hudson et al., 2012);(Lamond and Proverbs, 2009)] . It can also be defined as the ability of a system to reduce the chances of a shock, to absorb a shock if it occurs and to recover quickly after a shock (Cimellaro et al., 2010). According to their definitions a resilient system should have the following qualities:

- Low probability of failure
- Even if it fails, very low impact on the society in terms of loss of lives, damage and negative economic and social consequences
- Low recovery time

Figure 2.31 (a) shows the functionality of an infrastructure with time. At time  $T_0$ , the system was fully functioning [ $F(T_0, r_0)$ ] when the extreme event occurred. Functionality was reduced to  $F(T_0, r_d)$  due to the damage to the infrastructure system. At time  $T_R$ , the system completely recovered and started functioning as it was at time  $T_0$ . By considering the above qualities for a resilient system, it can be concluded that if the functionality due to damage is not much and/or if the recovery time is less, then the system is more resilient. Therefore if the area shown in Figure 2.31 (b) is less, the system is more resilient.

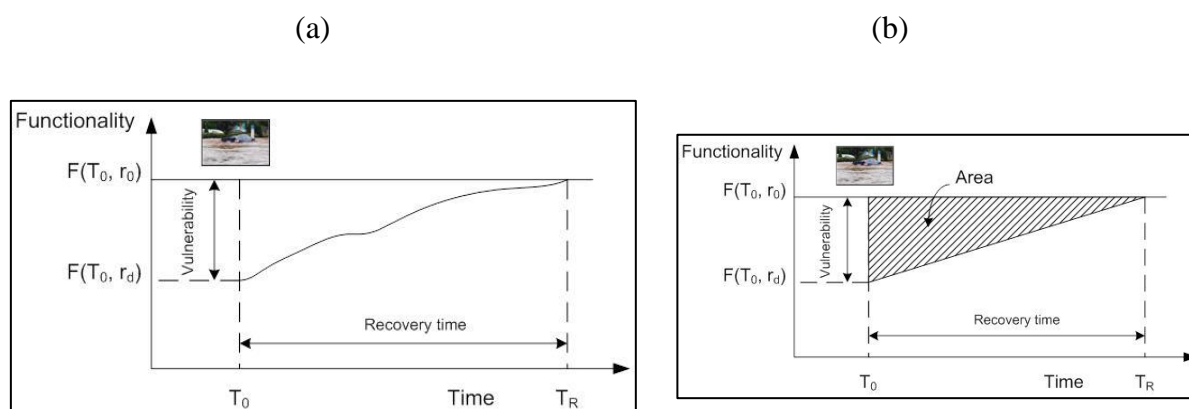


Figure 2.31: Representation of resilience and vulnerability

Where:

$r$  = functionality of a given system

$r_o$  = original functionality of the system before hazard

$r_d$  = reduced functionality of the system after hazard

$T_o$  = Initial time

$T_R$  = Recovery time

Delivering resilience is a cycle of identification, assessment, addressing and reviewing (Hudson et al., 2012). Evaluating or re-evaluating resilience can be related to the aftermath of an event, a near miss, or event affecting a similar infrastructure elsewhere.

### **2.9.2 Vulnerability Assessment**

The purpose of vulnerability assessment is to provide emergency-agencies and associated individuals, appropriate information for preparing better mitigation strategies from a long-term perspective. It is also very important for them to facilitate their activities regarding the use of temporary methods/tools for mitigating the impact in time and the responses (i.e., evacuation, search and rescue, protecting infrastructure, etc.) during the occurrence of floods. Therefore, the vulnerability assessment should provide the level of vulnerability for each infrastructure based on the varied timeline (long-term and just before/during/after) of the flood. For example, prediction of the level of vulnerability of an infrastructure as a flood develops, enables authorities to be proactive against the flood to mitigate the potential damage that the infrastructure may cause.

However, measuring the level of vulnerability is complicated due to unpredictability of flood events and the characteristics of infrastructure. During a flood, critical infrastructure such as levees and bridges are likely to be affected in the primary impact stage. Whereas, in the secondary stage, other adjacent (or indirectly inter-related) infrastructure will be affected by the damaged infrastructure as well as the flood water (Oh et al., 2010).

Thus, the level of vulnerability will vary according to the impact stages and the type of infrastructure. For determining the level of vulnerability, two types of information are important: probability of failure (or inundation) of each component (critical infrastructure, associated industries, and communities) due to a flood; and the extent of potential damage to them. It is noticeable that the probabilities of failure of the infrastructure are linked (or chained). For example, the probability of inundation of a road near a levee section depends on the probability of overflowing of the levee section. That is, if the probability of levee failure increases, then, the probability of failure of the road also increases. This conditional probability indicates the probable state of a variable that is dependent on the state of another variable.

A structure is vulnerable if relatively small damage leads to a disproportionately large consequence (Agarwal et al., 2003). Structural vulnerability assessment techniques could be divided into two categories: deterministic and probabilistic methods. Agarwal et al. (2003) proposed a deterministic vulnerability theory based on the concepts of structural form and connectivity. In practice, uncertainties of loading and structural parameters do exist and are unavoidable.

Probabilistic methods have been commonly used to assess vulnerability of structures under natural hazards such as earthquake, hurricanes and flood. In 2001, the Joint Committee on Structural Safety (JCSS) identified the reliability based assessment of existing structures as a topic of major importance (Diamantidis, 2001). Choices of desired levels of reliability for various types of structures have also been assessed and reported by the (JCSS) Faber and Sørensen (2002).

Ellingwood and Dusenberry (2005) suggested that the capability of a structure to withstand damage without collapse could be assessed using structural reliability and the probability-based method. Chen and Lui (2005) defined vulnerability as the probability of having a specific level of damage given a specific level of hazard. Elnashai et al. (2004) used deformation-based functions to assess the vulnerability of transportation structures under seismic effects. The vulnerability functions for reinforced concrete bridges were derived analytically using earthquake records and inelastic dynamic analysis techniques. Lee and Rosowsky (2006) considered the snow load effect in a seismic fragility analysis and performed multiple performance-based design for wood-frame structures. Probabilistic risk

assessment methods were also developed by Li and Ellingwood (2006) to evaluate the performance and reliability of low-rise light-frame wood residential structures under hurricanes.

## 2.10 Quantifying damage to bridges under flood for decision making

In the last decade, researchers have investigated various different indicators for damage identification. Initial studies for damage detection focused on the use of natural frequencies and/or mode shapes as the vibration signature parameters (Alampalli et al., 1997). Zimmerman and Kaouk (1994) published a paper whose indicator of damage is based on changes in stiffness. Estimates of downtime and repair cost are important factors for loss modelling of natural hazard events (Alampalli et al., 1997). As indicated by Comerio (2006), documentation of empirical data regarding repair and recovery along with associated costs is essential to refine loss models to assess the consequences and impacts of natural hazard events to communities and regions.

Blong (2003) used a damage index expressed as an equivalent number of houses (HE) totally destroyed in any natural hazard. For a major city severely damaged in an earthquake, damage might reach  $10^6$  HE (1 million House Equivalents). Such large numbers make comparisons different. It is also recognised that informed estimates have been multiplied by approximations in arriving at HE values. Here the number of HE is converted to a Damage Index by taking  $\log_2$  HE.  $\log_2$  HE provides a convenient range of values.

For example,

$$\log_2 32 \text{ HE} = 5,$$

$$\log_2 1,024 \text{ HE} = 10,$$

$$\log_2 1,048,576 \text{ HE} = 20$$

$$\text{The Damage Index for } 20 \text{ HE} = \log_{10} 20 / \log_{10} 2 = 4.32.$$

Thus the Damage Index,  $DI = 4.3$ .

Whitman and Biggs (1974), Whitman (1972), Whitman et al. (1973) developed a method for seismic damage assessment of buildings. The severity of ground motions is represented by the MMI scale, and seismic damage is expressed by the ratio of the cost of repair to the replacement cost of a building (damage ratio).

Blume (1977) proposed the spectral matrix method for potential damage assessment of a building or a group of buildings. A Ground motion characteristic is represented by the velocity response spectrum, and the structural capacity is expressed by the base shear at yielding. The spectral velocity corresponding to the base shear is then calculated. The overall damage is expressed by the ratio of cost of repair to the total replacement cost, which is crudely related to the ductility factor.

Bertero and Bresler (1977) attempted to give a more complete definition of damage, by defining local damageability, global damageability, and cumulative damageability. Local damageability is a measure of damage of the constituent components, expressed as a ratio of the maximum response to the ultimate deformation capacity. Global damageability is a measure of building damage defined as the sum of the local damages, weighted by an appropriate importance factor. Cumulative damageability is a measure of the overall damage as the result of previously sustained damage. Based on these definitions, Blejwas and Bresler (1979) proposed a method of damageability evaluation using a quasi-static structural analysis method. In applying this method to actual buildings, two critical quantities, namely, the ultimate deformation capacity of components and the appropriate importance factors should be specified. The use of relevant experimental data for the former and the appropriate engineering judgment for the latter were suggested.

As suggested in many of the foregoing studies, structural damage may be defined as a ratio of "demand," i. e., the response under earthquakes, to the ultimate structural capacity" Numerous studies have been made for obtaining the "demand" using dynamic response analysis; an extensive literature survey is available in (Umemura and Takizawa, 1982). On the other hand, the determination of the "capacity" is more limited in spite of its critical importance in damage assessment.

Gosain et al. (1977) proposed the "work index" as a measure of energy absorbing capacity of reinforced concrete components subjected to cyclic loadings. The incremental damage in

each cycle is expressed as a function of the ductility ratio, peak load, axial load, and the shear span ratio. Banon et al. (1980) proposed a more sophisticated damage model in which damage is represented by a two-dimensional failure surface of the total absorbed energy and the damage ratio defined by Lybas (1977)

## **2.11 Fragility analysis of bridges**

Defined as the relationship between hazard intensity and the probability that a bridge is damaged exceeding a certain level, bridge fragility curves have been widely used to express the structural vulnerability of a bridge subject to a variety of natural hazards. However, previous studies have mainly focused on the fragility curve derivation for bridges under earthquakes. For example, Basoz et al. (1999) and Shinozuka et al. (2000) developed empirical fragility curves using a data set of bridge damages resulting from the 1994 Northridge earthquake and the 1995 Kobe earthquake, respectively. Alternatively, Karim and Yamazaki (2001) generated analytical fragility curves of the highway bridge piers utilizing a numerical simulation based on the 1995 Kobe earthquake data.

Choi et al. (2004) modelled a type of bridge built in the central and south eastern United States to produce analytical fragility curves for identifying vulnerabilities under an earthquake. In addition, Yang et al. (2015) presented the analytical fragility curves of six bridge types such as multi-span simply supported concrete and steel bridges, multi-span continuous concrete and steel bridges, and single-span concrete and steel bridges.

Seo et al. (2016) proposed a method for fragility curve derivation considering unknown truck characteristics, to quantify the structural integrity of in-service highway bridges. In these studies, a wide variety of seismic fragility curves of bridges were obtained either empirically or analytically, and the results were used to assess the structural integrity of bridges under earthquakes. In comparison with seismic fragility analysis, fragility analysis related to floods has received less attention.

Decò and Frangopol (2011) generated the fragility curves of highway bridges under multiple hazards including earthquake, scour, traffic load, and environmental attack. With a similar

approach, Dong et al. (2013) derived seismic fragility curves of bridges considering the effects of scour and corrosion. In addition, Dawson et al. (2005) assessed the flood risk vulnerability of a fluvial dike system, and Witzany and Cejka (2007) performed a numerical analysis of flood fragility of a stone vault bridge structure. However, these studies mainly focused on the derivation of seismic fragility curves, while flood-related risk factors such as scour and corrosion were considered as an alternative cause of bridge failure in addition to earthquakes. As such, there have been few studies on the flood fragility estimation of bridges. However, various flood-related factors such as water stream pressure, debris accumulation, corrosion, and scour are reported as the most common causes of bridge failure. Wardhana and Hadipriono (2003), Cook (2014). In reality, a flood often generates a rapid water flow with accumulated debris, which yields a combined loading impact on bridges via the service loads and may bring about structural damage or collapse. Furthermore, if the structural integrity of a bridge is significantly degraded by the corrosion of steel reinforcements in addition to the scour-induced removal of soil resistances, the failure risk of bridges under flood events increases and their failure modes can become more complex.

## **2.12 Chapter summary**

Design standards around the world have considered flood loading on bridges differently. Three main bridge design standards have been studied in this research. In general, every design standards consider same types of forces on bridges resulting from water flow. However they give different definitions and corresponding equations to calculate these forces. The primary types of flood related forces are drag and lift forces on bridge piers and superstructures, debris forces and log impact force.

Researchers have used a series of laboratory based prototype models to quantify the hydrodynamic forces exerted on to the different components of the bridge. They arrived at formulating equations, graphs and tables to calculate the relevant coefficients and the flood related forces on the bridge.

There are many ways that a bridge could be damaged in an extreme flood event. Approaches of a bridge could be damaged due to debris impact, settlement or depressions. Debris against substructure and superstructure, bank erosion and damage to scour protection will damage the waterways. Movement of abutments, wing walls, piers, rotation of piers and missing, damaged dislodged or poorly seating of the bearings are the major reasons for substructure

failure. Superstructure could be damaged due to the debris on deck, rotation of deck, dipping of deck over piers or damage of girders. Due to any of these reasons, the members of a bridge could be damaged and bridge may not be completely functional.

Different indicators or indices for damage identification or damage quantification have been used by researchers in the literatures. Some researchers have used changes in natural frequency or changes in stiffness to define the damage indices. Structural damage index, as a ratio of demand to ultimate structural capacity; Cost based damage index, as a ratio of repair cost to the replacement cost; and "work index" as a measure of energy absorbing capacity of reinforced concrete components subjected to cyclic loadings are some of the other methods to measure the damages to infrastructure under natural hazard.

Vulnerability assessment is necessary to provide emergency agencies appropriate information for providing better mitigation strategies. Level of vulnerability varies according to the impact stages and the type of infrastructure. Probability of failure of each component of a structure under a hazard and the extent of potential damage to them is required to assess the level of vulnerability.

Fragility curves have been widely used to express the structural vulnerability of a bridge subject to a variety of natural hazards. However, these studies mainly focused on the derivation of seismic fragility curves, while flood-related risk factors such as scour and corrosion were considered as an alternative cause of bridge failure in addition to earthquakes.

The comprehensive literature review indicated that significant research have been carried out on studying the vulnerability of building infrastructure under the influence of certain natural hazards such as earthquake, hurricane etc. However, little or no literature have been reported on quantifying vulnerability of road infrastructure under flood hazard which would subsequently help develop damage stat for bridge structures. The damage state then could be used by Emergency Management to assess evacuation routes, traffic access for response and time to reopening the bridge after flood hazard. Comprehensive research program presented in this thesis addresses this gap in knowledge.



### 3 Research Methodology

This chapter presents the research methodology used to deliver the research outcomes. The research questions and the approach used to address the questions are explained in detail.

A detailed literature survey has been undertaken to understand contributing factors for various failure modes and failure mechanisms of bridge structures exposed to extreme flood events around the globe. The contributing factors such as flood velocity, type of debris etc. for causing damages to a particular bridge or its geographical location may not be the same. Pritchard (2013) identified that urban debris such as cars; containers etc. and the insufficient bridge span to through that debris were the main cause for damaging bridges in the aftermath of 2011/2012 extreme flood events in Queensland. These findings lead to a question what failure mechanisms and contributing factors should be incorporated in the bridge design codes of practices to enable the bridges to be resilient during an extreme flood event.

The comprehensive review of literature identified the gaps in knowledge as

- Lack of a comprehensive methodology for vulnerability modelling of bridges under flood loads
- An analysis which includes the variability of flood loading and materials is not available
- A method to define the damage index to establish the level of damage to a structure under flood loading is not available. For example, in earth quake resistant design, Peak Ground Acceleration (PGA) is used as a base.

In this chapter, the research methodology adopted to address these gaps in knowledge is presented. Research questions used to develop the research program is presented here.

### 3.1 Research questions and the methodology

In order to address the gaps in knowledge identified above and considering the review of literature, following research questions were developed.

1. What are the typical failure modes of bridges during a flood event?
2. What are the causes of these observed failures?
3. How can a girder bridge be modelled to include flood loading?
4. What is the relationship between flood velocity, flood level and other input parameters [ $M^*$ (flood induced bending moment), deck displacement, scour, damage indices etc.] on failure of bridges?
5. How can the damage to bridges under flood be captured for decision making?

The challenge of the research presented here was that it combined a qualitative and a quantitative approach to address a complex problem.

First, the possible failure modes of the bridges had to be identified using real life data to establish the major areas to focus on. This was a qualitative part of the work, which was mainly based on data collected from a selected case study area. Once the failure modes were established, a preliminary analysis was required to understand the method of calculating the combinations of conditions contributing to failure.

Subsequently a numerical modelling approach was required to quantify the probability of failure of a selected cohort of bridges using a variable flood load determined from historical data.

Subsequent sections describe the research methodology which comprise of analysis of case studies, numerical modelling using a deterministic approach and numerical modelling using a probabilistic approach.

### 3.2 Analysis of case studies

Case study research is one of several forms of research methods adopted in literature. Others include experimental research, surveys, numerical modelling, and archival analyses such as economics or statistical modelling (Yin, 2013). This research began with the analysis of case

studies of bridges exposed to the 2011/12 extreme flood events in Queensland. There were 47 damaged bridges reported in the bridge inspection report sourced through Lockyer Valley Regional Council in Queensland. Each bridge in the report had necessary in depth details together with photographs taken in different angles enabling identification of the types of damage sustained. Failure mechanism of each bridge and the major failure mechanism of the groups of bridges were then established. These are further elaborated in Chapter 4.

The damage to the bridge is quantified using a damage index that is defined as the ratio of the flood induced bending moment ( $M^*$ ) to the existing moment capacity ( $\phi M_u$ ). Most common types of bridge (Concrete Girder Bridge) that collapsed due to one of the common established major failure mechanisms was chosen to be numerically modelled using ABAQUS finite element software. Flood impact loading on to the bridge girder from the AS 5100 bridge design code (Australia, 2004) and flood loading from the literature (Jempson, 2000) and past data were used to determine the loads applied on the structure. The other input parameters such as the support boundary conditions, material properties etc. were also identified. Upon the modelling and computational output, the maximum minor axis bending moment induced by the flood impact lateral loading on to the girder ( $M^*$ ) were derived.

Using the as built drawings of the selected case study bridges that included all detailed reinforcement arrangement to the girder, the minor axis bending moment capacity ( $\phi M_u$ ) was calculated with the use of an excel sheet. The neutral axis depth of the girder cross section was first established at the section where the total compressive and tensile forces add up to zero. The required bending moment was then calculated with respect to this neutral axis.

Sensitivity of the bridge to different flood exposure conditions such as flood velocity was done followed by deriving relevant vulnerability curves.

A second method of quantifying bridge damage using cost based damage index (Nishijima and Faber, 2009) is then introduced. Damage Index in this case is defined as the ratio of the repair cost of the bridge to its replacement cost.

The methods so devised above are validated using observed failure modes and the literature (Jempson, 2000). Finally these vulnerability curves and the flood past data are used for decision making to enhance the resilience of bridges

The overall research methodology is illustrated through a flow chart given in Figure 3.1.

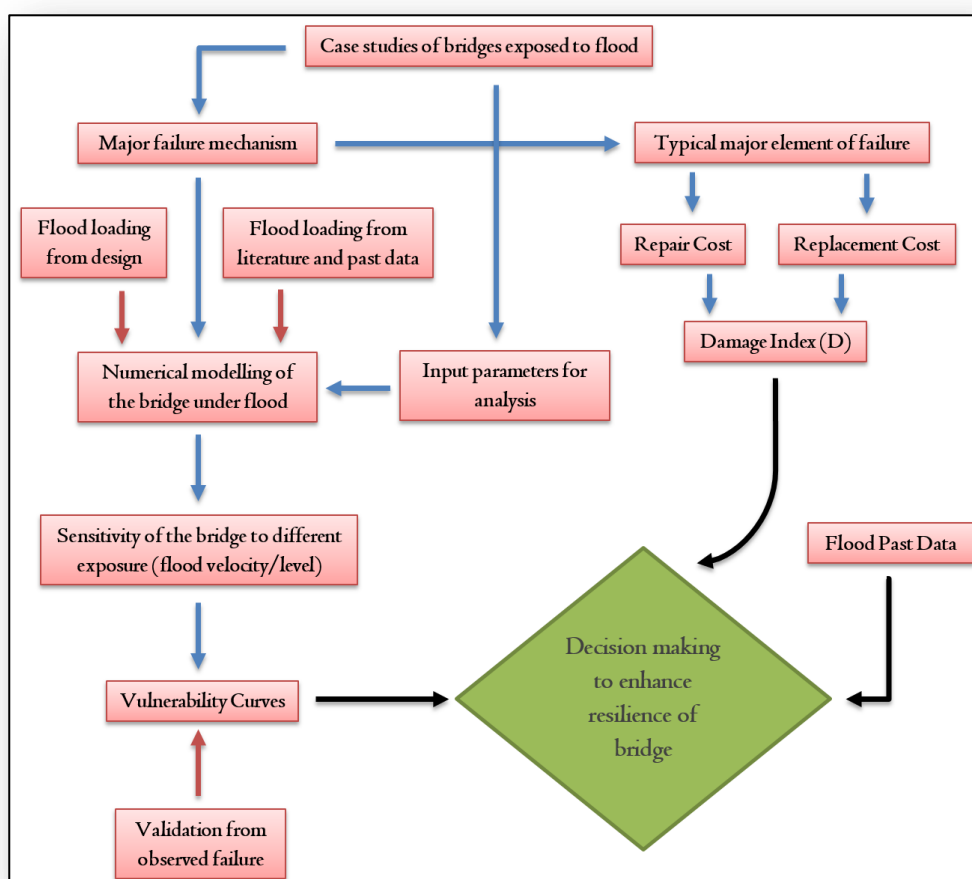


Figure 3.1: Research Methodology

2011/12 extreme flood events in Queensland (van den Honert and McAneney, 2011b) have been studied in detail in this research. Lockyer Valley Regional Council (LVRC) provided a comprehensive bridge inspection report to facilitate this research. There were total of 47 bridges inspected at level 1 that included the photographs of each bridge in the aftermath of this flood event. The data base contained physical parameters of the bridges such as length, width, span, age, location, elevation, bridge materials, roadway classification and average daily traffic. These information are summarized in Table 3-1(below)

Table 3-1: Summary of case study bridge details.

| Bridge Name                    | Type         | Deck       | Length | Width | Construction Date | Av Daily traffic | Road Type       | Longitude | Latitude | Elevation(m) | Possible Codes used for design |
|--------------------------------|--------------|------------|--------|-------|-------------------|------------------|-----------------|-----------|----------|--------------|--------------------------------|
| Evans Bridge                   | Timber       | Timber     | 6.3    | 3.7   | 19540101          | 10               | Rural Access    | 152.4935  | -27.5466 | 76           |                                |
| Weigels Crossing               | Box Culverts | Bitumen    | 44.6   | 7.5   | 19980101          | 220              | Rural Collector | 152.4585  | -27.5832 | 100          | NAASARA                        |
| Knopkes Crossing               | Box Culverts | Bitumen    | 8.1    | 3.4   | 19890101          | 198              | Rural Collector | 152.4485  | -27.6056 | 122          | NAASARA                        |
| Magarrigal Bridge              | Timber       | Unsurfaced | 11.3   | 3.7   | 18991230          | 30               | Rural Access    | 152.3644  | -27.6932 | 128          | NAASARA                        |
| Mcgrath Pedestrian Bridge      | Concrete     | Asphalt    | 42.3   | 3.7   | 19840101          | 0                | Rural Access    | 152.3637  | -27.7294 | 141          | NAASARA                        |
| Clarke Bridge                  | Timber       | PPLNK      | 6.1    | 7.4   | 19640101          | 100              | Rural Access    | 152.3731  | -27.7984 | 172          |                                |
| Maincamp creek                 | Box Culverts | Asphalt    | 23.5   | 4.9   | 20010101          | 40               | Rural Access    | 152.3573  | -27.8146 | 195          | 92 AUSTRROADS                  |
| Peters Bridge                  | Steel        | Asphalt    | 13.1   | 3.3   | 18991230          | 30               | Rural Access    | 152.3697  | -27.7757 | 185          |                                |
| Moon Bridge                    | Box Culverts | Concrete   | 24.3   | 8.2   | 19990101          | 70               | Rural Access    | 152.3244  | -27.6497 | 131          | 92 AUSTRROADS                  |
| Dotd Road Bridge               | Concrete     | Bitumen    | 20.1   | 4.1   | 20040101          | 100              | Rural Access    | 152.3496  | -27.5838 | 92           | AS5100                         |
| Whitehouse                     | Box Culverts | Unsurfaced | 11.8   | 3.6   | 19920101          | 10               | Rural Access    | 152.384   | -27.6124 | 97           | 92 AUSTRROADS                  |
| Old Laidley Forest Hill        | Box Culverts | Bitumen    | 13.1   | 8.6   | 19890101          | 1123             | Rural Arterial  | 152.5889  | -27.3727 | 150          | NAASARA                        |
| Crowley vale road              | Box Culverts | Bitumen    | 16.4   | 6.4   | 19890101          | 385              | Rural Arterial  | 152.3653  | -27.5562 | 82           | NAASARA                        |
| Lester Bridge                  | Box Culverts | Bitumen    | 16.5   | 9.8   | 20050101          | 200              | Rural Collector | 152.3899  | -27.4857 | 78           | AS5100                         |
| Main green swamp               | Box Culverts | Bitumen    | 15.3   | 6.7   | 19840101          | 412              | Rural Collector | 152.3693  | -27.4627 | 99           | NAASARA                        |
| Steinke's Bridge               | Concrete     | Asphalt    | 60     | 8.4   | 20091001          | 389              | Rural Collector | 152.3706  | -27.532  | 84           | AS5100                         |
| Quin Bridge                    | Concrete     | Bitumen    | 20.5   | 6     | 19890101          | 544              | Rural Collector | 152.4     | -27.5361 | 78           | NAASARA                        |
| Middletons Bridge              | Timber       | Bitumen    | 20.9   | 5.6   | 19640101          | 309              | Rural Collector | 152.4594  | -27.469  | 69           |                                |
| Narda Lagoon Suspension Bridge | Timber       | Unsurfaced | 85.5   | 1.6   | 19640101          | 0                |                 | 152.391   | -27.391  | 82           |                                |
| Daveys Bridge                  | Concrete     | Bitumen    | 21.6   | 4.1   | 19720101          | 1444             | Rural Collector | 152.2764  | -27.5525 | 99           |                                |
| Belford Bridge                 | Concrete     | Bitumen    | 17     | 7.3   | 19890101          | 1453             | Urban Arterial  | 152.2832  | -27.5448 | 98           | NAASARA                        |
| Liftn Bridge                   | Concrete     | Bitumen    | 20.7   | 4     | 19900101          | 5                |                 | 152.2722  | -27.5646 | 106          | NAASARA                        |
| Thistlethwaite Bridge          | Timber       | Bitumen    | 37.5   | 7     | 19570101          | 958              | Rural Arterial  | 152.2047  | -27.5835 | 116          |                                |
| Avs Bridge                     | Box Culverts | Bitumen    | 16.4   | 7.8   | 19970101          | 170              | Rural Collector | 152.1901  | -27.6246 | 134          | 92 AUSTRROADS                  |
| Logan Bridge                   | Concrete     | Bitumen    | 64.2   | 8     | 20040101          | 1161             | Rural Arterial  | 152.2145  | -27.6333 | 132          | AS5100                         |
| Frankie Steinhardt's Bridge    | Concrete     | Asphalt    | 42     | 9.6   | 20100701          | 247              | Rural Access    | 152.2374  | -27.5916 | 114          | AS5100                         |
| Robeck Bridge                  | Box Culverts | Concrete   | 10     | 9.2   | 20000101          | 150              | Rural Collector | 152.2513  | -27.6297 | 136          | AS5100                         |
| Clarke Bridge                  | Concrete     | PPLNK      | 19     | 7.4   | 19900101          | 2560             | Urban Arterial  | 152.2521  | -27.5878 | 109          | NAASARA                        |
| Hoger Bridge                   | Timber       | Bitumen    | 9.5    | 3.6   | 20000101          | 24               | Rural Access    | 152.2591  | -27.6577 | 161          | AS5100                         |
| Colouhoun Bridge               | Concrete     | Asphalt    | 15     | 5     | 20101101          | 30               | Rural Access    | 152.2502  | -27.6047 | 122          | AS5100                         |
| Sheep Station Bridge           | Timber       | Bitumen    | 15.3   | 4.5   | 19700101          | 230              | Urban Collector | 152.1227  | -27.5486 | 139          |                                |
| Mahon Bridge                   | Concrete     | Asphalt    | 36     | 8.4   | 20090801          | 189              | Rural Collector | 152.1473  | -27.5772 | 127          | AS5100                         |
| Hughes Bridge                  | Box Culverts | Concrete   | 8.9    | 7.8   | 20000101          | 554              | Urban Arterial  | 152.041   | -27.5818 | 303          | AS5100                         |
| Kapernicks Bridge              | Concrete     | CSLAB      | 66.1   | 7.6   | 19810101          | 729              | Rural Arterial  | 152.1408  | -27.5725 | 126          | NAASARA                        |
| Duncan Bridge                  | Concrete     | Bitumen    | 36.9   | 5.9   | 19650101          | 294              | Rural Arterial  | 152.1125  | -27.62   | 168          |                                |
| Murphy Bridge                  | Concrete     | Bitumen    | 36.6   | 3.4   | 19900101          | 191              | Rural Collector | 152.1227  | -27.5624 | 129          | NAASRA                         |
| Granny Williams Bridge         | Box Culverts | Bitumen    | 8.4    | 8.9   | 19900101          | 191              | Rural Collector | 152.1204  | -27.5743 | 141          | NAASRA                         |
| Evans Bridge                   | Box Culverts | Bitumen    | 6.1    | 6.8   | 20000101          | 85               | Rural Collector | 152.1022  | -27.0339 | 418          | AS5100                         |
| Cran Bridge                    | Timber       | Timber     | 8      | 3.6   | 19800101          | 119              | Rural Arterial  | 152.0646  | -27.634  | 207          | NAASRA                         |
| The Willows Bridge             | Concrete     | Asphalt    | 15     | 5     | 20101101          | 121              | Rural Collector | 152.0808  | -27.5072 | 162          | AS5100                         |
| The Dairy Bridge               | Concrete     | Concrete   | 22.1   | 5     | 20050101          | 77               | Rural Arterial  | 152.0732  | -27.4645 | 228          | AS5100                         |
| Kirsop Bridge                  | Concrete     | Concrete   | 12.1   | 4.8   | 18991230          | 422              | Rural Access    | 151.9791  | -27.4688 | 410          |                                |
| Greer Bridge                   | Concrete     | Concrete   | 36.8   | 8.4   | 20070101          | 1193             | Rural Arterial  | 152.0964  | -27.5457 | 155          | AS5100                         |
| Connole Bridge                 | Timber       | Bitumen    | 27.4   | 6.5   | 19800101          | 1193             | Rural Arterial  | 152.0686  | -27.5332 | 179          | NAASRA                         |
| McGraths Bridge                | Concrete     | Concrete   | 40     | 8     | 20090101          | 290              | Rural Collector | 152.3636  | -27.7292 | 140          | AS5100                         |
| Forestry Road Bridge           | Timber       | Timber     | 7.8    | 5.1   | 19660101          | 0                | Rural Collector | 152.263   | -27.4687 | 145          |                                |

In answering the first research question, a comprehensive analysis of the case studies of the failure of bridges in the Lockyer Valley Region was undertaken. This analysis enabled the identification of major failure mechanism of bridge structure. This was complimented by the literature review (Jempson, 2000) as well. Major failure mechanisms were identified and the scope of the research was defined.

### 3.3 Numerical modeling of the selected structures. (Deterministic)

The objective of this stage of research was to understand the effect of different types of flood loading on the bridge structure mentioned in AS5100 bridge design code (Australia, 2004) and understand the failure of the structure. Forces due to water flow, debris and log impacts are the main force that a bridge experiences under a flood event (Australia, 2004). It is noted that AS5100 (2017) has just been released and there are no major changes related to calculation of flood loading between AS 5100 (2004) and AS 5100(2017).

At this stage, the challenges in identifying the provision of as- built drawings were established and structural analysis process of a girder bridge under flood loading was established.

The process was validated using one case study of failure of a girder bridge. The main failure mode examined is the bending under minor axis.

Tenthill Creek bridge structure has been selected for the modelling in this research.

Since the first stage of any numerical modelling starts with some necessary input parameters, the following information in relation to the selected bridge structure has been gathered.

- As built Structural Drawing
- Concrete and Steel Material Properties
- Flood Loading as per AS 5100 bridge design standard.
- Flood intensity measure

### **3.3.1 As built Structural Drawing of the Tenthill Creek Bridge**

The first step in any numerical modelling is to input the structural part or component geometrically according to its actual dimensions followed by modelling the rest of the components such as rebar, support bearings etc. This information was obtained from the as built drawings of the Tenthill Creek Bridge.

### **3.3.2 Concrete and Steel Material Properties**

The model used for the compressive strength of concrete was the concrete damaged plasticity (CDP) model proposed in the paper (Carreira and Chu, 1985). The CDP model was chosen in the finite element software ABAQUS. The concrete damaged plasticity model is capable of carrying out the static and dynamic analysis of RC members with bars embedded. The model includes isotropic material, which accounts for tensile cracking and the compressive crushing modes. The response of concrete to uniaxial tension and uniaxial compression is shown in

Figure 3.2(below). For the CDP model, the default values of the dilation angle, eccentricity,  $f_{b0}/f_{c0}$ , K and viscosity parameter were used as 35, 0.1, 1.16, 0.667 and 0.01, respectively. The mechanical properties of concrete are summarized in Table 3-2, while the input constitutive relations and the damage parameters as a function of the compressive and tensile strengths are shown in Figure 3.3, Figure 3.4, Figure 3.5 and Figure 3.6

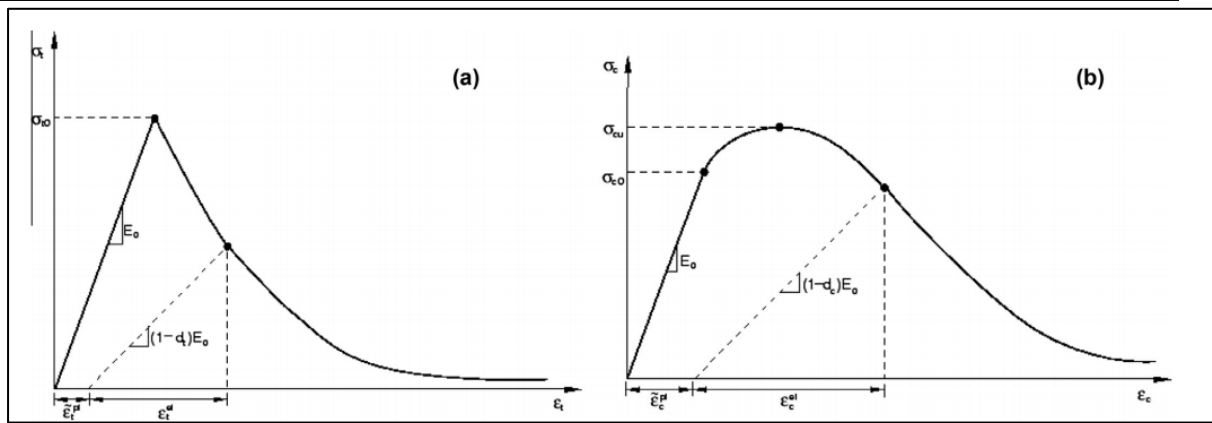


Figure 3.2: Response of concrete to uniaxial loading in tension (a) and compression (b). (Hanif et al., 2016)

Table 3-2: Mechanical properties of concrete (Hanif et al., 2016)

| Density<br>Tonne/mm <sup>3</sup> | $f_{cu}$<br>MPa | $f_{ct}$<br>MPa | $E_c$<br>MPa | $\nu$<br>- |
|----------------------------------|-----------------|-----------------|--------------|------------|
| 2.4E-9                           | 36.5            | 3.65            | 26957.85     | 0.15       |

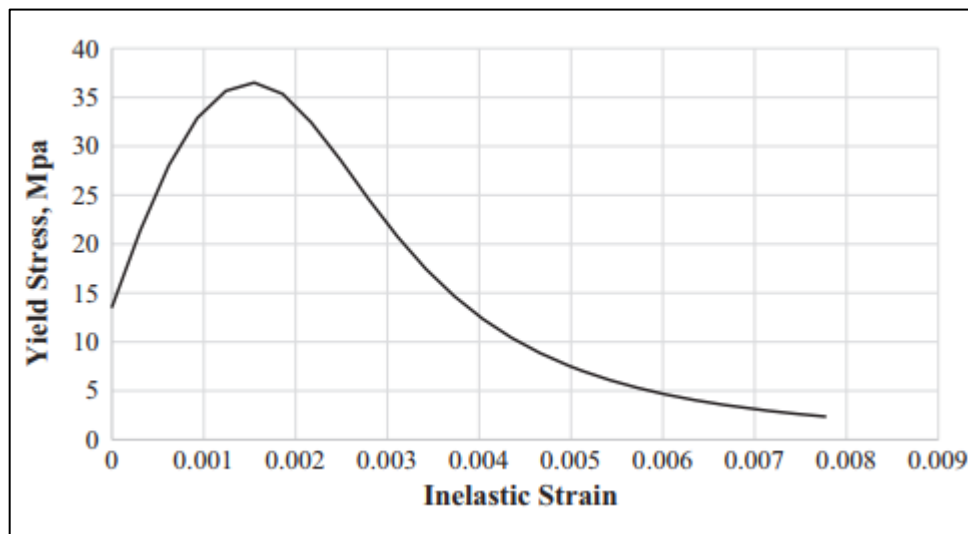


Figure 3.3: Compressive yield stress vs inelastic strain (Hanif et al., 2016)

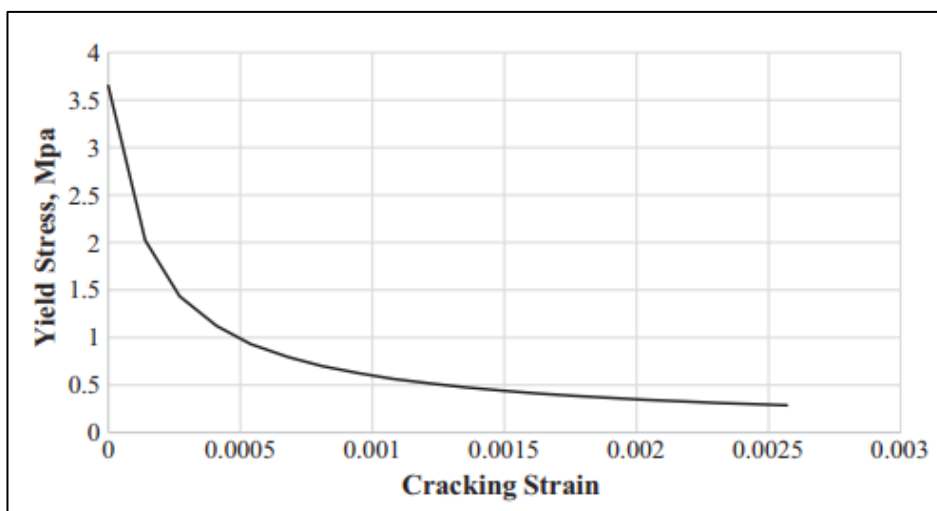


Figure 3.4: Concrete tensile softening model, yield stress vs cracking strain (Hanif et al., 2016).

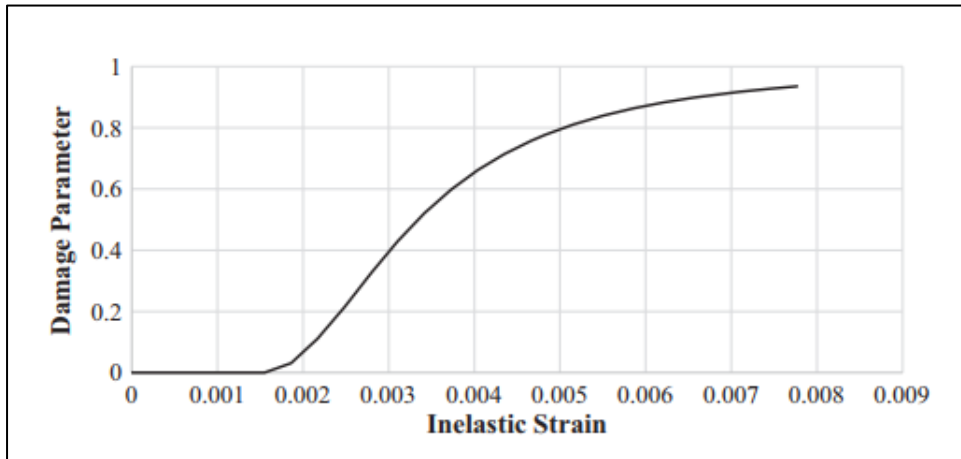


Figure 3.5: Damage parameter vs inelastic strain (Hanif et al., 2016)

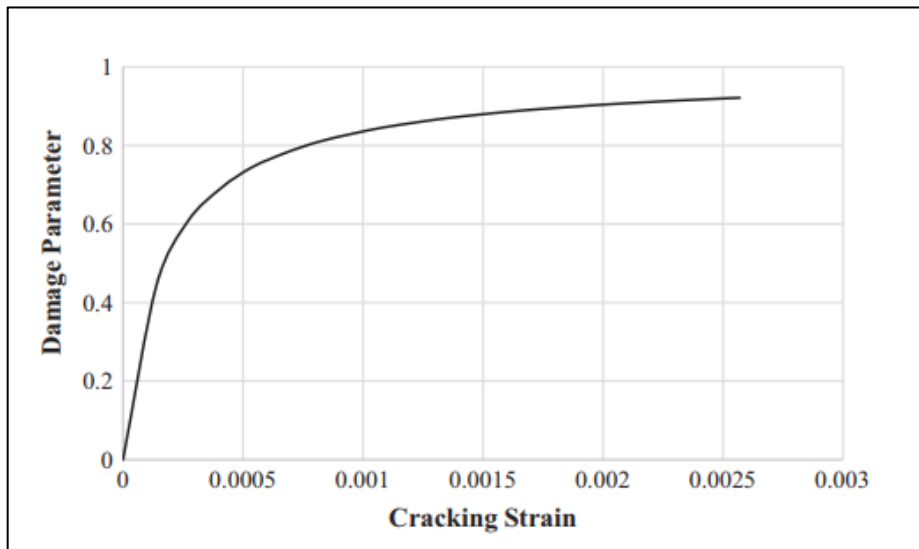


Figure 3.6: Damage parameter vs cracking strain (Hanif et al., 2016)

### Element types

This section describes the types of elements used in the ABAQUS model for the concrete girder bridge configuration and the steel reinforcement. There are various types of elements available from the [Abaqus/CAE User's - Abaqus/CAE User's Guide \(6.14\)](#). Some of the widely used element types are given in Figure 3.7, Figure 3.8, Figure 3.9. Many researchers have used ABAQUS Eight-node brick elements to model the solid concrete elements and 2-node linear beam element to model the reinforcement bars for most of the concrete structures such as beams, columns, slabs etc. [(Greg Rogencamp, 2012); (Weena.L and Sujeeva, 2013); (van den Honert and McAneney, 2011a); (QueenslandGovernment, 2013)]. With respect to this research, the concrete has been modelled using Eight-node brick element with reduced integration (C3D8R and F3D8R) whereas the steel reinforcement has been modelled using 2-node linear beam element (B31).

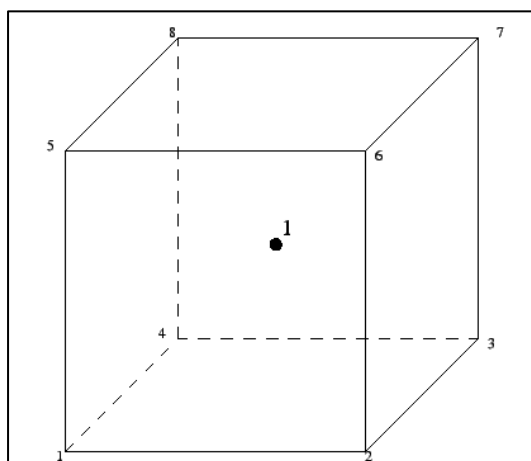


Figure 3.7: Eight-node element with reduced integration (C3D8R and F3D8R)(ABAQUS 6.14)

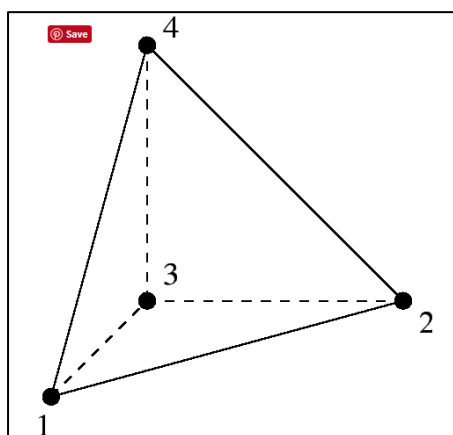


Figure 3.8: Four-node tetrahedral element (C3D4 and F3D4)(ABAQUS 6.14)

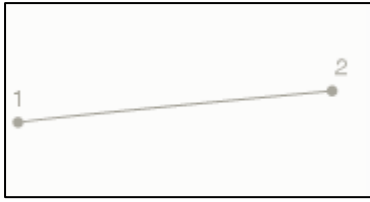


Figure 3.9: 2-node linear beam element (B31) (ABAQUS 6.14)

### Non-linear analysis.

The analysis of case study bridges exhibited severe damage and some large tensile cracks due to heavy flood impact loading exerted. This indicated that the structure could have exceeded the elastic limit in the stress- strain curve of the concrete materials and attained to the plastic or nonlinear region in the diagram. Hence, a nonlinear analysis in the software is necessary.

In nonlinear analysis, the total load applied to a finite element model is divided into a series of load increments called “load steps”. When the solution is completed at each increment, the stiffness matrix of the model is updated to reflect nonlinear changes in structural stiffness before proceeding to the next load increment. The ABAQUS program uses Newton-Raphson equilibrium iterations for adjusting the model stiffness. The Newton-Raphson iterative method provides convergence at the end of each load increment within the specified tolerance limits. Figure 3.10(below) shows the use of the Newton-Raphson approach in a single degree of freedom nonlinear analysis. It assesses the out-of-balance load vector, which is the difference between the restoring forces (the loads corresponding to the element stresses) and the applied loads, prior to each solution. Subsequently, the program performs a linear solution, using the out-of balance loads, and checks the convergence. If the convergence criteria are not satisfied, the out-of-balance load vector is re-evaluated, the stiffness matrix is adjusted, and a new solution is accomplished. This iterative procedure continues until the problem converges.

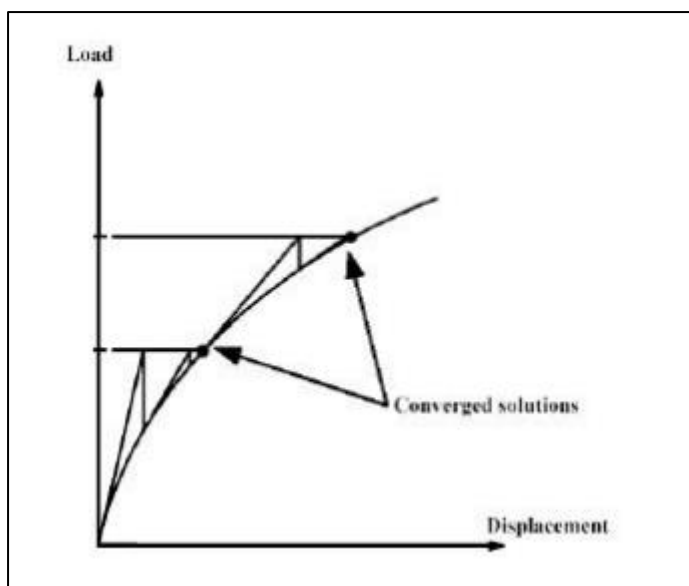


Figure 3.10: Newton-Raphson iteration in 2 load increments (ABAQUS 6.14)

In the ABAQUS program for the nonlinear analysis, automatic time stepping predicts and controls the load step sizes. If the convergence behaviour based on the former solution history and the physics of the models is smooth, automatic time stepping will increase the load increment up to a selected maximum load step size. Also, if the convergence behaviour is not smooth enough, automatic time stepping will reduce the load increment until it is equal to a selected minimum load step size. For the automatic time stepping, the maximum and minimum load step sizes are required.

The nominal steel rebar areas; nominal steel yield strength of 400 MPa for longitudinal reinforcement and 240 MPa for shear reinforcement and nominal concrete compressive strength of 20 MPa were used in the analysis

### 3.3.3 Flood Loading as per AS 5100 bridge design standard

As explained in Chapter 2, forces resulting from water flow given in AS 5100 has been fed to ABAQUS software as a static force exerted on to the bridge girder. Even though there was a provision to model the structure using CFD (Computational Fluid Dynamic) version of the ABAQUS software, this method was not used at this stage.

### 3.3.4 Flood Intensity Measure

Flood velocity has been the random variable parameter that is required to calculate various types of flood induced loading on a bridge structure such as drag force, lift force, debris force, log impact force etc. Flood velocity for a given river basin may vary depending on its

location and the river profile. The actual flood velocity can be calculated given that the river discharge, river profile and the depth of flood are known from the Equation 3-1

$$\text{Velocity}(V) = \frac{\text{Discharge}(Q)}{\text{River cross section area } (A)} \quad \text{Equation 3-1}$$

Water Monitoring Information Portal of Queensland Government has provided data for stream water level, stream discharge, profile of stream cross section etc. for various streams and creeks in Brisbane Basin. Figure 3.11(below) indicates the River profile of Lockyer Creek at Helidon Number 3 which is the closest monitoring station of the case study bridge in this research. An Excel formula was devised for calculating cross sectional area of the river for different stream water level. Corresponding flood velocity was then calculated using stream discharge and the river cross section area. It should be noted here that in the case of pipe flow, the velocity at the different points in the cross section would have changed. In this case, we have considered the average velocity of the stream.



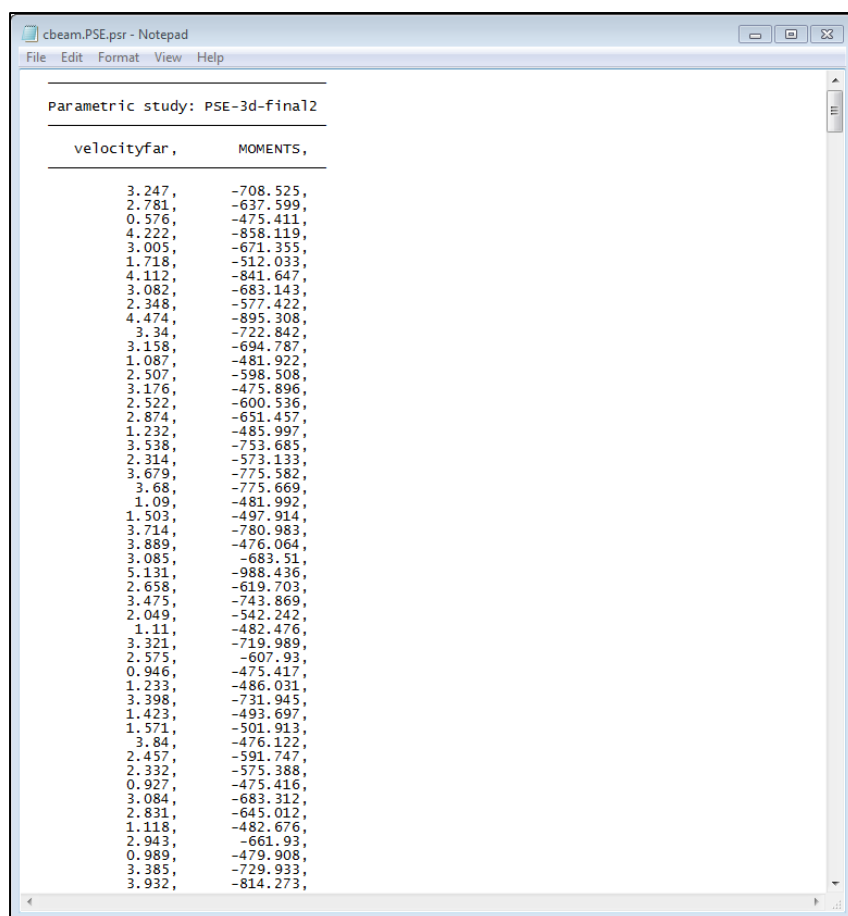
Figure 3.11: River profile of Lockyer Creek at Helidon Number 3

### 3.3.5 Method of analysis:

There are various types of modelling techniques and analysis available in any given FEA software. It's appropriate that a simple approach is adopted at the beginning followed by a complex approach. This ensures that comparison of results between different approach and the validation are achieved. We have adopted a simple linear analysis and a nonlinear analysis in this research.

### 3.3.5.1 Simple Linear Analysis:

Bridge I girder was modelled as a 2 node beam element. Linear elastic property of the concrete was considered in the material model. Unlike in the solid element, direct bending moment output is available in this simple method that is required to quantify the damage using damage index. However, actual simulation of the bridge girder with rebar is not possible here. Figure 3.12(below) shows the direct bending moment output obtained from a parametric study run in ABAQUS using a python script. Some limitation in using nonlinear property of the concrete was observed here when it came to python script study.



| velocityfar, | MOMENTS,  |
|--------------|-----------|
| 3.247,       | -708.525, |
| 2.781,       | -637.599, |
| 0.576,       | -475.411, |
| 4.222,       | -858.119, |
| 3.005,       | -671.355, |
| 1.718,       | -512.033, |
| 4.112,       | -841.647, |
| 3.082,       | -683.143, |
| 2.348,       | -577.422, |
| 4.474,       | -895.308, |
| 3.34,        | -722.842, |
| 3.158,       | -694.787, |
| 1.087,       | -481.922, |
| 2.507,       | -598.508, |
| 3.176,       | -475.896, |
| 2.522,       | -600.536, |
| 2.874,       | -651.457, |
| 1.232,       | -485.997, |
| 3.538,       | -753.685, |
| 2.314,       | -573.133, |
| 3.679,       | -775.582, |
| 3.68,        | -775.669, |
| 1.09,        | -481.992, |
| 1.503,       | -497.914, |
| 3.714,       | -780.983, |
| 3.889,       | -476.064, |
| 3.085,       | -683.51,  |
| 5.131,       | -988.436, |
| 2.658,       | -619.703, |
| 3.475,       | -743.869, |
| 2.049,       | -542.242, |
| 1.11,        | -482.476, |
| 3.321,       | -719.989, |
| 2.575,       | -607.93,  |
| 0.946,       | -475.417, |
| 1.233,       | -486.031, |
| 3.398,       | -731.945, |
| 1.423,       | -493.697, |
| 1.571,       | -501.913, |
| 3.84,        | -476.122, |
| 2.457,       | -591.747, |
| 2.332,       | -575.388, |
| 0.927,       | -475.416, |
| 3.084,       | -683.312, |
| 2.831,       | -645.012, |
| 1.118,       | -482.676, |
| 2.943,       | -661.93,  |
| 0.989,       | -479.908, |
| 3.385,       | -729.933, |
| 3.932,       | -814.273, |

Figure 3.12: Direct bending moment output from ABAQUS.

### 3.3.5.2 Nonlinear Analysis:

Case study analysis of the Tenthill Creek Bridge revealed that it experienced a heavy flood loading. There was some tension cracks appeared on the girder. This indicated that the concrete had reached the plastic limit or nonlinear state. Therefore we had to model the bridge structure using nonlinear constitutive model of the concrete. We used Concrete Damage Plasticity (CDP) (ABAQUS 6.14) model in this research. Unlike in our previous analysis discussed in section 3.3.5.1, we were able to model the rebar within the bridge girder

in this method. We used 8 node solid elements to enable inclusion of the rebar. Also solid elements yield better results in concrete nonlinear constitutive model such as Concrete Damage Plasticity (CDP) than that of being in beam elements. However, direct bending moment output is not possible from the solid elements in ABAQUS. Therefore we had to devise another method to calculate these bending moments from the relevant elemental stress output.

### 3.3.5.3 Calculation of Bending Moment from ABAQUS Elemental Stress output

The bending moment is directly computed with normal stress on the specified girder beam section as shown in equation Equation 3-2

$$M = \sum \sigma_i A_i l_i \quad \text{Equation 3-2}$$

Where  $\sigma_i$ = normal stress at the centroid of the element,  $A_i$ =corresponding area of the element, and  $l_i$ = distance between centroid of the element and the Neutral axis of the beam section (Figure 3.13)

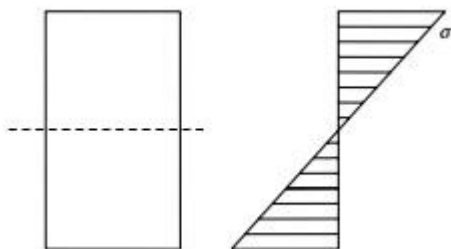


Figure 3.13: Beam section stress distribution

Since the flood loading acts laterally on the I-girder, minor axis bending moment has to be considered. Neutral axis is located in between where the elemental normal stress changes from tensile stress to compressive stress or vice versa. The exact location of the neutral axis is obtained by interpolating between these two stresses.

### 3.4 Numerical modeling of the selected structures. (Probabilistic)

Probabilistic modelling of the bridge is required to capture the influences of uncertain factors on river bridge safety evaluation. A sampling approach such as a Monte Carlo simulation (MCS) or importance sampling is often adopted using @Risk software, an add in application of Microsoft Excel. The random variable considered here includes flood velocity that forms the demand model of the system while Concrete compressive strength, geometry of the bridge section and the span form the capacity model of the system. Simulation is performed using ABAQUS Command software through an ABAQUS Script written in Python Language to capture the uncertainty in the demand model. Figure 3.14(below) shows the model development of the bridge deck and the girders. Further details on this will be discussed in chapter 6

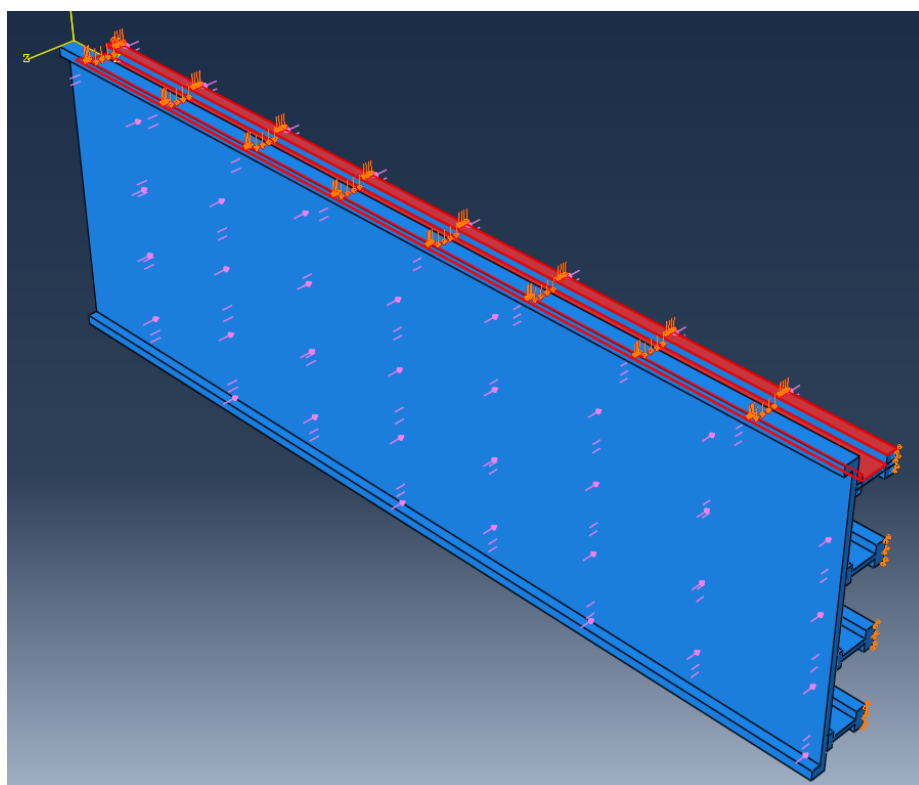


Figure 3.14: Model development of bridge and deck in ABAQUS

### 3.5 Fragility curves

Fragility curves are tools that determine the probability of failure/damage of any given structure under a set of uncertain loading conditions. The uncertain nature of the flood velocity, flood depth and the amount of accumulated debris/log impact etc. are considered in deriving these fragility curves. Further details on this will be discussed in chapter 6.

### 3.6 Chapter Summary

In summary, the research methodology adopted following research techniques:

- Analysis of case studies to identify major failure modes of bridges under flood loading.
- Numerical modelling of bridges to develop deterministic load response of the structures.
- Developing fragility curves incorporating variability of flood loads and variability of material properties.

Each of these methods is discussed in detail in the following chapters.

#### Relationship between chapters 4, 5 and 6

This research has initiated from the analysis of case study bridges that were affected during the severe flood events in Queensland in 2011 and 2013. Chapter 4 presents the detailed analysis of this case study bridges. Flood impact damage to the bridges has initially been investigated through a deterministic approach. Two of the bridges physically affected in Lockyer Valley region were numerically modelled in this approach using ABAQUS software. Flood exerted loading on the bridges was determined using equations given in AS5100 bridge design code and necessary reactions such as bending moments were derived. This approach is presented in great details in Chapter 5. Deterministic approach would yield necessary output that is applicable only to one or two bridges that are fixed in their geometric configuration, material strength and the flood loading exerted etc. and in no way it could give rise to a generic methodology that is applicable for multiple bridges in a region. To overcome this restriction, a probabilistic approach has been adopted to analyse the bridges incorporating the variability of bridge material strength, geometric configuration, and the exposed flood intensity. Broader aspects of this probabilistic method are covered in Chapter 6.



## 4 Analysis of Case Studies

### 4.1 Introduction

The case study approach adopted in this research examined the actual bridge inspection report compiled during aftermath of 2013 severe flooding incident in Queensland [(Pritchard, 2013), (QueenslandGovernment, 2012)].

Yin (2013) encourages the use of multiple case studies, stating that the results from a multiple case study approach are more robust and compelling than those from a single case study.

#### Triangulation of Data

Triangulation involves using several data sources or investigative approaches to get additional viewpoints to confirm the phenomenon being explored. According to Yin (2013):

*‘The most important advantage presented by using multiple sources of evidence is the development of converging lines of enquiry. Any case study finding or conclusion is likely to be more convincing and accurate if it is based on several different sources of information’*

If triangulation can be achieved, it should contribute to the validity and reliability of the study as a whole (Yin, 2013). This research has been triangulated using the following sources of information:

- Bridge Inspection Report sourced through Lockyer Valley Regional Council.
- Published documents and literature on the damage to bridge infrastructure under natural hazards (Flood)
- Finite Element Modelling of the case study bridge.
- Consultation with practitioners

The bridge inspection data for the bridges in the case study area is analysed to understand the major failure mechanisms of the bridges.

Lockyer Valley Region of Queensland has been selected as a case study for this research. 2011/2013 floods had severely affected road and bridge infrastructure which enormously impacted on the community in the Lockyer Valley region. This case study aims at identifying all possible attributes of bridges contributing to failure such as bridge superstructure with

girders, bridge approaches, bridge substructure with piers, waterway etc. It further analyses the failure criteria/ mode of failure of different types of bridges.

## **4.2 Overview of case study analysis**

Lockyer Valley Regional Council in Queensland has compiled a comprehensive bridge inspection report for about 46 bridges in the region before they open the bridges for traffic after the flood has receded. The study on this report indicated that the damage to bridge structures are complex and requires a detailed knowledge of underlying design principles, current classification of roads/bridges as well as construction methods adopted during different periods of design and construction. Critical analysis of this bridge inspection data that included the photos of the affected bridges revealed that the failure of the bridges was primarily due to the flood impacts on the attributes of bridge such as bridge girders and decks, bridge approaches, relieving slabs, abutments, wing walls and misalignment of piers. The report also revealed that some of the bridges were inundated as long as 96 hours and the fill under the relieving slab had undermined. The impact load of the huge rocks, ship containers, vehicles and the other unexpected debris that were carried along the flood water with high velocity was the primary cause of damage to bridge superstructure, abutments, wing walls and piers. There are many ways that a bridge could be damaged in an extreme flood event. If the structure is completely inundated during the flood, the damage to the property depends on the length of time it was submerged as well as the elements collected around or passing the structure. Even after the flood water recedes, extra care should be taken to inspect the supports of the bridges. Approaches of a bridge could be damaged due to debris impact, settlement or depressions. Debris against substructure and superstructure, bank erosion and damage to scour protection will damage the waterways. Movement of abutments, wing walls, and piers, rotation of piers and missing, damaged, dislodged or poorly seating of the bearings are the major reasons for substructure failure. Superstructure could be damaged due to the debris on deck, rotation of deck, dipping of deck over piers or damage of girders due to log impact. Due to any of these reasons, the members of a bridge could be damaged and bridge may not be completely functional. Some of the snap shots of the affected bridges are illustrated in Figure 4.1.



Figure 4.1: Some of the snap shots of the affected bridges

### 4.3 Inspection data for damaged bridges

A bridge inspection template had been prepared to undertake inspections of bridges after the January 2013 flood event. These inspections were undertaken in accordance with the Queensland Transport Main Roads Level 1 bridge inspection. They used a template to record the assessment for each inspected bridge and the template included the following information for each inspection element of the bridge.

- Approaches
  - signs and delineation- missing, damaged or obscured
  - guardrails – missing or damaged
  - road drainage – blocked inlets/ outlets
  - road surface – missing or damaged, settlement or depression
- Bridge surface
  - Bridge surface – missing or damaged, scuppers blocked

- Footpaths – damaged
- Barriers/handrails – damaged, missing fixings, loose post base
- expansion joints – loose or damaged, missing or damaged seal, obstructions in gap
- Waterway
  - debris against substructure
  - debris against superstructure
  - bank erosion
  - scour holes
  - damage to scour protection
- Substructure (abutments)
  - Movement of abutments
  - Movement of wing walls
  - Scour of spill through
- Substructure (piers)
  - Movement of piers
  - Rotation of piers
  - Scour around piers
- Substructure (bearings)
  - Missing, damaged or dislodged
  - Poorly sealed
- Superstructure (deck)
  - Damage

- Debris on deck
- Rotation of deck
- Dipping of deck over piers
- Superstructure (girders)
  - damage

Figure 4.2 and Figure 4.3 illustrate typical pages as extracted from the bridge inspection report.

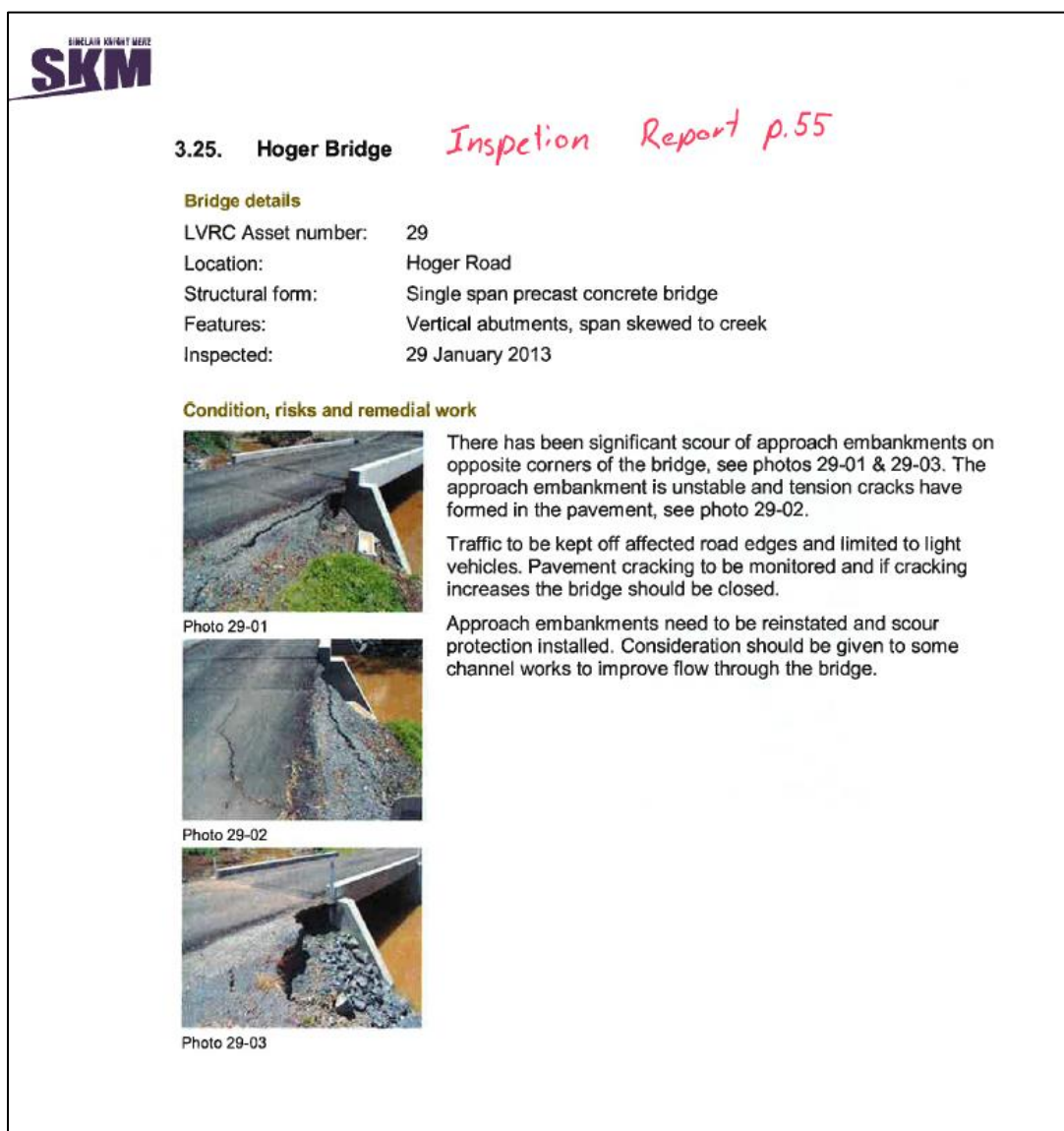


Figure 4.2: Illustrative page from bridge inspection report

| Post Flood Inspection Report |             |                   |                  |  |
|------------------------------|-------------|-------------------|------------------|--|
| Structure Id                 | Hoyer Road  |                   |                  |  |
| Road Name                    | Hoyer Road  | River/Creek Name  | Deep Gully       |  |
| Structure Type               | single span | Construction Type | precast concrete |  |
| Construction Material        | concrete    |                   |                  |  |
| Inspector                    | D. Loren    |                   |                  |  |
| Date                         | 29-1-13     | Time              | 12:45            |  |

| Inspection Elements            | Problem |     | Location and Comments   | Impact Opening |   |
|--------------------------------|---------|-----|---|----------------|---|
|                                | Y       | N   |   | Y              | N |
| <b>Approaches</b>              |         |     |   |                |   |
| <b>1 Signs and Delineation</b> |         |     |   |                |   |
| Missing, damaged or obscured   |         | N   |   |                |   |
| <b>2 Guardrails</b>            |         |     |   |                |   |
| Missing or damaged             |         | N   |   |                |   |
| <b>3 Road Drainage</b>         |         |     |   |                |   |
| Blocked inlets/outlets         |         | N   |   |                |   |
| Scour of outlets               |         |     |   |                |   |
| <b>4 Road Surface</b>          |         |     |   |                |   |
| Missing or damaged             |         | Y   | Roundover water corner<br>asphalt ramp tension cracks<br>in pavement. |                |   |
| Settlement or depressions      |         |     |   |                |   |
| <b>Bridge Surface</b>          |         |     |   |                |   |
| <b>5 Bridge Surface</b>        |         |     |   |                |   |
| Missing or damaged             |         | N   |   |                |   |
| Scuppers blocked               |         |     |   |                |   |
| <b>6 Footpaths</b>             |         |     |   |                |   |
| Damaged                        |         | N/A |   |                |   |
| <b>7 Barriers/handrails</b>    |         |     |   |                |   |
| Damaged                        |         | N/A |   |                |   |
| Missing fixings                |         |     |   |                |   |
| Loose post base                |         |     |   |                |   |
| <b>8 Expansion Joints</b>      |         |     |   |                |   |
| Loose or damaged               |         | N/A |   |                |   |
| Missing or damaged seal        |         |     |   |                |   |
| Obstructions in gap            |         |     |   |                |   |

Figure 4.3: Extract from bridge inspection report

Each report further included information about the damages to services by inspection and the damage to brackets or conduits. Finally it gave recommendations such as bridge ok to open or bridge requires work prior to opening or further assessment required.

The report contained details of damage to 46 bridges in the Lockyer Valley region. Oh et al. (2010) described that vulnerability of an infrastructure would depend on its physical characteristics such as bridge elevation, height, type of material and construction practice used. Having identified the importance of physical characteristics, an Excel sheet has been prepared by the author to summarize finer details of the bridges such as bridge type, length, width, number of spans, location of the bridge, elevation, average daily traffic and possible design codes used Table 4-2(below).

Different bridges have been designed using different types of bridge standards applicable at the time of construction of the bridge under consideration. Table 4-1(below) gives details of the bridge design standards used in Australia. It covers the period from 1927 to date.

Table 4-1: Australian bridge design standards

| <b>Design Standards – Pre-1948</b>  |                |          |                           |
|-------------------------------------|----------------|----------|---------------------------|
| (i)                                 | PWD            | Pre-1927 | Traction Engine Standard  |
| (ii)                                | PWD            | Pre-1927 | Standard UDL + Pt. Loads  |
| (iii)                               | DMR            | 1927     | Standard UDL + Pt. Loads  |
| (iv)                                | DMR            | 1938     |                           |
| <b>Design Standard – MS18</b>       |                |          |                           |
| (i)                                 | DMR            | 1948     | Standard Truck (MS18)     |
| <b>Design Standards – Post-1976</b> |                |          |                           |
| (i)                                 | NAASRA BDS     | 1976     | Standard Truck            |
| (ii)                                | NAASRA BDS     | 1976     | Abnormal Vehicle Standard |
| (iii)                               | Ordinance 30C  | 1982     | Articulated Vehicle       |
| (iv)                                | Austrroads '92 | 1992     | Standard T44 Truck & HLP  |
| (v)                                 | Austrroads '92 | 1992     | HLP 320 & HLP 400 (abn)   |
| (vi)                                | AS 5100        | 2004     | SM1600                    |

Bridges in the bridge inspection report, were classified based on the materials used to construct them such as concrete, steel and timber bridges. It also included some box culverts. These are graphically shown in Figure 4.4(below)

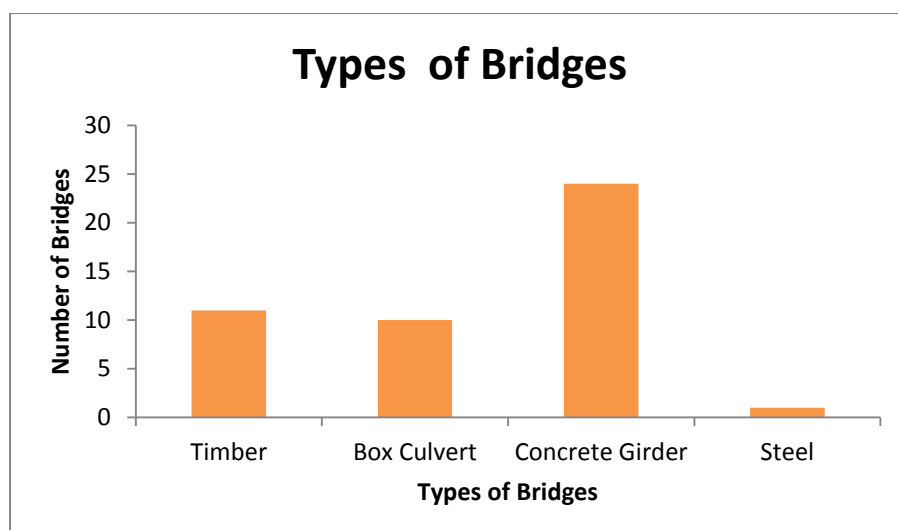


Figure 4.4: Types of bridges included in the bridge inspection report

Detail about the the types of road that the bridges served were also given in the report. These were rural access, rural collector and urban areterial roads. Global location of each bridge was given in terms of Longitude and Lattitude. Using this location detail, the elevation of each bridge was obtained through google earth. Construction date, average daily traffic flow and percentage of heavy vehicles usage for each bridge were also given in the table.

It has been observed from the given bridge inspection report that different bridges have different types of failure mechanisms. In a performance based design, it is important to investigate the consequences of individual member behavior on the performance of the structural system (Bonstrom and Corotis, 2010). Some bridges have failed because of loss of bridge approach while some other bridges have failed due to scouring at the bridge pier or bridge abutment/wing wall etc.

Table 4-3(below) illustrates different failure mechanisms for different bridges. It also describes the most common failure mechanisms of the bridge.

Table 4-2: Details of damaged bridges

|    | Bridge Name               | Road Name                    | Type         | Deck       | Length | Width | Construction Date | Av Daily traffic | % of Heavy Vehicles | Road Type       | Elevation(m) | Possible codes used for design |
|----|---------------------------|------------------------------|--------------|------------|--------|-------|-------------------|------------------|---------------------|-----------------|--------------|--------------------------------|
| 1  | Evans Bridge              | Evans Road                   | Timber       | Timber     | 6.3    | 3.7   | 19540101          | 10               | 10                  | Rural Access    | 76           |                                |
| 2  | Weigels Crossing          | Summerholm Road              | Box Culverts | Bitumen    | 44.6   | 7.5   | 19980101          | 220              | 11                  | Rural Collector | 100          | NAASARA                        |
| 3  | Knopkes Crossing          | Summerholm Road              | Box Culverts | Bitumen    | 8.1    | 3.4   | 19890101          | 198              | 12.3                | Rural Collector | 122          | NAASARA                        |
| 4  | Magarrigal Bridge         | Magarrigal Road              | Timber       | Unsurfaced | 11.3   | 3.7   | 18991230          | 30               | 10                  | Rural Access    | 128          | NAASARA                        |
| 5  | Mcgrath Pedestrian Bridge | Mulgowie School Road         | Concrete     | Asphalt    | 42.3   | 3.7   | 19840101          | 0                | 0                   | Rural Access    | 141          | NAASARA                        |
| 6  | Clarke Bridge             | Thornton School Road         | Timber       | PPLNK      | 6.1    | 7.4   | 19640101          | 100              | 10                  | Rural Access    | 172          |                                |
| 7  | Maincamp creek            | Maincamp Creek Road          | Box Culverts | Asphalt    | 23.5   | 4.9   | 20010101          | 40               | 10                  | Rural Access    | 195          | 92 AUSTRROADS                  |
| 8  | Peters Bridge             | Peters Road                  | Steel        | Asphalt    | 13.1   | 3.3   | 18991230          | 30               | 10                  | Rural Access    | 185          |                                |
| 9  | Moon Bridge               | Ropeley Road                 | Box Culverts | Concrete   | 24.3   | 8.2   | 19990101          | 70               | 18.6                | Rural Access    | 131          | 92 AUSTRROADS                  |
| 10 | Dotd Road Bridge          | Dotd Road                    | Concrete     | Bitumen    | 20.1   | 4.1   | 20040101          | 100              | 10                  | Rural Access    | 92           | AS 5100                        |
| 11 | Whitehouse                | Whitehouse                   | Box Culverts | Unsurfaced | 11.8   | 3.6   | 19920101          | 10               | 20                  | Rural Access    | 97           | 92 AUSTRROADS                  |
| 12 | Old Laidley Forest Hill   | Old Laidley Forest Hill Road | Box Culverts | Bitumen    | 13.1   | 8.6   | 19890101          | 1123             | 6                   | Rural Arterial  | 150          | NAASARA                        |

Chapter 4: Analysis of Case Studies

|    |                                |                       |              |            |        |       |                   |                  |                     |                 |              |                                |
|----|--------------------------------|-----------------------|--------------|------------|--------|-------|-------------------|------------------|---------------------|-----------------|--------------|--------------------------------|
| 13 | Crowley vale road              | Crowley Vale Road     | Box Culverts | Bitumen    | 16.4   | 6.4   | 19890101          | 385              | 8.4                 | Rural Arterial  | 82           | NAASARA                        |
| 14 | Lester Bridge                  | Lester Road           | Box Culverts | Bitumen    | 16.5   | 9.8   | 20050101          | 200              | 10                  | Rural Collector | 78           | AS 5100                        |
| 15 | Main green swamp               | Main green swamp Road | Box Culverts | Bitumen    | 15.3   | 6.7   | 19840101          | 412              | 11.7                | Rural Collector | 99           | NAASARA                        |
| 16 | Steinke's Bridge               | Lake Clarendon Road   | Concrete     | Asphalt    | 60     | 8.4   | 20091001          | 389              | 15.8                | Rural Collector | 84           | AS 5100                        |
|    | Bridge Name                    | Road Name             | Type         | Deck       | Length | Width | Construction Date | Av Daily traffic | % of Heavy Vehicles | Road Type       | Elevation(m) | Possible codes used for design |
| 17 | Quin Bridge                    | Harm Drive            | Concrete     | Bitumen    | 20.5   | 6     | 19890101          | 544              | 5.8                 | Rural Collector | 78           | NAASARA                        |
| 18 | Middletons Bridge              | Lockrose Road North   | Timber       | Bitumen    | 20.9   | 5.6   | 19640101          | 309              | 13.6                | Rural Collector | 69           |                                |
| 19 | Narda Lagoon Suspension Bridge | Narda Lagoon          | Timber       | Unsurfaced | 85.5   | 1.6   | 19640101          | 0                | 0                   |                 | 82           |                                |
| 20 | Daveys Bridge                  | Smithfield Road       | Concrete     | Bitumen    | 21.6   | 4.1   | 19720101          | 1444             | 4.3                 | Rural Collector | 99           |                                |
| 21 | Belford Bridge                 | Allan Street          | Concrete     | Bitumen    | 17     | 7.3   | 19890101          | 1453             | 6.3                 | Urban Arterial  | 98           | NAASARR                        |
| 22 | Liftin Bridge                  | Robinsons road        | Concrete     | Bitumen    | 20.7   | 4     | 19900101          | 5                | 14                  |                 | 106          | NAASARR                        |
| 23 | Thistlethwaite Bridge          | Grantham Winwill road | Timber       | Bitumen    | 37.5   | 7     | 19570101          | 958              | 8.7                 | Rural Arterial  | 116          |                                |
| 24 | Avis Bridge                    | Ma Ma Lilydale Road   | Box Culverts | Bitumen    | 16.4   | 7.8   | 19970101          | 170              | 18.7                | Rural Collector | 134          | 92 AUSTRROADS                  |
| 25 | Logan Bridge                   | Tenthill Creek Road   | Concrete     | Bitumen    | 64.2   | 8     | 20040101          | 1161             | 10.2                | Rural Arterial  | 132          | AS 5100                        |
| 26 | Frankie Steinhardt's Bridge    | Lower Tenthill road   | Concrete     | Asphalt    | 42     | 9.6   | 20100701          | 247              | 18.8                | Rural Access    | 114          | AS 5100                        |

Chapter 4: Analysis of Case Studies

|    |                        |                              |              |          |        |       |                   |                  |                     |                 |              |                                |
|----|------------------------|------------------------------|--------------|----------|--------|-------|-------------------|------------------|---------------------|-----------------|--------------|--------------------------------|
| 27 | Robeck Bridge          | Manteuffell road             | Box Culverts | Concrete | 10     | 9.2   | 20000101          | 150              | 20                  | Rural Collector | 136          | AS 5100                        |
| 28 | Clarke Bridge          | Tenthill creek road          | Concrete     | PPLNK    | 19     | 7.4   | 19900101          | 2560             | 13.5                | Urban Arterial  | 109          | NAASRA                         |
| 29 | Hoger Bridge           | Hogers road                  | Timber       | Bitumen  | 9.5    | 3.6   | 20000101          | 24               | 4.5                 | Rural Access    | 161          | AS 5100                        |
| 30 | Colquhoun Bridge       | Colquhouns road              | Concrete     | Asphalt  | 15     | 5     | 20101101          | 30               | 5                   | Rural Access    | 122          | AS 5100                        |
| 31 | Sheep Station Bridge   | Gunn street                  | Timber       | Bitumen  | 15.3   | 4.5   | 19700101          | 230              | 7.5                 | Urban Collector | 139          |                                |
| 32 | Mahon Bridge           | Carpendale road              | Concrete     | Asphalt  | 36     | 8.4   | 20090801          | 189              | 37                  | Rural Collector | 127          | AS 5100                        |
|    | Bridge Name            | Road Name                    | Type         | Deck     | Length | Width | Construction Date | Av Daily traffic | % of Heavy Vehicles | Road Type       | Elevation(m) | Possible codes used for design |
| 33 | Hughes Bridge          | Blanchview Road              | Box Culverts | Concrete | 8.9    | 7.8   | 20000101          | 554              | 5.1                 | Urban Arterial  | 303          | AS 5100                        |
| 34 | Kapernicks Bridge      | Flagstone Creek road         | Concrete     | CSLAB    | 66.1   | 7.6   | 19810101          | 729              | 26.5                | Rural Arterial  | 126          | NAASRA                         |
| 35 | Duncan Bridge          | Flagstone Creek Road         | Concrete     | Bitumen  | 36.9   | 5.9   | 19650101          | 294              | 34.1                | Rural Arterial  | 168          |                                |
| 36 | Murphy Bridge          | Back Flagstone Creek Road    | Concrete     | Bitumen  | 36.6   | 3.4   | 19900101          | 191              | 12.1                | Rural Collector | 129          | NAASRA                         |
| 37 | Granny Williams Bridge | Back Flagstone Creek Road    | Box Culverts | Bitumen  | 8.4    | 8.9   | 19900101          | 191              | 12.1                | Rural Collector | 141          | NAASRA                         |
| 38 | Evans Bridge           | Back Flagstone Creek road    | Box Culverts | Bitumen  | 6.1    | 6.8   | 20000101          | 85               | 14.9                | Rural Collector | 418          | AS 5100                        |
| 39 | Cran Bridge            | Helidon Flagstone Creek Road | Timber       | Timber   | 8      | 3.6   | 19800101          | 119              | 4.8                 | Rural Arterial  | 207          | NAASRA                         |
| 40 | The Willows Bridge     | Lockyer Siding               | Concrete     | Asphalt  | 15     | 5     | 20101101          | 121              | 5.3                 | Rural           | 162          | AS 5100                        |

Chapter 4: Analysis of Case Studies

|    |                      | road                 |          |          |      |     |          |      |      | Collector       |     |         |
|----|----------------------|----------------------|----------|----------|------|-----|----------|------|------|-----------------|-----|---------|
| 41 | The Dairy Bridge     | Fifteen Mile road    | Concrete | Concrete | 22.1 | 5   | 20050101 | 77   | 11.8 | Rural Arterial  | 228 | AS 5100 |
| 42 | Kirsop Bridge        | Spring Bluff Road    | Concrete | Concrete | 12.1 | 4.8 | 18991230 | 422  | 5.2  | Rural Access    | 410 |         |
| 43 | Greer Bridge         | Postmans Ridge road  | Concrete | Concrete | 36.8 | 8.4 | 20070101 | 1193 | 6.7  | Rural Arterial  | 155 | AS 5100 |
| 44 | Connole Bridge       | Postmans Ridge road  | Timber   | Bitumen  | 27.4 | 6.5 | 19800101 | 1193 | 6.7  | Rural Arterial  | 179 | NAASRA  |
| 45 | McGraths Bridge      | Mulgowie School Road | Concrete | Concrete | 40   | 8   | 20090101 | 290  | 47   | Rural Collector | 140 | AS 5100 |
| 46 | Forestry Road Bridge | Forestry Road        | Timber   | Timber   | 7.8  | 5.1 | 19660101 | 0    | 0    | Rural Collector | 207 |         |

Table 4-3: Failure mechanisms of selected bridges

| <b>Name of bridge</b>    | <b>Bridge type</b>                       | <b>Submerged?</b> | <b>Mode of failures</b>   | <b>Most affected bridge component</b>              |
|--------------------------|--|-------------------|---|--|
| <b>Maggarigal Bridge</b> | 2 Span Deck Unit                         | Yes               | Deck and the bridge girder significantly damaged; Built up of mud and debris on the structure and approach  | Bridge girder and Deck/<br>Scouring or undermining |
| <b>Peters Bridge</b>     | 4 Span Precast Concrete Deck Unit        | Yes               | Both run on slabs have been undermined; Abutment headstock not connected to piles; Headstock not centrally located on piles; Some cracking and spalling of piles              | Both run on slabs/ scouring or undermined          |
| <b>Middleton Bridge</b>  | 4 Span Timber Deck                       | Yes               | Scouring in front of North Abutment; Undercut beneath the southern abutment.  | Abutments/ Scouring                                |
| <b>Davey Bridge</b>      | 2 Span Blade pier R/C vertical abutments | Yes               | Significant scour behind the western abutment; Substantial crack in the downstream western wing wall; Downstream western guardrail had been damaged due to build-up of debris | Abutment wing wall/scoured and cracked             |

|                                    |                                     |             |  |  |
|------------------------------------|-------------------------------------|-------------|--|--|
| <b>Belford Bridge</b>              | 2 Span I Girder Bridge              | Yes         | Scour and slumping of the southern upstream rock spill; Relieving slab and the deck has been undermined; Substantial crack appeared in the bridge girder                       | Bridge deck and the girder affected.                       |
| <b>Logan Bridge</b>                | 4 Span deck unit bridge             | Yes         | Section of one approach has been damaged<br><br>Headstock has been undermined<br><br>Cracks noted in the surfacing of the first end girder                                     | Bridge girder affected together with the headstock         |
| <b>Frankie Steinhardt's Bridge</b> | Single Span precast concrete bridge | No (Medium) | Significant scour of approach<br><br>The approach embankment is unstable and tension cracks have been formed in the pavement and the girder                                    | Both approach embankments/scouring/damage to bridge girder |
| <b>Sheep Station Bridge</b>        | Single span precast deck unit       | No (Medium) | Western upstream spill through has been undermined<br><br>Abutment wing wall has dropped and rotated with a large crack opened<br><br>Wing wall not connected to the headstock | Abutment wing walls/scouring or undermining                |

|                           |  |           |  |   |
|---------------------------|--|-----------|--|---|
| <b>Duncan Bridge</b>      | 4 span deck unit                         | Yes       | Small scour hole has formed on the downstream eastern abutment<br><br>Road shoulder at the end of bridge has been lost | Bridge approach and abutments/scouring  |
| <b>Murphy Bridge</b>      | Concrete Deck Unit                       | Yes       | Significant build-up of debris on the deck<br><br>Bridges girders damaged significantly                                | Bridge deck and the girder suffered significant damage                                    |
| <b>The Willows Bridge</b> | Single precast deck unit                 | Yes       | Both approaches sustained substantial damage<br><br>Bridge guardrails ripped off<br><br>Tension cracks on the girder   | Both bridge approach/scouring/failure of bridge girder with appearance of tension cracks. |
| <b>The Dairy Bridge</b>   | 2 span timber girder -concrete deck      | Yes       | Loss of rip rap spill through protection with some minor undercutting of abutment headstocks                           | Abutments/ scouring or undermining  |
| <b>Greer Bridge</b>       | 4 span timber girders with Concrete deck | No (High) | Scour protection has been washed away from the face of the spill through<br><br>Scouring of spill through              | Spill through/scouring  |

|                                 |                               |            |   |   |
|---------------------------------|-------------------------------|------------|---|---|
| <p><b>Kapernicks Bridge</b></p> | <p>3 Span I girder bridge</p> | <p>Yes</p> | <p>Substantial crack on the bridge girder.<br/>Scour and erosion observed on both bridge approach</p>   | <p>Substantial damage to the bridge superstructure</p>                                |
| <p><b>Clerk Bridge</b></p>      | <p>3 Span Deck Unit</p>       | <p>Yes</p> | <p>Edge delineation had been damaged by debris<br/><br/>Bridge girder sustained damage due to debris impact<br/><br/>Some bank scour on the downstream side of the bridge</p> | <p>Wing wall or bank / Scouring<br/><br/>Bridge girder and the deck got affected.</p> |

#### **4.4 Major failure modes/mechanism**

Inspection report for the bridges affected by recent flood event (January 2013) indicated different types of failure mechanisms for different bridges. The observed failure mechanisms were as follows:

- Deck and the bridge girders were significantly damaged
- Pier / Abutment scouring
- Significant built up of mud and debris on the structure and approaches
- Both run on slabs had been undermined
- Substantial crack in the abutment wing walls
- Abutment headstock not connected to piles.

Damage to bridge girders due to heavy log impact such as containers, vehicles, leisure crafts that were carried along the floodwater, Losses of road approach, embankment and pier and abutment scouring have been identified as major causes of failure for the bridges in Lockyer Valley region.

#### **4.5 Focus on concrete girder bridges**

There are several types of bridges commonly adopted in the world. Depending on the location and the intended purpose of the bridge, the designer selects the suitable types of bridge. The beam bridges/girder bridges are the cheapest and most common bridges across the world. They come in various size and shapes. They can be built over water or inland. They are simple, easy to build, and serves the purpose.

Reinforced or pre-stressed concrete girder bridges are a common design configuration used in Australia. Analysis on the performance of bridges under 2011/2013 flood in Lockyer Valley Region, Queensland indicated that vulnerability of girder bridges was observed by significant damage to these structures. The details of some of the bridges obtained from the Lockyer Valley Regional Council Bridge Inspection Data report are given in Table 4-2(above). Concrete girder bridges are the most recurrent types of bridge in Australia and it was observed that most of the bridges in the case study bridge region (Lockyer Valley Region)

were concrete girder bridges. Hence concrete girder bridges have been selected for case studies in this research to derive structural vulnerability models and determine vulnerable structures in the road network.

#### **4.6 Chapter summary**

Nearly 46 bridges sustained damage in Lockyer valley Region during the severe flood events in 2013. Much of the damage was to the superstructures, where typical damage included severe damage to bridge girders and unseating or drifting of decks. Bridge inspections showed that several bridges suffered damage due to debris impact in the form of leisure crafts, containers and vehicles. Other less severe forms of damage was a result of scour.

Considering that a major failure mode observed is the damage to superstructure of the concrete girder bridges due to impact of flood and debris as well as object impact, a decision was made to focus this research on vulnerability modelling of girder bridges under flood loading. Chapter 5 presents vulnerability modelling of a case study concrete girder bridge under flood, debris and log impact.

## 5 Numerical modelling of the case study bridge – Deterministic analysis

### 5.1 Introduction

In the previous chapters the case study based research methodology is discussed. This chapter presents the methodology and the outcomes of the analysis of two case study bridges selected for the analysis: Tenthill Creek Bridge and Kapernicks Bridge.

The research has focussed on the concrete girder bridges which form more than 60% of the bridge stock in Australia. Both bridges are located in a flood hazard zone and one of them had failed during 2011 floods in the Lockyer Valley Region in Queensland.

The chapter presents input data derived from the as built drawings, the analysis methods and assumptions and outcomes. Loading regimes is developed based on AS5100 and modified using field observation during disasters. Damage index derived based on structural capacity is also presented.

The analysis presented here is using a deterministic approach to understand the level of vulnerability of structures under different loading regimes. Variability of input parameters is taken into account in the next chapter (Chapter 6).

### 5.2 ABAQUS Finite Element Software

ABAQUS finite element analysis software is used in both the academic and industrial world and it has a broad usage among engineers. It is important to understand the theory and the methods limitations for the user. ABAQUS is the chosen software for this thesis. Each analyse in ABAQUS involves three stages, see Figure 5.1(below)

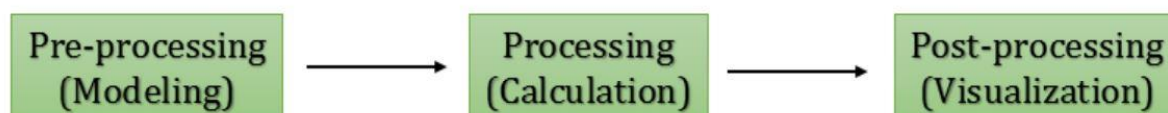


Figure 5.1: Solution sequence in ABAQUS

The first one is called pre-processing or modelling (Kuntjoro, 2005). In this stage the geometry of the current part or assembly is created. Some of the parameters that have to be considered are loads, material properties, boundary conditions and what output is required.

This is also called creating an input file. This stage can be performed by compatible CAD software or text editors. In the second step the actual analysis are performed which is called processing/solution. In this stage an output file is created and the nodal field values are calculated. The third and final stage is called post-processing. It is a visual rendering stage where the results can be described visually from the output file (Kuntjoro, 2005).

ABAQUS consist of five core software products which are based on the solution sequence described above.

### **5.2.1 ABAQUS/CAE**

CAE means Complete ABAQUS Environment. The application can be used to create the model as part of the pre-processing stage. It can also be used during the processing stage by monitoring and visualizing the results from the analysis, post-processing. (DassaultsSystems, 2015)

### **5.2.2 ABAQUS/Standard**

ABAQUS/Standard performs traditional calculations with an implicit integration scheme. The application is well suited for analyses which are static and low-speed dynamic and also steady state transport. It is possible to analyse the model in time and frequency domain in the same simulation. Combined with the CAE application where one can perform pre- and post-processing the whole solution sequence is fulfilled as the standard application perform the processing stage (Kuntjoro, 2005).

### **5.2.3 ABAQUS/Explicit**

The explicit application provides the opportunity to solve severely nonlinear systems. It is suitable to simulate transient dynamic problems. The application is part of the processing stage and can be combined with the CAE application and its modelling environment where both pre- and post-processing occurs (Kuntjoro, 2005). The results from ABAQUS/Explicit can be used as baseline for further calculations in ABAQUS/Standard. In the same way, the results from ABAQUS/Standard can be used as input in ABAQUS/Explicit. The advantage of this flexibility is that the explicit application calculates problems where high-speed, nonlinear and transient response dominates the solution. The standard application on the other hand is more suitable for to the parts of the analysis that are more appropriate to an implicit solution technique, e.g. static, low-speed dynamic or steady state transport analyses (Kuntjoro, 2005).

#### **5.2.4 ABAQUS/ CFD**

With the support for pre- and post-processing provided in the CAE application the CFD (Computational Fluid Dynamics) software supply advanced computational fluid dynamics capabilities in the processing stage. The application is able to solve incompressible flow problems such as laminar and turbulent, thermal convective and deforming- mesh arbitrary langrangian eulerian problems (Kuntjoro, 2005)

#### **5.2.5 ABAQUS/Multiphysics**

The application solves computational multi physical problem such as hydrodynamic wave loading and electrical coupling (Kuntjoro, 2005)

#### **5.2.6 User developed subroutines**

Subroutine is a programming tool which can be seen as a single part of a bigger program, where the program is divided into smaller parts. When the program needs the function that is written in the subroutines the user calls the subroutine. In ABAQUS this method is called User Subroutines and it is used if it is not possible to run the analysis by ABAQUS built-in model. FORTAN is the only program ABAQUS accepts for writing a subroutine in ABAQUS/Standard and ABAQUS/Explicit (DassaultsSystems, 2015).

### **5.3 Description of the case study bridges**

Two bridges were selected from the bridge inspection report for this purpose.

#### **5.3.1 Tenthill Creek Bridge**

This bridge has been constructed with 12 numbers of concrete I girders and has 3 spans. Structural details with reinforcement were also available for this bridge from the sourced as built drawings.

##### **5.3.1.1 Location of the bridge**

This bridge was built in 1976 and used to carry a state highway of Ipswich-Toowoomba over Tenthill Creek in Gatton, Queensland, Australia. The bridge has now been bypassed by the 4 lanes Gatton Bypass. It is now on road 314 Gatton Clifton. The location of the bridge is shown in Figure 5.2(below)



Figure 5.2 Location of Tenthill Bridge

### 5.3.1.2 Details of the Bridge

The bridge is 82.15 m long and about 8.6 m wide and is supported by a total of 12 concrete 27.38 m long beams over three spans of 27.38 m. Side and cross views of the Tenthill Bridge are shown in Figure 5.3 and Figure 5.4. The beams are supported by two abutments and two headstocks. A headstock elevation view is shown in Figure 5.5(below)



Figure 5.3 Photos of the Tenthill Bridge



Figure 5.4 Photos of the Tenthill Bridge

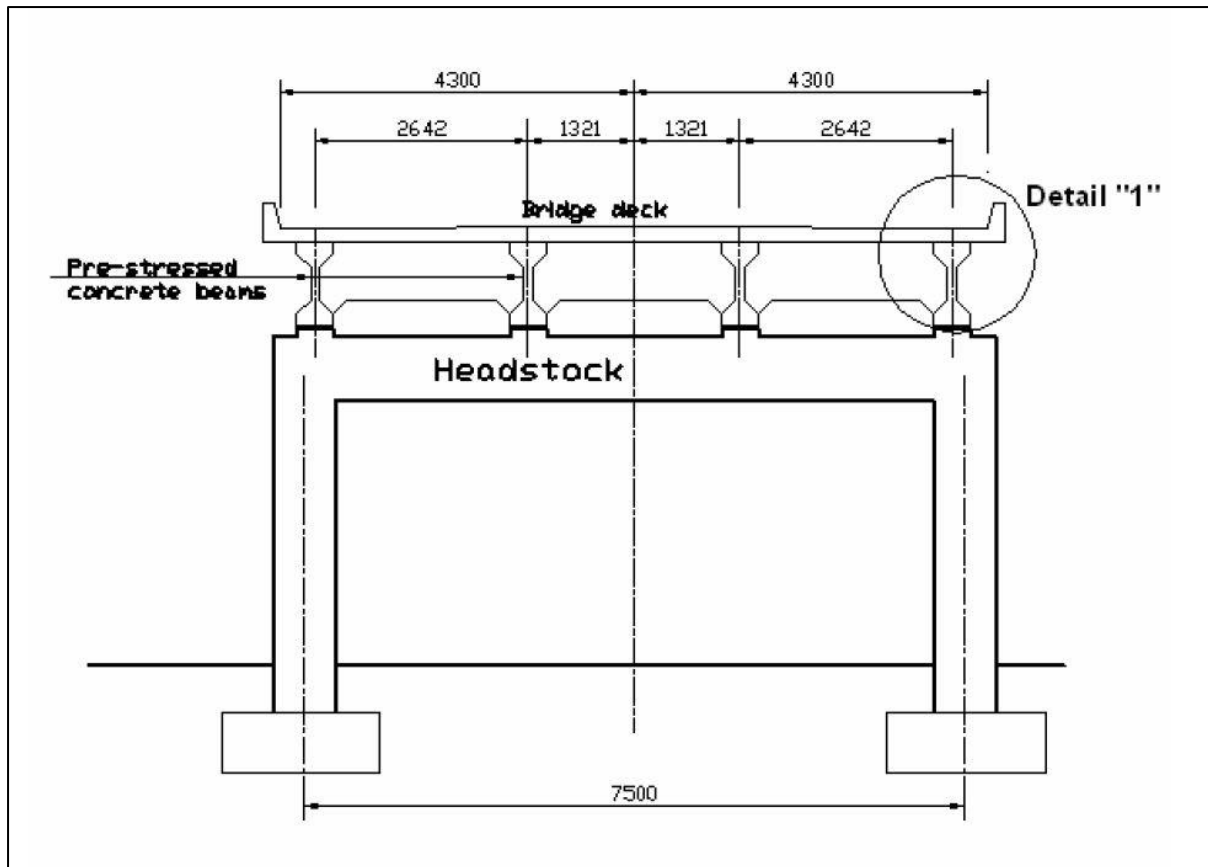
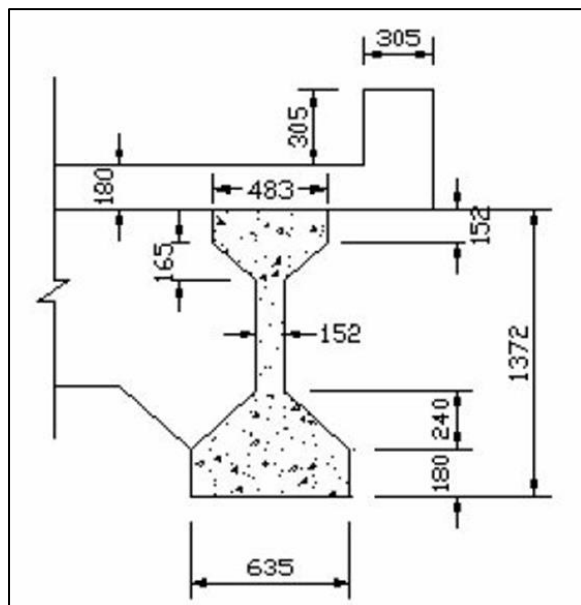


Figure 5.5 Schematic Details of the Headstock and superstructure



Beam span = 27382mm

Detail "1"

### 5.3.2 Kapernicks bridge

This bridge was chosen to be one of the case study bridges because in the aftermath of 2011 severe flood event in Queensland, this was completely washed away and Queensland Reconstruction Authority and QDTMR (Queensland Department of Transport and Main Roads) replaced this bridge with a new bridge. The new design flood velocity used for this new construction was used to validate the findings of the critical flood velocity in this research.

#### 5.3.2.1 Location of the bridge

Kapernicks Bridge is a three span; two lanes precast concrete Girder Bridge located on Flagstone Creek Road.

#### 5.3.2.2 Detail of the bridge

The bridge is 43.40 m long and about 8.56 m wide and is supported by a total of 12 concrete girders. Mid span consists of 22.0m long girders while the end span consists of 11.7m long girders on either side of the bridge approaches. Photo views of the Kapernicks Bridge are shown in Figure 5.6 and Figure 5.7. Sectional view of the bridge with all 4 girders is shown in Figure 5.8(below)



Figure 5.6: Kapernicks bridge Photo #1



Figure 5.7: Kapernicks bridge photo #2

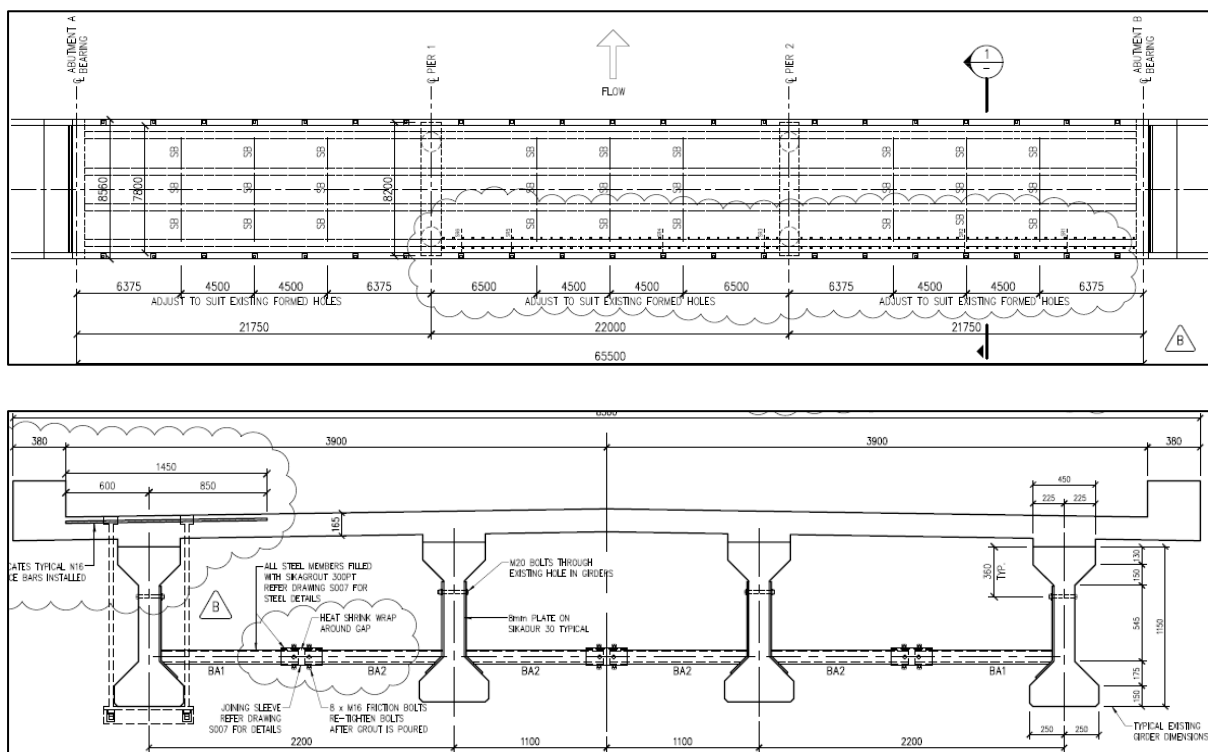


Figure 5.8: Kapernicks bridge sectional view

## 5.4 Deriving Flood Induced Bending Moment on the Girder

As mentioned in section 3.3.5, the bridge I girder was modelled using two different approaches and corresponding flood induced bending moments were derived.

#### 5.4.1 Method 1: Modelling of Bridge Girder using beam elements.

In this simple method, Bridge I girder was modelled using ABAQUS two-node beam elements (B31). Corresponding section bending moment (SM2) output was requested from the field output request. Maximum flood induced bending moment at the mid-span section was derived for calculating the relevant damage indices. Figure 5.9(below) shows the rendered view of the I girder beam profile.

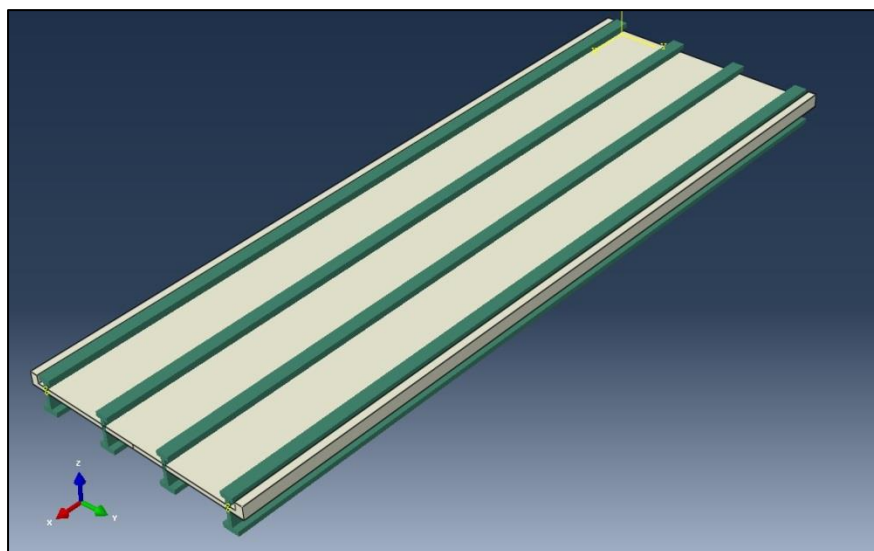


Figure 5.9: Rendered view of the I girder beam profile

#### 5.4.2 Method 2: Modelling of Bridge Girder using solid elements

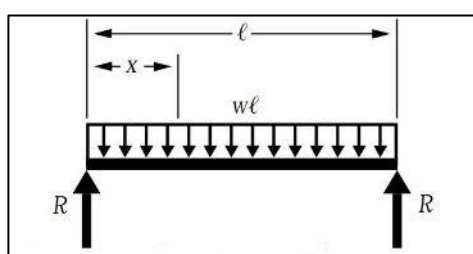
As discussed in section 3.3.5.2 (Chapter3), the bridge girder in this method was modelled using ABAQUS eight-node solid elements (C3D8R) to actually simulate the original condition of the bridge structure. Reinforcement bars within the girder were modelled as wire elements. Concrete Damaged Plasticity (CDP) Hanif et al. (2016) material property module was used in the analysis to account for the nonlinear behaviour of the concrete. Graphical representations of the concrete constitutive model used in the ABAQUS model are given in section 3.3.2 (Chapter3). Corresponding elemental normal stress outputs (S11) were obtained to calculate the maximum flood induced bending moment on the girder. Excel sheets as shown in Table 5-2(below) and Table 5-3(below) were used for this purpose.

## 5.5 Model Validation

In this section, the validation of the actual model and the adopted different methods to calculate the bending moments are discussed in details.

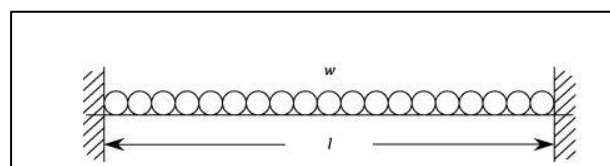
### 5.5.1 Method validation when the bridge girder was modelled using beam elements

In this case, a single beam subjected to a vertical uniformly distributed load (udl) was modelled and the mid-span bending moment was derived from the ABAQUS for two different types of boundary conditions at the beam supports as shown in Figure 5.10(below). Both pinned and fixed support conditions were considered. These results were compared with the text book manual calculations as shown in Table 5-1(below). The results give a 99.9% close estimation that validates this method.



Both end pinned condition

$$\text{Mid-span moment} = \frac{wl^2}{8}$$



Both end fixed condition

$$\text{Mid-span moment} = \frac{wl^2}{24}$$

Figure 5.10 Illustration of beam support conditions

Table 5-1: Comparisons of bending moments (beam elements)

|                        | ABAQUS value(kNm) | Manual Value(kNm) | % Error |
|------------------------|-------------------|-------------------|---------|
| <b>Both end pinned</b> | 11.23             | 11.25             | 0.17    |
| <b>Both end fixed</b>  | 3.74              | 3.75              | 0.19    |

W= 10kN/m ; L=3m

### 5.5.2 Method validation when the bridge girder was modelled using solid elements

Since no direct bending moment output is available for solid elements in any FEA, relevant elemental normal stress (S11) at the mid-span section of the beam were derived from the ABAQUS post processing step. These elemental stresses were then used to calculate the bending moment as discussed in 3.3.5.3. Neutral axis of the section was located in between where the stress value changed its sign from tensile to compressive or vice versa. Pinned and fixed support boundary conditions were considered here as well. Figure 5.11 and Figure 5.12 show the beam considered for the calculation of bending moment. Table 5-2 and Table 5-3(below) illustrate the stress obtained from ABAQUS analysis and the corresponding bending moments calculated. The results indicate that a 99.9% close estimation for pinned support condition whereas it gives 99.5% close estimation for fixed support condition and hence validate the method adopted. It should be noted here that Figure 5.11 and Figure 5.12 depicts just a single girder arrangement in the ABAQUS modelling for verification purpose of the method used to calculate bending moment from elemental stress output. However, in the actual modelling of the selected two case study bridges, all 4 girders and the deck on top of them were modelled and the mid span stress output from the end girder was considered for moment calculation since the mid span would experience the maximum bending moment. Also the flood load was applied laterally to the girder to simulate the actual impact.

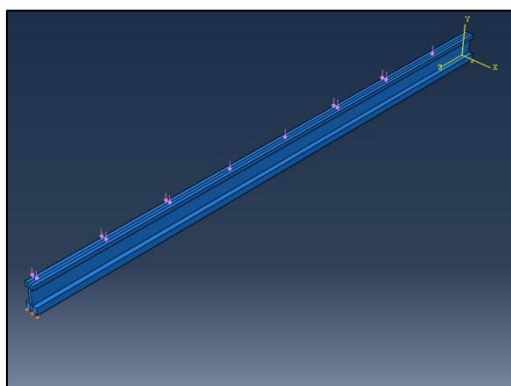


Figure 5.12: Simply supported Bridge Girder

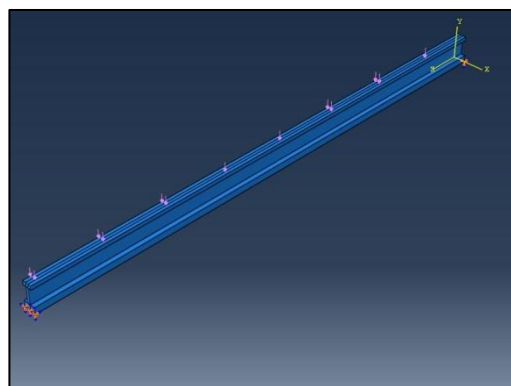


Figure 5.11: Fixed supported Girder

Table 5-2: Moment Calculation table for simply supported condition

| Ele#  | Ele. Id | Stress    | width | height | Force     | distance | moment    | absmom        |            |
|-------|---------|-----------|-------|--------|-----------|----------|-----------|---------------|------------|
| Ele1  | 10649   | 5.11E+04  | 0.65  | 0.05   | 1.66E+03  | 0.562    | 9.33E+02  | 932.8776      |            |
| Ele2  | 9654    | 4.65E+04  | 0.65  | 0.05   | 1.51E+03  | 0.512    | 7.74E+02  | 774.0179      |            |
| Ele3  | 8659    | 4.20E+04  | 0.65  | 0.05   | 1.36E+03  | 0.462    | 6.30E+02  | 630.0039      |            |
| Ele4  | 7664    | 3.74E+04  | 0.65  | 0.05   | 1.22E+03  | 0.412    | 5.01E+02  | 500.8155      |            |
| Ele5  | 6669    | 3.28E+04  | 0.65  | 0.05   | 1.07E+03  | 0.362    | 3.86E+02  | 386.425       |            |
| Ele6  | 5674    | 2.83E+04  | 0.65  | 0.05   | 9.19E+02  | 0.312    | 2.87E+02  | 286.8373      |            |
| Ele7  | 4679    | 2.37E+04  | 0.65  | 0.05   | 7.71E+02  | 0.262    | 2.02E+02  | 202.0363      |            |
| Ele8  | 33723   | 1.93E+04  | 0.15  | 0.05   | 1.45E+02  | 0.212    | 3.07E+01  | 30.67046      |            |
| Ele9  | 33724   | 1.48E+04  | 0.15  | 0.05   | 1.11E+02  | 0.162    | 1.80E+01  | 17.99038      |            |
| Ele10 | 33725   | 1.03E+04  | 0.15  | 0.05   | 7.73E+01  | 0.112    | 8.66E+00  | 8.660232      |            |
| Ele11 | 33726   | 5.82E+03  | 0.15  | 0.05   | 4.36E+01  | 0.062    | 2.71E+00  | 2.705561      |            |
| Ele12 | 33727   | 1.32E+03  | 0.15  | 0.05   | 9.92E+00  | 0.012    | 1.19E-01  | 0.119034      |            |
| Ele13 | 33728   | -3.17E+03 | 0.15  | 0.05   | -2.38E+01 | 0.038    | -9.03E-01 | 0.902712      |            |
| Ele14 | 33729   | -7.66E+03 | 0.15  | 0.05   | -5.75E+01 | 0.088    | -5.06E+00 | 5.057976      |            |
| Ele15 | 33730   | -1.22E+04 | 0.15  | 0.05   | -9.12E+01 | 0.138    | -1.26E+01 | 12.57929      |            |
| Ele16 | 33731   | -1.67E+04 | 0.15  | 0.05   | -1.25E+02 | 0.188    | -2.35E+01 | 23.47876      |            |
| Ele17 | 33732   | -2.11E+04 | 0.15  | 0.05   | -1.59E+02 | 0.238    | -3.77E+01 | 37.74008      |            |
| Ele18 | 33733   | -2.56E+04 | 0.15  | 0.05   | -1.92E+02 | 0.288    | -5.54E+01 | 55.38931      |            |
| Ele19 | 33734   | -3.01E+04 | 0.15  | 0.05   | -2.26E+02 | 0.338    | -7.64E+01 | 76.39501      |            |
| Ele20 | 33735   | -3.46E+04 | 0.15  | 0.05   | -2.60E+02 | 0.388    | -1.01E+02 | 100.805       |            |
| Ele21 | 33736   | -3.91E+04 | 0.15  | 0.05   | -2.94E+02 | 0.438    | -1.29E+02 | 128.5631      |            |
| Ele22 | 33737   | -4.36E+04 | 0.15  | 0.05   | -3.27E+02 | 0.488    | -1.60E+02 | 159.7272      |            |
| Ele23 | 33738   | -4.81E+04 | 0.15  | 0.05   | -3.61E+02 | 0.538    | -1.94E+02 | 194.2372      |            |
| Ele24 | 33739   | -5.27E+04 | 0.15  | 0.05   | -3.95E+02 | 0.588    | -2.32E+02 | 232.3977      |            |
| Ele25 | 20795   | -5.70E+04 | 0.5   | 0.05   | -1.42E+03 | 0.638    | -9.09E+02 | 909.0176      |            |
| Ele26 | 21392   | -6.16E+04 | 0.5   | 0.05   | -1.54E+03 | 0.688    | -1.06E+03 | 1058.774      |            |
| Ele27 | 21989   | -6.61E+04 | 0.5   | 0.05   | -1.65E+03 | 0.738    | -1.22E+03 | 1220.06       |            |
| Ele28 | 22586   | -7.07E+04 | 0.5   | 0.05   | -1.77E+03 | 0.788    | -1.39E+03 | 1392.617      |            |
|       |         |           |       |        |           |          |           | <b>9380.9</b> | <b>kNm</b> |

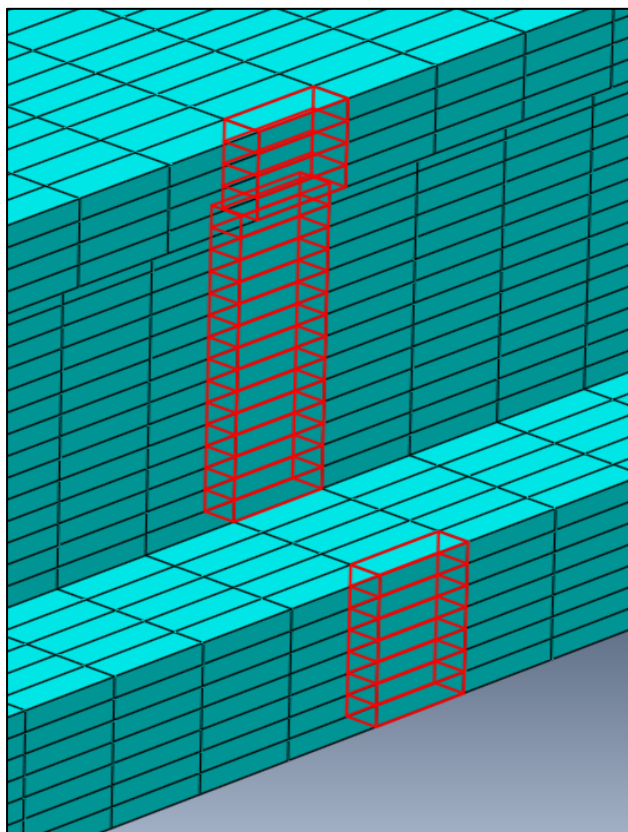


Figure 5.13: Considered mid-span elements

Table 5-3: Moment Calculation table for fixed supported condition

| Ele#  | Ele. Id | Stress    | width | height | Force     | distance | moment          | absmom     |
|-------|---------|-----------|-------|--------|-----------|----------|-----------------|------------|
| Ele1  | 10649   | 1.71E+04  | 0.65  | 0.05   | 5.56E+02  | 0.562    | 3.12E+02        | 312.4027   |
| Ele2  | 9654    | 1.55E+04  | 0.65  | 0.05   | 5.05E+02  | 0.512    | 2.59E+02        | 258.6921   |
| Ele3  | 8659    | 1.40E+04  | 0.65  | 0.05   | 4.55E+02  | 0.462    | 2.10E+02        | 210.0644   |
| Ele4  | 7664    | 1.24E+04  | 0.65  | 0.05   | 4.04E+02  | 0.412    | 1.67E+02        | 166.5127   |
| Ele5  | 6669    | 1.09E+04  | 0.65  | 0.05   | 3.54E+02  | 0.362    | 1.28E+02        | 128.0032   |
| Ele6  | 5674    | 9.32E+03  | 0.65  | 0.05   | 3.03E+02  | 0.312    | 9.45E+01        | 94.5408    |
| Ele7  | 4679    | 7.76E+03  | 0.65  | 0.05   | 2.52E+02  | 0.262    | 6.61E+01        | 66.11548   |
| Ele8  | 33723   | 6.33E+03  | 0.15  | 0.05   | 4.75E+01  | 0.212    | 1.01E+01        | 10.06171   |
| Ele9  | 33724   | 4.85E+03  | 0.15  | 0.05   | 3.64E+01  | 0.162    | 5.89E+00        | 5.889032   |
| Ele10 | 33725   | 3.35E+03  | 0.15  | 0.05   | 2.51E+01  | 0.112    | 2.81E+00        | 2.814823   |
| Ele11 | 33726   | 1.86E+03  | 0.15  | 0.05   | 1.40E+01  | 0.062    | 8.65E-01        | 0.865374   |
| Ele12 | 33727   | 366.452   | 0.15  | 0.05   | 2.75E+00  | 0.012    | 3.30E-02        | 0.032981   |
| Ele13 | 33728   | -1.12E+03 | 0.15  | 0.05   | -8.42E+00 | 0.038    | -3.20E-01       | 0.319833   |
| Ele14 | 33729   | -2.62E+03 | 0.15  | 0.05   | -1.96E+01 | 0.088    | -1.73E+00       | 1.727286   |
| Ele15 | 33730   | -4.11E+03 | 0.15  | 0.05   | -3.08E+01 | 0.138    | -4.25E+00       | 4.249814   |
| Ele16 | 33731   | -5.60E+03 | 0.15  | 0.05   | -4.20E+01 | 0.188    | -7.90E+00       | 7.899469   |
| Ele17 | 33732   | -7.09E+03 | 0.15  | 0.05   | -5.32E+01 | 0.238    | -1.27E+01       | 12.66006   |
| Ele18 | 33733   | -8.59E+03 | 0.15  | 0.05   | -6.44E+01 | 0.288    | -1.86E+01       | 18.55747   |
| Ele19 | 33734   | -1.01E+04 | 0.15  | 0.05   | -7.56E+01 | 0.338    | -2.56E+01       | 25.56091   |
| Ele20 | 33735   | -1.16E+04 | 0.15  | 0.05   | -8.69E+01 | 0.388    | -3.37E+01       | 33.71672   |
| Ele21 | 33736   | -1.31E+04 | 0.15  | 0.05   | -9.81E+01 | 0.438    | -4.30E+01       | 42.97043   |
| Ele22 | 33737   | -1.46E+04 | 0.15  | 0.05   | -1.09E+02 | 0.488    | -5.34E+01       | 53.37817   |
| Ele23 | 33738   | -1.61E+04 | 0.15  | 0.05   | -1.21E+02 | 0.538    | -6.49E+01       | 64.8824    |
| Ele24 | 33739   | -1.76E+04 | 0.15  | 0.05   | -1.32E+02 | 0.588    | -7.78E+01       | 77.78446   |
| Ele25 | 20795   | -1.89E+04 | 0.5   | 0.05   | -4.73E+02 | 0.638    | -3.02E+02       | 301.9479   |
| Ele26 | 21392   | -2.05E+04 | 0.5   | 0.05   | -5.12E+02 | 0.688    | -3.53E+02       | 352.502    |
| Ele27 | 21989   | -2.21E+04 | 0.5   | 0.05   | -5.52E+02 | 0.738    | -4.07E+02       | 407.09     |
| Ele28 | 22586   | -2.36E+04 | 0.5   | 0.05   | -5.91E+02 | 0.788    | -4.65E+02       | 465.4361   |
|       |         |           |       |        |           |          | <b>3126.678</b> | <b>kNm</b> |

Table 5-4: Comparisons of bending moments (solid elements)

|                                       | <b>ABAQUS<br/>value(kNm)</b> | <b>Manual<br/>Value(kNm)</b> | <b>%<br/>Error</b> |
|---------------------------------------|------------------------------|------------------------------|--------------------|
| <b>Simply supported<br/>condition</b> | 9380.90                      | 9384.50                      | 0.04               |
| <b>Fixed support condition</b>        | 3126.68                      | 3128.17                      | 0.05               |

W = 100kN/m and length of beam = 27.4m

## 5.6 Development of Vulnerability Curves.

Deterministic vulnerability curves were derived for two of the case study bridges namely Tenthill Creek Bridge and Kapernicks Bridge. This analysis enabled us to find out the

threshold magnitude of the flood intensity. In other words, the maximum flood velocity the bridge structure could withstand before it would fail.

### 5.6.1 Definition of Vulnerability/Resilience

There are many definitions reported in the literature for resilience. It can be defined as the ability to maintain functionality and return to normality following an extreme event making sure that the damage is tolerable and affordable (Hudson et al., 2012); (Lamond and Proverbs, 2009). It was defined as the ability of a system to reduce the chances of a shock, to absorb a shock if it occurs and to recover quickly after a shock (Cimellaro et al., 2010). According to their definition a resilient system should have the following qualities:

- Low probability of failure
- Even if it fails, very low impact on the society in terms of loss of lives, damage and negative economic and social consequences
- Low recovery time

Figure 5.14(a) shows the functionality of an infrastructure with time. At time  $T_0$ , the system was fully functioning [ $F(T_0, r_0)$ ] when the extreme event occurred. Functionality was reduced to  $F(T_0, r_d)$  due to the damage to the infrastructure system. At time  $T_R$ , the system completely recovered and started functioning as it was at time  $T_0$ . By considering the above qualities for a resilient system, it can be concluded that if the functionality due to damage is not much and/ or if the recovery time is less, then the system is more resilient. Therefore if the area shown in Figure 5.14(b) is less, the system is more resilient.

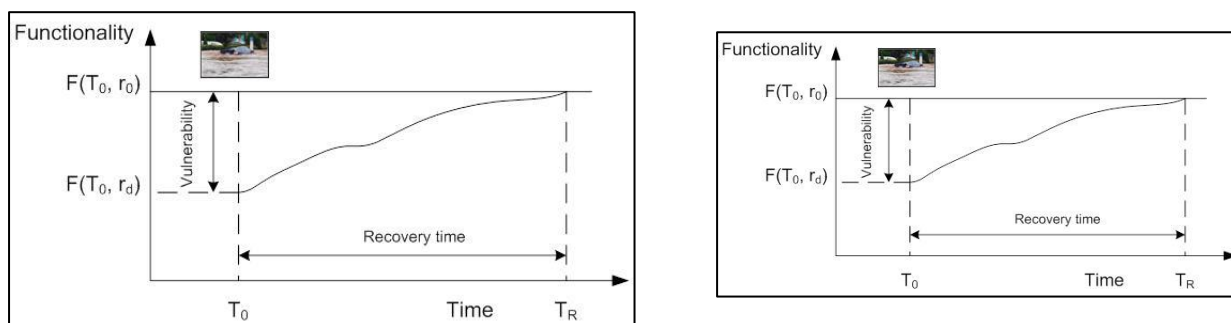


Figure 5.14: Representation of resilience

(a)

(b)

## 5.6.2 Forces on bridge resulting from flood event

AS 5100 Bridge Design code (Section 15 of AS 5100.2-2004) Australia (2004) gives relevant equations to calculate the flood induced forces on bridge resulting from water flow, debris and log impact. Relevant equations given in all 3 major bridge design specifications (American, European and Australian) to calculate the flood induced force on the bridge structure were compared and found that they didn't exhibit huge difference between them. Given the virtue of its simplicity, applicability for Australia's context and the recent published work which confirmed the appropriateness of the values given Nasim et al. (2017), this has been chosen to be used in this research.

### 5.6.2.1 Forces on superstructure due to water flow

When the bridge superstructure is partially or fully inundated in a flood, it is subjected to a horizontal drag force ( $F_d$ ) normal to its longitudinal axis and a vertical lift force ( $F_l$ ) as given in AS 5100.

$$(F_d) = 0.5C_dV^2A_s \quad \text{Equation 5-1}$$

Where  $C_d$  = drag coefficient read from the chart given in the code

$V$  = mean velocity of water flow (flood) (m/s)

$A_s$  = wetted area of the superstructure, including any railings or parapets, projected on a plane normal to the water flow ( $m^2$ ), and ( $F_d$ ) would be in kN.

$$(F_l) = 0.5C_lV^2A_l \quad \text{Equation 5-2}$$

Where  $C_l$  = lift coefficient read from the chart given in the code

$V$  = mean velocity of water flow (flood) (m/s)

$A_l$  = Plan deck area of the superstructure ( $m^2$ ) and ( $F_l$ ) would be in kN.

### 5.6.2.2 Forces due to Debris

Debris load acting on superstructures is given by the code as,

$$F_{deb} = 0.5C_dV^2A_{deb} \quad \text{Equation 5-3}$$

Where  $C_d$  = drag coefficient read from the chart given in the code

$V$  = mean velocity of water flow (flood) (m/s) ;  $F_{deb}$  would be in kN

$A_{deb}$  = Projected area of the debris mat described in the code ( $m^2$ ).

### 5.6.2.3 Forces due to Log Impact

Where floating logs are a possible hazard, the drag forces exerted by such logs directly hitting bridge girder (superstructure) shall be calculated on the assumptions that a log with a minimum mass of 2t will be stopped in a distance of 75mm for such solid girder (superstructure). However for the bridge in question, this mass was taken equivalent to a mass of a shipping container to simulate the actual condition.

$F_{log}$  shall thus be given by the following Equation 5-4

$$F_{log} = \frac{mV^2}{2d} \quad \text{Equation 5-4}$$

Where  $m$ = mass of a shipping container (24000kg),  $d$ = 0.075m and  $V$ = flood velocity (m/s)

### 5.6.3 Characterization of Damage / measure of the structural damage

There are several quantitative damage measures that characterize the state of structures in the aftermath of any natural hazard. Most of the definitions consider damage to individual elements and are based on ductility ratio or dissipated energy (Banon et al., 1980). Examples of damage indices for reinforced concrete structures include those by Park et al. (1985), Chung et al. (1989) and DiPasquale and Cakmak (1990). The Krawinkler index by Krawinkler (2009) is a measure frequently used to quantify damage in steel components.

For reinforced concrete structures, (Park et al., 1985) model has been widely used in recent years because it is simple and because it has been calibrated using data from various structures damaged during past earthquakes.

Newmark and Rosenblueth (1971) proposed that the ductility ratio, defined as the ratio of the maximum displacement to the yielding displacement  $\frac{X_M}{X_y}$  be used as a measure of the structural damage. Other measures or indices, always expressed as a function of the maximum displacement, have been introduced by Oliveira (1975) and by Bresler (1977), who took into account the cumulative nature of damage, as well as the complexity of a structure, considered as an assemblage of  $m$  elements. The damage index for the global structure was defined as

$$\delta = \frac{1}{\sum_{i=1}^m \omega_i} \sum_{i=1}^m \frac{\omega_i \eta_i S_i}{\gamma_i r_i} \quad \text{Equation 5-5}$$

Where  $S_i$  is the demand and  $r_i$  is the capacity, corresponding to the  $i^{th}$  element, the  $\omega_i$  are weights, to account for the relative importance of different elements, and  $\eta_i$  and  $\gamma_i$  are service factors, that model the cumulative nature of the damage.

Banon and Veneziano (1982) pointed out the necessity to consider separately the two components of damage. They defined a damage function

$$\delta = f(FDR, NCR) \quad \text{Equation 5-6}$$

where the flexural damage ratio (FDR) is the ratio between the initial flexural stiffness  $K_f$  to the reduced secant stiffness  $K_r$  for a reinforced concrete cantilevered element.

$$FDR = \frac{K_f}{K_r} \quad \text{Equation 5-7}$$

The normalized cumulative rotation NCR is the ratio between the cumulative plastic rotation in 'n' numbers of cycles and the yielding rotation of the nonlinear spring, considered in their model

$$NCR = \frac{\sum_{i=1}^{ncycle} |\theta_i|}{\theta_y} \quad \text{Equation 5-8}$$

Park et al. (1985) suggested the use of a linear combination of ductility and of an energy factor, defining an index  $\delta$

$$\delta = \frac{X_M}{X_u} + \beta \frac{\int dE}{F_y X_u} \quad \text{Equation 5-9}$$

Where  $X_u$  is the ultimate displacement,  $F_y$  the yielding force,  $dE$  the elementary energy dissipated in the system, and  $\beta$  a parameter, estimated from experimental data.

According to Park et al. (1985) this linear relationship must be viewed as a first order approximation to a more complicated, unknown function. This approximation is valid in the region, close to the ultimate displacement of the element.

Stephens (1985) developed a damage function, on the basis of a hypothesis formulated by Yao and Munse (1963). The damage, subsequent to the  $i^{th}$  cycle of deformation, is given by:

$$\Delta\delta_i = \left( \frac{\Delta\delta_{pt}}{\Delta\delta_{pf}} \right)_i^\alpha \quad \text{Equation 5-10}$$

Where

$\Delta\delta_{pt}$ = positive change in plastic deformation

$\Delta\delta_{pf}$ = positive change in plastic deformation to failure

$\alpha = 1 - br_l$ , where b is a constant and  $r_l$  is relative deformation ratio,  $\frac{\Delta\delta_{pt}}{\Delta\delta_{pf}}$ , between the negative and the positive change in plastic deformation over a cycle. This index takes into account the dissymmetry in the behaviour of reinforced concrete elements, as well as the influence of the geometry of the cycle on the accumulation mechanism.

Different types of Damage Indices described above are all summarized in the Table 5-5(below):

Table 5-5: Damage indices

| Damage Index        | Formula   | Literature                                 |
|---------------------|---|--|
| Ductility ratio     | $\frac{X_M}{X_y}$   | (Newmark and Rosenblueth, 1971)            |
| $\delta_{Bertero}$  | $\frac{1}{\sum_{i=1}^m \omega_i} \sum_{i=1}^m \frac{\omega_i \eta_i S_i}{\gamma_i r_i}$   | (Bertero and Bresler, 1977)                |
| $\delta_{Banon}$    | $f\left(\frac{K_f}{K_r}, \frac{\sum_{i=1}^{ncycle}  \theta_i }{\theta_y}\right)$          | (Banon and Veneziano, 1982)                |
| $\delta_{Park}$     | $\frac{X_M}{X_u} + \beta \frac{\int dE}{F_y X_u}$   | (Park et al., 1985)                        |
| $\delta_{Stephens}$ | $\sum_{i=1}^{ncycle} \left( \frac{\Delta\delta_{pt}}{\Delta\delta_{pf}} \right)_i^\alpha$ | (Stephens, 1985) and (Yao and Munse, 1963) |

For a network level analysis of structures, the above indices are complex and cannot be accommodated in a generic analysis method. To simplify the understanding of the vulnerability based on risk of failure, we have defined a damage index as

$$\frac{\text{Applied load induced design action}}{\text{Structural Capacity}}$$

Equation 5-11

Whilst this is a simplified measure, for quantifying failure of structure this is considered to be adequate. This definition is based on structural capacity which is an indirect representation of the displacement. However a displacement ratio may not directly define failure of a structure and the proposed index can directly give the likelihood of failure.

#### 5.6.4 Deriving Damage Index

In this research, the structural damage to the bridge girder is measured using Damage Index (DI) that is defined as the ratio between the moment induced by flood loading on the bridge girder ( $M^*$ ) and the existing moment capacity of the bridge girder ( $\phi M_u$ ) as given in Equation 5-12. Damage Indices are first derived to generate vulnerability curves for the Bridges under different flood exposure conditions. The effects of flood flow, debris and the log impact on the bridge girder have been considered to derive the damage indices. The damage index can also be defined using the costs associated with retrofitting/repairing the bridge under flood.

It is noted here that the definition of failure using  $\frac{M^*}{\phi M_u}$  only consider flexural failure. Shear failure can also be critical in the case of short span structures which are not considered in this study because most of the bridges reported are long span bridges.

$$\text{Damage Index DI} = \frac{M^*}{\phi M_u} \quad \text{Equation 5-12}$$

#### 5.6.5 Calculation of the existing moment capacity of the girder ( $\phi M_u$ )

In accordance with the Australian codes of practice for structural design, the capacity analysis methods contained in this section are based on ultimate limit-state philosophy. This ensures that a member will not become unfit for its intended use. The capacity analysis results would be compared with structural analysis results to identify the deficiencies. This approach sets acceptable levels of safety against the occurrence of all possible failure situations. The nominal strength of a member is assessed based on the possible failure modes and subsequent strains and stresses in each material.

A typical bridge girder section is shown in Figure 5.15(below). The positive and negative flexural and shear capacities of the section were calculated in accordance with Australian standards (AS3600, 1988). The nominal steel reinforcing bars areas; nominal steel yield strength of 400 MPa for longitudinal reinforcement and 240 MPa for shear reinforcement and nominal concrete compressive strength of 20 MPa were used in the section capacity analysis. The degradation due to corrosion of the steel and creep and shrinkage of the concrete were ignored.

A detailed study on the arrangement of the reinforcement bars and cover blocks placed inside the girder was first warranted to derive the actual existing flexural capacity of the girder. An excel sheet as shown in Table 5-6(below) was utilized to calculate the positive and negative flexural force and the moments resulting from the reinforcing bars and the concrete. Since the flood impact loading was exerted laterally on the girder, the minor axis bending moment was considered. First the position of the neutral axis of the girder about the minor axis was established. Neutral axis would lie where the total tensile and compressive force add up to zero. An initial guess for the neutral axis depth ( $d_n$ ) was made and subsequent tensile and compressive force were calculated based on this assumption. Neutral axis depth ( $d_n$ ) was solved for using Excel add in “solver”. Finally the required existing moment capacity was calculated using the established neutral axis depth. Based on the above assumptions and the procedures, the existing moment capacity of the concrete girder section was found to be 600kNm.

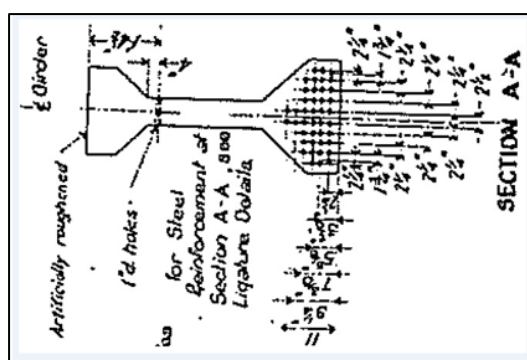


Figure 5.15: Bridge girder section

Table 5-6: Excel Sheet for Moment Capacity calculation

| parameter              | delta                      | inches | value    | Stain   | Stress | no       | A (mm2)  | F(N)(+ve tension | M(Nmm)                         |                     |
|------------------------|----------------------------|--------|----------|---------|--------|----------|----------|------------------|--------------------------------|---------------------|
| dn                     |                            |        | 209.006  | mm      |        |          |          |                  |                                |                     |
| 10                     | 1.5                        | 1.5    | 38.1     | mm      | 0.0025 | 4.91E+02 | 3        | 339.292          | -1.66E+05 -6.34E+06            |                     |
| 9                      | 2.25                       | 3.75   | 95.25    | mm      | 0.0016 | 3.27E+02 | 4        | 452.3893         | -1.48E+05 -1.41E+07            |                     |
| 8                      | 1.75                       | 5.5    | 139.7    | mm      | 0.0010 | 1.99E+02 | 4        | 452.3893         | -9.00E+04 -1.26E+07            |                     |
| 7                      | 2.25                       | 7.75   | 196.85   | mm      | 0.0002 | 3.49E+01 | 4        | 452.3893         | -1.58E+04 -3.11E+06            |                     |
| 6                      | 13                         | 2.25   | 10       | 254     | mm     | 0.0006   | 1.29E+02 | 12               | 1357.168                       | 1.75E+05 4.45E+07   |
| 5                      | 12                         | 2.25   | 12.25    | 311.15  | mm     | 0.0015   | 2.93E+02 | 12               | 1357.168                       | 3.98E+05 1.24E+08   |
| 4                      |                            | 2.25   | 14.5     | 368.3   | mm     | 0.0023   | 4.57E+02 | 4                | 452.3893                       | 2.07E+05 7.62E+07   |
| 3                      |                            | 2.25   | 16.75    | 425.45  | mm     | 0.0031   | 6.21E+02 | 4                | 452.3893                       | 2.81E+05 1.20E+08   |
| 2                      |                            | 1.75   | 18.5     | 469.9   | mm     | 0.0037   | 7.49E+02 | 4                | 452.3893                       | 3.39E+05 1.59E+08   |
| 1                      |                            | 2.25   | 20.75    | 527.05  | mm     | 0.0046   | 9.13E+02 | 3                | 339.292                        | 3.10E+05 1.63E+08   |
| 14                     |                            |        |          | 114.1   | mm     | 0.0014   | 2.72E+02 | 2                | 226.1947                       | -6.16E+04 -7.03E+06 |
| 11                     |                            |        |          | 520.9   | mm     | 0.0045   | 8.95E+02 | 2                | 226.1947                       | 2.03E+05 1.05E+08   |
| mm in 1 inch           |                            |        | 25.4     | mm/inch |        |          |          |                  | 7.49E+08                       |                     |
| E (steel)              |                            |        | 2.00E+05 | Mpa     |        |          |          |                  |                                |                     |
| ε                      |                            |        | 0.003    |         |        |          |          |                  |                                |                     |
| Rebar area             |                            |        | 113.0973 | mm2     |        |          |          |                  |                                |                     |
| stress (F/area) * 0.85 |                            |        | 27.2     | MPa     |        |          |          |                  |                                |                     |
| Dimensio               | total right (height        |        | 635      | mm      |        |          |          |                  |                                |                     |
|                        | middle (height             |        | 152      | mm      |        |          |          |                  |                                |                     |
|                        | total_left_height          |        | 483      | mm      |        |          |          |                  |                                |                     |
|                        | width (right)              |        | 180      | mm      |        |          |          |                  |                                |                     |
|                        | width (left)               |        | 152      | mm      |        |          |          |                  |                                |                     |
|                        | width(left_slant           |        | 165      | mm      |        |          |          |                  |                                |                     |
|                        | width (right_slant         |        | 240      | mm      |        |          |          |                  |                                |                     |
|                        | width_middle               |        | 635      | mm      |        |          |          |                  |                                |                     |
|                        | width_total                |        | 1372     | mm      |        |          |          |                  |                                |                     |
|                        | height_right_slant         |        | 241.5    | mm      |        |          |          |                  |                                |                     |
|                        | height_right_slant+rectang |        | 393.5    |         |        |          |          |                  |                                |                     |
|                        | Area_1 (A)                 |        | 103265.2 | mm2     |        |          |          |                  |                                |                     |
|                        | Area_2 (A+B)               |        | 311809.2 | mm2     |        |          |          |                  |                                |                     |
|                        | total Area                 |        | 431063.5 | mm2     |        |          |          |                  |                                |                     |
|                        | width_slant_right          |        | 387.7078 | mm      |        |          |          |                  |                                |                     |
|                        | C_trapizium; x is from b   |        |          |         |        |          |          |                  | $x = [(b+2a) / (3*(a+b))] * h$ |                     |
|                        | height_left_slant          |        | 133.006  | mm      |        |          |          |                  |                                |                     |
|                        | width_slant_left           | b      | 204.238  | mm      |        |          |          |                  |                                |                     |

### 5.6.6 Estimating flood induced bending moment (M\*)

In order to estimate flood induced bending moment on the bridge girder, general purpose finite element software, ABAQUS was used to model the bridge deck and the girders for both the bridges. Self-weight of the bridge, the drag and the lift force due to water flow, debris force and the log impact force were considered in the analysis. Flood load was applied in the y-direction as a uniform pressure all along the end girder face perpendicular to y-direction as shown in Figure 5.16

ABAQUS model was run for different flood velocities ranging from 0.5m/s to 5.0m/s in steps of 0.50m/s increment. The model was run separately for the effect of flood flow, debris impact, log (container in this case) impact. Figure 5.16(below) depicts the bridge deck model used in the analysis.

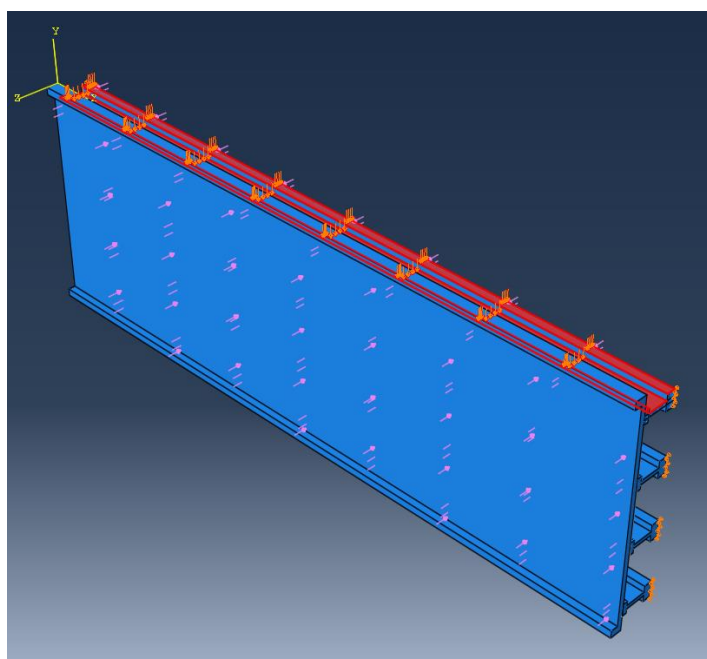


Figure 5.16: ABAQUS bridge Deck Model

Normal stress (S22) that caused minor axis bending moment to the end girder in the mid span section were all extracted from the output and the required bending moment  $M^*$  were calculated using the established method in section 5.3.2.

It is obvious that the end girder would resist more impact than the rest of the inner girders because the moving flood water would have already lost some of its kinetic energy when it hit the other girders in the series. It was observed that the support reactions at the girders were descending in the direction of flood flow. First end girder shared the highest support reaction force while the last girder (4<sup>th</sup> girder in the direction of flood flow) shared the lowest as shown in Table 5-7. ABAQUS output data obtained for these support reactions are given in Appendix 2

Table 5-7: Support reactions at girders

| Position of girders | Support reactions (kN)  |                          |        |
|---------------------|-------------------------|--------------------------|--------|
|                     | Left hand support (LHS) | Right hand support (RHS) | Total  |
| First end girder    | 102.22                  | 77.30                    | 179.52 |
| First inner girder  | 99.45                   | 74.84                    | 174.29 |
| Second inner girder | 96.15                   | 73.58                    | 169.73 |
| Third inner girder  | 81.16                   | 71.02                    | 152.18 |

Using Equation 5-12(above), damage indices for different flood intensities were calculated as shown in Table 5-8(below) for Kapernicks Bridge and Table 5-9(below) for Tenthill Creek Bridge

Table 5-8: Damage Indices for Kapernicks Bridge

| <b>Flood Velocity (m/s)</b> | <b><math>M^*</math> (kNm)</b> | <b><math>DI = \frac{M^*}{\phi M_u}</math></b> |
|-----------------------------|-------------------------------|---|
| 0.5                         | 85.68                         | 0.18  |
| 1.0                         | 107.54                        | 0.22  |
| 1.5                         | 143.97                        | 0.30  |
| 2.0                         | 194.98                        | 0.41  |
| 2.5                         | 260.56                        | 0.54  |
| 3.0                         | 340.72                        | 0.71  |
| 3.5                         | 435.44                        | 0.91  |
| 4.0                         | 544.73                        | 1.14  |
| 4.5                         | 668.64                        | 1.39  |
| 5.0                         | 807.10                        | 1.69  |

Table 5-9: Damage Indices for Tenthill Creek Bridge

| <b>Flood Velocity (m/s)</b> | <b><math>M^*</math> (kNm)</b> | <b><math>DI = \frac{M^*}{\phi M_u}</math></b> |
|-----------------------------|-------------------------------|---|
| 0.5                         | 8.54                          | 0.02  |
| 1.0                         | 48.35                         | 0.01  |
| 1.5                         | 114.71                        | 0.24  |
| 2.0                         | 207.61                        | 0.43  |
| 2.5                         | 327.04                        | 0.68  |
| 3.0                         | 473.02                        | 0.99  |
| 3.5                         | 645.53                        | 1.35  |

|     |         |      |
|-----|---------|------|
| 4.0 | 844.57  | 1.75 |
| 4.5 | 1070.2  | 2.22 |
| 5.0 | 1324.27 | 2.78 |

$M_u = 600\text{kNm}$  (Existing capacity of the girder as calculated from the section analysis of the reinforced concrete girder)

$\phi = 0.8$  (Safety factor for the moment capacity as per AS 5100)

Table 5-10 and Table 5-11 summarize Damage Indices calculated for all three different types of flood impact conditions considered for both the bridges in the analysis.

Table 5-10: Damage Indices for different types of flood impact for Kapernicks Bridge

| Flood Velocity (m/s) | DI              |                 |                 |
|----------------------|-----------------|-----------------|-----------------|
|                      | Flood impact #1 | Flood impact #2 | Flood impact #3 |
| 0.5                  | 0.18            | 0.20            | 0.41            |
| 1.0                  | 0.22            | 0.30            | 1.15            |
| 1.5                  | 0.30            | 0.47            | 2.38            |
| 2.0                  | 0.41            | 0.71            | 4.17            |
| 2.5                  | 0.54            | 1.02            | 6.25            |
| 3.0                  | 0.71            | 1.39            | 9.09            |
| 3.5                  | 0.91            | 1.85            | 12.50           |
| 4.0                  | 1.14            | 2.38            | 16.67           |
| 4.5                  | 1.39            | 2.94            | 20.00           |
| 5.0                  | 1.69            | 3.57            | 25.00           |

Table 5-11: Damage Indices for different types of flood impact for Tent hill Creek Bridge

| Flood Velocity (m/s) | DI              |                 |                 |
|----------------------|-----------------|-----------------|-----------------|
|                      | Flood impact #1 | Flood impact #2 | Flood impact #3 |
| 0.5                  | 0.02            | 0.04            | 0.26            |
| 1.0                  | 0.10            | 0.20            | 1.05            |
| 1.5                  | 0.24            | 0.48            | 2.38            |
| 2.0                  | 0.43            | 0.87            | 4.17            |
| 2.5                  | 0.68            | 1.37            | 6.67            |
| 3.0                  | 0.99            | 1.96            | 10.00           |
| 3.5                  | 1.35            | 2.70            | 14.29           |
| 4.0                  | 1.79            | 3.57            | 16.67           |
| 4.5                  | 2.22            | 4.55            | 20.00           |
| 5.0                  | 2.78            | 5.26            | 25.00           |

Flood impact #1: Impact from flood flow only

Flood impact #2: Impact from (flood flow + Debris)

Flood impact #3: Impact from (flood flow + Debris + Container)

### 5.6.7 Deriving Deterministic Vulnerability Curves

Damage Indices values are plotted against the flood exposure condition (flood velocity in this case) to develop vulnerability curves. These curves are generated for the above three different types of flood impacts for both the bridges and are shown in Figure 5.17 and Figure 5.18(below).

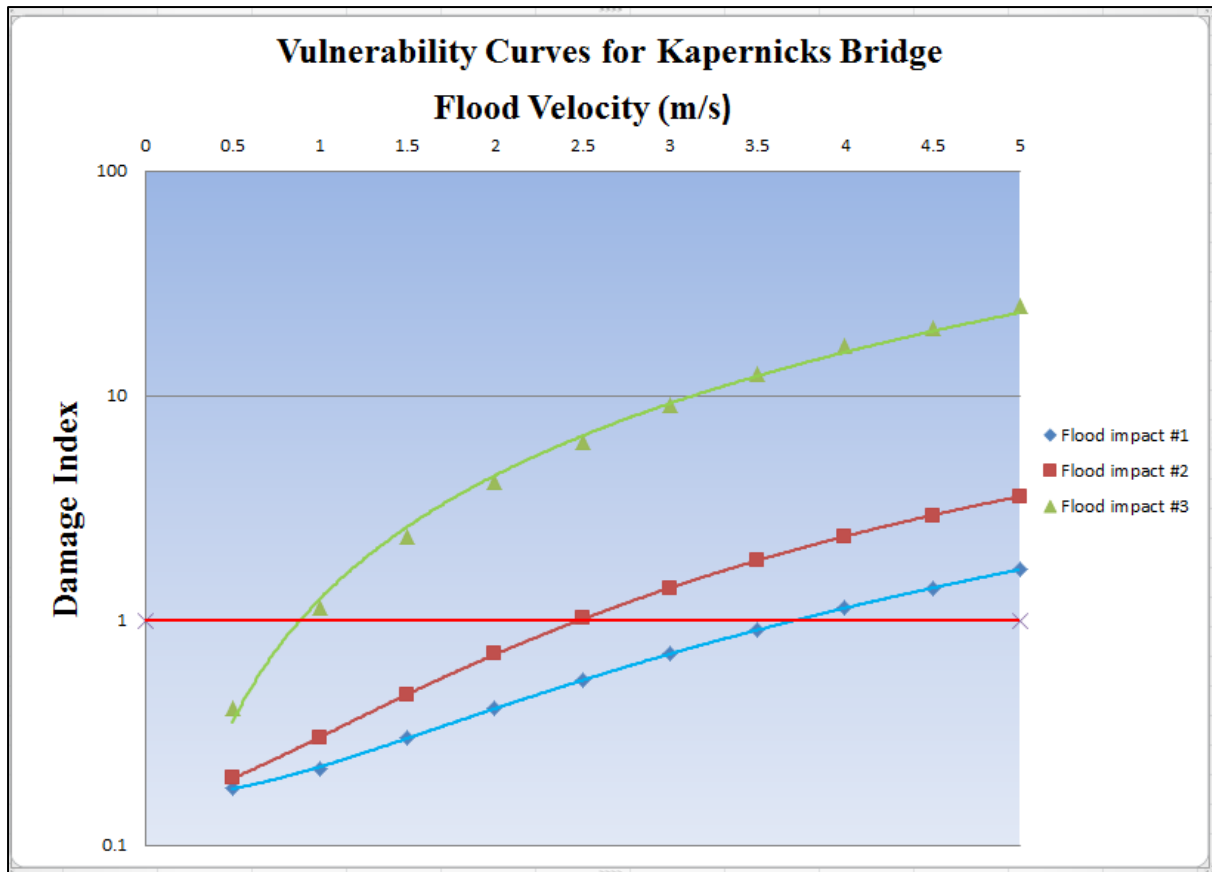


Figure 5.17: Vulnerability curves for Kapernicks bridge

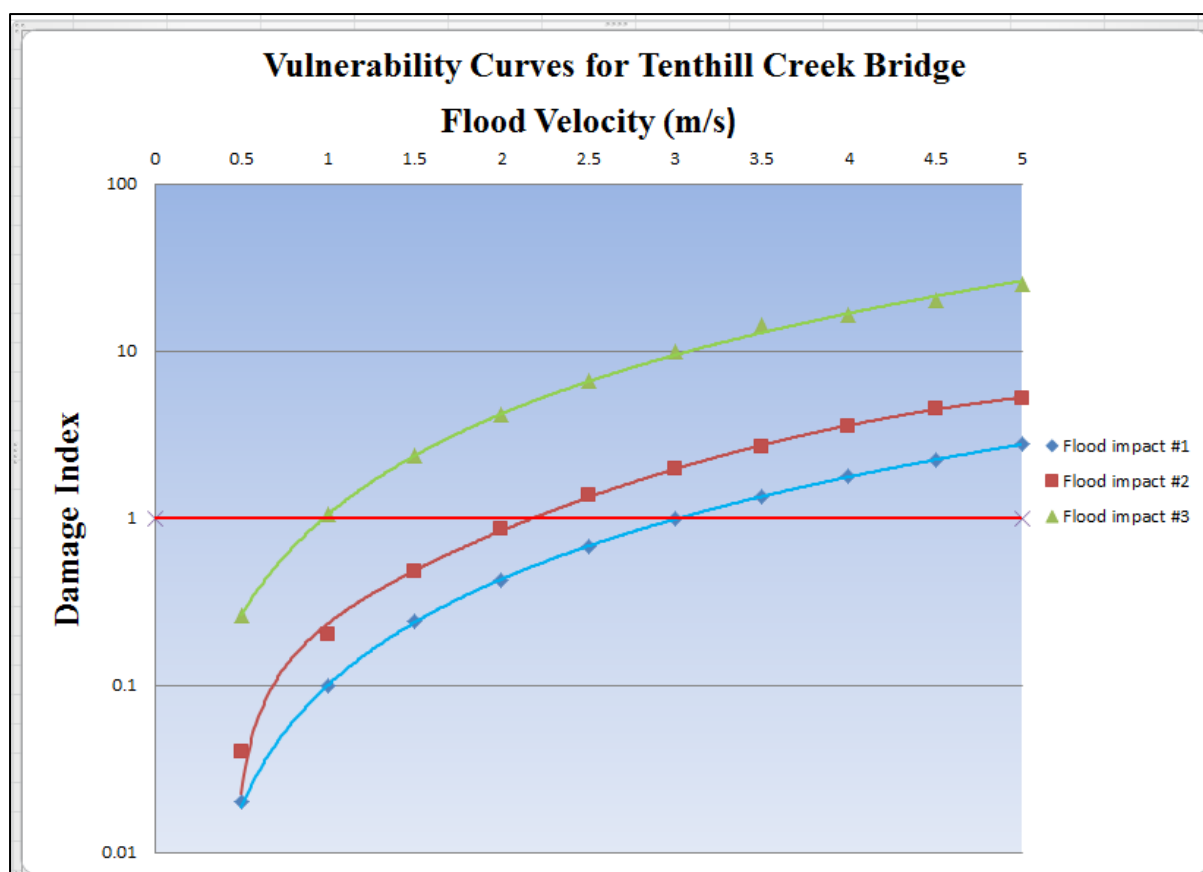


Figure 5.18: Vulnerability curves for Tenthill Creek bridge

### 5.6.8 Severity of Damage

A Facility Condition Index (FCI) has been used in the past, initially by the U.S. Navy to evaluate the condition of vessels and later in the 1990s to do the same for buildings in order to prioritize funding for repair/replacement (Facility Condition Index 2011). An FCI gives a numerical value for the condition of a building by considering any needed repair or upgrade requirements of the building with respect to the replacement value of relevant building components of interest. Similar to the FCI for buildings, a damage index (DI) proposed by Nishijima and Faber (2009) has been used in the past to assess the condition of infrastructure. The FCI as well as DI completely depend on the condition assessment of the inspector. Benchmarking the level of FCI or DI for an infrastructure depends on the rules and regulations, budget constraints, and the service level defined by the organization to which the infrastructure belongs. In this research, it was decided to use Equation 5-13(below) to estimate the severity of damage. It provides a comparative indication of the flood induced bending moment ( $M^*$ ) with respect to the existing moment capacity of the bridge girder ( $\phi M_u$ ).

$$DI = \frac{M^*}{\phi M_u} \quad \text{Equation 5-13}$$

Theoretically, a DI equal to one warrants complete damage according to the above defined equation. Higher DI values indicate higher severity in terms damage. Therefore, DI can be used as a measure of damage severity. This thesis proposes five levels of damage severity based on DI values as discussed below.

#### **5.6.8.1 Complete Damage**

If the calculated DI value from Equation 5-13(above) is equal to or greater than one, it warrants a full replacement of the structure. Generally, the decision to replace a damaged bridge can be made based on the site investigations, without calculating the DI.

#### **5.6.8.2 Extreme Damage**

When the DI value is in the range of 0.8-1.0, it can be classified as extreme damage. In such cases, the decision to repair should be critically assessed with respect to design life and associated maintenance cost. In some instances, particularly, when the DI is very close to one, replacement is worth considering rather than repair, if the whole life-cycle cost can be minimized by replacement.

#### **5.6.8.3 Major Damage**

Bridge can be deemed to be subjected to major damage if the DI falls within the 0.7–0.8 range. In such cases, great attention should be given to areas that have been subjected to major damage. Vulnerability of such areas to future events should be critically assessed and relevant measures should be taken to avoid further damage, assuming that there is a possibility of another extreme flood event occurring in the near future.

#### **5.6.8.4 Moderate Damage**

Cases with DI values between 0.6 and 0.7 can be categorized as moderate damage. However, when the DI is closer to upper limit, it may be worth examining the accuracy of prediction as well as the criticality of the damage zone. Generally, bridges with moderate damage can be rectified very quickly to minimize indirect costs associated with closure of the bridge.

#### **5.6.8.5 Minor Damage**

When the DI value is between 0.5-0.6, it is classified as a minor damage. Such incidents can be repaired very quickly without any significant impact to the performance of the bridge.

The above severity classifications are summarized in the Table 5-12(below)

Table 5-12: Table of damage severity classification

| Severity of Damage | Damage Index |
|--------------------|--------------|
| Complete Damage    | $\geq 1.0$   |
| Extreme Damage     | 0.8-1.0      |
| Major Damage       | 0.7-0.8      |
| Moderate Damage    | 0.6-0.7      |
| Minor Damage       | 0.5-0.6      |

### 5.6.9 Results and discussion

Reinforced or pre-stressed concrete girder bridges are a common design configuration used in Australia. During the Lockyer Valley floods in 2013, vulnerability of girder bridges was observed by significant damage to these structures. Structural performances of Kapernicks concrete girder bridge and Tent hill concrete girder bridge have been investigated. For the girder to fail under the flooding the damage index (DI) must be equal to or greater than one. The maximum allowable flood velocity to satisfy this condition could be read from the above structural vulnerability curves. For both the bridges under investigation, the threshold hazard intensity measure (Flood velocity) when  $DI = 1$ , are shown in Table 5-13 and

Table 5-14(below) while the hazard intensity measure (Flood velocity) for different severity of damage are shown in

Table 5-15 and

Table 5-16(below) based on the deterministic analysis.

Table 5-13: Threshold hazard intensity measure for Kapernicks bridge (DI=1)

| <b>Type of flood impact</b> | <b>Threshold hazard intensity measure<br/>(Flood velocity when DI =1)</b> |
|-----------------------------|---|
| Flood Impact #1             | 3.71  |
| Flood Impact #2             | 2.46  |
| Flood Impact #3             | 0.93  |

Table 5-14: Threshold hazard intensity measure for Tenthill creek bridge (DI=1)

| <b>Type of flood impact</b> | <b>Threshold hazard intensity measure<br/>(Flood velocity when DI =1)</b> |
|-----------------------------|---|
| Flood Impact #1             | 3.02  |
| Flood Impact #2             | 2.11  |
| Flood Impact #3             | 0.97  |

Table 5-15: Hazard Intensity Measure for Kapernicks Bridge

| <b>Severity of Damage</b> | <b>Hazard Intensity Measure – Flood Velocity (m/s)</b> |                        |                        |
|---------------------------|--|------------------------|------------------------|
|                           | <b>Flood Impact #1</b>                                 | <b>Flood Impact #2</b> | <b>Flood Impact #3</b> |
| Complete Damage           | 3.48-3.71  | 2.31-2.46              | 0.88-0.93              |
| Extreme Damage            | 3.24-3.48  | 2.15-2.31              | 0.82-0.88              |
| Major Damage              | 2.97-3.24  | 1.97-2.15              | 0.76-0.82              |
| Moderate Damage           | 2.68-2.97  | 1.78-1.97              | 0.70-0.76              |
| Minor Damage              | 2.36-2.68  | 1.56-1.78              | 0.63-0.70              |

Table 5-16: Hazard Intensity Measure for Tenthill Creek Bridge

| Severity of Damage | Hazard Intensity Measure – Flood Velocity (m/s) |                 |                 |
|--------------------|---|-----------------|-----------------|
|                    | Flood Impact #1                                 | Flood Impact #2 | Flood Impact #3 |
| Complete Damage    | 2.86-3.02                                       | 2.00-2.11       | 0.94-0.97       |
| Extreme Damage     | 2.70-2.86                                       | 1.89-2.00       | 0.90-0.94       |
| Major Damage       | 2.53-2.70                                       | 1.77-1.89       | 0.86-0.90       |
| Moderate Damage    | 2.35-2.53                                       | 1.64-1.77       | 0.82-0.86       |
| Minor Damage       | 2.15-2.35                                       | 1.50-1.64       | 0.78-0.82       |

### 5.7 Validation of this research

It was reported that Kapernicks Bridge failed during 2011 flood event in Queensland and fully replaced by Queensland Road Authority. The new design flood velocity for the bridge was taken as 4.00 m/s considering the actual flood velocity the bridge experienced in 2011 flood event. As shown in Table 5-13, this research has found the threshold velocity for Kapernicks Bridge as 3.71 m /s which gives 93% accuracy to the actual value. This validates researcher’s findings in this thesis.

### 5.8 Conclusions of Chapter 5

This chapter presented numerical modelling of the case study bridge. Brief description about ABAQUS finite element software used to model the bridge superstructure has been presented. Bridge geometry and its structural details have then been captured.

Bridge deck and the girder have been modelled in ABAQUS using two types of elements available from ABAQUS element library. Maximum bending moment at the mid span of the girder was derived either using direct bending moment out or elemental normal stress.

A method to calculate the bending moment from elemental normal stress output has been proposed and the methodology has been validated.

The calculated flood velocity which would cause failure of the Kapernicks Bridge was shown to be close to the observed value during 2011 floods which created failure of the bridge.

Vulnerability curves for 2 case study bridges have been derived. Damage to the bridge girder is quantified using structural capacity based Damage Index. Damage index versus hazard intensity (Flood velocity) is plotted to generate these deterministic vulnerability curves.

Severity of Damage to the bridge girder is defined using 5 different scales from complete damage to minor damage and the threshold flood velocity for each damage severity has been derived for both the bridges.

## 6 Numerical Modelling of the case study bridge – Probabilistic Analysis

### 6.1 Introduction

Chapter 5 presented the deterministic analysis of the structural vulnerability of concrete girder bridge decks under flood loading. Fragility modelling gives a quantified performance measure, including uncertainty, and reliability of a structural system under a set of loading conditions. A fragility curve is a statistical function which describes the performance (or damage state) for a given demand (or loading condition). The curves are typically S-shaped, which describes the uncertainty in the system's capacity to withstand a loading condition (Schultz et al., 2010). For example, a gradual curve implies a high uncertainty in the performance for a given demand, whereas a steep curve implies a high certainty in the performance. Fragility curves with high uncertainty may lead to an under prediction of performance at low demands, and over prediction of performance at high demands (Schultz et al., 2010). There are typically four methods used to develop fragility curves: judgmental, empirical, analytical, and hybrid (Schultz et al., 2010). An advantage of using fragility curves is that they incorporate all of the hazards and uncertainty into a single function

We need to identify the conditions or limit states in which the structural system fails a certain performance objective, which can be either strength or deformation related. The probability of a limit state or a function subjected to loading can be expressed as

$$P (LS) = \sum P (LS | D = x)P(D = x) \quad \text{Equation 6-1}$$

Where D is a random demand on the system, e.g., damage index, inundation ratio, wind speed or spectral acceleration, and  $P (LS|D= x)$  is the conditional probability of demand equalling the limit state. The hazard is defined by the probability  $P(D= x)$  and the fragility is defined as the conditional probability  $P(LS|D= x)$ . If the hazard is defined as a continuous function of  $x$ , then the summation in Equation 6-1 is replaced by the convolution integral of structural reliability theory (Rosowsky and Ellingwood, 2002).

Rosowsky and Ellingwood (2002) state that the fragility provides a less informative measure of safety than a fully coupled risk analysis; however, there are numerous benefits from pure fragility analysis. A fragility analysis is less cumbersome than a fully coupled risk analysis

and the hazard probability is not required. In addition, it is independent of location since only the structure and loading intensity are used in its development.

The fragility of a structural component or system is often modelled by a lognormal cumulative distribution function, CDF,

$$FR(x) = \Phi \left[ \ln \left( \frac{x}{\lambda_R} \right) / \xi_R \right] \quad \text{Equation 6-2}$$

in which  $\lambda_R$  is the logarithmic mean of capacity, R, and  $\xi_R$  is the logarithmic standard deviation (Rosowsky and Ellingwood, 2002)

When performing a risk analysis, hazard curves can be obtained from a number of sources or from a statistical analysis. For example, flood discharge values can be obtained from the insurance agency or department of meteorology in the area of interest. Figure 6.1(below) displays a set of fragilities based on a certain demand. In the research presented here, the demand would be a range of damage indices calculated for different flood demand.

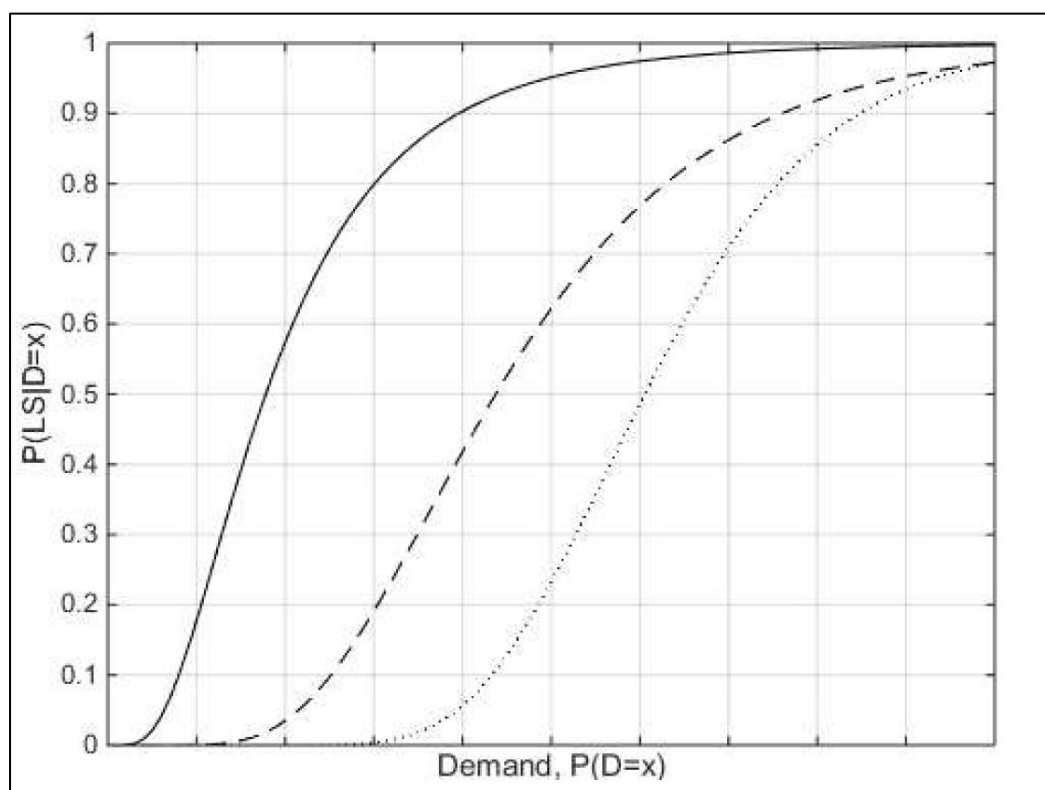


Figure 6.1: Example fragilities for illustration

Development of probability-based design began with the American National Standards Institute (ANSI) Standard A58 (Ellingwood, 1980). This was the first use of reliability theory to determine load and resistance factors for design of civil engineering structures and was

widely accepted. However, Load and Resistance Factor Design (LRFD) wasn't introduced into bridge construction until 1994 when The American Association State Highway Transportation Officials AASHTO (1998) published the first edition of AASHTO (1998) LRFD Bridge Design Specification (AASHTO, 1998). In LRFD, the safety performance requirement is expressed by the following equation AASHTO (1998) where:

$$\Phi R_n > \sum \gamma_i Q_i$$

$R_n$  = Nominal Capacity of a member, connection, or a component;

$\Phi$  = Resistance Factor that takes into account the uncertainties in the material strength;

$Q_i$  = Load effect such as moment, shear or axial load;

$\gamma_i$  = load factor that takes into account the uncertainties in the load.

Reliability analysis begins with the formulation of a limit state function,  $g(x)$ , such that failure corresponds to  $g(x) < 0$ , where  $x$  = vector of basic variables (e.g. material properties, geometric properties, etc.). The form of the limit state function is often expressed as

$$g(x) = R - S \quad \text{Equation 6-3}$$

where  $R$  = structural resistance or capacity model and  $S$  = load effect or demand model. Both can either be a random variable or a function of multiple random variables. The failure probability,  $P_f$ , can be calculated using any one of several numerical techniques (e.g. MCS. FORM, etc.).

However, in this research, the form of the limit state function is expressed in terms of damage index (DI) as follows;

$$g(x) = DI = \frac{S}{R} = \frac{M^*}{\Phi M_u} \quad \text{Equation 6-4}$$

such that failure corresponds to  $g(x) > 1$

For this research, only the bridge superstructure was considered (i.e. the girders and bridge deck).

For the purpose of modelling the bridge, a bridge that carries a state route of Ipswich-Toowoomba road over Tenthill Creek in Gatton, Queensland, Australia has been selected. This is a simple span reinforced concrete, I-girder bridge built in 1970's. The bridge is 82.15m long and about 8.6m wide and is supported by a total of 12 pre-stressed 27.38m long beams over three spans of 27.38m. The beams are supported by two abutments and two headstocks.

General purpose finite element software, ABAQUS has been used to model the bridge deck and all 4 girders to analyse the flood loading effect on them. All four girders were assumed simply supported and to rest on the headstock of the piers. The reinforced concrete deck is modelled as supported on the girder and connected to the girder. Self-weight of the bridge



Figure 6.2: Tenthill creek bridge configuration

and the flood and log impact loads acting laterally to one of the end girder were considered in the analysis since the end girder was the most affected as described in section 5.5.6. The flood load was fed as a pressure on the face of the end girder. Figure 6.2 illustrates the Tenthill Creek bridge configuration. Section details of the bridge deck and the girder is given in Figure 6.3.

Assumption of flood loading as a uniform pressure is the recommendation of all bridge design codes reviewed in chapter 2. Nasim et al. (2017) performed a rigorous analysis of the fluid structure interaction using ANSYS Fluent and confirmed that this was appropriate for the fragility analysis.

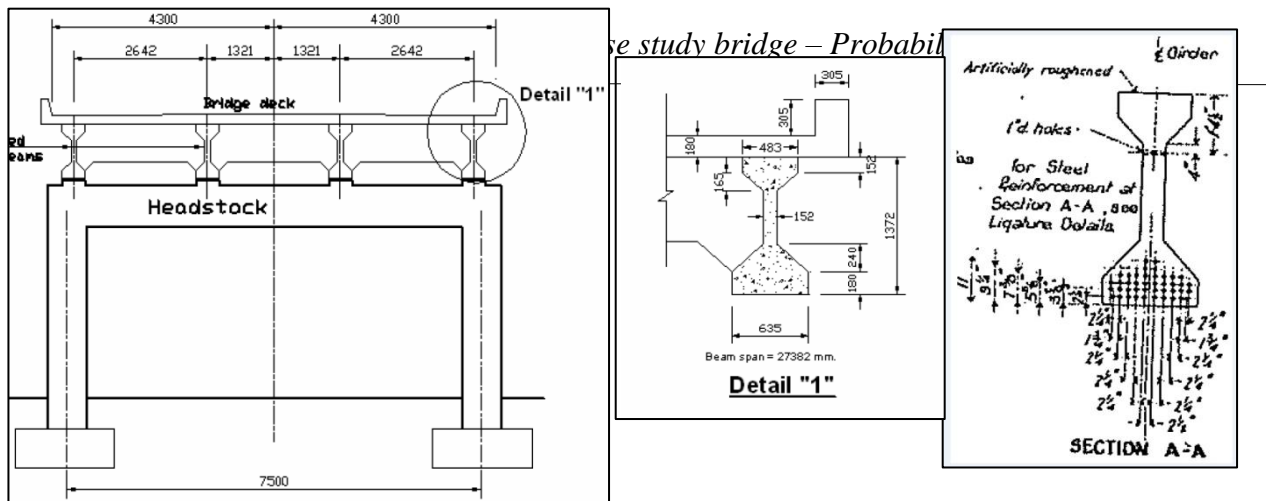


Figure 6.3: Section detail of the bridge deck and girder

## 6.2 Effect of Flood Intensity (Demand Model)

To capture the influences of uncertain factors on river bridge safety evaluation, a probabilistic approach was adopted in these types of analysis. A sampling approach such as a Monte Carlo simulation (MCS) or importance sampling is often adopted. The random variable considered here includes flood velocity. Simulation is performed using ABAQUS software through an ABAQUS Script written in Python Language to capture the uncertainty in the random variable. Figure 6.4 shows the model development of the bridge deck and the girders.

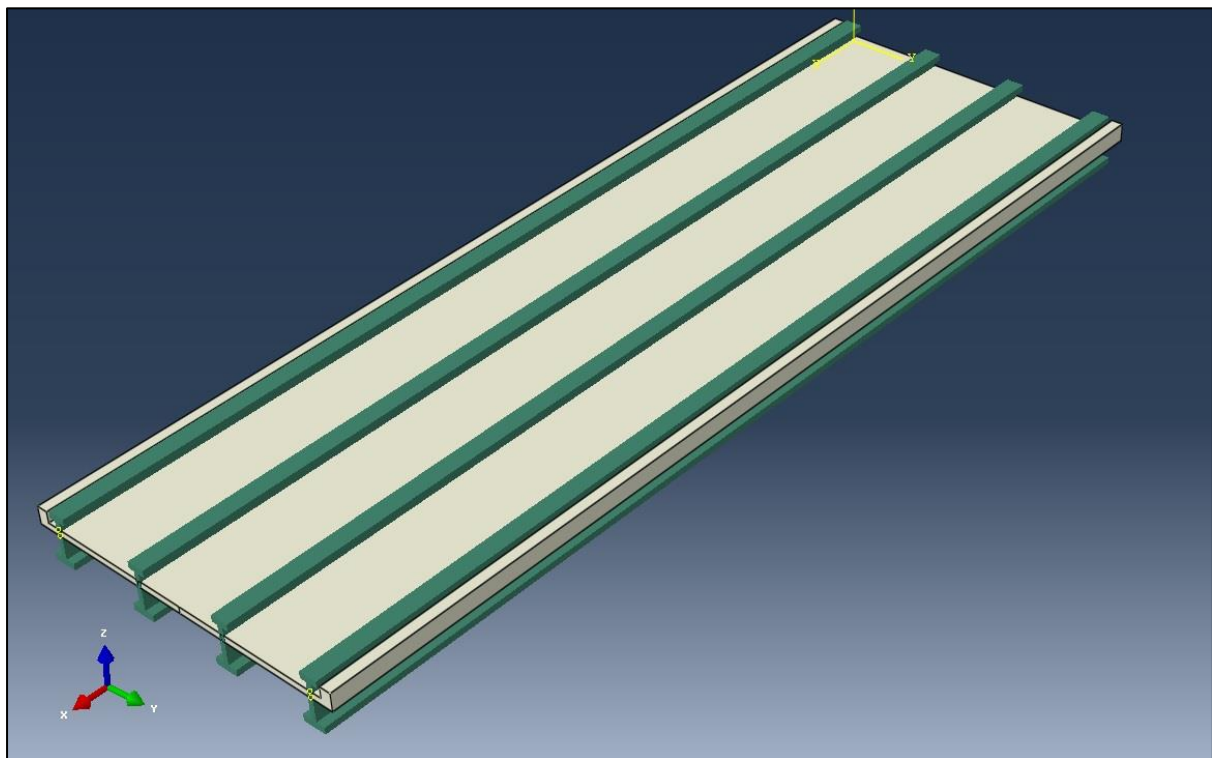


Figure 6.4: ABAQUS Bridge Deck Model

### 6.2.1 Analysis of flood data

Flood data required for this research has been sourced through water monitoring committee of Queensland Government. This web based data set (Figure 6.5) provided the flood discharge, flood height and the creek river profile data for all rainfall monitoring stations across the state. Figure 6.6(below) indicates the River profile of Lockyer Creek at Helidon Number 3 which is the closest monitoring station of the case study bridge in this research. The recorded data are available from as old as 1987 to date. Simple open channel flow equation (Equation 6-5) was used to derive the required flood velocity. Given river profile was first drawn in AutoCAD to get the corresponding cross sectional area at different flood heights. River profile was modified into a number of simplified trapezium to make ease of calculating cross sectional area as shown in Figure 6.7(below)

$$V = \frac{Q}{A}$$

Equation 6-5

Where V= Flood velocity

Q= Flood discharge

A= Creek cross sectional area at the given flood height

An Excel formula was devised for calculating cross sectional area of the river for different stream water level. Corresponding flood velocity was then calculated using stream discharge and the river cross section area.

| Time and Date    | 143203C       | 143203C | 143203C        |      |                    |   |
|------------------|---------------|---------|----------------|------|--------------------|---|
|                  | 10            | 100     | 140            |      |                    |   |
|                  | Rainfall (mm) |         | Level (Metres) |      | Discharge (Cumecs) |   |
|                  | Point         | Qual    | Point          | Qual | Point              | Qual  |
| 19/11/1987 11:40 |               |         | 0.54           | 9    | 0.028              | 20 Sites:                                     |
| 19/11/1987 12:33 |               |         | 0.55           | 9    | 0.037              | 20 143203C -                                  |
| 19/11/1987 12:41 |               |         | 0.56           | 9    | 0.048              | 20  |
| 19/11/1987 12:48 |               |         | 0.56           | 9    | 0.048              | 20 Variables:                                 |
| 19/11/1987 13:02 |               |         | 0.57           | 9    | 0.061              | 20 10 - Rainfall (millimetres)                |
| 19/11/1987 13:53 |               |         | 0.56           | 9    | 0.048              | 20 100 - Stream Water Level (Metres)          |
| 19/11/1987 14:03 |               |         | 0.55           | 9    | 0.037              | 20 140 - Stream Discharge (Cumecs)            |
| 19/11/1987 14:14 |               |         | 0.55           | 9    | 0.037              | 20  |
| 19/11/1987 15:40 |               |         | 0.55           | 9    | 0.037              | 20 Qualities:                                 |
| 19/11/1987 16:41 |               |         | 0.55           | 9    | 0.037              | 20 1 - Good (actual)                          |
| 19/11/1987 17:43 |               |         | 0.54           | 9    | 0.028              | 20 9 - CITEC - Normal Reading                 |
| 19/11/1987 21:47 |               |         | 0.54           | 9    | 0.028              | 20 10 - Good                                  |
| 20/11/1987 7:19  |               |         | 0.54           | 9    | 0.028              | 20 15 - Water level below threshold (no flow) |
| 20/11/1987 12:57 |               |         | 0.55           | 9    | 0.037              | 20 20 - Fair                                  |
| 20/11/1987 13:40 |               |         | 0.56           | 9    | 0.048              | 20 30 - Poor                                  |
| 20/11/1987 14:44 |               |         | 0.56           | 9    | 0.048              | 20 59 - CITEC - Derived Height                |
| 20/11/1987 16:18 |               |         | 0.56           | 9    | 0.048              | 20 60 - Estimate                              |
| 20/11/1987 22:53 |               |         | 0.57           | 9    | 0.061              | 20 83 - Non standard rainfall                 |
| 21/11/1987 9:08  |               |         | 0.57           | 9    | 0.061              | 20 130 - Not coded value                      |
| 21/11/1987 9:22  |               |         | 0.57           | 9    | 0.061              | 20 151 - Data not yet available               |
| 21/11/1987 9:51  |               |         | 0.56           | 9    | 0.048              | 20 160 - Suspect                              |
| 21/11/1987 10:38 |               |         | 0.55           | 9    | 0.037              | 20 200 - Water level below threshold          |
| 21/11/1987 12:11 |               |         | 0.55           | 9    | 0.037              | 20 255 - No data exists                       |
| 21/11/1987 16:09 |               |         | 0.54           | 9    | 0.028              | 20  |
| 21/11/1987 20:20 |               |         | 0.54           | 9    | 0.028              | 20  |

Figure 6.5: Extraction of as given data from water monitoring committee of QLD government (Station: Helidon No.3)



Figure 6.6: River profile of Lockyer Creek at Helidon Number 3

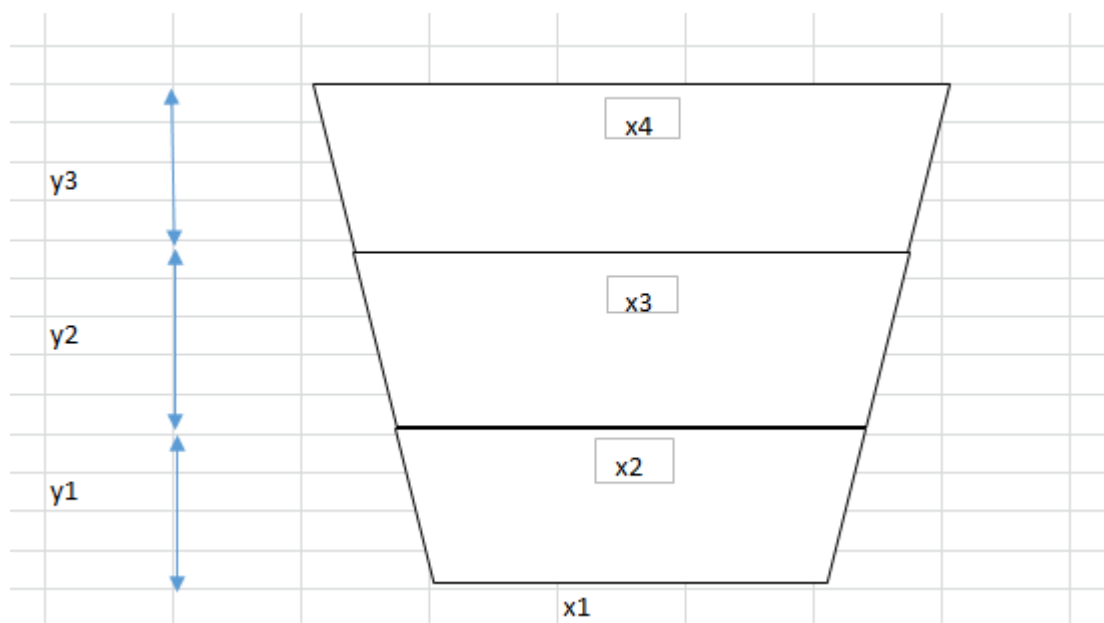


Figure 6.7: Simplified river profile (Exaggerated figure)

### 6.2.2 Analysis of Actual Flood Velocity Distribution

Distributive nature of the flood velocity for the period between 1987 and 2016 was obtained using @Risk software simulation techniques as shown in Figure 6.8, Figure 6.9 and Figure 6.10(below). Three different distinct period of the flood velocity analysis have been carried out. It is worth to note that Lockyer Valley Region had experienced severe rain between beginning of December 2010 and end of January 2011 and in particularly on 7, 8, 9 and 10<sup>th</sup> of January 2011. Table 6-1(below) gives the summary of the flood velocity data analysis.

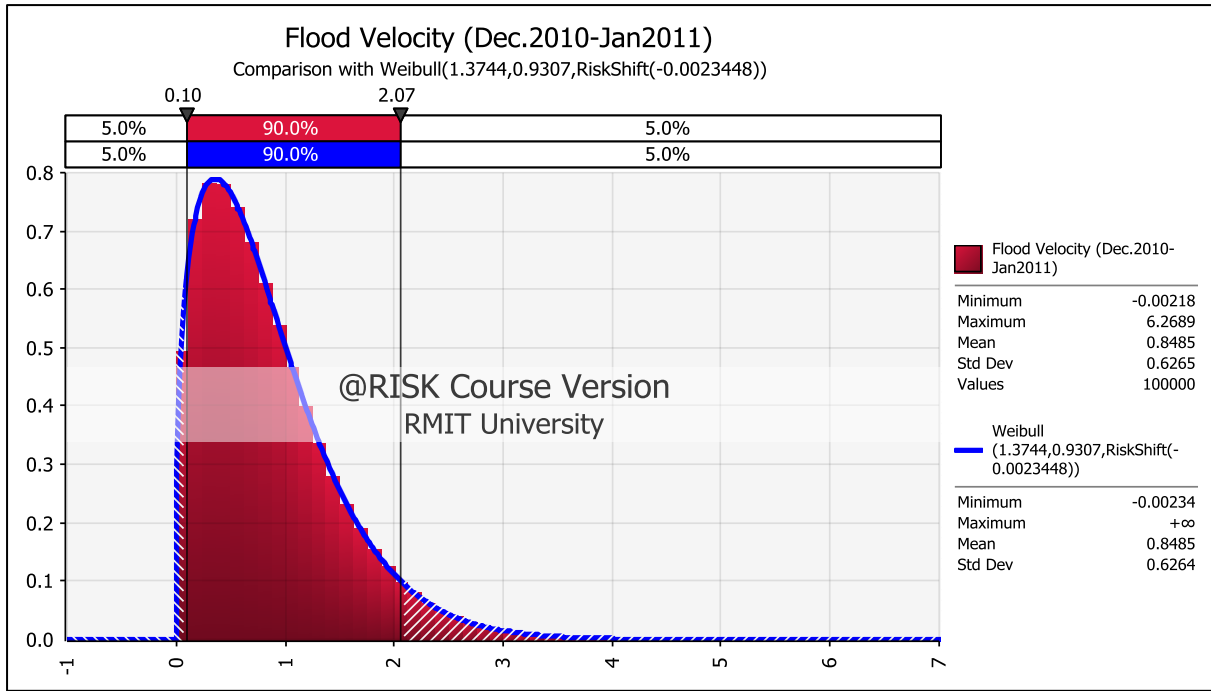


Figure 6.8: Flood Velocity Distribution (Dec.2010 – Jan 2011)

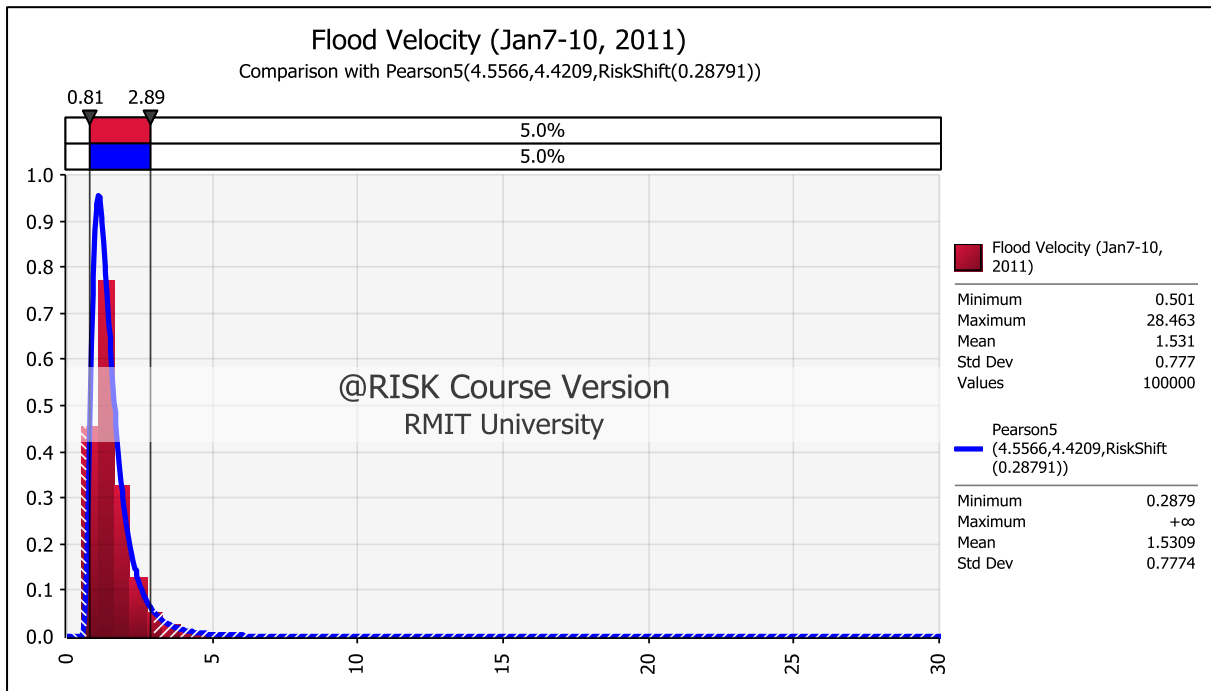


Figure 6.9: Flood Velocity Distribution (Jan 7-10, 2011)

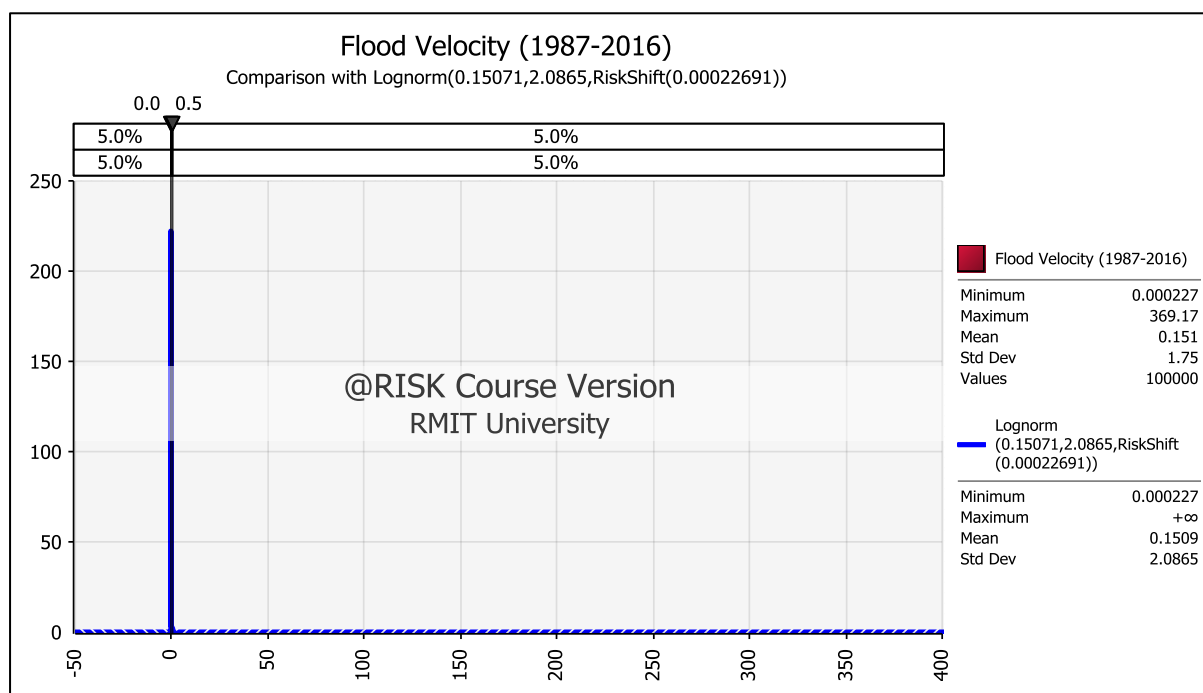


Figure 6.10: Flood Velocity Distribution (1987-2016)

Table 6-1: Summary of the Flood Velocity Data Analysis

| Analysis of Flood Velocity Distribution (m/s) |             |               |                |                             |                             |
|---|-------------|---------------|----------------|-----------------------------|-----------------------------|
| Period  | Type of fit | Mean Velocity | Std. Deviation | 05 <sup>th</sup> Percentile | 95 <sup>th</sup> Percentile |
| Dec 2010 – Jan 2011                           | Weibull     | 0.85          | 0.63           | 0.10                        | 2.07                        |
| Jan 7-10, 2011                                | Pearson 5   | 1.53          | 0.78           | 0.81                        | 2.89                        |
| 1987 - 2017                                   | Lognorm     | 0.15          | 2.08           | 0.00                        | 0.50                        |

From the above analysis, 100 random velocity values were generated using @ Risk for parametric study as shown in Table 6-2(below)

Table 6-2: Flood Velocity values used in the parametric study

|       |       |       |       |       |
|-------|-------|-------|-------|-------|
| 2.172 | 1.745 | 1.635 | 1.694 | 2.002 |
| 1.745 | 1.828 | 2.608 | 2.015 | 1.881 |
| 2.469 | 1.649 | 1.635 | 1.912 | 1.628 |
| 1.707 | 2.146 | 1.934 | 2.538 | 2.305 |
| 2.118 | 1.727 | 2.643 | 1.733 | 2.012 |
| 2.329 | 1.708 | 1.683 | 1.831 | 1.659 |
| 1.988 | 1.734 | 1.716 | 2.203 | 1.779 |
| 1.772 | 1.894 | 2.427 | 1.744 | 1.609 |
| 1.88  | 1.895 | 2.376 | 1.921 | 2.597 |
| 1.94  | 2.177 | 2.263 | 1.618 | 3.175 |
| 2.843 | 2.084 | 1.69  | 1.558 | 2.318 |
| 1.666 | 1.793 | 2.399 | 3.653 | 1.698 |
| 2.078 | 1.994 | 1.621 | 1.76  | 2.799 |
| 2.028 | 1.604 | 1.954 | 2.766 | 2.369 |
| 1.78  | 1.626 | 1.566 | 1.729 | 1.746 |
| 1.679 | 2.146 | 1.804 | 1.846 | 2.019 |
| 1.65  | 1.785 | 1.878 | 2.783 | 1.784 |
| 1.669 | 1.728 | 2.026 | 1.572 | 1.634 |
| 2.176 | 1.682 | 2.908 | 1.868 | 1.552 |
| 1.659 | 2.075 | 1.798 | 1.68  | 1.599 |

### 6.3 Parametric Study in ABAQUS

ABAQUS uses python as the programming language. Scripting is necessary when it comes to doing a recurring task. In order to capture the variability in the flood intensity or flood velocity, it was necessary to construct python script. It was constructed in 3 steps as follows using the method proposed by Bahmani (2015):

#### Step1: Creating the model in CAE environment

Case study bridge configuration and the reinforcement details were modelled in the ABAQUS CAE environment. Node or element sets, for specific point required to report data, were created. And also a history data for those node or element was defined.

#### Step2: Modifying the INP file

The ABAQUS CAE environment automatically creates an input file that contains all the command descriptions used through the Graphical User Interface (GUI). This (.inp) file needs to be modified to include additional commands and do a parametric study. \*PARAMETER

key word in the python language is used to define the parameter. In this case, the parameter was the flood velocity under the load module.

### Step3: Constructing Python Script

The following steps were followed in the given sequential order to construct the required python script for the parametric study. Necessary Keywords and commands were obtained from the ABAQUS 6.14 user manual.

1. Create parametric study.
2. Define parameters: define parameter type (continuous or discrete valued)
3. Sample parameters: specify sampling option and data
4. Combine parameter samples to create sets of designs
5. Constrain designs (optional)
6. Generate designs and analysis job data
7. Execute the analysis jobs for selected designs of the study
8. Gather key results for selected designs of the study
9. Report gathered results.

Some of the above steps could be neglected or treated optional depending on the type of study.

Python Script constructed in this research is given in Figure 6.11(below)

```

#cbeam=ParStudy(par=('FLOODX','FLOODY'))
cbeam=ParStudy(par=('velocityfar'))
#cbeam.define(DISCRETE,par='FLOODX',domain=(0))
cbeam.define(DISCRETE,par='velocityfar',domain=(1.635,2.608,1.635,1.934,2.643,1.683,1.716,2.427,2.376,2.263))
#cbeam.sample(INTERVAL,par='FLOODX',interval=1)
cbeam.sample(NUMBER,par='velocityfar',number=10)
cbeam.combine(MESH,name='csr')
cbeam.generate(template='correct25417')
cbeam.execute(ALL)
cbeam.output(step=1,file=ODB)
cbeam.gather(results='STRESS',variable='S11',element=27294,request=HISTORY,instance="igirder-1")
cbeam.report(FILE,results=('STRESS'),par=('velocityfar'),file='cbeam.PSE27294.psr')
cbeam.gather(results='STRESS',variable='S11',element=27073,request=HISTORY,instance="igirder-1")
cbeam.report(FILE,results=('STRESS'),par=('velocityfar'),file='cbeam.PSE27073.psr')
cbeam.gather(results='STRESS',variable='S11',element=26852,request=HISTORY,instance="igirder-1")
cbeam.report(FILE,results=('STRESS'),par=('velocityfar'),file='cbeam.PSE26852.psr')
cbeam.gather(results='STRESS',variable='S11',element=26631,request=HISTORY,instance="igirder-1")
cbeam.report(FILE,results=('STRESS'),par=('velocityfar'),file='cbeam.PSE26631.psr')
cbeam.gather(results='STRESS',variable='S11',element=26410,request=HISTORY,instance="igirder-1")
cbeam.report(FILE,results=('STRESS'),par=('velocityfar'),file='cbeam.PSE26410.psr')
cbeam.gather(results='STRESS',variable='S11',element=7183,request=HISTORY,instance="igirder-1")
cbeam.report(FILE,results=('STRESS'),par=('velocityfar'),file='cbeam.PSE7183.psr')
cbeam.gather(results='STRESS',variable='S11',element=6962,request=HISTORY,instance="igirder-1")
cbeam.report(FILE,results=('STRESS'),par=('velocityfar'),file='cbeam.PSE6962.psr')
cbeam.gather(results='STRESS',variable='S11',element=6741,request=HISTORY,instance="igirder-1")
cbeam.report(FILE,results=('STRESS'),par=('velocityfar'),file='cbeam.PSE6741.psr')
cbeam.gather(results='STRESS',variable='S11',element=25745,request=HISTORY,instance="igirder-1")
cbeam.report(FILE,results=('STRESS'),par=('velocityfar'),file='cbeam.PSE25745.psr')
cbeam.gather(results='STRESS',variable='S11',element=25746,request=HISTORY,instance="igirder-1")
cbeam.report(FILE,results=('STRESS'),par=('velocityfar'),file='cbeam.PSE25746.psr')
cbeam.gather(results='STRESS',variable='S11',element=25747,request=HISTORY,instance="igirder-1")
cbeam.report(FILE,results=('STRESS'),par=('velocityfar'),file='cbeam.PSE25747.psr')
cbeam.gather(results='STRESS',variable='S11',element=25748,request=HISTORY,instance="igirder-1")
cbeam.report(FILE,results=('STRESS'),par=('velocityfar'),file='cbeam.PSE25748.psr')

```

Figure 6.11: ABAQUS Script for Parametric study

The bridge deck and the girders were modelled using ABAQUS CAE module and the input file (.inp file) was extracted and modified to run the parametric study in the ABAQUS command module. Element numbers for all the elements in the mid span girder were carefully identified to feed them in the python script so that the required elemental stress output could be obtained to calculate the flood induced bending moments ( $M^*$ ) for all 100 random velocity values. Figure 6.12 (below) shows the stress values obtained for just one element.

```

Parametric study: zaf9th10

velocityfar,      STRESS,
-----
2.002,           2832.31,
1.881,           2384.74,
1.628,           1877.08,
2.305,           4527.38,
2.012,           2842.33,
1.659,           2515.02,
1.779,           2090.85,
1.609,           2177.46,
2.597,           6311.85,
3.175,           10493.6,
    
```

Figure 6.12: Parametric study report for stress output

Table 6-3 (below) shows typical M\* calculation for some of the flood velocity values using the method described in section 5.3.2

Table 6-3: Typical M\* calculation

| V1(2.172) |          |       |        |          |          |          |          | V2(1.745) |          |       |        |          |          |          |          |
|-----------|----------|-------|--------|----------|----------|----------|----------|-----------|----------|-------|--------|----------|----------|----------|----------|
|           | stress   | width | height | force    | distance | Moment   | absmom   |           | stress   | width | height | force    | distance | Moment   | absmom   |
| S1        | -20511.5 | 0.05  | 0.35   | -358.951 | 0.096    | -34.4593 | 34.45932 | S1        | -10940.8 | 0.05  | 0.35   | -191.464 | 0.096    | -18.3805 | 18.38054 |
| S2        | -11103.2 | 0.05  | 0.35   | -194.306 | 0.046    | -8.93808 | 8.938076 | S2        | -5137.22 | 0.05  | 0.35   | -89.9014 | 0.046    | -4.13546 | 4.135462 |
| S3        | 2360.44  | 0.05  | 0.55   | 64.9121  | 0.004    | 0.259648 | 0.259648 | S3        | 1126.4   | 0.05  | 0.55   | 30.976   | 0.004    | 0.123904 | 0.123904 |
| S4        | 3008.2   | 0.05  | 0.55   | 82.7255  | 0.054    | 4.467177 | 4.467177 | S4        | 1285.82  | 0.05  | 0.55   | 35.36005 | 0.054    | 1.909443 | 1.909443 |
| S5        | 2223.85  | 0.05  | 0.55   | 61.15588 | 0.104    | 6.360211 | 6.360211 | S5        | 2237.12  | 0.05  | 0.55   | 61.5208  | 0.104    | 6.398163 | 6.398163 |
| S6        | 3151.83  | 0.05  | 1.4    | 220.6281 | 0.154    | 33.97673 | 33.97673 | S6        | 1547.7   | 0.05  | 1.4    | 108.339  | 0.154    | 16.68421 | 16.68421 |
| S7        | 2727.61  | 0.05  | 1.4    | 190.9327 | 0.204    | 38.95027 | 38.95027 | S7        | 2600.21  | 0.05  | 1.4    | 182.0147 | 0.204    | 37.131   | 37.131   |
| S8        | 3062.46  | 0.05  | 1.4    | 214.3722 | 0.254    | 54.45054 | 54.45054 | S8        | 1359.23  | 0.05  | 1.4    | 95.1461  | 0.254    | 24.16711 | 24.16711 |
| S9        | 3158.25  | 0.05  | 0.55   | 86.85188 | 0.304    | 26.40297 | 26.40297 | S9        | 2317.74  | 0.05  | 0.55   | 63.73785 | 0.304    | 19.37631 | 19.37631 |
| S10       | 3429.45  | 0.05  | 0.55   | 94.30988 | 0.354    | 33.3857  | 33.3857  | S10       | 2754.42  | 0.05  | 0.55   | 75.74655 | 0.354    | 26.81428 | 26.81428 |
| S11       | 3768.09  | 0.05  | 0.55   | 103.6225 | 0.404    | 41.86348 | 41.86348 | S11       | 2096.85  | 0.05  | 0.55   | 57.66338 | 0.404    | 23.296   | 23.296   |
| S12       | 4149.62  | 0.05  | 0.35   | 72.61835 | 0.454    | 32.96873 | 32.96873 | S12       | 2263.51  | 0.05  | 0.35   | 39.61143 | 0.454    | 17.98359 | 17.98359 |
| S13       | 4585.52  | 0.05  | 0.35   | 80.2466  | 0.504    | 40.44429 | 40.44429 | S13       | 2747.71  | 0.05  | 0.35   | 48.08493 | 0.504    | 24.2348  | 24.2348  |
|           |          |       |        |          | Total    | 356.9271 |          |           |          |       |        |          | Total    | 220.6348 |          |
| V3(2.329) |          |       |        |          |          |          |          | V4(1.988) |          |       |        |          |          |          |          |
|           | stress   | width | height | force    | distance | Moment   | absmom   |           | stress   | width | height | force    | distance | Moment   | absmom   |
| S1        | -24239.7 | 0.05  | 0.35   | -424.195 | 0.096    | -40.7227 | 40.7227  | S1        | -16734.4 | 0.05  | 0.35   | -292.852 | 0.096    | -28.1138 | 28.11379 |
| S2        | -14142.3 | 0.05  | 0.35   | -247.49  | 0.046    | -11.3846 | 11.38455 | S2        | -8190.99 | 0.05  | 0.35   | -143.342 | 0.046    | -6.59375 | 6.593747 |
| S3        | 3258.82  | 0.05  | 0.55   | 89.61755 | 0.004    | 0.35847  | 0.35847  | S3        | 1607.33  | 0.05  | 0.55   | 44.20158 | 0.004    | 0.176806 | 0.176806 |
| S4        | 2324.74  | 0.05  | 0.55   | 63.93035 | 0.054    | 3.452239 | 3.452239 | S4        | 2559.49  | 0.05  | 0.55   | 70.38598 | 0.054    | 3.800843 | 3.800843 |
| S5        | 3291.44  | 0.05  | 0.55   | 90.5146  | 0.104    | 9.413518 | 9.413518 | S5        | 1814.89  | 0.05  | 0.55   | 49.90948 | 0.104    | 5.190585 | 5.190585 |
| S6        | 2654.79  | 0.05  | 1.4    | 185.8353 | 0.154    | 28.61864 | 28.61864 | S6        | 2924.17  | 0.05  | 1.4    | 204.6919 | 0.154    | 31.52255 | 31.52255 |
| S7        | 3024.9   | 0.05  | 1.4    | 211.743  | 0.204    | 43.19557 | 43.19557 | S7        | 3117.6   | 0.05  | 1.4    | 218.232  | 0.204    | 44.51933 | 44.51933 |
| S8        | 3339.84  | 0.05  | 1.4    | 233.7888 | 0.254    | 59.38236 | 59.38236 | S8        | 2928.9   | 0.05  | 1.4    | 205.023  | 0.254    | 52.07584 | 52.07584 |
| S9        | 3696.61  | 0.05  | 0.55   | 101.6568 | 0.304    | 30.90366 | 30.90366 | S9        | 2471.76  | 0.05  | 0.55   | 67.9734  | 0.304    | 20.66391 | 20.66391 |
| S10       | 4138.45  | 0.05  | 0.55   | 113.8074 | 0.354    | 40.28781 | 40.28781 | S10       | 2603.63  | 0.05  | 0.55   | 71.59983 | 0.354    | 25.34634 | 25.34634 |
| S11       | 4679.45  | 0.05  | 0.55   | 128.6849 | 0.404    | 51.98869 | 51.98869 | S11       | 2895.17  | 0.05  | 0.55   | 79.61718 | 0.404    | 32.16534 | 32.16534 |
| S12       | 5170.29  | 0.05  | 0.35   | 90.48008 | 0.454    | 41.07795 | 41.07795 | S12       | 3162.02  | 0.05  | 0.35   | 55.33535 | 0.454    | 25.12225 | 25.12225 |
| S13       | 5648.2   | 0.05  | 0.35   | 98.8435  | 0.504    | 49.81712 | 49.81712 | S13       | 3491.56  | 0.05  | 0.35   | 61.1023  | 0.504    | 30.79556 | 30.79556 |
|           |          |       |        |          | Total    | 410.6033 |          |           |          |       |        |          | Total    | 306.0869 |          |

### 6.3.1 Log Impact Analysis on the bridge girder

Pritchard (2013) identified that urban debris such as cars; containers etc. and the insufficient bridge span to through that debris were the main cause for damaging bridges in the aftermath of 2011/2012 extreme flood events in Queensland as shown in Figure 6.13(below). Visual inspection on the damaged bridge photos given in the bridge inspection report has also supported this finding.



Figure 6.13: Urban debris (Toowoomba); cars and four-wheel drives

Thus, the impact from this urban debris has also been considered in the numerical analysis of the case study bridges. A commercial container as shown in Figure 6.14(below) was considered hitting at the mid span of the girder in the analysis. Relevant ABAQUS input files used in this parametric study has been annexed as appendices (Appendix1) at the end of this thesis.



Figure 6.14: Commercial container

## 6.4 Effect of Compressive Strength for Concrete (Capacity Model)

### 6.4.1 Resistance Statistics

Moment capacity of reinforced concrete girders which is a function of cross section and the reinforcement configuration is influenced by several variables. The compressive strength of the concrete, the steel component area and the yield strength are the most influential. The geometry of the concrete girder is also an important factor that influences the compressive moment capacity of the bridge girder. Table 6-4(below) shows the parameters used in the Monte Carlo simulation for generating suitable distributions of the nominal moment capacity i.e. the resistance in the Equation 6-6 (below). In Monte Carlo simulation, a system is simulated a large number of times (e.g. 100000 times) where each simulation is equally likely to occur, which is often denoted as a realization of the system. Several random numbers are generated between 0 and 1 which then pull values from the uncertain variable CDF (Cumulative Density Function) function. This results in a large numbers of separate and independent values, each representing a probable outcome for the system. The final results are fitted to probability density function (PDF), which represents all the possible values the system can take. In this research, the system is equal to Equation 6-6 and the resulting PDF is the nominal moment capacity of the girder. The variables are either a normal or lognormal distribution which requires the input of two parameters: the mean and standard deviation. For the standard deviation, the calculated mean is multiplied by the coefficient of variation.

To capture the influences of uncertain factors on the property of the concrete material and the geometry of the bridge, the associated random variables were defined using distributions found in the literature as shown in table 5. Fundamental Beam section analysis was carried out to the bridge I- Girder section. Neutral Axis depth for the section was established when the total tensile and the compressive forces added up to zero. Moment Capacity was then

calculated as shown in Equation 6-6 by taking moments about this neutral axis to the section. Figure 6.15 shows the geometry of the I Girder. Relevant random variable terms in this equation were simulated using @Risk software.

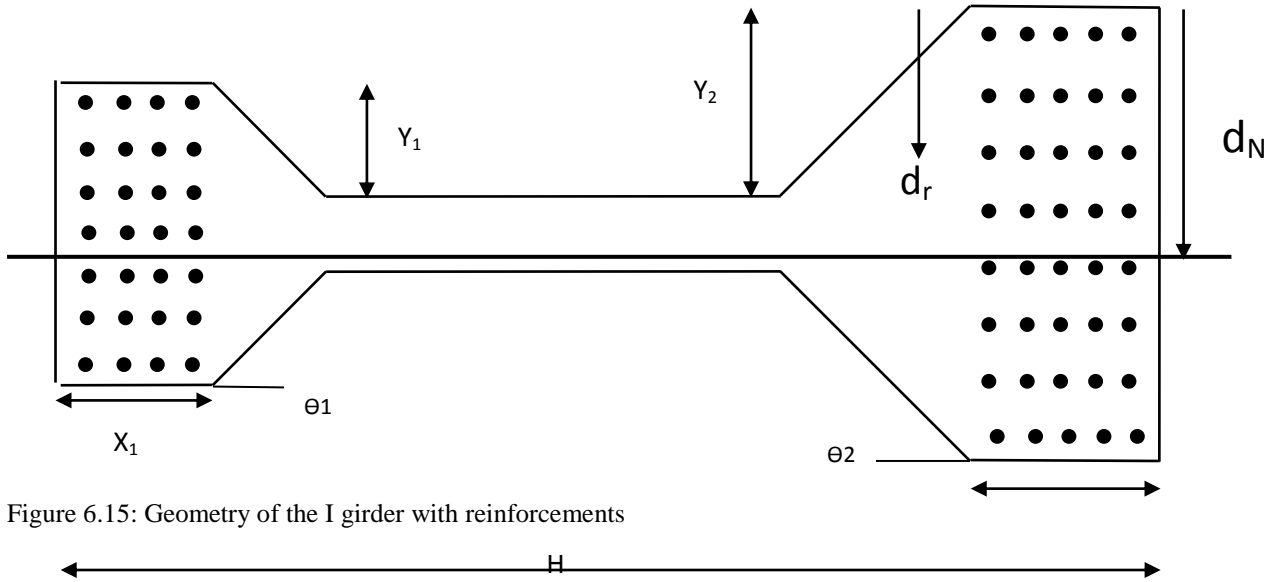


Figure 6.15: Geometry of the I girder with reinforcements

$$\begin{aligned}
 M_u = E_s \frac{\epsilon_c}{d_n} \sum_1^n a_r (d_n - d_r)^2 & \\
 + 0.85 f_c' \left[ x_1 y_1 \left( \lambda + \frac{y_1}{2} \right) \right. & \\
 + \frac{y_1^2}{2 \tan \theta_1} \left( \lambda + \frac{y_1}{3} \right) + x_2 y_2 \left( \lambda + \frac{y_2}{2} \right) & \quad \text{Equation 6-6} \\
 \left. + \frac{y_2^2}{2 \tan \theta_2} \left( \lambda + \frac{y_2}{3} \right) + \frac{H}{2} \lambda^2 \right] &
 \end{aligned}$$

where

$$\lambda = (0.9 d_n - y_2)$$

$E_s$  = Elasticity of Steel

$\epsilon_c$  = Concrete yield strain

$d_n$  = Neutral Axis Depth

$f'_c$  = concrete compressive stress

$d_r$  = depth to  $r^{th}$  layer of the steel.

$a_r$  = rebar cross section areas at the  $r^{th}$  layer

H = Height of the concrete I Girder

$M_u$  = Moment capacity

$X_1, X_2, Y_1, Y_2, \theta_1, \theta_2$  = Dimensions as shown in the Figure 6.15(above)

Table 6-4: Random variable parameters (Adopted from Tavares (2011))

| Variable      | Mean   | COV           | Distribution | Std. Dev |
|---------------|--------|---------------|--------------|----------|
| Es(Mpa)       | 200000 | 0.1           | Normal       | 20000    |
| $\varepsilon$ | 0.0035 | Deterministic |              |          |
| fc'(Mpa)      | 30     | 0.1           | Normal       | 3        |
| x1(mm)        | 152    | 0.015         | Normal       | 2.28     |
| y1(mm)        | 165.5  | 0.018         | Normal       | 2.979    |
| x2(mm)        | 180    | 0.015         | Normal       | 2.7      |
| y2(mm)        | 241.5  | 0.018         | Normal       | 4.347    |
| H(mm)         | 1372   | 0.015         | Normal       | 20.58    |
| $\theta_1$    | 0.7854 | Deterministic |              |          |
| $\theta_2$    | 0.7854 | Deterministic |              |          |

### Monte Carlo Simulation Techniques in @Risk Software

This section describes the procedure adopted to obtain the fragility curves in this research. As mentioned in Figure 6.1, the demand is measured using damage index for the generation of fragility curves. The damage index is a function of  $M^*$  and  $\Phi M_u$  both of which are represented by distributions to accommodate the uncertainties in the demand and capacity model. The demand model ( $M^*$ ) is accounted for variation in flood velocity while the capacity model ( $\Phi M_u$ ) is meant for uncertainties in concrete compressive strength, steel rebar yield strength and the geometry of the bridge girder. The demand and capacity models are simulated first to obtain the distribution for the damage index from which the fragility

curves are finally generated. Figure 6.16 (below) gives a screen shot of @Risk software interface to understand the procedures to be explained in the following section.

| Layer | distance | strain   | Stress    | #bars | A(m2)    | F(N)      | Moment(Nm) | Moment(kNm) |
|-------|----------|----------|-----------|-------|----------|-----------|------------|-------------|
| d1    | 0.05     | 0.002656 | 5.84E+08  | 3     | 3.39E-04 | 1.98E+05  | 3.12E+04   | 3.12E+01    |
| d2    | 0.1      | 0.001812 | 3.99E+08  | 3     | 3.39E-04 | 1.35E+05  | 1.45E+04   | 1.45E+01    |
| d3    | 0.125    | 0.00139  | 3.06E+08  | 2     | 2.26E-04 | 6.91E+04  | 5.69E+03   | 5.69E+00    |
| d4    | 0.15     | 0.000968 | 2.13E+08  | 3     | 3.39E-04 | 7.22E+04  | 4.14E+03   | 4.14E+00    |
| d5    | 0.2      | 0.000123 | 2.71E+07  | 5     | 5.65E-04 | 1.54E+04  | 1.12E+02   | 1.12E-01    |
| d6    | 0.3      | -0.00156 | -3.44E+08 | 7     | 7.92E-04 | -2.73E+05 | 2.53E+04   | 2.53E+01    |
| d7    | 0.35     | -0.00241 | -5.30E+08 | 7     | 7.92E-04 | -4.20E+05 | 5.99E+04   | 5.99E+01    |
| d8    | 0.45     | -0.0041  | -9.01E+08 | 3     | 3.39E-04 | -3.06E+05 | 7.42E+04   | 7.42E+01    |
| d9    | 0.5      | -0.00494 | -1.09E+09 | 3     | 3.39E-04 | -3.69E+05 | 1.08E+05   | 1.08E+02    |
| d10   | 0.525    | -0.00536 | -1.18E+09 | 2     | 2.26E-04 | -2.67E+05 | 8.48E+04   | 8.48E+01    |
| d11   | 0.55     | -0.00579 | -1.27E+09 | 3     | 3.39E-04 | -4.32E+05 | 1.48E+05   | 1.48E+02    |
| d12   | 0.6      | -0.00663 | -1.46E+09 | 3     | 3.39E-04 | -4.95E+05 | 1.94E+05   | 1.94E+02    |
|       |          |          |           |       |          | -2.07E+06 |            | 7.50E+02    |

| Part             | Area     | Force     | Distance | Moment(Nm) | Moment(kNm) |
|------------------|----------|-----------|----------|------------|-------------|
| C1               | 0.064791 | 1.99E+06  | 0.103655 | 2.07E+05   | 2.07E+02    |
| C2               | 0.021449 | 6.60E+05  | 0.056056 | 3.70E+04   | 3.70E+01    |
| C3               | -0.02697 | -8.29E+05 | -0.01757 | 1.46E+04   | 1.46E+01    |
| Total Conc Force |          | 1.82E+06  |          |            | 2.58E+02    |

|        |             |
|--------|-------------|
| Es     | 2.20E+11 Pa |
| ec     | 3.50E-03    |
| oc     | 3.08E+07 Pa |
| Østeel | 1.20E-02 m  |

Figure 6.16: @Risk software interface

### Procedure to obtain the distribution for $M^*$ using @Risk software

1. As mentioned in section 5.4.2, elemental stress output for all the mid span elements of the girder were first extracted. These were then substituted in the established excel Table 6-3 (above) to obtain the relevant  $M^*$  values.
2. All these  $M^*$  values were then transferred to @Risk software and stored in a column.
3. These values were then fitted a distribution using “Distribution Fitting” icon in @Risk software and stored in a cell (Say cell A)

4. This cell (Cell A) was then added an Output using “Add Output” icon in @Risk software and simulated for 100000 times using “Start Simulation” icon in the software.

Procedure to obtain the distribution for ( $\Phi M_u$ ) using @Risk software

1. Each random variable on the right hand side of Equation 6-6 (above) was defined relevant distributions in @Risk software and saved to different cells in a column.
2. The equation for Mu was then written on a new cell using the cell reference for each random variable.
3. The cell assigned for Mu was added an output using “Add Output” icon in @Risk software.
4. This cell (Say cell B) was then simulated for 100000 times using “Start Simulation” icon in the software.

Procedure to obtain the distribution for damage index (DI) using @Risk software

1. A new cell (Say cell C) was chosen for this and an equation was written for that cell by dividing cell A by Cell B to obtain the damage index as defined in Equation 5-12
2. This new cell (Cell C) was simulated 100000 times and the relevant fragility curves were obtained.

## 6.5 Determination of Failure Probability of the bridge

Failure of the bridge against flood is measured through Damage Index ( $DI = \frac{M^*}{\Phi M_u}$ ) that is defined as the ratio between the flood induced bending moment ( $M^*$ ) on the girder and the existing moment capacity ( $\Phi M_u$ ). When the limiting value of the Damage is equal to greater than 1.0, the bridge is considered failed. Using @Risk software, the Damage Index value was simulated and the corresponding probability curves (the “S” curves) or fragility curves were obtained. Fragility curves were derived for both Tenthill Creek Bridge and Kapernicks

Bridge in the case study region. These were obtained for different flood scenarios such as flood only and flood with log impacts etc.

These are shown in Figure 6.17 - Figure 6.20(below)

### 6.5.1 Fragility curves for Tenthill Creek Bridge

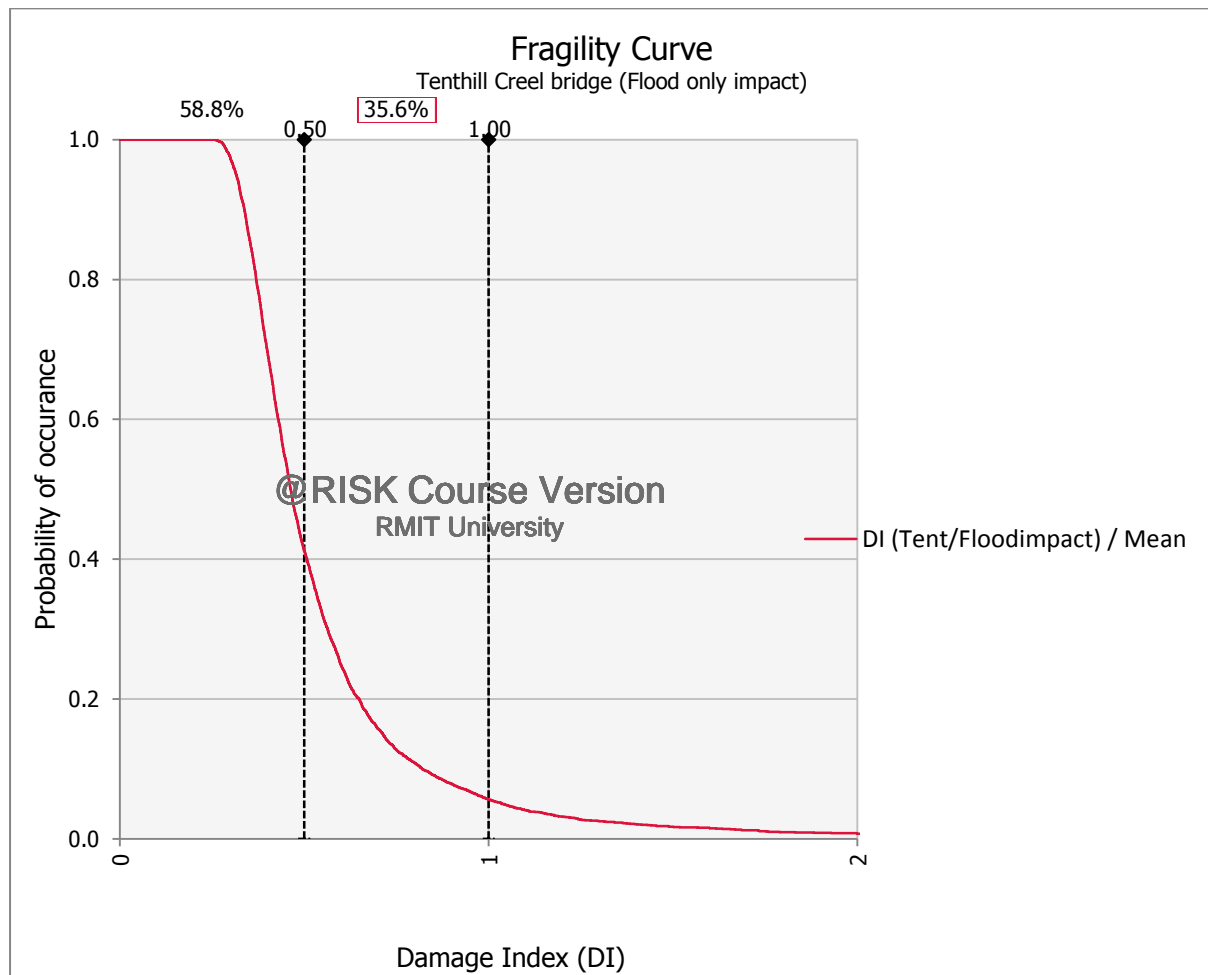


Figure 6.17: Fragility curve for Tenthill Creek Bridge under flood only impact

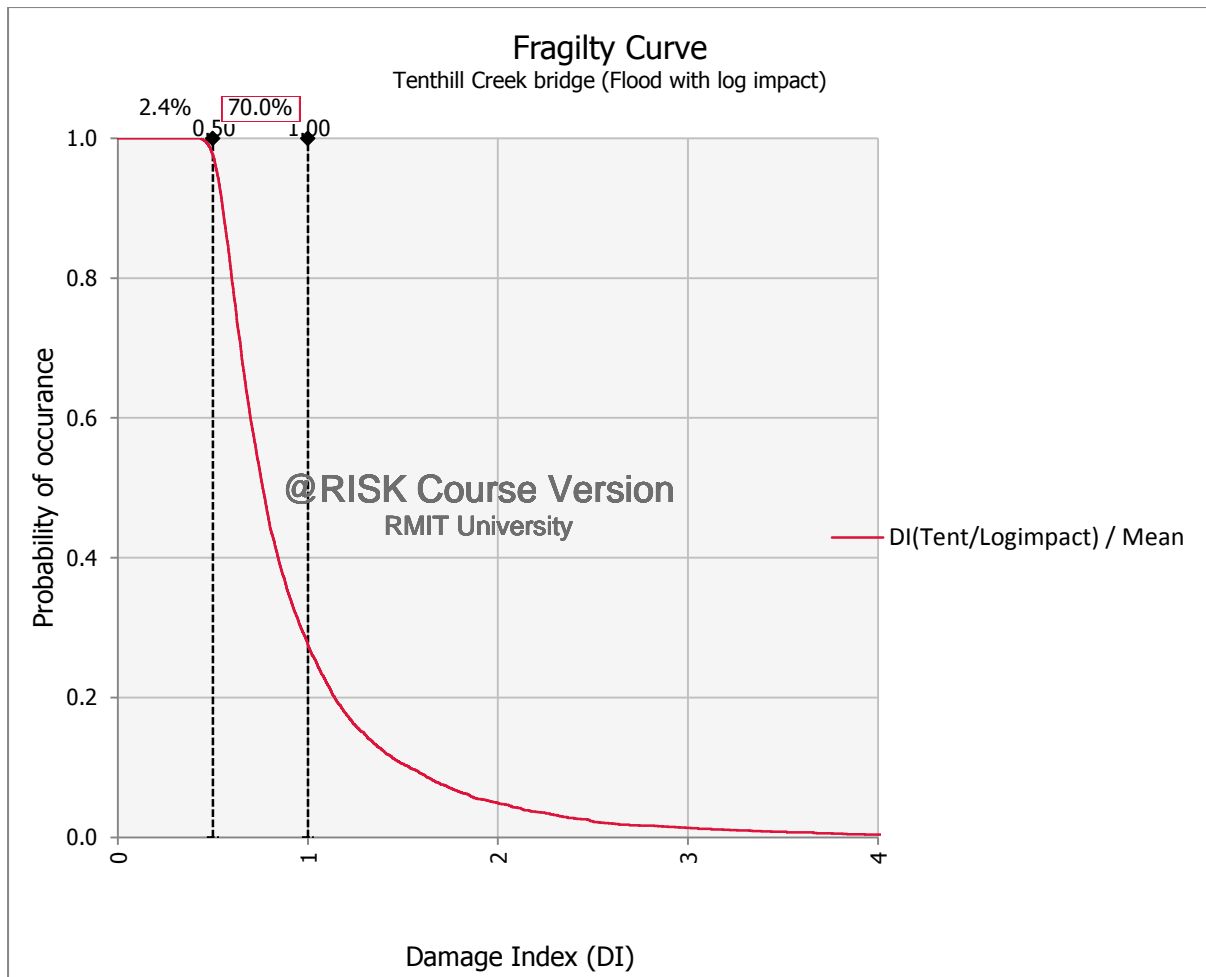


Figure 6.18: Fragility curve for Tenthill Creek Bridge under flood and log impact

### 6.5.2 Fragility curves for Kapernicks Bridge

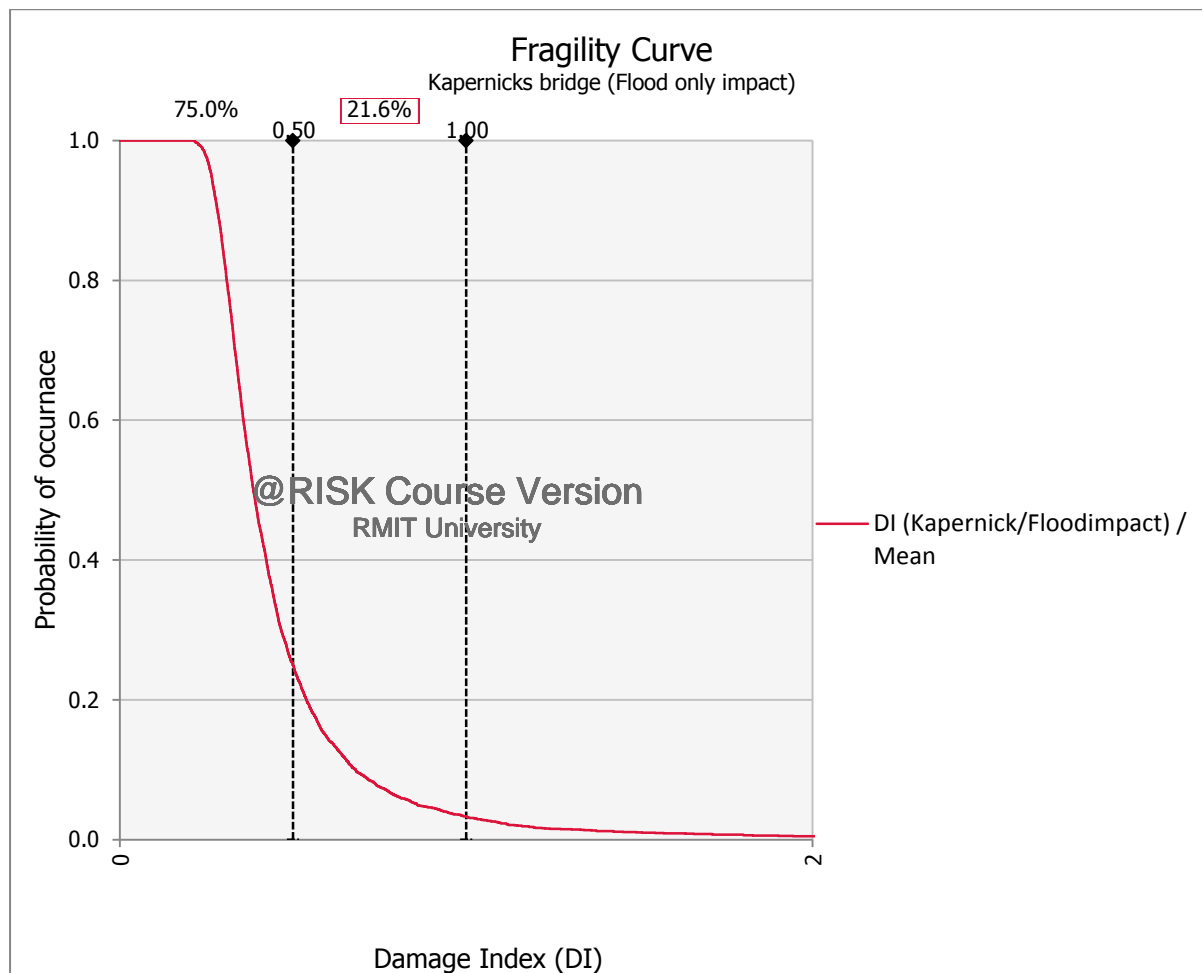


Figure 6.19: Fragility curve for Kapernicks Bridge under flood only impact

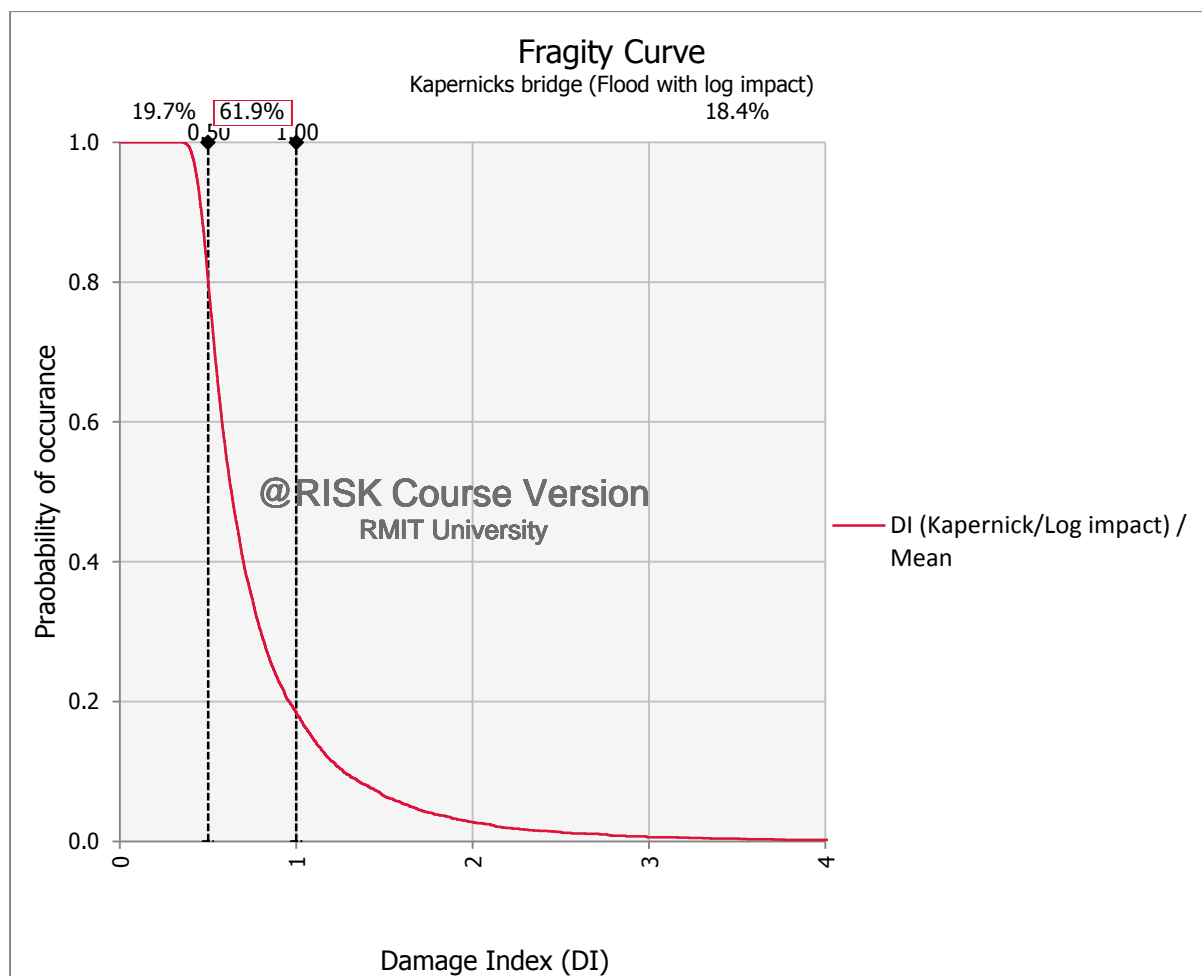


Figure 6.20: Fragility curve for Kapernicks Bridge under flood and log impact

Failure probability of the above two bridges are summarized in Table 6-5(below);

Table 6-5: Failure Probability for Case study bridges

| Considered Flood Effect | Probability of Failure |                   |
|-------------------------|------------------------|-------------------|
|                         | Tenthill Creek Bridge  | Kapernicks Bridge |
| Plain Flood             | 5.6%                   | 3.3%              |
| Flood with Log Impact   | 27.6%                  | 18.4%             |

Tenthill Creek Bridge gives 5.6% probability of failure when it's under the influence of a plain flood. AS 5100 Bridge Design standard allows 5% failure probability for all bridges. Bridge Design Standards assume rural flood condition rather than an urban flood condition that would include the effect of log impact.

Kapernicks Bridge has a shorter span (22.0m) than that of Tenthill Creek Bridge (27.4m) and this gives a less probability of failure (3.2%) to Kapernicks Bridge when it is under plain flood condition.

Hence, both the bridges are in good agreement to AS 5100 Bridge Design standard that allows 5% probability of failure for all the bridges

## **6.6 Parametric study for fragility curves**

The objective of this parametric study is to examine the effect of different bridge span and a different flood velocity distribution to its fragility curves. The other effects such as support conditions are not considered in this parametric study owing to extended computing time.

### **6.6.1 Effect of different bridge span**

For this study, a lower bound span of 15m bridge and an upper bound span of 45 m bridge were considered. The depth of the beam was adjusted to meet the requirement of Australia (2004) Bridge superstructures with the new dimensions were modelled using ABAQUS. Procedures described in section 6.3 were repeated to obtain the relevant fragility curves as shown in Figure 6.21 - Figure 6.24(below)

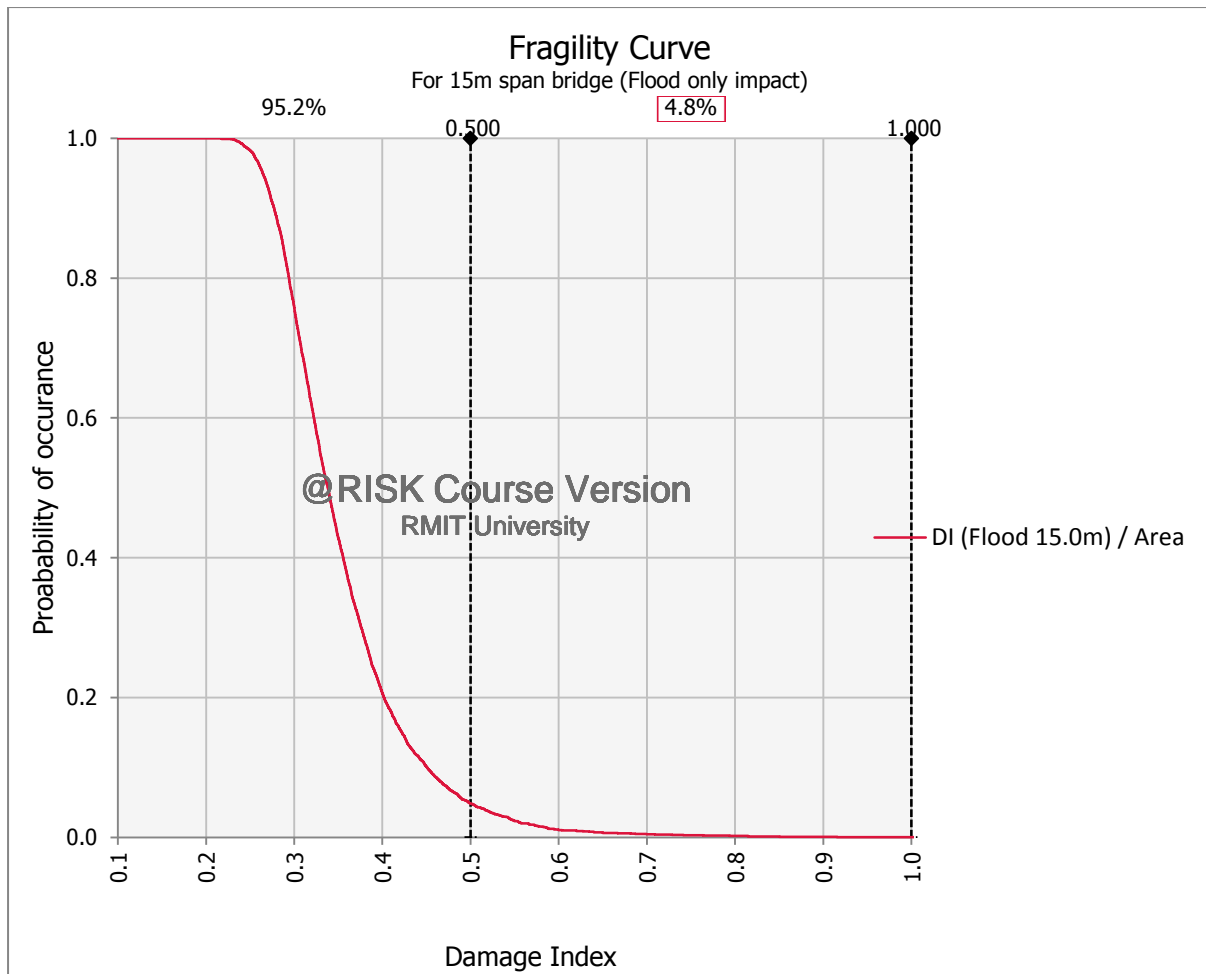


Figure 6.21: Fragility curve for 15m span bridge under flood only impact

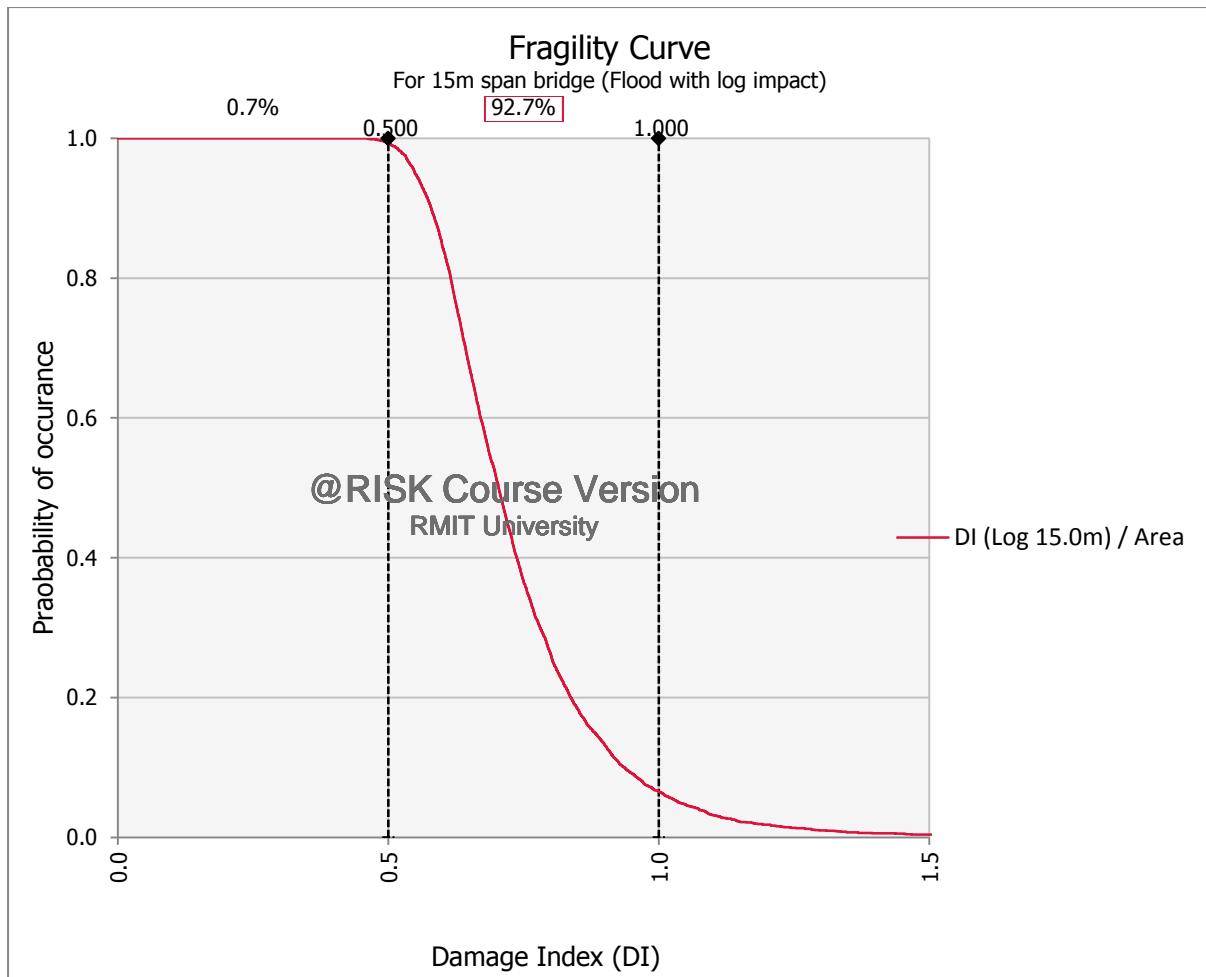


Figure 6.22: Fragility curve for 15m span bridge under flood and log impact

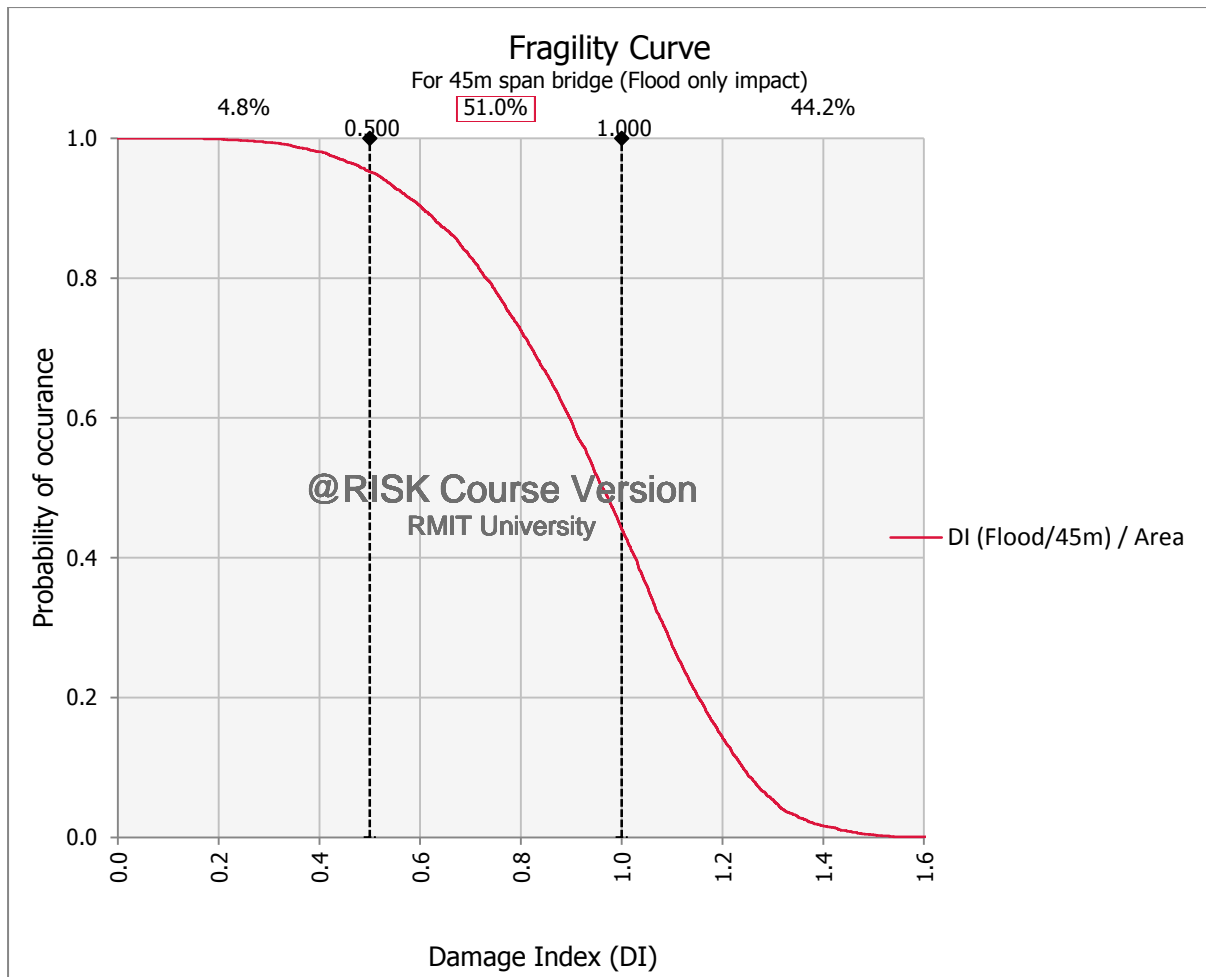


Figure 6.23: Fragility curve for 45m span bridge under flood only impact

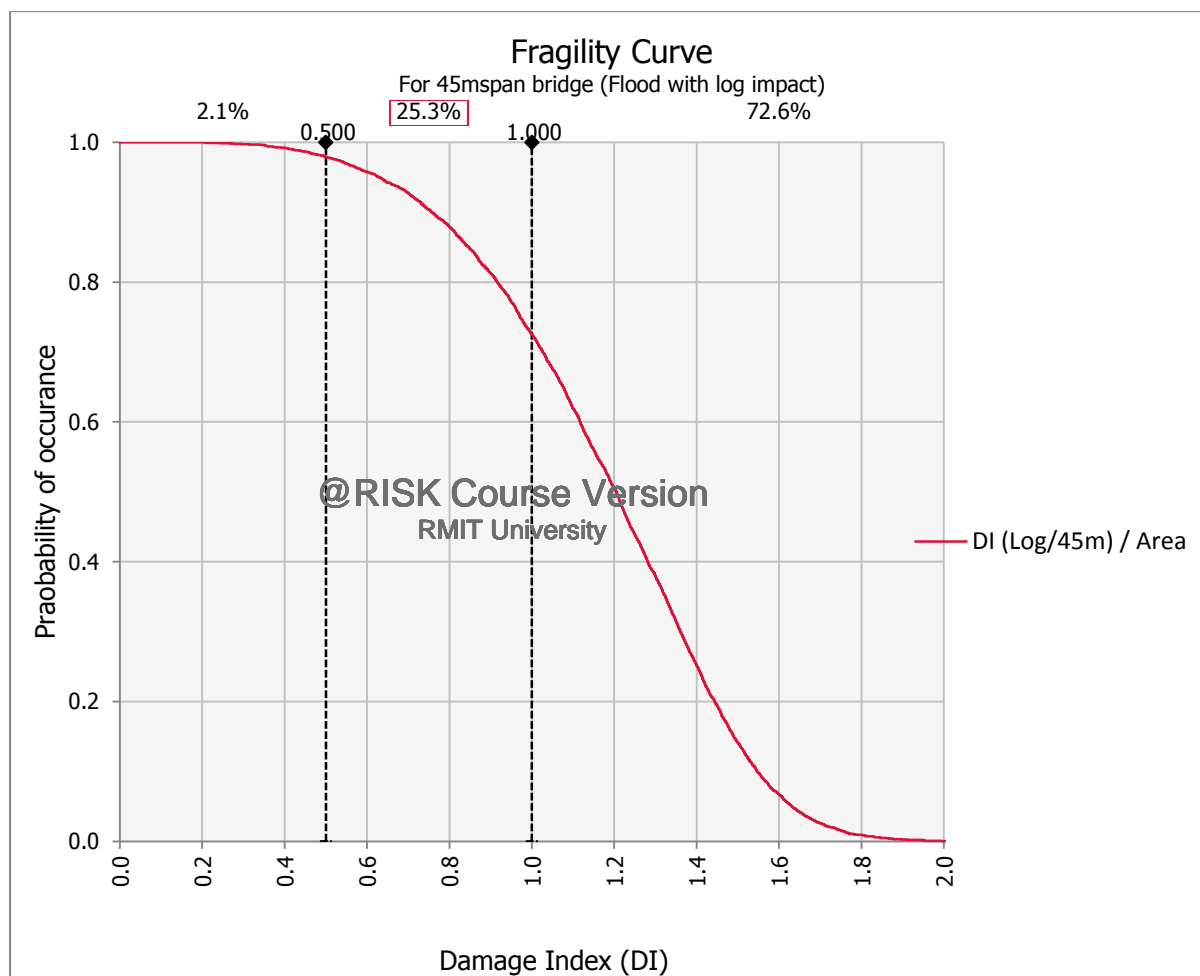


Figure 6.24: Fragility curve for 45m span bridge under flood and log impact

Failure probability of the above two hypothetical bridges are summarized in Table 6-6(below);

Table 6-6: Failure Probability for hypothetical bridges of two different spans.

| Considered Flood Effect | Probability of Failure |                   |
|-------------------------|------------------------|-------------------|
|                         | 15.0m span Bridge      | 45.0m span Bridge |
| Plain Flood             | 0.0%                   | 42.1%             |
| Flood with Log Impact   | 8.0%                   | 71.8%             |

The outcome of the analysis indicates that the long span bridges would have significantly higher probabilities of failure under flood loading. However, it should be noted here that the vulnerability of the bridge piers could be higher in a shorter span bridge.

### 6.6.2 Effect of different flood velocity distribution

Flood discharge data recorded for Brisbane River at Linville (Monitoring station No. 143007A) was used here. These data were obtained from water monitoring committee of Queensland Government and all the procedures mentioned in 6.2.1 were repeated to obtain the required flood velocity distribution for this study. Figure 6.25(below) depicts the River profile of Brisbane River at Linville (143007A)

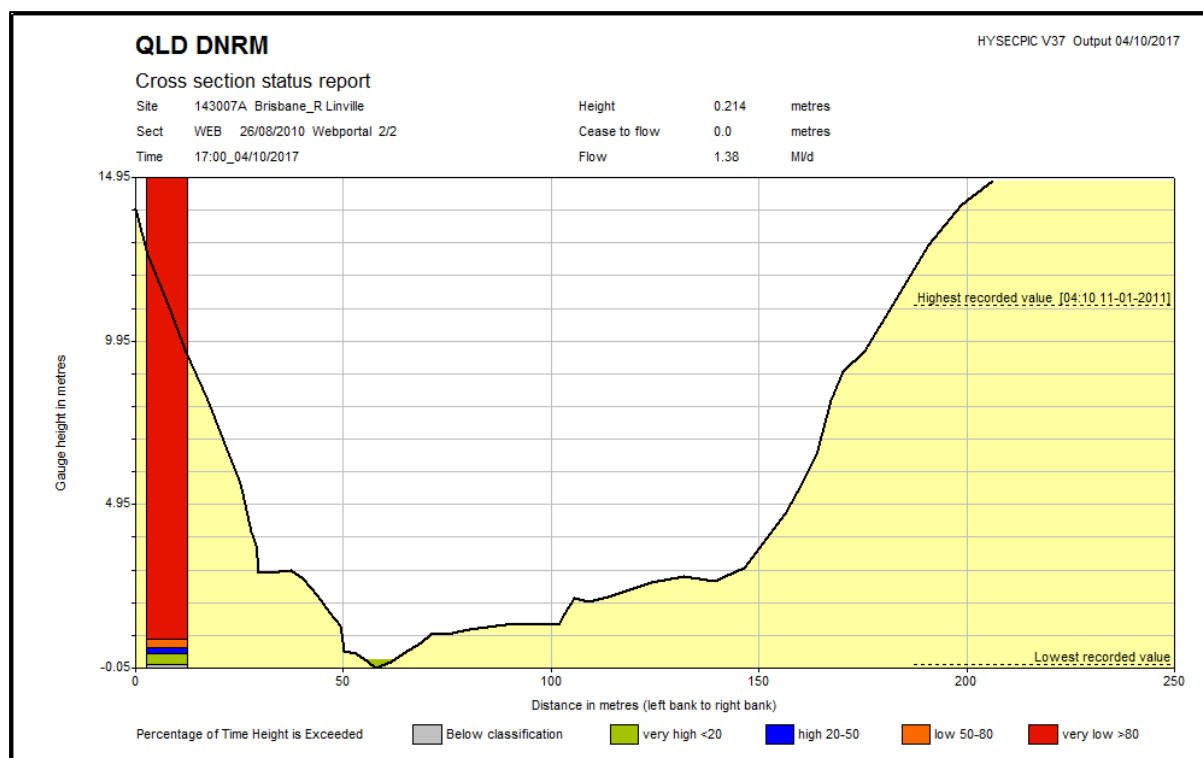


Figure 6.25: River profile of Brisbane River at Linville (143007A)

Flood velocity distribution obtained for the above geographical location is shown in Figure 6.26(below)

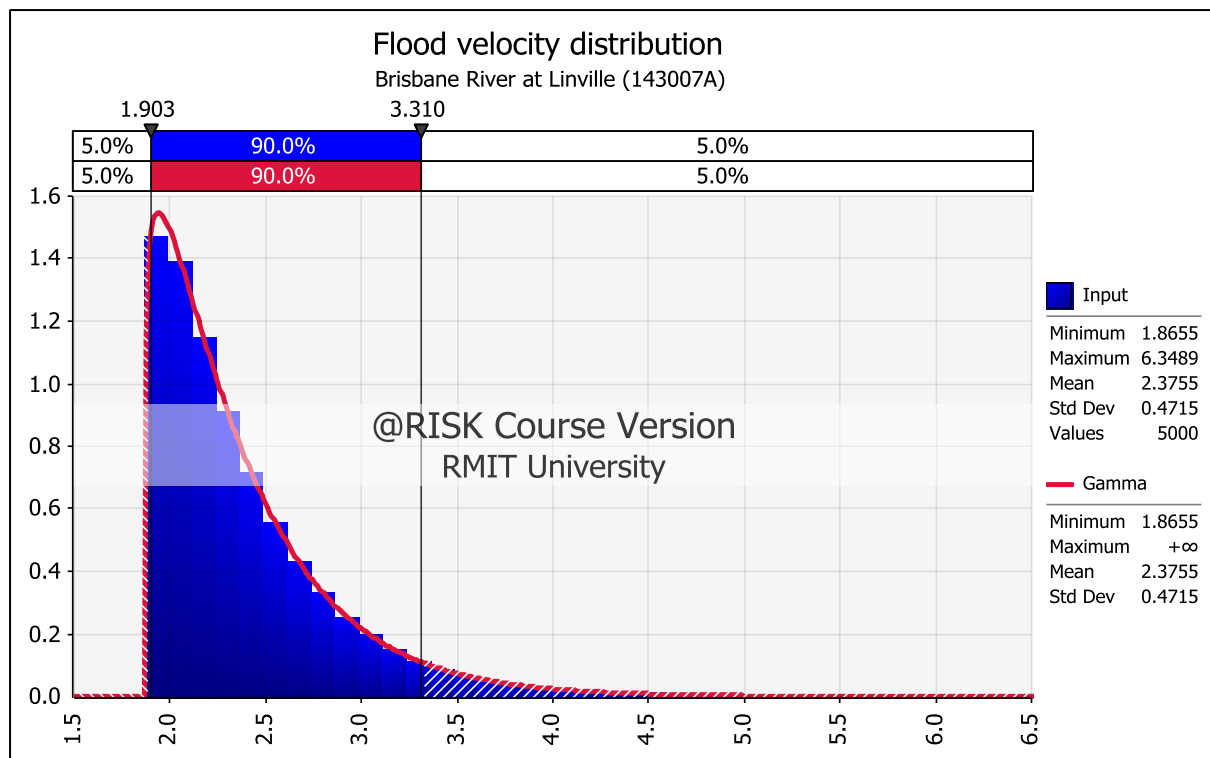


Figure 6.26: Flood Velocity Distribution for Brisbane River at Linville (143007A)

This new velocity distribution was applied to obtain the new fragility curves for Tenthill Creek Bridge as shown in Figure 6.27 and Figure 6.28(below). Due to constraint of computing time, Kapernicks Bridge was not considered for this scenario.

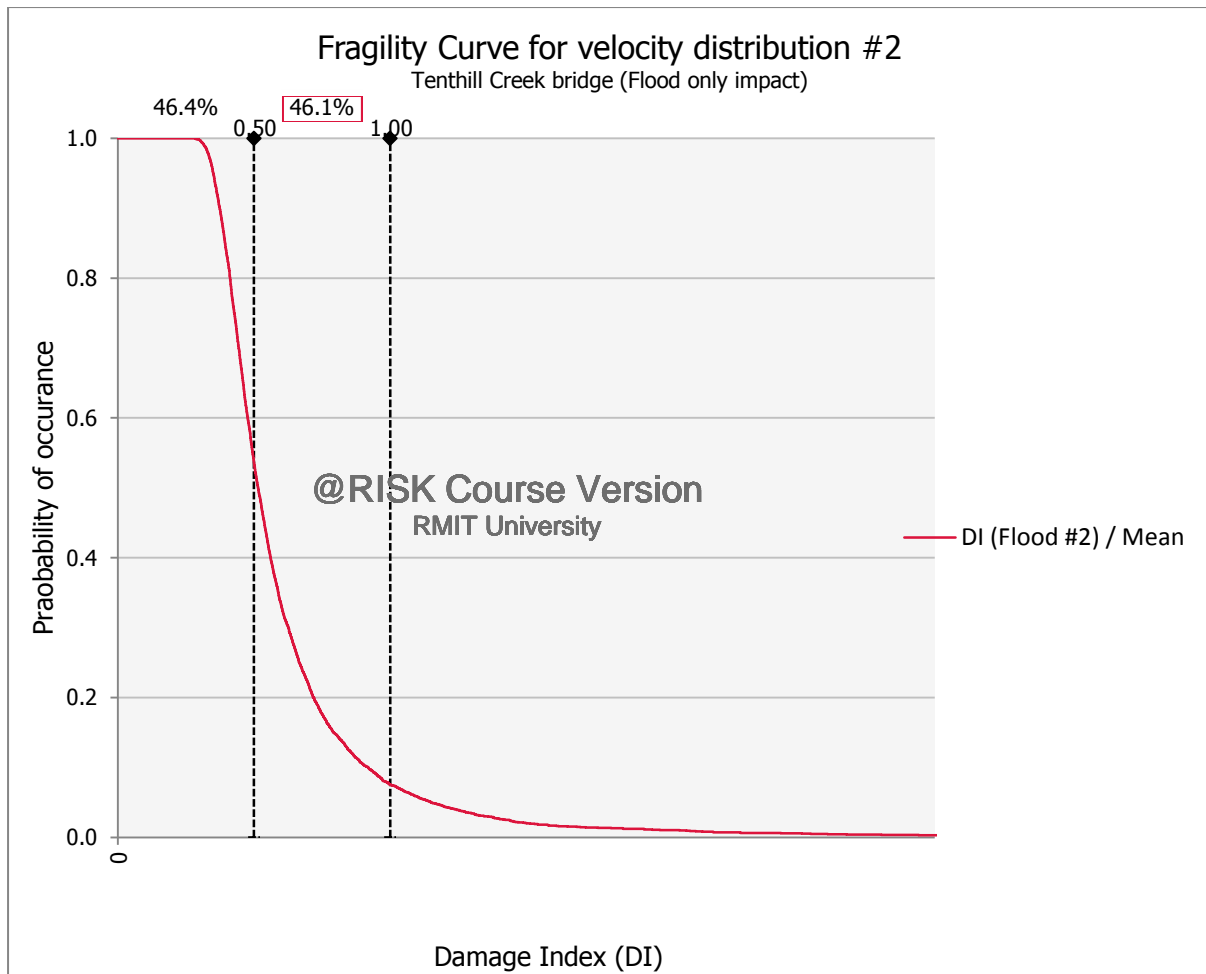


Figure 6.27: Fragility curve for velocity distribution # 2 (Flood only impact for Tenthill creek bridge)

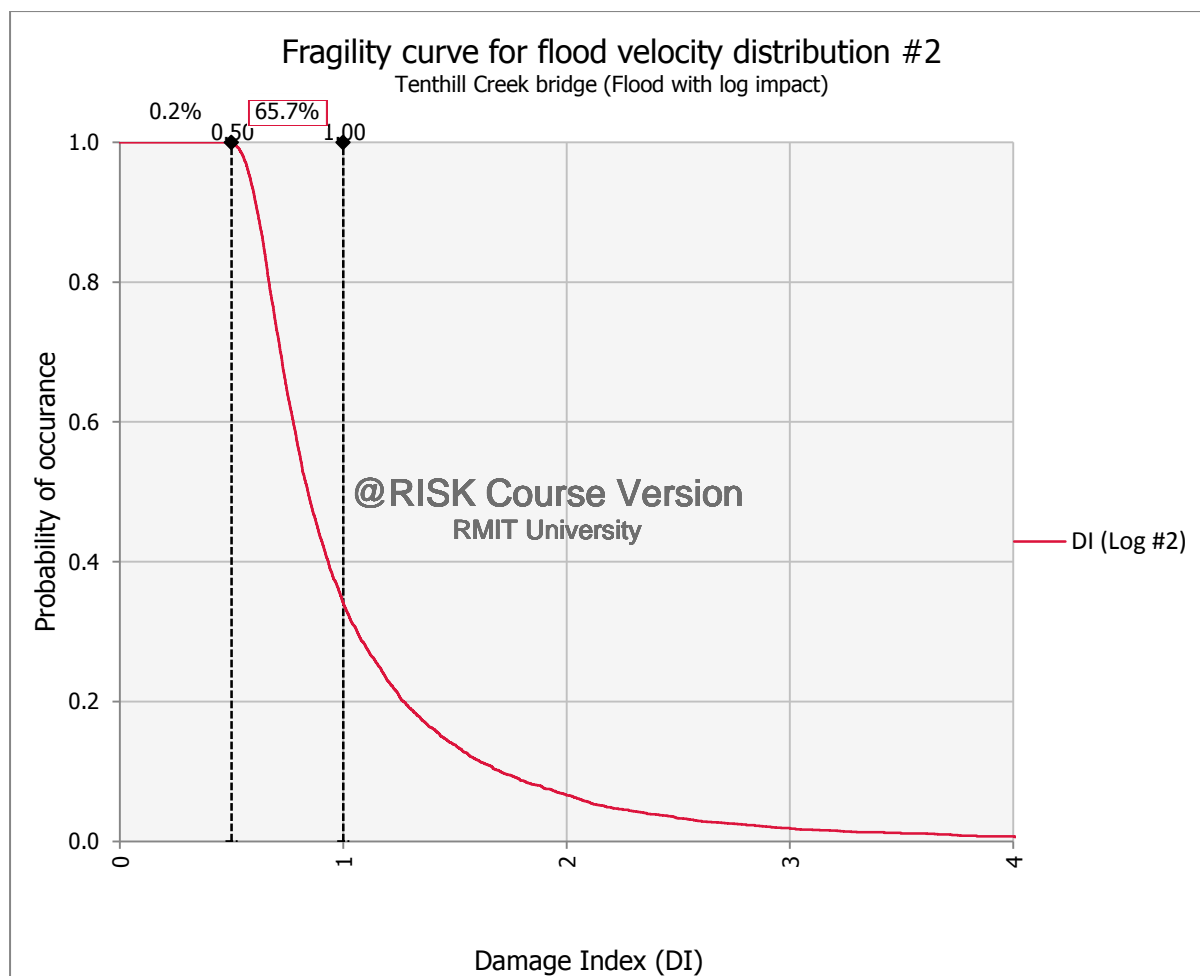


Figure 6.28: Fragility curve for velocity distribution # 2 (Flood and log impact for Tenthill creek bridge)

Table 6-7: Failure probability of bridges when the flood velocity changed

| Flood velocity distribution                | Probability of failure (when DI=1.0) |
|--|--------------------------------------|
| Distribution # 1 (Mean velocity = 2.55m/s) | 5.6%                                 |
| Distribution # 2 (Mean velocity = 2.75m/s) | 7.5%                                 |

## 6.7 Summary of the Chapter

This chapter was meant to elaborate the procedures for modelling the case study bridges probabilistically and generate fragility curves to study the effect of uncertain nature of the flood intensity measure and the material strength of the concrete. Fundamental theory on generating fragility curve and the bridge configurations are presented first.

Historical flood data for the case study bridge area has been sourced through water monitoring committee of Queensland Government. The data has been analysed and the flood velocity distribution has been obtained.

Parametric studies have been carried out to assess the effect of different bridge span and different flood velocity distribution to the fragility curves. Graphical representation of such fragility curves is presented.

The probability of failure of the Tenthill Creek and Kapernicks bridges under flood loading was observed to be 5.6% and 3.3% respectively while flood and log impact this increases to 27.6% and 18.4%.

A parametric study indicated that the increase in bridge span from 15m to 45m will increase the probability of failure by up to nine fold.

Similarly the increase in velocity distribution will also have a profound increase in the probability of failure of the bridges.

The methodology presented here can be used to explore the effect of climate change on the failure of bridge structure under natural hazards.

## 7 Damage Indices for Practical Application

### 7.1 Introduction

The research presented in this thesis covered development of a vulnerability modelling methodology for concrete girder bridges using two case studies.

A deterministic analysis demonstrated that at as built condition and under observed flood loading both bridges can be significantly vulnerable.

A fragility analysis method was developed to ascertain the probability of failure of the bridges considering the variability of flood loading and the variability of structural capacity due to degradation of the structure.

It is noted that under observed loading, the probability of failure of the structure can be as high as 28% which is significantly higher than the designed probability of 5%.

This chapter focuses on the methods of presenting damage to structure for practical application. Two methods of quantifying the damage to structures are presented which can be implemented by practitioners.

### 7.2 Types of damage indices.

Damage indices are used to quantify the damage to structures. They are defined using several methods. Two types of damage indices identified during the review of literature were used in this research. These indices were then used to derive damage curves for bridges under flood for various exposure conditions.

#### 7.2.1 Structural Capacity based Damage Index

In this method, the Damage Index (DI) is measured as the ratio between the moment induced by flood loading on the bridge girder ( $M^*$ ) and the moment capacity of the bridge girder ( $\phi M_u$ ).

$$\text{Damage Index (DI)} = \frac{M^*}{\phi M_u} \quad \text{Equation 7-1}$$

This method requires analysis of bridge structure under the following different exposure conditions

- Bridge Elevation
- Flood Velocity
- Flood Water Level

Method of determining the capacity based damage indices is given in chapters 5 and 6.

### 7.2.2 Cost based Damage Index

A cost based damage index provides a simplified method for practitioners and can be significantly valuable. In this method, Nishijima and Faber (2009) define the Damage Index as the ratio between the repair cost and the replacement cost of the bridge under flood. Replacement cost is calculated based on the assumption that the bridge is completely damaged.

$$Damage\ Index(DI) = \frac{Repair\ cost}{Replacement\ cost} \quad \text{Equation 7-2}$$

In simple terms, we would require two types of cost data to calculate this damage index. If the actual monetary value of the repair and replacement cost are known, this would then be such a straight forward method. Table 7-2(below) shows such simple actual damage indices calculated for four bridges from the case study area. However, such data may not be available readily.

In such circumstances, an approximate method has been proposed and demonstrated in this research using bridge inspection reports, without referring to detailed cost estimations. This process required general understanding of failure mechanisms and associated cost for repair/reconstruction work. Full reconstruction work for a bridge typically included items 1-10 as listed below.

1. Construction of temporary road
2. Demolishing and removing existing structures such as bridge approach, bridge deck, pier/abutment and headstock
3. Reconstruction of bridge approach
4. Reconstruction of bridge deck
5. Reconstruction of bridge pier/abutment
6. Placing riprap /rock fill for scour protection.
7. Construction of wing wall / gabion wall for approach embankment
8. Replacing attachment of services to bridge
9. Replacing sign posts and standard road signs
10. Clearing debris material

Bridges with partial damage warranted only combination of some items from the above list and hence would be a fraction of the total replacement cost. For example, cracking in reinforced concrete bridge deck mainly require temporary access road (Item 1), demolishing reinforced concrete deck slab (Item 2), and Reconstruction of concrete bridge deck (Item 3). Based on estimated costs, it can calculate the repair cost and the DI. Alternatively, Equation 7-3 can be used to calculate contribution factors for all relevant items and then add them to obtain the DI using Equation 7-5.

$$\text{Contribution Factor for item 'i'} = \frac{\text{Repair Cost for item 'i'}}{\text{Estimated replacement cost}} \quad \text{Equation 7-3}$$

Where; the numerator, repair cost for item 'i', represented any individual item from the above list and the denominator, Estimated replacement cost, represented the total cost for complete replacement (i.e. summation of replacement cost for all items, 1-10).

$$DI = \sum \text{Contributing Factors for items 'i'} \quad \text{Equation 7-4}$$

Based on Equation 7-3, DI for the above example (i.e. damage to reinforced concrete bridge deck) can be expressed as:

$$DI \text{ for example} = \sum_{i=A,B,C} (\text{Contributing factors for items A, B and C})$$

Equation 7-5

Contributing factors may subject to change based on number of items, accuracy of the information as well as the severity of damage. For better estimation, above ten items could be further categorised into sub-items. For an example, item D may be sub-divided into two main categories, namely, damage to road wearing concrete slab and damage to concrete girder beams. Extent of damage can also be incorporated as another dimension for further improvement. However, these contribution factors may be subject to change from one region to another. Next section provides approximate contribution factors for 10 items listed above based on cost estimation values obtained from LVRC.

### Damage Index

DI method is used to quantify the severity of damage. For a completely damaged bridge, DI values are taken as 1. Cost estimations for partially damaged bridge were only available for Belford Bridge, Clarke Bridge, Logan Bridge and The Willows Bridge. For these four bridges, DI values were calculated based on the actual repair cost as well as the method proposed above. For other partially damaged bridge, DI values were calculated only based on Equation 7-3 and Equation 7-5 given in the above section. Next section defines the contribution factors for individual items 1-10 for the purpose of DI calculation.

### Contribution factors for items 1-10

Table 7-1 (below) summarises cost per each items 1-10 as a fraction of the total replacement cost, assuming fully damaged condition. These fractional values were determined based on estimated costs for fully damaged bridge sites in the Lockyer Valley Regional Council area. Therefore, given fractional values correspond with complete failure of individual item. In other terms, contribution factors given in Table 7-1(below) represent maximum value for a given item. If a given item is deemed to be partially damaged, the contribution factor should

be taken as a value between 0 and the corresponding maximum value. This may require detailed observations and relevant engineering judgements made using detailed inspection reports. Conservatively, 80% of the maximum contribution factor can be used for the DI calculation, if detailed inspection reports are not available.

Table 7-1: Maximum contribution factors for items 1-10

| Item No. | Item  | Maximum fraction Cost |
|----------|---|-----------------------|
| 1        | Construction of temporary road                                  | 0.05                  |
| 2        | Demolishing and removing existing structures                    | 0.07                  |
| 3        | Reconstruction of bridge approach                               | 0.15                  |
| 4        | Reconstruction of bridge deck                                   | 0.35                  |
| 5        | Reconstruction of bridge pier/abutment                          | 0.20                  |
| 6        | Placing riprap /rock fill for scour protection                  | 0.01                  |
| 7        | Construction of wing wall / gabion wall for approach embankment | 0.10                  |
| 8        | Replacing attachment of services to bridge                      | 0.03                  |
| 9        | Replacing sign posts and standard road signs                    | 0.02                  |
| 10       | Clearing debris material  | 0.02                  |
|          |   | Σ 1.0                 |

As maximum contribution factors (i.e. equals to maximum fractional cost) indicated, damage to bridge deck can lead to higher DI value. Therefore, bridge deck can be categorised as the most important item in terms of reduction in repair cost. Secondly, bridge pier/abutment is important, as it accounts approximately for 20% of total cost of replacement. Therefore, future studies on improving resilience of bridge should focus more on cost effective solutions for strengthening works or damage mitigation methods for bridge deck and pier/abutment.

Table 7-2: Actual Damage Index for the bridges

| <b>Bridge Name</b> | <b>Description of damage</b>  | <b>Repair Cost (AUD)</b> | <b>Estimated Replace cost (AUD)</b> | <b>DI</b> |
|--------------------|---|--------------------------|-------------------------------------|-----------|
| Belford Bridge     | Scour and slumping of the southern upstream rock spill; Relieving slab and approach road kerb has been undermined; Substantial crack appeared in the downstream western wing wall         | 91,592                   | 220,776                             | 0.41      |
| Clarke Bridge      | Edge delineation had been damaged by debris; Some bank scour on the downstream side of the bridge   | 21,535                   | 98903                               | 0.21      |
| Logan Bridge       | Whole section of one approach has been damaged<br>Significant scour of the eastern abutment<br>Headstock has been undermined<br>Cracks noted in the surfacing behind the eastern abutment | 67,547                   | 290,965                             | 0.23      |
| The Willows Bridge | Both approaches sustained substantial damage<br>Bridge guardrails ripped off<br>Upstream edge of the bridge broken  | 71,301                   | 85,485                              | 0.83      |

Estimated DI values and severity of damage

Table 7-3 (below) presents the estimated DI value for Belford Bridge using the Equation 7-3 and Equation 7-5

Table 7-3: Estimation of DI for Belford bridge

| <b>Bridge Name</b> | <b>Reported damage condition</b>   | <b>Corresponding Item</b> | <b>Contribution factor</b> | <b>DI</b> |
|--------------------|--|---------------------------|----------------------------|-----------|
| Belford Bridge     | Scour and slumping of the southern upstream rock spill; Relieving slab and approach road kerb has been undermined; Substantial crack appeared in the downstream western wing wall (Assuming fully damaged condition for each item) | F                         | 0.01                       | 0.38      |
|                    |  | A                         | 0.05                       |           |
|                    |  | B                         | 0.07                       |           |
|                    |  | C                         | 0.15                       |           |
|                    |  | G                         | 0.10                       |           |

Similarly DI values for other bridge sites have been calculated.

Figure 7.1(below) indicates good agreement between estimated DI values and actual DI values for Belford Bridge, Clarke Bridge, Logan Bridge and The Willows Bridge and hence validates the proposed method.

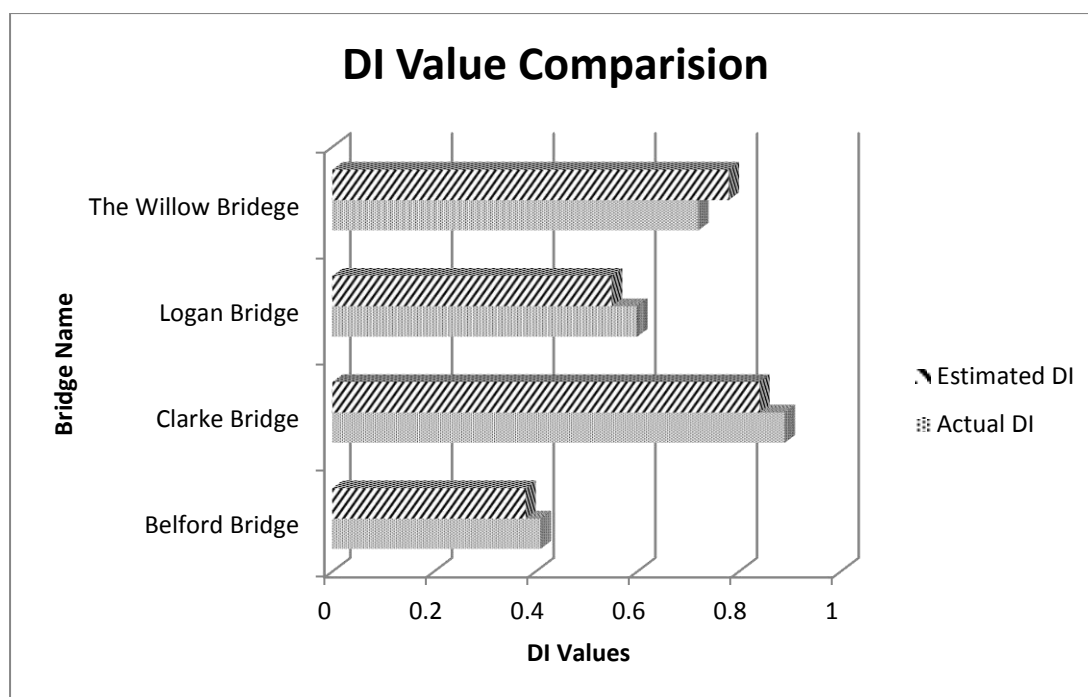


Figure 7.1: Comparison of Actual DI and Estimated DI

### 7.3 Damage Interpretation

The damage occurring in a concrete structure could be the result of loads exceeding its structural capacity or deformation. Generally a concrete structure is deemed to have failed when its tensile stress exceeds the maximum tensile stress as specified in AS 3600 as follows:

$$f'_{ct} = 0.36\sqrt{f'_c}$$

Equation 7-6

$f'_{ct}$  = concrete tensile stress and

$f'_c$  = nominal concrete compressive strength

When it comes to deformation criteria, the concrete structure is deemed to have failed when its strain reaches the value of 0.0035.

### 7.3.1 Concrete Plastic Damage Model

The structural behaviour of RC structures is highly complex due to the composite nature of the material. Concrete behaviour is brittle, but, under stress reversal, tensile cracks might close, then broken parts may be reassembled. Conversely, steel behaviour is ductile, with extremely rare fractures, and broken parts cannot be reunited. Therefore, concrete behaviour can be better used to describe damage models, whereas plasticity models better represent steel behaviour. Nevertheless, since steel brings additional ductility, the behaviour of reinforced concrete can be even better described with models that combine damage and plasticity. These models are particularly well suited for reproducing failure modes that are based on tensile cracking and compression crushing. In this research, steel behaviour is simulated with a uniaxial plasticity model and concrete is described with a multi axial model that considers parallel combination of scalar (isotropic) damaged elasticity and no associated multi-hardening plasticity. This model is termed as ‘‘Concrete Plastic Damage Model’’ (CPDM).

Figure 7.2(below) displays uniaxial stress-strain plot of damage-plasticity models.  $E_0$  is the initial (undamaged) elastic stiffness (deformation modulus), and  $\epsilon^{el}$  and  $\epsilon^{pl}$  are the elastic (recoverable) and plastic (irrecoverable) strain, respectively. Fig. 1 shows that damage generates stiffness degradation since the slope of unloading/reloading branch is  $(1 - d)E_0$  where  $d$  is a damage variable ranging between 0 (no damage) and 1 (destruction).

For uniaxial compression and tension, the stress-strain relation under uniaxial loading in the damage-plasticity behaviour displayed in Fig. 1, can be written as:

$$\sigma_c = (1 - d_c)E_0(\epsilon_c - \epsilon_c^{pl}) \quad \text{Equation 7-7}$$

$$\sigma_t = (1 - d_t)E_0(\epsilon_t - \epsilon_t^{pl}) \quad \text{Equation 7-8}$$

Subindices ‘c’ and ‘t’ refer to compression and tension, respectively.

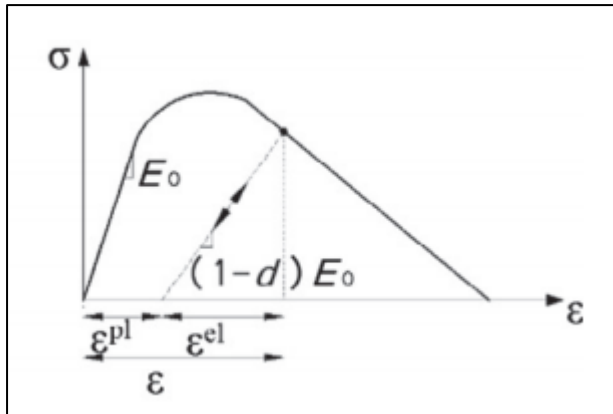


Figure 7.2: Uniaxial stress – strain plot (ABAQUS 6.14)

## 7.4 Damage Measurement

Mid span section of the bridge deck and the girder was modelled using ABAQUS and the flood force was applied to the first end girder. Figure 7.3 and Figure 7.4 show the concrete tension damage and concrete compression damage respectively for one particular output data base file from ABAQUS. There were 100 such files generated for each corresponding flood velocity fed to the system. The above figures correspond to the maximum flood velocity the bridge girder experienced. The damage is measured using damage variable ( $d$ ) ranging between 0 (no damage) and 1 (destruction). As can be seen from the Figure 7.4 it's obvious that the bridge superstructure didn't sustain any compression damage but tension damage.

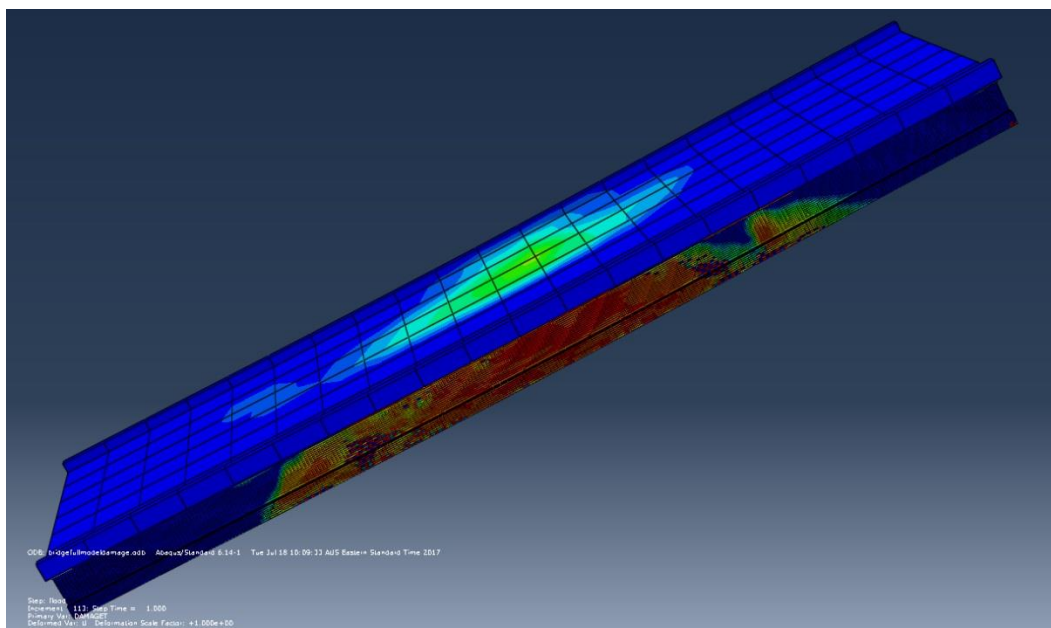


Figure 7.3: Concrete Tension Damage Parameter ( $dt$ )

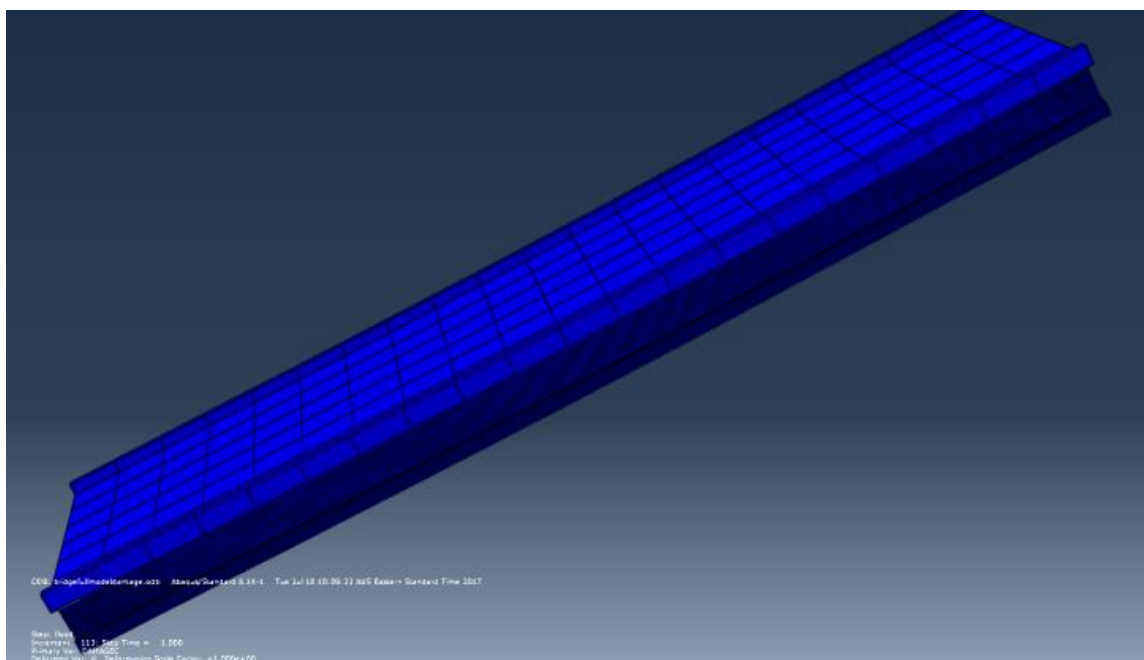


Figure 7.4: Concrete Compression Damage Parameter ( $d_c$ )

#### 7.4.1 Calculating the damage parameters ( $d_c$ & $d_t$ ) for damaged plasticity model in ABAQUS

Damage to the bridge girder are measured using the damage parameters ( $d_c$  &  $d_t$ ) that takes any value between 0 (No Damage) and 1 (Complete Damage) as defined by ABAQUS user manual. These parameters are extracted for each and every elements of the bridge girder. The overall damage to the girder was measured using the ratio between the number of elements that contained any value for damage parameter and the total number of elements. For this study only concrete tension Damage Parameter ( $d_t$ ) was used since no concrete compression damage was sustained in the concrete girder as shown in Figure 7.3. It was observed that not all the elements sustained same degree of damage.

#### 7.4.2 Classification of damage state to the bridge girder

Bridge inspectors use the method of area loss to ascertain the severity of damage to bridge structures. It is usually calculated as a percentage of area that is lost due to deterioration of the aging structure. Ramesh (2009) used similar kind of method to measure the damage to concrete beams in buildings using ABAQUS concrete tension damage parameters ( $d_t$ ).

Severity of damage has been defined as shown in Table 7-4(below). Accordingly the structure experiences a complete damage when the damage index takes a value of 1 and no damage when it takes a value of 0. It should be stated that this classification of damage severity and the classification of damage severity discussed in chapters 5 and 6 are not the same. The classification of damage severity discussed in this section is based on the definition of damage parameters ( $d_c$  and  $d_t$ ) given in ABAQUS manual. The damage severity defined here gives an indication of the repair cost and can be more suited to practical application.

Table 7-4: Classification of damage severity ((Ramesh, 2009))

| <b>Severity of Damage</b> | <b>concrete tension Damage Parameter (<math>d_t</math>)</b> |
|---------------------------|---|
| Complete Damage           | $0.8 < d_t < 1.0$   |
| Major Damage              | $0.5 < d_t < 0.8$   |
| Moderate Damage           | $0.2 < d_t < 0.5$   |
| Minor Damage              | $0.0 < d_t < 0.2$   |

There were 48772 elements that built up the bridge end girder in the ABAQUS model created. Damage parameter ( $d_t$ ) values were extracted for each and every elements when the bridge girder was under the influence of the maximum flood velocity that would eventually induce the maximum damage to the girder. Number of elements that would fit the corresponding damage index range were calculated using an excel sheet operation. For example, for major damage, the number of elements that corresponds to the value between 0.5 and 0.8 were counted. Table 7-5(below) summarizes this operation.

Table 7-5: Damage Interpretation table

| <b>Severity of Damage</b> | <b>dt</b>        | <b>Number of Elements</b> | <b>% of Elements</b> |
|---------------------------|------------------|---------------------------|----------------------|
| Complete Damage           | $0.8 < dt < 1.0$ | 12205                     | 25.02%               |
| Major Damage              | $0.5 < dt < 0.8$ | 9134                      | 18.72%               |
| Moderate Damage           | $0.2 < dt < 0.5$ | 2740                      | 5.62%                |
| Minor Damage              | $0.0 < dt < 0.2$ | 3289                      | 6.74%                |

Table 7-5(above) tells us that 25.02% of the bridge end girder would undergo a complete damage while 18.72% of it would experience a major damage and so on. This information assists in determining the possible cost of refurbishment of the girder.

## 7.5 Interpretation of Damage Curves

This section presents graphical comparisons of all fragility curves developed in chapter 6

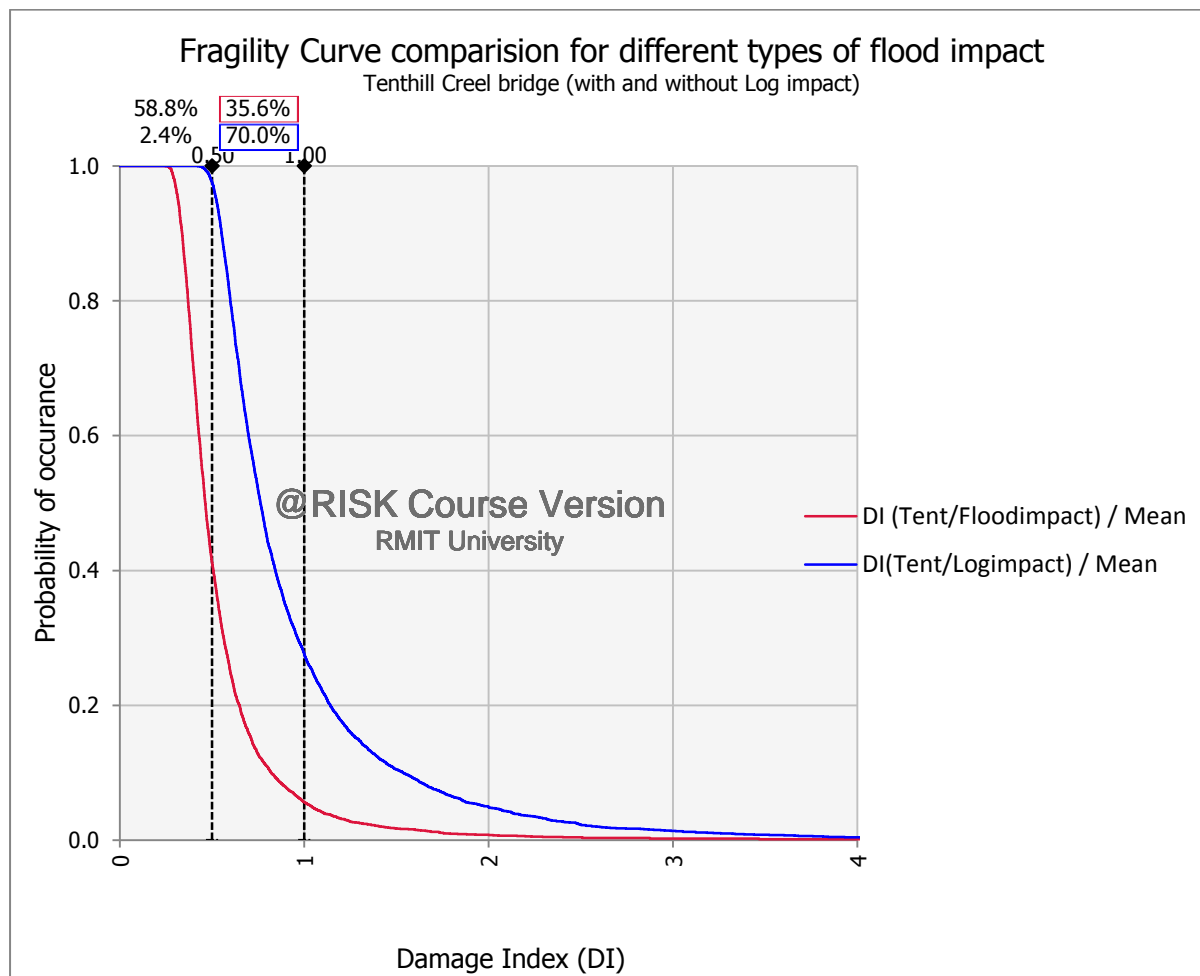


Figure 7.5: Fragility curve comparisons for Tenthill Creek Bridge under flood and log impact

Table 7-6: Comparison of failure probability for different types of flood impact (Tenthill Creek Bridge)

| Types of flood impact | Probability of failure (when DI=1.0) |
|-----------------------|--------------------------------------|
| Plain flood           | 5.6%                                 |
| Flood with log impact | 27.6%                                |

It is noted here that the bridge under investigation (Tenthill creek bridge) incur a higher probability of failure when it is hit by a flood that carries unusual debris such as vehicles, containers, leisure crafts etc.

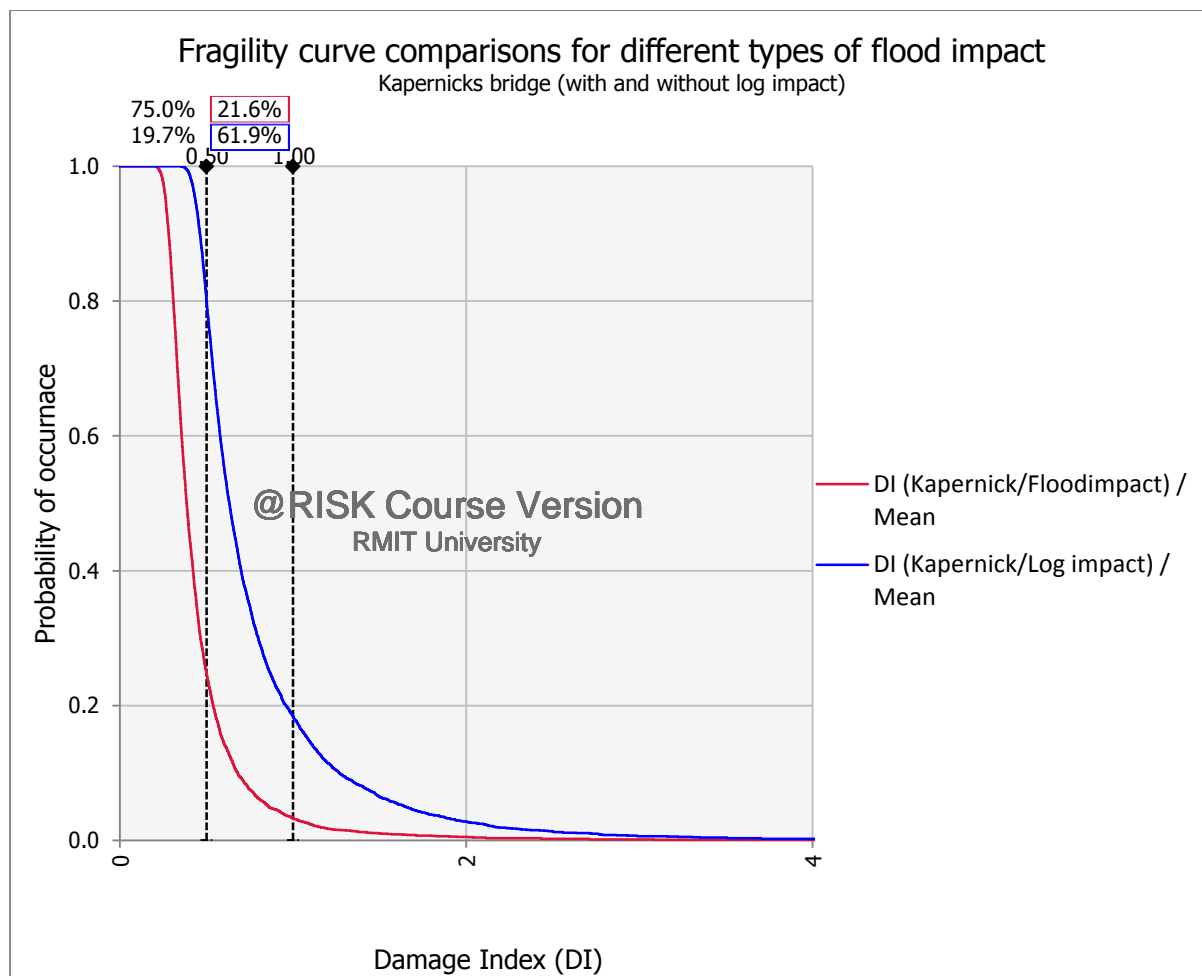


Figure 7.6: Fragility curve comparison for Kapernicks Bridge under flood and log impact

Table 7-7: Comparison of failure probability for different types of flood impact (Kapernicks Bridge)

| Types of flood impact | Probability of failure (when DI=1.0) |
|-----------------------|--------------------------------------|
| Plain flood           | 3.3%                                 |
| Flood with log impact | 18.4%                                |

It is noted here that the bridge under investigation (Kapernicks bridge) incur a higher probability of failure when it is hit by a flood that carries unusual debris such as vehicles, containers, leisure crafts etc. Comparatively, this bridge shows lower probability of failure than that of Tenthill Creek Bridge because this bridge is having a shorter span than that of Tenthill Creek bridge.

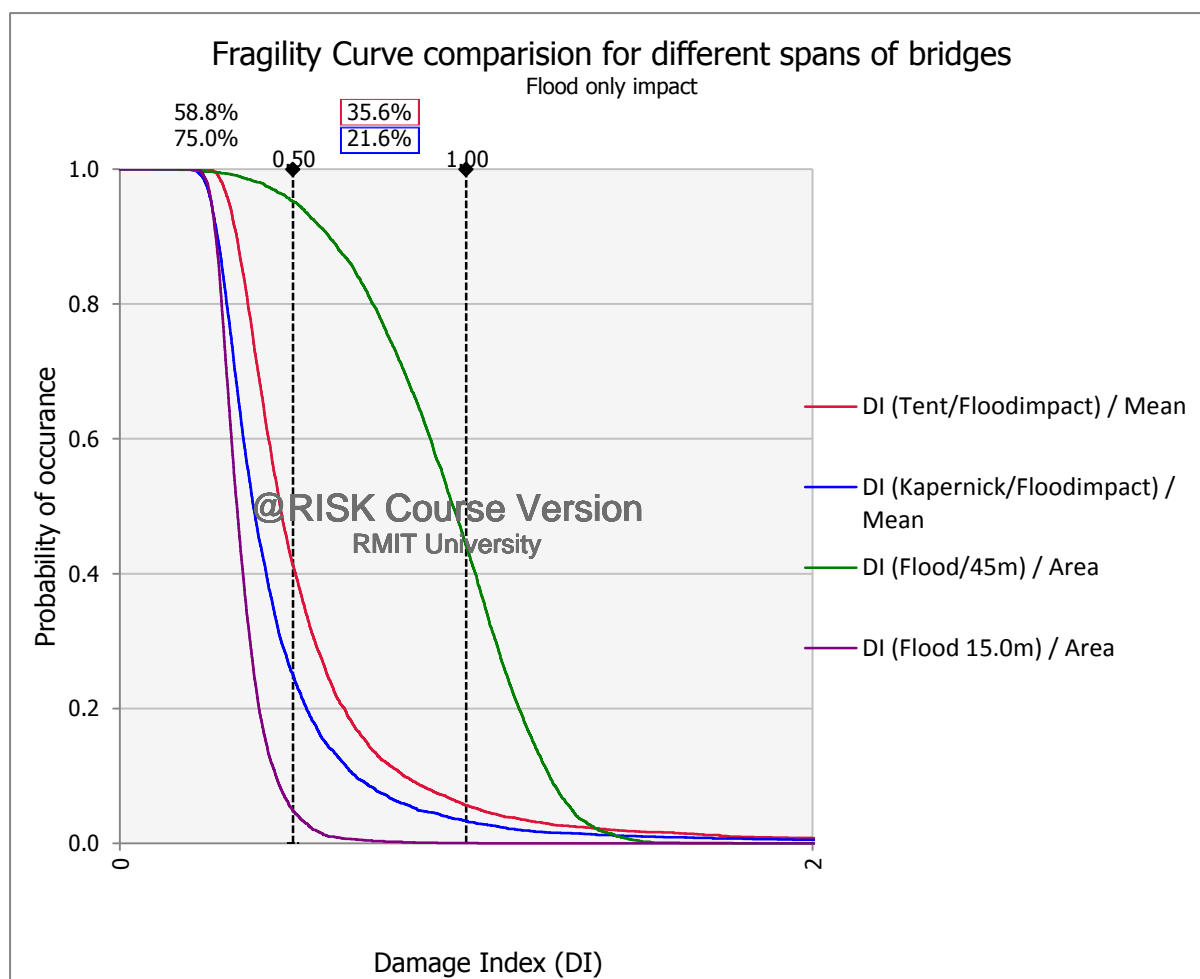


Figure 7.7: Fragility curve comparison for different span of bridges under flood only impact

Table 7-8: Comparisons of failure probability for different span length of the bridge (Flood only impact)

| Bridge girder span length (m) | Probability of failure (when DI =1.0) |
|-------------------------------|---------------------------------------|
| 15                            | 0%                                    |
| 22 (Kapernicks Bridge)        | 3.3%                                  |
| 27.4 (Tenthill Creek Bridge)  | 5.6%                                  |
| 45                            | 42.1%                                 |

It is observed here that the higher the span length of the bridge, the higher the probability of failure for same construction types of bridge. In this research concrete girder bridges have been studied. Different material types of bridges may exhibit different probability of failure for same span length.

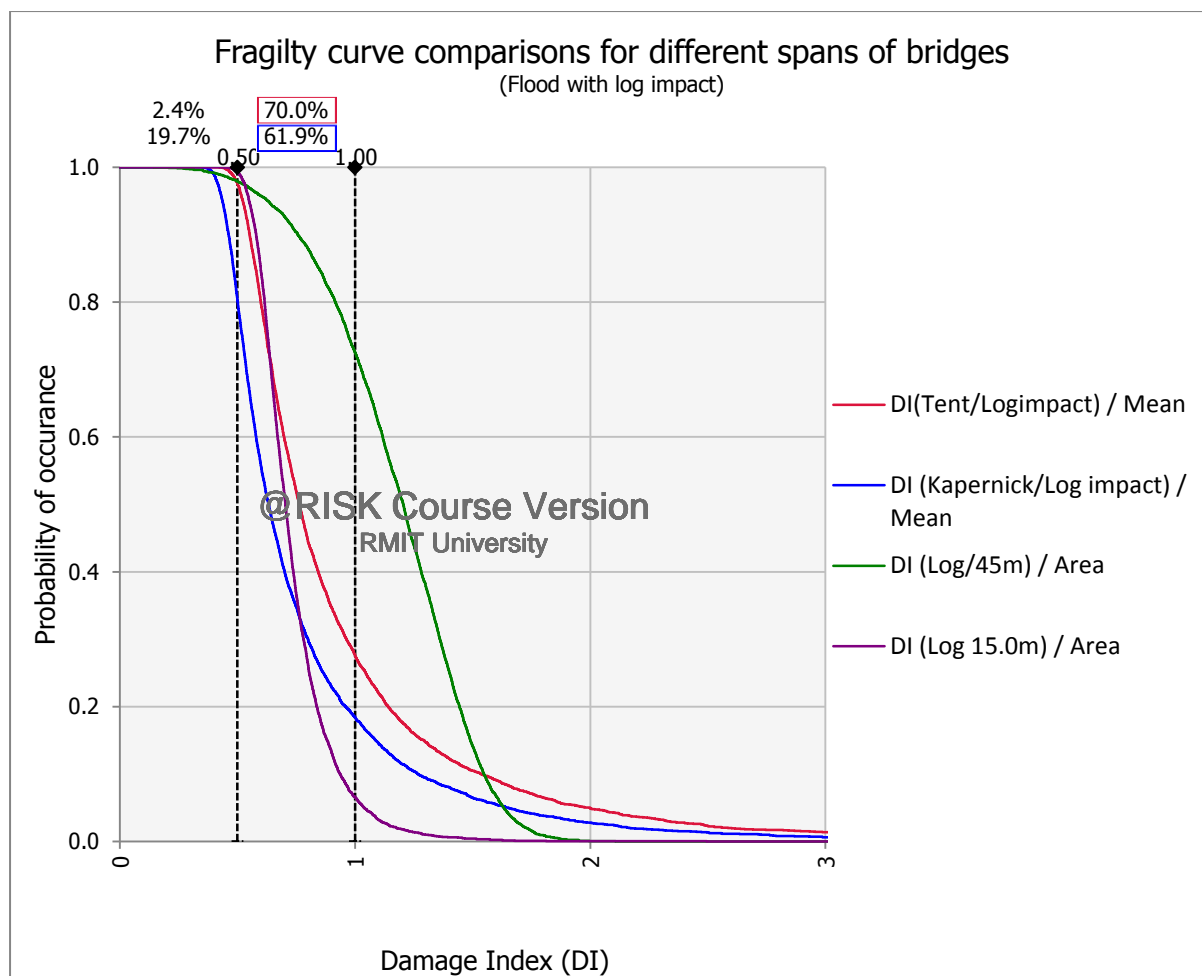


Figure 7.8: Fragility curve comparison for different span of bridges under flood and log impact

Table 7-9: Comparisons of failure probability for different span length of the bridge (Flood with log impact)

| Bridge girder span length (m) | Probability of failure (when DI =1.0) |
|-------------------------------|---------------------------------------|
| 15                            | 8.0%                                  |
| 22 (Kapernicks Bridge)        | 18.4%                                 |
| 27.4 (Tenthill Creek Bridge)  | 27.6%                                 |
| 45                            | 71.8%                                 |

It is observed here the bridges show the same trend as in the previous case but with higher probability of failure than that of previous case.

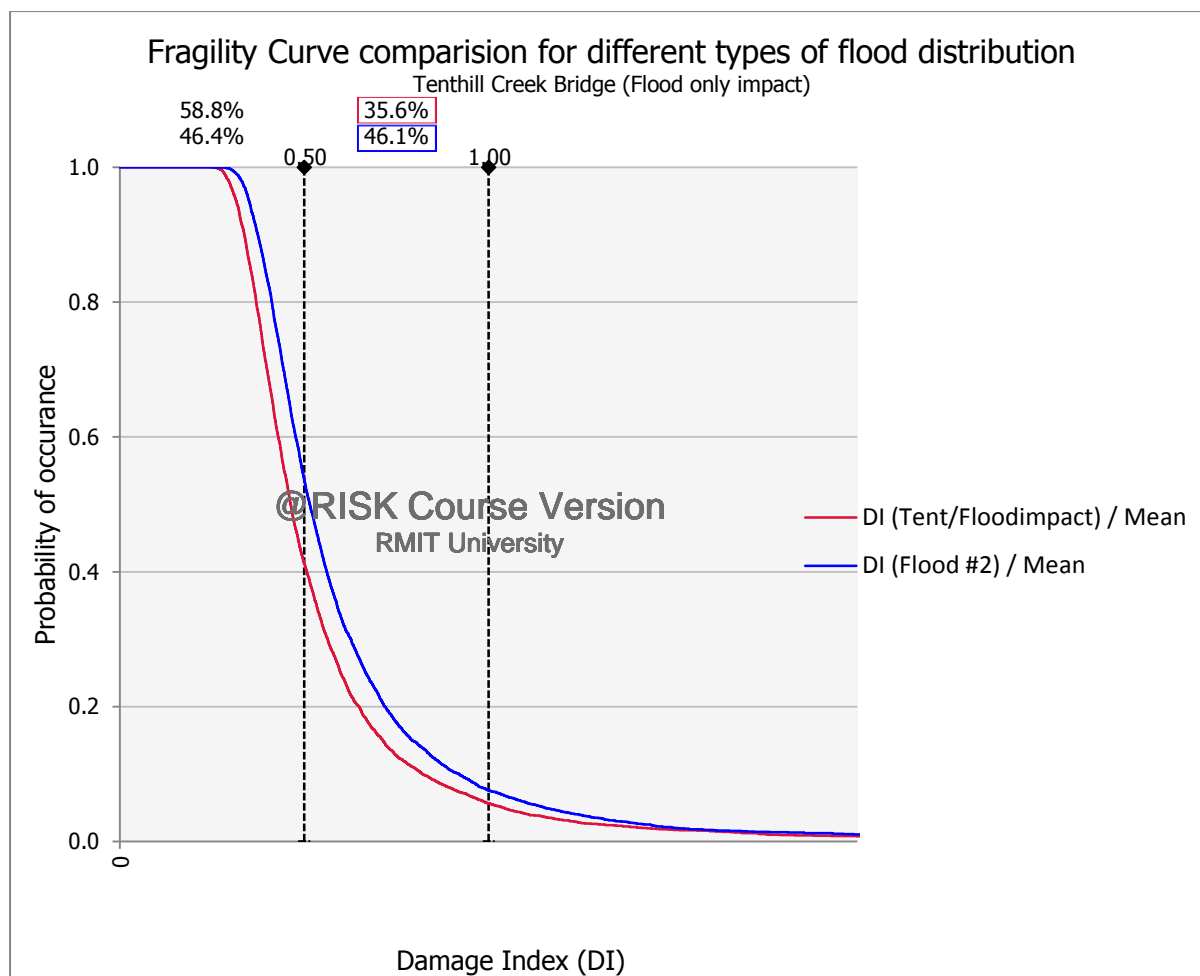


Figure 7.9: Fragility curve comparison for different types of flood velocity distribution for Tenthill bridge under flood only impact

Table 7-10: Comparisons of probability of failure for different flood velocity distribution (Tenthill creek bridge under flood only impact)

| Flood velocity distribution                | Probability of failure (when DI=1.0) |
|--|--------------------------------------|
| Distribution # 1 (Mean velocity = 2.55m/s) | 5.6%                                 |
| Distribution # 2 (Mean velocity = 2.75m/s) | 7.5%                                 |

It is noted here that when the bridge is hit by a higher flood velocity distribution, it experiences a higher probability of failure as shown in Table 7-10

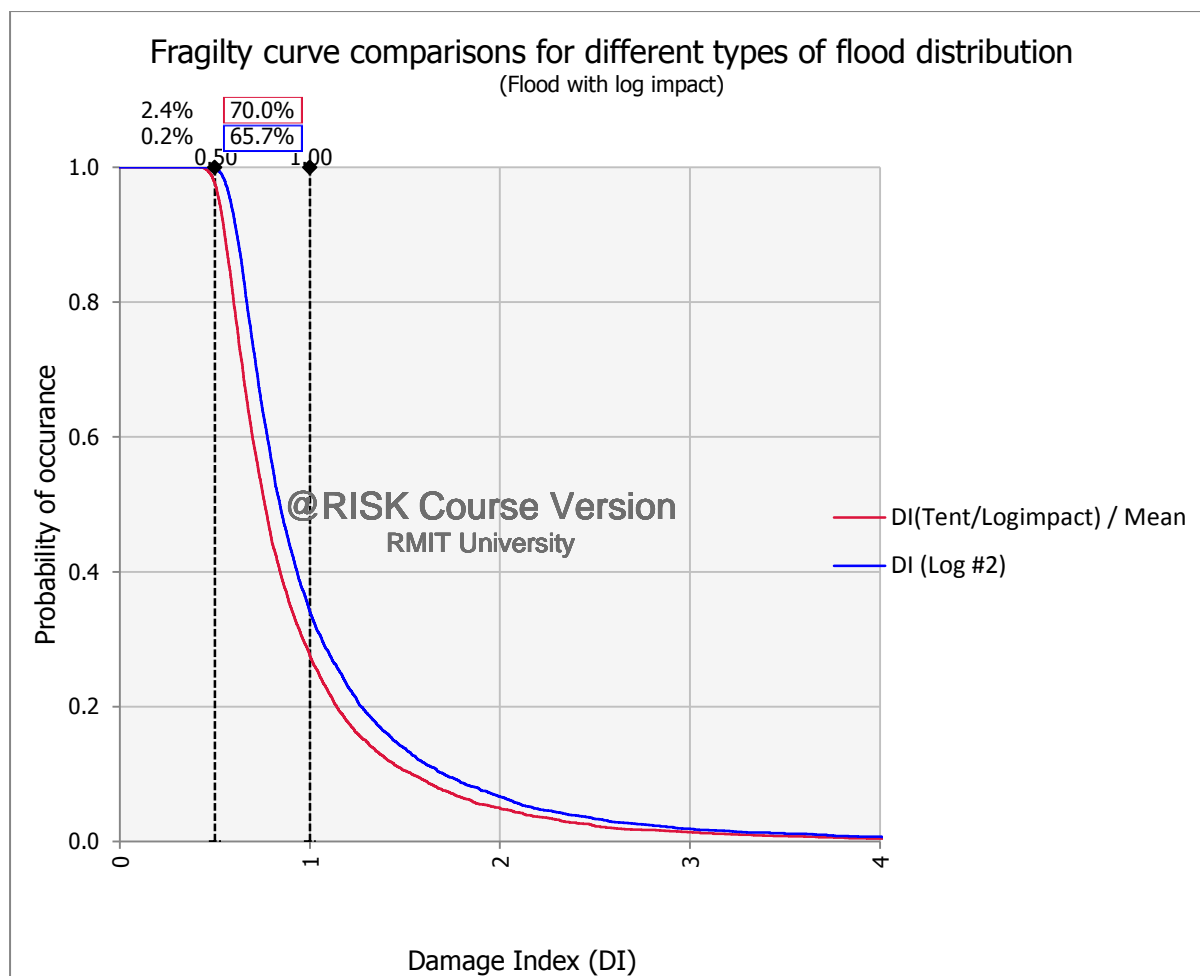


Figure 7.10: Fragility curve comparison for different types of flood velocity distribution for Tenthill bridge under flood and log impact

Table 7-11: Comparisons of probability of failure for different flood velocity distribution (Tenthill creek bridge under flood with log impact)

| Flood velocity distribution                | Probability of failure (when DI=1.0) |
|--|--------------------------------------|
| Distribution # 1 (Mean velocity = 2.55m/s) | 27.6%                                |
| Distribution # 2 (Mean velocity = 2.75m/s) | 34.1%                                |

Table 7-11 indicates that when the bridge experience a flood with log impact it undergoes even a higher probability of failure than that of it being hit by just plain flood.

## 7.6 Application of fragility curves for end users and decision makers.

The methodology developed for deriving fragility curves for concrete girder bridges can be used to evaluate the bridge stock of a road authority using the point stream flow data and known variability of bridge materials and structures. The fragility curves allow the bridge engineer to understand the vulnerability of a given structure under expected annual exceedance probability of a flood and also material and structure degradation of aging structures

A summary of findings of the research are given in Table 7-12 and Table 7-13 for concrete girder bridges

Table 7-12: Probability of failure for different scenarios (DI=1.0)

| <b>Analysis</b>        | <b>Probability of failure (DI=1.0)</b> |
|------------------------|--|
| Tenthill (Flood)       | 5.6%                                   |
| Tenthill (Flood/Log)   | 27.6%                                  |
| Kapernicks (Flood)     | 3.3%                                   |
| Kapernicks (Flood/Log) | 18.4%                                  |
| 15m span (Flood)       | 0.0%                                   |
| 15m span (Flood/Log)   | 8.0%                                   |
| 45m span (Flood)       | 42.1%                                  |
| 45m span (Flood/Log)   | 71.8%                                  |
| Tenthill(Flood #2)     | 7.5%                                   |
| Tenthill(Flood/Log #2) | 34.1%                                  |

Table 7-13: Probability of failure for different scenarios (different damage severity)

| Analysis               | Probability of occurrence (%) for damage severity |          |       |           |          |
|------------------------|---|----------|-------|-----------|----------|
|                        | Minor   | Moderate | Major | Extensive | Complete |
| Tenthill (Flood)       | 16.4  | 9.1      | 4.9   | 3.0       | 2.2      |
| Tenthill (Flood/Log)   | 17.9  | 20.1     | 15.2  | 9.7       | 7.1      |
| Kapernicks (Flood)     | 10.5  | 5.3      | 3.0   | 1.6       | 1.3      |
| Kapernicks (Flood/Log) | 24.6  | 15.7     | 10.0  | 7.1       | 4.5      |
| 15m span (Flood)       | 3.8   | 0.6      | 0.2   | 0.1       | 0.1      |
| 15m span (Flood/Log)   | 14.9  | 33.2     | 25.0  | 13.0      | 6.6      |
| 45m span (Flood)       | 4.9   | 7.3      | 10.5  | 13.0      | 15.3     |
| 45m span (Flood/Log)   | 2.1   | 3.1      | 4.8   | 6.6       | 8.7      |
| Tenthill(Flood #2)     | 20.4  | 11.3     | 7.1   | 4.3       | 3.0      |
| Tenthill(Flood/Log #2) | 7.2   | 19.1     | 17.4  | 12.8      | 9.2      |

## 7.7 Chapter summary

This chapter describes the types of damage indices used in this research and derivation of damage curves for concrete girder bridges under flood hazard. An approximate method of calculating cost based damage index, in the absence of actual cost data, has been illustrated using some of the bridges (Belford bridge, Clarke bridge, Logan bridge and The Willows bridge) reported in the bridge inspection report from Lockyer Valley Regional council.

Measuring severity of damage to bridge structure using concrete tension damage parameter (dt) in ABAQUS has been explained.

Fragility curves generated in chapter 6 are presented graphically to compare the difference between different scenarios considered.

Cost based damage indices were shown to be a useful method for practitioners to determine the strength of the bridge network during pre-disaster planning. The method proposed offers a reasonable accuracy and can be further developed as a method useful to practitioners.

The tension damage parameters can be used to determine the area of refurbishment and the corresponding cost in one structural element. This method will complement the cost based damage index and the fragility of a bridge.

Combining the three parameters: cost based damage index, fragility and the tension damage parameter a comprehensive management strategy for concrete girder bridges can be developed for the infrastructure owners to assist in enhancing resilience of critical bridges in the network.

## **8 Summary, conclusions and recommendation**

### **8.1 Summary**

Bridges are critical links in the road network and they play a critical role in evacuation and search and rescue operation during and aftermath of any natural hazard. Reinforced or pre-stressed concrete girder bridges are a common design configuration used in Australia. During the Lockyer Valley floods in 2013, vulnerability of girder bridges was observed to have undergone significant damage.

With global climate change, the intensity and frequency of severe weather events such as flooding are increasing. It is reported that flood events cost the most damage to infrastructure compared to any other natural hazards in the world. Quantifying vulnerability of road infrastructure such as bridges has therefore become necessary.

Extensive literature review under this research has indicated that significant research has been carried out on the vulnerability of building structures under the influence of other natural hazard such as earth quake, hurricane etc. but little or no research has been done on the vulnerability of road infrastructure such as bridges under the influence of flood hazard which was the gap in knowledge identified in this research programme.

The major contribution to knowledge from this research is the development of a generic methodology for vulnerability assessment and vulnerability indices for concrete girder bridges incorporating the uncertain nature of flood induced loading and the capacity of aging bridge structures. This, in turn, gives road authorities tools required to make decision on strengthening of the aging bridge structures to be resilient to flood hazards.

It should be noted that although the research has been conducted on concrete girder bridges, many of the concepts introduced will be applicable to other types of bridges such as steel and timber bridges.

### **8.2 Conclusions**

The research presented here aimed to develop a methodology for vulnerability modelling of bridges under flood loading considering the uncertainty in the flood velocity and the structural capacity of ageing structures.

First objective of this research has been achieved through exploration of case study bridges from Lockyer Valley region in Queensland. There were 46 bridges reported partially or fully damaged in the aftermath of 2011 and 2013 severe flood event in the region. Extensive analysis of these bridges identified the failure modes of the bridges as summarised in tables 4.2 and 4.3 in section 4.3.

Having identified that the majority of the bridge stocks, as shown in figure 4.4, are concrete girder bridges, two bridges were selected for structural analysis as described in section 5.1.

It was necessary to understand the provisions of bridge design codes to analyse the selected two bridges structurally to establish the bridge responses to flood impact. This objective has been addressed in sections 2.3 and 2.4. Globally renowned 3 major bridge design codes, AASHTO, Euro and AS 5100, were discussed and AS 5100 was chosen to be used because the bridges analysed were all from Australian region.

Third objective achieved through this research is numerically modelling the selected bridges as described in Chapters 5 and 6. The bridges were first modelled using simple beam elements available in ABAQUS. The actual configuration of the bridge girder that includes reinforcement bars inside was unable to be modelled using ABAQUS beam elements. This restriction was overcome by using ABAQUS solid elements as described in section 5.4.2 and the accuracy of the analysis was enhanced.

Having established the knowledge gap as detailed in section 1.4, an attempt has been made to arrive at a generic methodology to develop fragility curves for concrete girder bridge decks. The bridges were analysed through a probabilistic approach in this model to account for variation in bridge material strength, geometric configuration and flood intensity. The actual flood velocity distribution for the case study area was obtained for the analysis as described in sections 6.2.1 and 6.2.2. The relationship between flood exposure and the corresponding damage are established through development of fragility curves as depicted in figures 6.17 through 6.24 in section 6.5.

The major conclusions are summarized in the following sections.

### **8.2.1 Findings from the review of literature**

The review of previous work explored the provisions of the design standards given to cover flood loading. This review confirmed that all standards follow a similar approach and the impact of flood is taken as a uniformly distributed load on the structure.

Study of research literature indicated that damage to infrastructure resulting from the impact of natural hazards is measured using damage indices. Different researchers adopted different concepts to define these damage indices from a simple cost based damage index to a complex energy based damage index.

Further it was noted that the vulnerability of the structures can be determined using either a deterministic analysis or a full probabilistic analysis. A deterministic analysis can be used to calculate the flood velocity at which the structure would fail. A full probabilistic analysis can provide the probability of failure of the structure in the form of fragility curves.

### **8.2.2 Findings from the analysis of the case studies**

Lockyer Valley region in Queensland, Australia is the most adversely affected area during recent flood events. It suffered two nationally prominent extreme flood disasters in the recent past, one in 2011 and the other in 2013. Comprehensive review of bridge inspection reports from Lockyer Valley Regional council revealed that different bridges failed due different failure mechanisms. Damage to concrete girder bridge decks was observed to be one of the major failure mechanisms of the affected bridge stock of the region. It also revealed that some of the bridges failed mainly because of unusual floating debris such as shipping containers, cars and river-craft (for example 300t vessels).

Analysis of bridge inspection reports indicated that most of the bridges reported were concrete girder bridges and they exhibited most of the damage happening on the bridge decks. This specific observation paved way to narrow down this research to concentrate detailed analysis on concrete girder bridge decks.

### **8.2.3 Findings from the numerical modelling of the case study bridge – Deterministic approach**

Two bridges have been selected to case study in this research to establish the major failure mode and the necessary input parameters for numerical modelling. One of them in fact failed

during the 2013 flood event. Damage to bridges was quantified using capacity based damage index. These bridges were numerically modelled using ABAQUS to study the effect of flood impact to the bridge. A simple deterministic vulnerable modelling method was first adopted to generate vulnerability curves to establish threshold values of flood velocity before the structure would fail. Calculated failure flood velocity was compared with the field observations and was observed to have reasonable agreement.

Vulnerability curves for concrete girder bridges under flood hazard have been generated and relevant flood intensity values have been established for different flood scenarios. It was observed and justified here that the bridge would fail at a lower flood velocity under the combined effect of flood and log impact.

#### **8.2.4 Findings from the numerical modelling of the case study bridge – Probabilistic approach**

In order to incorporate the uncertain nature of the flood intensity (flood velocity) and the structural capacity of the bridge structure due to deterioration, a probabilistic fragility modelling method was adopted to establish the probability of failure of the bridge structure under flood hazard.

A comprehensive method to establish relevant flood velocity values for use in this research was devised using simple open channel flow equations. This involved use of AutoCAD software to draw the corresponding river profile that enabled calculating corresponding cross sectional area for every depth of the flood recorded over a long period of time at the corresponding water monitoring stations.

Both the bridges examined here showed that they had the probability of failure of less than 5.0% as per the provision allowed in all the bridge design codes worldwide. However, they showed a higher probability of failure when they were under the influence of unusual debris such as containers, vehicles and leisure crafts.

Damage to bridge structure before it would fail in its entirety has been classified into 5 levels of damage from minor damage to complete damage to help the authority to estimate the associated cost for refurbishment and to prioritise necessary retrofitting activities.

### 8.2.5 Findings from damage indices for practical application

Application of two types of damage indices has been demonstrated. An approximate method of calculating cost based damage index showed that it yielded close result in the absence of actual repair cost data available for the bridges.

It was shown that concrete damage parameters defined in the concrete damage plasticity model (CDP) could be used to calculate the area loss of the damaged bridge structure and the retrofitting actions could be planned accordingly.

Fragility curves, considering the variability of flood intensity and capacity of the aging bridge structure, have been constructed for different flood scenarios. A sensitivity analysis has also been carried out to study the effect of different span length of the bridge and different flood distribution that may arrive from some other parts of the case study area. Generation of these fragility curves have shown the following observations:

- Bridge structure would experience a higher probability of failure when they are impacted by flood that would carry huge floating objects. It was observed that the increase was as high as five fold.
- Parametric study on the effect of increasing bridge span showed that the bridge would experience higher probability of failure. It was shown that the probability of failure was increased up to nine fold when the bridge span was increased from 15m to 45m.
- Sensitivity analysis on the effect of increasing flood velocity showed that the bridge would experience higher probability of failure with the increase in flood velocity. It was shown that the probability of failure was increased from 5.6% to 7.5% when the mean flood velocity was increased from 2.55m/s to 2.75m/s. The probability increased from 27.6% to 34.1% when the effect of log impact was considered for the same flood velocity increase.

Finally Damage Index (DI), vulnerability curves, fragility curves and concrete damage parameters would provide adequate information for making decisions to enhance the resilience of the bridge exposed extreme flood event.

It should be noted here that the decision to strengthen may consider the impact of the failure of the bridge on the community. This is considered to be beyond the scope of this research.

### 8.3 Recommendations for future research:

Although the research aimed to generate fragility curves for concrete girder bridges under flood hazard, some aspects were beyond the scope of this project. Therefore to extend and continue this research the following recommendations are made:

- Fragility curves generated in this research are applicable only for the deck of a concrete girder bridge for concrete girder bridge. This work should be extended to cover the other components of the bridge such as bridge piers, bridge approach and bridge foundation etc. Analysis of the case study bridges indicated that another phenomenon called “bridge scour” has also played significant role in making severe damages to the bridges during the aftermath of 2013 Queensland severe flood event. Hence vulnerability of bridge piers including the bridge foundation should be carried out to capture the effect of bridge scour on the developed fragility curves.
- One of the other aspects observed from the bridge inspection report was that some of the bridges were failed because of loss of supports between the girder and the headstock. This should also be given attention in the future work.
- Given the virtue of its simplicity, the flood induced force on the bridge girder has been calculated as per AS5100 bridge design code and applied to the structure as a static load in this research. It is, however, recommended to use ABAQUS CFD (Computational Fluid Dynamics) modules to get a better result that takes into account the dynamic nature of the flood force.
- It is postulated that the AS 5100 Bridge Design Code was written mainly for traditional rural applications. This research examined the actual loads that urban bridges were subjected to including floating debris such as shipping containers, cars and river-craft (for example 300 t vessels) that should be incorporated in future revisions of AS 5100. It is suggested that in future, bridge design codes should consider the context and location of bridges for connectivity and post disaster functionality. It is recommended that AS 5100:2004 be amended to account for the knowledge gained during Queensland’s extreme event. Areas to review include:
  - Flood loads on all bridges including road, pedestrian and rail bridges
  - Ship impact during flood
  - Debris type in urban areas, for example, containers that can cause both debris loads and buoyancy loads
  - Debris loads on piers

- Abutment scour
- Armouring of stream bed against scour
- Storm surge events from cyclone and other extreme events
- Land use changes from urban development
- Climate change including changes to rainfall patterns
- Sea level change
- Post disaster functionality for bridges on critical transport links.

**REFERENCES**

---

- Historic Winter Flood Along Mississippi River Sets Record in Cape Girardeau, January 6, 2016.* [Online]. Available: <https://weather.com/news/news/mississippi-river-flooding-december-2015>. [Accessed 12 January 2017].
- Stream Stability at Highway Structures. 2nd Edition, Hydraulic Engineering Circular (HEC) No. 20.* U.S. Department of Transportation, FHWA, November 1995. [Online]. Available: <http://www.fhwa.dot.gov/engineering/hydraulics/pubs/hec/hec20si.pdf>. [Accessed March 15 2016].
- AASHTO, L. 1998. Bridge design specifications. American Association of State Highway and Transportation Officials, Washington, DC.
- AASHTO, L. 2012. Bridge design specifications, customary US units, (6th Edition). American Association of State Highway and Transportation Officials, Washington, DC.
- AGARWAL, J., BLOCKLEY, D. & WOODMAN, N. 2003. Vulnerability of structural systems. *Structural Safety*, 25, 263-286.
- ALAMPALLI, S., FU, G. & DILLON, E. W. 1997. Signal versus noise in damage detection by experimental modal analysis. *Journal of Structural Engineering*, 123, 237-245.
- APELT, C. Flood forces on bridges. AUSTRALIAN ROAD RESEARCH BOARD PROCEEDINGS, 1986.
- ATAEI, N. & PADGETT, J. E. 2012. Probabilistic modeling of bridge deck unseating during hurricane events. *Journal of Bridge Engineering*, 18, 275-286.
- AUSTRALIA, S. A. O. 2004. Australian Standard Bridge Design Part 2. AS 5100.2. Sydney NSW 2001, Australia: Standards Australia.
- AUSTROAD'92 1992. *Bridge design code*, Surry Hills, NSW, Austroads.

- AZADBAKHT, M. & YIM, S. C. 2014. Simulation and estimation of tsunami loads on bridge superstructures. *Journal of Waterway, Port, Coastal, and Ocean Engineering*, 141, 04014031.
- BAHMANI, M. 2015. *Parametric Study in ABAQUS* [Online]. Available: <https://www.youtube.com/watch?v=yR2DKliOZHA> [Accessed 03/04/2015 2015].
- BANON, H., BIGGS, J. M. & IRVINE, H. 1980. *Prediction of seismic damage in reinforced concrete frames*. Massachusetts Institute of Technology.
- BANON, H. & VENEZIANO, D. 1982. Seismic safety of reinforced concrete members and structures. *Earthquake Engineering & Structural Dynamics*, 10, 179-193.
- BASOZ, N. I., KIREMIDJIAN, A. S., KING, S. A. & LAW, K. H. 1999. Statistical analysis of bridge damage data from the 1994 Northridge, CA, earthquake. *Earthquake Spectra*, 15, 25-54.
- BERTERO, V. & BRESLER, B. 1977. Design and engineering decision: failure criteria (limit states), developing methodologies for evaluating the earthquake safety of existing buildings. Report No. EERC-77-6, University of California, Berkeley, CA.
- BLEJWAS, T. E. & BRESLER, B. 1979. *Damageability in existing buildings*, University of California, Earthquake Engineering Research Center.
- BLONG, R. 2003. A new damage index. *Natural Hazards*, 30, 1-23.
- BLUME, J. A. Engineering intensity scale data for the 1971 San Fernando earthquake. Proc. World Conf. Earthquake Eng., New Delhi, 1977. 2-375.
- BOCCHINI, P. & FRANGOPOL, D. M. 2012. Restoration of bridge networks after an earthquake: multicriteria intervention optimization. *Earthquake Spectra*, 28, 426-455.
- BONSTROM, H. L. & COROTIS, R. B. 2010. Structural reliability and sustainable resilience.

- BRESLER, B. 1977. Developing Methodologies for Evaluating the Earthquake Safety of Existing Buildings.
- BUREAU OF METEOROLOGY. 2003. '*Floods - warning, preparedness and safety*' [Online]. Available: [http://www.bom.gov.au/australia/flood/EMA\\_Floods\\_warning\\_preparedness\\_safety.pdf](http://www.bom.gov.au/australia/flood/EMA_Floods_warning_preparedness_safety.pdf).
- CARREIRA, D. J. & CHU, K.-H. Stress-strain relationship for plain concrete in compression. *Journal Proceedings*, 1985. 797-804.
- CHEN, Q., WANG, L. & ZHAO, H. 2009a. Hydrodynamic investigation of coastal bridge collapse during Hurricane Katrina. *Journal of Hydraulic Engineering*, 135, 175-186.
- CHEN, W.-F. & LUI, E. M. 2005. *Handbook of structural engineering*, Crc Press.
- CHEN, Z., HAN, Y., HUA, X. & LUO, Y. 2009b. Investigation on influence factors of buffeting response of bridges and its aeroelastic model verification for Xiaoguan Bridge. *Engineering Structures*, 31, 417-431.
- CHOI, E., DESROCHES, R. & NIELSON, B. 2004. Seismic fragility of typical bridges in moderate seismic zones. *Engineering Structures*, 26, 187-199.
- CHUNG, Y. S., MEYER, C. & SHINOZUKA, M. 1989. Modeling of concrete damage. *Structural Journal*, 86, 259-271.
- CIMELLARO, G. P., REINHORN, A. M. & BRUNEAU, M. 2010. Seismic resilience of a hospital system. *Structure and Infrastructure Engineering*, 6, 127-144.
- COMERIO, M. C. 2006. Estimating downtime in loss modeling. *Earthquake Spectra*, 22, 349-365.
- COOK, W. 2014. Bridge Failure Rates, Consequences, and Predictive Trends.

- DANIELS, J., HUGHES, D., RAMEY, G. E. & HUGHES, M. L. 2007. Effects of bridge pile bent geometry and levels of scour and P loads on bent pushover loads in extreme flood/scour events. *Practice Periodical on Structural Design and Construction*, 12, 122-134.
- DASSAULTSSYSTEMS. 2015. *ABAQUS UNIFIED FEA. COMPLETE SOLUTIONS FOR REALISTIC SIMULATION* [Online]. Available: <http://www.3ds.com/productservices/simulia/products/abaqus/> [Accessed 10 May 2017].
- DAWSON, R., HALL, J., SAYERS, P., BATES, P. & ROSU, C. 2005. Sampling-based flood risk analysis for fluvial dike systems. *Stochastic Environmental Research and Risk Assessment*, 19, 388-402.
- DECÒ, A. & FRANGOPOL, D. M. 2011. Risk assessment of highway bridges under multiple hazards. *Journal of Risk Research*, 14, 1057-1089.
- DENG, L., WANG, W. & YU, Y. 2015. State-of-the-art review on the causes and mechanisms of bridge collapse. *Journal of Performance of Constructed Facilities*, 30, 04015005.
- DENSON, K. H. 1982. Steady-state drag, lift and rolling-moment coefficients for inundated inland bridges.
- DEPARTMENT OF INFRASTRUCTURE AND REGIONAL DEVELOPEMNT, A. G. 2008. *About Australia's Regions 2008* [Online]. Available: [https://bitre.gov.au/publications/2008/other\\_005.aspx](https://bitre.gov.au/publications/2008/other_005.aspx) [Accessed 12.12.2013 2013].
- DEPARTMENTOFMAINROADS. 2006. *Road Planning and Design Manual* [Online]. Available: <https://www.tmr.qld.gov.au/business-industry/Technical-standards-publications/Road-planning-and-design-manual.aspx>.

- DESROCHES, R., CHOI, E., LEON, R. T., DYKE, S. J. & ASCHHEIM, M. 2004. Seismic response of multiple span steel bridges in central and southeastern United States. I: As built. *Journal of Bridge Engineering*, 9, 464-472.
- DIAMANTIDIS, D. 2001. *Report 32: Probabilistic Assessment of Existing Structures-A publication for the Joint Committee on Structural Safety (JCSS)*, RILEM publications.
- DIPASQUALE, E. & CAKMAK, A. 1990. Seismic damage assessment using linear models. *Soil Dynamics and Earthquake Engineering*, 9, 194-215.
- DONG, Y., FRANGOPOL, D. M. & SAYDAM, D. 2013. Time-variant sustainability assessment of seismically vulnerable bridges subjected to multiple hazards. *Earthquake Engineering & Structural Dynamics*, 42, 1451-1467.
- DURMUS, A. Geospatial assessment of sustainable built infrastructure assets and flood disaster protection. Masters Abstracts International, 2012.
- ELLINGWOOD, B. 1980. *Development of a probability based load criterion for American National Standard A58: Building code requirements for minimum design loads in buildings and other structures*, US Department of Commerce, National Bureau of Standards.
- ELLINGWOOD, B. R. & DUSENBERRY, D. O. 2005. Building design for abnormal loads and progressive collapse. *Computer-Aided Civil and Infrastructure Engineering*, 20, 194-205.
- ELNASHAI, A., BORZI, B. & VLACHOS, S. 2004. Deformation-based vulnerability functions for RC bridges. *Structural Engineering and Mechanics*, 17, 215-244.
- EUROCODE 2005. Eurocode. *Part 1.7*. London: European Authority.
- EYRE, T., FERGUSON, D., HOURIGAN, C., SMITH, G., MATHIESON, M., KELLY, A., VENZ, M., HOGAN, L. & ROWLAND, J. 2012. Terrestrial vertebrate fauna survey assessment guidelines for Queensland. Department of Science. *Information Technology, Innovation and the Arts, Queensland Government, Brisbane*.

- EZEAJUGH, L. Restoration of scoured out bridge approaches and foundations: a Queensland Department of Transport and Main Roads (QDTMR) perspective. Austroads Bridge Conference, 9th, 2014, Sydney, New South Wales, Australia, 2014.
- FABER, M. & SØRENSEN, J. D. 2002. Reliability based code calibration. *The Joint Committee on Structural Safety, Zurich, Switzerland*.
- GOSAIN, N. K., BROWN, R. H. & JERSA, J. 1977. Shear requirements for load reversals on RC members. *Journal of the Structural Division*, 103.
- GREG ROGENCAMP, J. B. 2012. *The Lockyer Creek Flood of January 2011: What Happened and How Should We Manage Hazard for Rare Floods* [Online]. Queensland. Available: <http://www.floodplainconference.com/papers2012.php> [Accessed 20 January 2015].
- GUO, J. 2010. Computational design tool for bridge hydrodynamic loading in inundated flows of Midwest Rivers.
- HAMPTON, M. A. 1972. The role of subaqueous debris flow in generating turbidity currents. *Journal of Sedimentary Research*, 42.
- HANIF, M. U., IBRAHIM, Z., JAMEEL, M., GHAEDI, K. & ASLAM, M. 2016. A new approach to estimate damage in concrete beams using non-linearity. *Construction and Building Materials*, 124, 1081-1089.
- HASHIMOTO, K. & CHOUW, N. 2003. Investigation of the effect of Kobe earthquake on a three-dimensional soil–structure system. *JSCE Journal of Earthquake Engineering*, 27, 1-8.
- HE, X., SHENG, X., SCANLON, A., LINZELL, D. & YU, X. 2012. Skewed concrete box girder bridge static and dynamic testing and analysis. *Engineering Structures*, 39, 38-49.
- HONG, J.-H., CHIEW, Y.-M., LU, J.-Y., LAI, J.-S. & LIN, Y.-B. 2011. Houfeng bridge failure in Taiwan. *Journal of Hydraulic Engineering*, 138, 186-198.

- HUDSON, S., CORMIE, D., TUFTON, E. & INGLIS, S. Engineering resilient infrastructure. Proceedings of the ICE-Civil Engineering, 2012. Thomas Telford, 5-12.
- HUGHES, D., RAMEY, G. E. & HUGHES, M. L. 2007. Bridge pile bent number of piles and X-bracing system: impact on pushover capacity as scour increases. *Practice Periodical on Structural Design and Construction*, 12, 82-95.
- IBISWORLD. 2011. *Queensland floods: The economic impact Special Report* [Online]. Available: <http://www.ibisworld.com.au/common/pdf/QLD%20floods%20special%20report.pdf> [Accessed 23 May 2013].
- IVERSON, R. M. 2000. Landslide triggering by rain infiltration. *Water resources research*, 36, 1897-1910.
- JEMPSON, M. 2000. Flood and debris loads on bridges.
- JEMPSON, M. & APELT, C. Hydrodynamic Forces on Partially and Fully Submerged Bridge Superstructures. PROCEEDINGS, 16TH ARRB CONFERENCE, 9-13 NOVEMBER 1992, PERTH, WESTERN AUSTRALIA; VOLUME 16, PART 3, 1992.
- JONES, C. 2001. *Coastal Construction Manual: Principles and Practices of Planning, Siting, Designing, Constructing and Maintaining Residential Buildings in Coastal Areas*, DIANE Publishing.
- KARIM, K. R. & YAMAZAKI, F. 2001. Effect of earthquake ground motions on fragility curves of highway bridge piers based on numerical simulation. *Earthquake engineering & structural dynamics*, 30, 1839-1856.
- KERENYI, K., SOFU, T. & GUO, J. 2009. Hydrodynamic forces on inundated bridge decks.
- KIM, S. J., HOLUB, C. J. & ELNASHAI, A. S. 2010. Analytical assessment of the effect of vertical earthquake motion on RC bridge piers. *Journal of Structural Engineering*, 137, 252-260.

- KONG, D., SETUNGE, S., MOLYNEAUX, T., ZHANG, G. & LAW, D. 2013. Structural resilience of core port infrastructure in a changing climate.
- KRAWINKLER, H. Loading histories for cyclic tests in support of performance assessment of structural components. The 3rd international conference on advances in experimental structural engineering, San Francisco, 2009.
- KUNNATH, S. K., ERDURAN, E., CHAI, Y. & YASHINSKY, M. 2008. Effect of near-fault vertical ground motions on seismic response of highway overcrossings. *Journal of Bridge Engineering*, 13, 282-290.
- KUNTJORO, W. 2005. *An Introduction to the Finite Element Method*, Singapore, McGraw-Hill.
- LAMOND, J. E. & PROVERBS, D. G. 2009. Resilience to flooding: lessons from international comparison. *Proceedings of the ICE-Urban design and Planning*, 162, 63-70.
- LEE, K. H. & ROSOWSKY, D. V. 2006. Fragility analysis of woodframe buildings considering combined snow and earthquake loading. *Structural Safety*, 28, 289-303.
- LEVY, C. 2011. *Etude instrumentale et numérique de la réponse dynamique d'une écaille calcaire potentiellement instable*. Université de Grenoble.
- LI, Y. & ELLINGWOOD, B. R. 2006. Hurricane damage to residential construction in the US: Importance of uncertainty modeling in risk assessment. *Engineering structures*, 28, 1009-1018.
- LIN, C., BENNETT, C., HAN, J. & PARSONS, R. L. 2010. Scour effects on the response of laterally loaded piles considering stress history of sand. *Computers and Geotechnics*, 37, 1008-1014.
- LOKUGE, W. & SETUNGE, S. Evaluating disaster resilience of bridge infrastructure when exposed to extreme natural events. Proceedings of the 3rd International Conference on Building Resilience 2013, 2013. University of Salford, 1-12.

- LWIN, M. M., YEN, W. P. & SHEN, J. J. 2013. Effects of Hurricane Katrina on the performance of US highway bridges. *Journal of Performance of Constructed Facilities*, 28, 40-48.
- LYBAS, J. M. 1977. *Effect of beam strength and stiffness on dynamic behavior of reinforced concrete coupled walls*. University of Illinois at Urbana-Champaign.
- MALAVASI, S. & GUADAGNINI, A. 2003. Hydrodynamic loading on river bridges. *Journal of Hydraulic Engineering*, 129, 854-861.
- MURRAY, G. & KEMP, A. Remediation of bridges after the Queensland January 2011 flood. Austroads Bridge Conference, 8th, 2011, Sydney, New South Wales, Australia, 2011.
- NASIM, M., MOHSENI, H., SETUNGE, S., ZHOU, S. & DISSANAYAKE, A. An Investigation to the Behaviour of water flow on Bridge Pier in Flood Event. ABC Conference, 2017 Melbourne.
- NEWMARK, N. M. & ROSENBLUETH, E. 1971. Fundamentals of earthquake engineering. *Civil engineering and engineering mechanics series*, 12.
- NIELSON, B. G. & DESROCHES, R. 2006. Influence of modeling assumptions on the seismic response of multi-span simply supported steel girder bridges in moderate seismic zones. *Engineering structures*, 28, 1083-1092.
- NISHIJIMA, K. & FABER, M. H. 2009. Societal performance of infrastructure subject to natural hazards. *Australian journal of structural engineering*, 9, 9-16.
- OH, E. H., DESHMUKH, A. & HASTAK, M. Vulnerability assessment of critical infrastructure, associated industries, and communities during extreme events. Construction Research Congress, 2010. 449-58.
- OKEIL, A. M. & CAI, C. 2008. Survey of short-and medium-span bridge damage induced by Hurricane Katrina. *Journal of Bridge Engineering*, 13, 377-387.

- OLIVEIRA, C. S. 1975. *Seismic risk analysis for a site and a metropolitan area*, University of California, Berkeley, Earthquake Engineering Research Center.
- PADGETT, J., DESROCHES, R., NIELSON, B., YASHINSKY, M., KWON, O.-S., BURDETTE, N. & TAVERA, E. 2008. Bridge damage and repair costs from Hurricane Katrina. *Journal of Bridge Engineering*, 13, 6-14.
- PAN, Y., AGRAWAL, A. K., GHOSN, M. & ALAMPALLI, S. 2010. Seismic fragility of multispan simply supported steel highway bridges in New York State. II: Fragility analysis, fragility curves, and fragility surfaces. *Journal of Bridge Engineering*, 15, 462-472.
- PARK, Y.-J., ANG, A. H.-S. & WEN, Y. K. 1985. Seismic damage analysis of reinforced concrete buildings. *Journal of Structural Engineering*, 111, 740-757.
- PAROLA, A. C. 2000. *Debris forces on highway bridges*, Transportation Research Board.
- PRITCHARD, R. W. 2013. 2011 to 2012 Queensland floods and cyclone events: Lessons learnt for bridge transport infrastructure. *Australian Journal of Structural Engineering*, 14, 167-176.
- QUEENSLANDGOVERNMENT. 2010. *Increasing Queensland's resilience to inland flooding in a changing climate*: [Online]. Available: <http://www.ehp.qld.gov.au/climatechange/pdf/inland-flood-study.pdf> [Accessed 30 April 2014].
- QUEENSLANDGOVERNMENT. 2012. *Rebuilding a stronger, more resilient Queensland* [Online]. Available: <http://www.qldreconstruction.org.au/u/lib/cms2/rebuilding-resilient-qld-full.pdf> [Accessed 12 October 2013].
- QUEENSLANDGOVERNMENT. 2013. *Extreme Flood Event in Queensland* [Online]. Available: <http://www.chiefscientist.qld.gov.au/publications/understanding-floods/what-is-a-flood> [Accessed 03 March 2016].

- RAMESH, K., ZHANG, MALIK 2009. Damage to concrete beams in buildings - A Case study.
- ROBERTSON, I. N., RIGGS, H. R., YIM, S. C. & YOUNG, Y. L. 2007. Lessons from Hurricane Katrina storm surge on bridges and buildings. *Journal of Waterway, Port, Coastal, and Ocean Engineering*, 133, 463-483.
- ROSOWSKY, D. V. & ELLINGWOOD, B. R. 2002. Performance-based engineering of wood frame housing: Fragility analysis methodology. *Journal of Structural Engineering*, 128, 32-38.
- SAADEGHVAZIRI, M. A. & YAZDANI-MOTLAGH, A. 2008. Seismic behavior and capacity/demand analyses of three multi-span simply supported bridges. *Engineering Structures*, 30, 54-66.
- SCHULTZ, M. T., GOULDBY, B. P., SIMM, J. D. & WIBOWO, J. L. 2010. Beyond the factor of safety: Developing fragility curves to characterize system reliability. ENGINEER RESEARCH AND DEVELOPMENT CENTER VICKSBURG MS GEOTECHNICAL AND STRUCTURES LAB.
- SEO, J., HATFIELD, G. & KIMN, J.-H. 2016. Probabilistic structural integrity evaluation of a highway steel bridge under unknown trucks. *Journal of Structural Integrity and Maintenance*, 1, 65-72.
- SHINOZUKA, M., FENG, M. Q., KIM, H.-K. & KIM, S.-H. 2000. Nonlinear static procedure for fragility curve development. *Journal of engineering mechanics*.
- SIDDHARTHAN, R. V., EL-GAMAL, M. & MARAGAKIS, E. A. 1997. Stiffnesses of abutments on spread footings with cohesionless backfill. *Canadian Geotechnical Journal*, 34, 686-697.
- STEPHENS, J. 1985. *Structural damage assessment using response measurements*. Ph. D. Thesis, School of Civil Engineering, Purdue University, West Lafayette, IN.

- TAKAHASHI, T. 1978. Mechanical characteristics of debris flow. *Journal of the Hydraulics Division*, 104, 1153-1169.
- TAVARES, D. 2011. *Seismic risk assessment for bridges in quebec using fragility curves*. PhD thesis. Sherbrooke (QC): Faculté de Génie, Département de Génie Civil, Université de Sherbrooke.
- UMEMURA, H. & TAKIZAWA, H. 1982. *Dynamic response of reinforced concrete buildings*, Iabse.
- UNDERSTANDINGFLOODS. 2011. *Understanding Floods Q&A* [Online]. Available: [http://www.chiefscientist.qld.gov.au/images/documents/chiefscientist/pubs/floods/understanding-floods\\_full\\_colour.pdf](http://www.chiefscientist.qld.gov.au/images/documents/chiefscientist/pubs/floods/understanding-floods_full_colour.pdf) [Accessed 03 Jan 2013 2013].
- VAN DEN HONERT, R. C. & MCANENEY, J. 2011a. The 2011 Brisbane Floods: Causes, Impacts and Implications. *Water*, 3, 1149.
- VAN DEN HONERT, R. C. & MCANENEY, J. 2011b. The 2011 Brisbane floods: causes, impacts and implications. *Water*, 3, 1149-1173.
- VARNES, D. J. 1984. *Landslide hazard zonation: a review of principles and practice*.
- VELETZOS, M. J., RESTREPO, J. I. & SEIBLE, F. 2006. Seismic response of precast segmental bridge superstructures. *SSRP*, 6, 18.
- WALTON, C. M., YU, C.-P., NG, P. & TOBIAS, S. 1982. An assessment of recent state truck size and weight studies. *Center for Transportation Research, Austin, TX*.
- WANG, W., LIU, R. & WU, B. 2014. Analysis of a bridge collapsed by an accidental blast loads. *Engineering Failure Analysis*, 36, 353-361.
- WARDHANA, K. & HADIPRIONO, F. C. 2003. Analysis of recent bridge failures in the United States. *Journal of performance of constructed facilities*, 17, 144-150.

- WEENA.L & SUJEEVA, S. 2013. *Evaluating disaster resilience of bridge infrastructure when exposed to extreme natural events* [Online]. Available: <https://eprints.usq.edu.au/24202/> [Accessed 15 September 2015].
- WELLWOOD, N. & FENWICK, J. A flood loading methodology for bridges. Australian Road Research Board (ARRB) Conference, 15th, 1990, Darwin, Northern Territory, 1990.
- WHITMAN, R. & BIGGS, J. 1974. Seismic Design Decision Analysis-Methodology and Pilot Application, Report R 74-57, M. LT., July.
- WHITMAN, R. V. 1972. *Methodology and initial damage statistics*, MIT Department of Civil Engineering.
- WHITMAN, R. V., HONG, S.-T. & REED, J. W. 1973. *Damage statistics for high-rise buildings in the vicinity of the San Fernando Earthquake*, Department of Civil Engineering, School of Engineering, Massachusetts Institute of Technology.
- WITZANY, J. & CEJKA, T. 2007. Reliability and failure resistance of the stone bridge structure of Charles Bridge during floods. *Journal of civil engineering and management*, 13, 227-236.
- WITZANY, J., CEJKA, T. & ZIGLER, R. 2008. Failure resistance of historic stone bridge structure of Charles bridge. II: Susceptibility to floods. *Journal of Performance of Constructed Facilities*, 22, 83-91.
- XU, G. & CAI, C. 2014. Wave forces on Biloxi Bay Bridge decks with inclinations under solitary waves. *Journal of Performance of Constructed Facilities*, 29, 04014150.
- YANG, C.-S. W., WERNER, S. D. & DESROCHES, R. 2015. Seismic fragility analysis of skewed bridges in the central southeastern United States. *Engineering Structures*, 83, 116-128.

- YAO, J. & MUNSE, W. Low-cycle axial fatigue behavior of mild steel. Symposium on Fatigue Tests of Aircraft Structures: Low-Cycle, Full-Scale, and Helicopters, 1963. ASTM International.
- YIM, S. C., WEI, Y., AZADBAKHT, M., NIMMALA, S. & POTISUK, T. 2014. Case study for tsunami design of coastal infrastructure: Spencer Creek Bridge, Oregon. *Journal of Bridge Engineering*, 20, 05014008.
- YIN, R. K. 2013. *Case study research: Design and methods*, Sage publications.
- ZHONG, S., CLARK, M., HOU, X. Y., ZANG, Y. L. & FITZGERALD, G. 2013. 2010–2011 Queensland floods: using Haddon's Matrix to define and categorise public safety strategies. *Emergency Medicine Australasia*, 25, 345-352.
- ZIMMERMAN, D. C. & KAOUK, M. 1994. Structural damage detection using a minimum rank update theory. *TRANSACTIONS-AMERICAN SOCIETY OF MECHANICAL ENGINEERS JOURNAL OF VIBRATION AND ACOUSTICS*, 116, 222-222.

## Appendix1: Input files for ABAQUS parametric study

Below is an extract of the above file that contained more than 2000 odd pages. This illustrates only the important parts of the files highlighted in different colours. For access to the entire file the author could be contacted on [farook.kalendher@rmit.edu.au](mailto:farook.kalendher@rmit.edu.au)

```

*Heading
** Job name: pythonlog Model name: Model-1
** Generated by: Abaqus/CAE 6.14-1
*Preprint, echo=NO, model=NO, history=NO, contact=NO
**
*PARAMETER
velocityfar = 0
FLOODY=0.5*2.2*velocityfar*velocityfar
CONTY=15.873*velocityfar*velocityfar
** PARTS
**
*Part, name=igirder
*Node
    1, 0.075000003, 1.20000005, 12.5
    2, 0.25, 1.20000005, 12.5
    3, 0.25, 1.20000005, 13.6999998
    4, 0.075000003, 1.20000005, 13.6999998
    5, 0.25, 1.39999998, 12.5
    6, 0.25, 1.39999998, 13.6999998
    7, 0.075000003, 1.39999998, 13.6999998
    8, 0.075000003, 1.39999998, 12.5
    9, 0.400000006, 0.349999994, 12.5
    10, 0.649999976, 0.349999994, 12.5
    11, 0.649999976, 0.349999994, 0.
    12, 0.400000006, 0.349999994, 0.
    13, 0.649999976, 0., 12.5
    14, 0.649999976, 0., 0.
    15, 0.400000006, 0., 0.
    16, 0.400000006, 0., 12.5
    17, 0.25, 0.349999994, 12.5

    62140, 0.300000012, 1.29999995, 27.
    62141, 0.300000012, 1.25, 27.
    62142, 0.300000012, 1.35000002, 27.1000004
    62143, 0.300000012, 1.29999995, 27.1000004
    62144, 0.300000012, 1.25, 27.1000004
    62145, 0.300000012, 1.35000002, 27.2000008
    62146, 0.300000012, 1.29999995, 27.2000008
    62147, 0.300000012, 1.25, 27.2000008
    62148, 0.300000012, 1.35000002, 27.2999992
    62149, 0.300000012, 1.29999995, 27.2999992
    62150, 0.300000012, 1.25, 27.2999992

```

```

*Element, type=C3D8R
  1, 138, 5011, 32451, 4945, 1, 81, 4901, 106
  2, 5011, 5012, 32452, 32451, 81, 82, 4902, 4901
  3, 5012, 142, 4978, 32452, 82, 2, 83, 4902
  4, 4945, 32451, 32453, 4946, 106, 4901, 4903, 105
  5, 32451, 32452, 32454, 32453, 4901, 4902, 4904, 4903
  6, 32452, 4978, 4979, 32454, 4902, 83, 84, 4904
  7, 4946, 32453, 32455, 4947, 105, 4903, 4905, 104
  8, 32453, 32454, 32456, 32455, 4903, 4904, 4906, 4905
  9, 32454, 4979, 4980, 32456, 4904, 84, 85, 4906
 10, 4947, 32455, 32457, 4948, 104, 4905, 4907, 103
 11, 32455, 32456, 32458, 32457, 4905, 4906, 4908, 4907
 12, 32456, 4980, 4981, 32458, 4906, 85, 86, 4908
 13, 4948, 32457, 32459, 4949, 103, 4907, 4909, 102
 14, 32457, 32458, 32460, 32459, 4907, 4908, 4910, 4909
 15, 32458, 4981, 4982, 32460, 4908, 86, 87, 4910
 16, 4949, 32459, 32461, 4950, 102, 4909, 4911, 101
 17, 32459, 32460, 32462, 32461, 4909, 4910, 4912, 4911
 18, 32460, 4982, 4983, 32462, 4910, 87, 88, 4912

48763, 62143, 62144, 62147, 62146, 20220, 20344, 20345, 20221
48764, 62144, 30856, 30857, 62147, 20344, 3588, 3589, 20345
48765, 32443, 62145, 62148, 32444, 3216, 20097, 20098, 3215
48766, 62145, 62146, 62149, 62148, 20097, 20221, 20222, 20098
48767, 62146, 62147, 62150, 62149, 20221, 20345, 20346, 20222
48768, 62147, 30857, 30858, 62150, 20345, 3589, 3590, 20346
48769, 32444, 62148, 32448, 4899, 3215, 20098, 3591, 68
48770, 62148, 62149, 32449, 32448, 20098, 20222, 3592, 3591
48771, 62149, 62150, 32450, 32449, 20222, 20346, 3593, 3592
48772, 62150, 30858, 4599, 32450, 20346, 3590, 71, 3593

*Nset, nset=Set-1, generate
  1, 62150, 1
*Elset, elset=Set-1, generate
  1, 48772, 1
** Section: concrete
*Solid Section, elset=Set-1, material=concrete
,
*End Part
**
*Part, name=rebarpil2
*Node
  1, 0., 0., 0.
  2, 0.100000001, 0., 0.
  3, 0.200000003, 0., 0.
  4, 0.300000012, 0., 0.
  5, 0.400000006, 0., 0.
  6, 0.5, 0., 0.
  7, 0.600000024, 0., 0.
  8, 0.699999988, 0., 0.
  9, 0.800000012, 0., 0.
 10, 0.899999976, 0., 0.
 11, 1., 0., 0.
 12, 1.10000002, 0., 0.

```

## Appendices

---

```

    13, 1.20000005, 0., 0.
    14, 1.29999995, 0., 0.
    261, 26., 0., 0.
    262, 26.1000004, 0., 0.
    263, 26.2000008, 0., 0.
    264, 26.2999992, 0., 0.
    265, 26.3999996, 0., 0.
    266, 26.5, 0., 0.
    267, 26.6000004, 0., 0.
    268, 26.7000008, 0., 0.
    269, 26.7999992, 0., 0.
    270, 26.8999996, 0., 0.
    271, 27., 0., 0.
    272, 27.1000004, 0., 0.
    273, 27.2000008, 0., 0.
    274, 27.2999992, 0., 0.
    275, 27.3999996, 0., 0.
*Element, type=T3D2
  1, 1, 2
  2, 2, 3
  3, 3, 4
  4, 4, 5
  5, 5, 6
  6, 6, 7
  7, 7, 8
  8, 8, 9
  9, 9, 10
 10, 10, 11
 11, 11, 12
 12, 12, 13
 13, 13, 14

267, 267, 268
268, 268, 269
269, 269, 270
270, 270, 271
271, 271, 272
272, 272, 273
273, 273, 274
274, 274, 275
*Nset, nset=Set-1, generate
  1, 275, 1
*Elset, elset=Set-1, generate
  1, 274, 1
** Section: rebar
*Solid Section, elset=Set-1, material=steel
0.000113097,
*End Part
**
**
** ASSEMBLY
**
*Assembly, name=Assembly
**
*Instance, name=igirder-1, part=igirder
  27.4, 1.67776611483187e-15, -1.02733545112337e-31
```

## Appendices

---

```
27.4, 1.67776611483187e-15, -1.02733545112337e-31,
27.977350279552, -0.577350279552041, -0.577350279552042,
119.999999109416
*End Instance
**
*Instance, name=rebarpi12, part=rebarpi12
3.06161699786838e-18, -0.05, 0.05
3.06161699786838e-18, -0.05, 0.05, 1.,
-0.05, 0.05, 90.
*End Instance
**
*Instance, name=rebarpi12-lin-2-1, part=rebarpi12
6.12323399573677e-18, -0.1, 0.05
6.12323399573677e-18, -0.1, 0.05, 1.,
-0.1, 0.05, 90.
*End Instance
**
*Instance, name=rebarpi12-lin-3-1, part=rebarpi12
9.18485099360515e-18, -0.15, 0.05
9.18485099360515e-18, -0.15, 0.05, 1.,
-0.15, 0.05, 90.
*End Instance
**
*Instance, name=rebarpi12-lin-4-1, part=rebarpi12
1.22464679914735e-17, -0.2, 0.05
1.22464679914735e-17, -0.2, 0.05, 1.,
-0.2, 0.05, 90.
*End Instance
**
*Instance, name=rebarpi12-lin-6-1, part=rebarpi12
1.83697019872103e-17, -0.3, 0.05
**
*Instance, name=rebarpi12-lin-7-1-lin-1-3-li-lin-1-2-2,
part=rebarpi12
3.2146978477618e-17, -0.525, 1.25
3.2146978477618e-17, -0.525, 1.25, 1.,
-0.525, 1.25, 90.
*End Instance
**
*Elset, elset=Set-4, instance=igirder-1
45412,
*Elset, elset=Set-5, instance=igirder-1
45411,
*Elset, elset=Set-6, instance=igirder-1
45410,
*Elset, elset=Set-7, instance=igirder-1
45409,
*Elset, elset=Set-8, instance=igirder-1
45408,
*Elset, elset=Set-9, instance=igirder-1
34288,
*Elset, elset=Set-10, instance=igirder-1
34287,
*Elset, elset=Set-11, instance=igirder-1
34286,
*Elset, elset=Set-12, instance=igirder-1
```

```
22882,
*Elset, elset=Set-13, instance=igirder-1
22883,
*Elset, elset=Set-14, instance=igirder-1
22884,
*Elset, elset=Set-15, instance=igirder-1
22885,
*Elset, elset=Set-16, instance=igirder-1
22886,
*Nset, nset=lhs, instance=igirder-1
49, 50, 60, 75, 2007, 2008, 2009, 2010, 2886, 2887, 4138,
4139, 4140, 4141
*Elset, elset=lhs, instance=igirder-1
17725, 17726, 17727, 17728, 17729, 20214, 20215, 20216, 29670,
29671, 29672, 29673, 29674
*Nset, nset=m_Set-1, instance=rebarpi12, generate
1, 275, 1
*Nset, nset=m_Set-1, instance=rebarpi12-lin-2-1, generate
1, 275, 1
*Nset, nset=m_Set-1, instance=rebarpi12-lin-3-1, generate
1, 275, 1
*Nset, nset=m_Set-1, instance=rebarpi12-lin-9-1, generate
1, 275, 1
*Nset, nset=m_Set-1, instance=rebarpi12-lin-1-2, generate
1, 275, 1
*Nset, nset=m_Set-1, instance=rebarpi12-lin-6-1-lin-1-2, generate
1, 275, 1
*Nset, nset=m_Set-1, instance=rebarpi12-lin-7-1-lin-1-3-lin-1-3,
generate
1, 275, 1
*Nset, nset=m_Set-1, instance=rebarpi12-lin-9-1-lin-1-2, generate
1, 275, 1
*Nset, nset=m_Set-1, instance=rebarpi12-lin-3-1-lin-1-2, generate
1, 275, 1
*Nset, nset=m_Set-1, instance=rebarpi12-lin-10-1-lin-1-2, generate
1, 275, 1
*Nset, nset=m_Set-1, instance=rebarpi12-lin-7-1-lin-1-3-li-lin-2-1,
generate
1, 275, 1
*Nset, nset=m_Set-1, instance=rebarpi12-lin-6-1-lin-1-3-lin-1-2,
generate
1, 275, 1
*Nset, nset=m_Set-1, instance=rebarpi12-lin-7-1, generate
1, 275, 1
*Nset, nset=m_Set-1, instance=rebarpi12-lin-2-1-lin-1-2, generate
1, 275, 1
*Nset, nset=m_Set-1, instance=rebarpi12-lin-7-1-lin-1-2, generate
1, 275, 1
*Nset, nset=m_Set-1, instance=rebarpi12-lin-6-1-lin-1-3-li-lin-1-2,
generate
1, 275, 1
*Nset, nset=m_Set-1, instance=rebarpi12-lin-11-1-lin-1-2, generate
1, 275, 1
*Nset, nset=m_Set-1, instance=rebarpi12-lin-11-1, generate
1, 275, 1
*Nset, nset=m_Set-1, instance=rebarpi12-lin-12-1-lin-1-2, generate
```

```
1, 275, 1
*Nset, nset=m_Set-1, instance=rebarpi12-lin-7-1-lin-1-3-li-lin-1-2-
1, generate
1, 275, 1
*Nset, nset=m_Set-1, instance=rebarpi12-lin-4-1-lin-1-2, generate
1, 275, 1
*Nset, nset=m_Set-1, instance=rebarpi12-lin-6-1-lin-1-3-lin-1-4,
generate
1, 275, 1
*Nset, nset=m_Set-1, instance=rebarpi12-lin-4-1, generate
1, 275, 1
*Nset, nset=m_Set-1, instance=rebarpi12-lin-6-1, generate
1, 275, 1
*Nset, nset=m_Set-1, instance=rebarpi12-lin-1-3, generate
1, 275, 1
*Nset, nset=m_Set-1, instance=rebarpi12-lin-6-1-lin-1-3, generate
1, 275, 1
*Nset, nset=m_Set-1, instance=rebarpi12-lin-7-1-lin-1-3-lin-1-4,
generate
1, 275, 1
*Nset, nset=m_Set-1, instance=rebarpi12-lin-9-1-lin-1-3, generate
1, 275, 1
*Nset, nset=m_Set-1, instance=rebarpi12-lin-10-1, generate
1, 275, 1
*Nset, nset=m_Set-1, instance=rebarpi12-lin-10-1-lin-1-3, generate
1, 275, 1
*Nset, nset=m_Set-1, instance=rebarpi12-lin-7-1-lin-1-3-li-lin-2-1-
1, generate
1, 275, 1
*Nset, nset=m_Set-1, instance=rebarpi12-lin-3-1-lin-1-3, generate
1, 275, 1
*Nset, nset=m_Set-1, instance=rebarpi12-lin-6-1-lin-1-3-lin-1-3,
generate
1, 275, 1
*Nset, nset=m_Set-1, instance=rebarpi12-lin-12-1, generate
1, 275, 1
*Nset, nset=m_Set-1, instance=rebarpi12-lin-2-1-lin-1-3, generate
1, 275, 1
*Nset, nset=m_Set-1, instance=rebarpi12-lin-7-1-lin-1-3, generate
1, 275, 1
*Nset, nset=m_Set-1, instance=rebarpi12-lin-7-1-lin-1-3-li-lin-1-2,
generate
1, 275, 1
*Nset, nset=m_Set-1, instance=rebarpi12-lin-11-1-lin-1-3, generate
1, 275, 1
*Nset, nset=m_Set-1, instance=rebarpi12-lin-4-1-lin-1-3, generate
1, 275, 1
*Nset, nset=m_Set-1, instance=rebarpi12-lin-12-1-lin-1-3, generate
1, 275, 1
*Nset, nset=m_Set-1, instance=rebarpi12-lin-7-1-lin-1-3-li-lin-1-2-
2, generate
1, 275, 1
*Nset, nset=m_Set-1, instance=rebarpi12-lin-7-1-lin-1-3-lin-1-2,
generate
1, 275, 1
*Elset, elset=m_Set-1, instance=rebarpi12, generate
```

```
1, 274, 1
*Elset, elset=m_Set-1, instance=rebarpil2-lin-2-1, generate
1, 274, 1
*Elset, elset=m_Set-1, instance=rebarpil2-lin-3-1, generate
1, 274, 1
*Elset, elset=m_Set-1, instance=rebarpil2-lin-9-1, generate
1, 274, 1
*Elset, elset=m_Set-1, instance=rebarpil2-lin-1-2, generate
1, 274, 1
*Elset, elset=m_Set-1, instance=rebarpil2-lin-6-1-lin-1-2, generate
1, 274, 1
*Elset, elset=m_Set-1, instance=rebarpil2-lin-7-1-lin-1-3-lin-1-3,
generate
1, 274, 1
*Elset, elset=m_Set-1, instance=rebarpil2-lin-9-1-lin-1-2, generate
1, 274, 1
*Elset, elset=m_Set-1, instance=rebarpil2-lin-3-1-lin-1-2, generate
1, 274, 1
*Elset, elset=m_Set-1, instance=rebarpil2-lin-10-1-lin-1-2, generate
1, 274, 1
*Elset, elset=m_Set-1, instance=rebarpil2-lin-7-1-lin-1-3-li-lin-2-
1, generate
1, 274, 1
*Elset, elset=m_Set-1, instance=rebarpil2-lin-6-1-lin-1-3-lin-1-2,
generate
1, 274, 1
*Elset, elset=m_Set-1, instance=rebarpil2-lin-7-1, generate
1, 274, 1
*Elset, elset=m_Set-1, instance=rebarpil2-lin-2-1-lin-1-2, generate
1, 274, 1
*Elset, elset=m_Set-1, instance=rebarpil2-lin-7-1-lin-1-2, generate
1, 274, 1
*Elset, elset=m_Set-1, instance=rebarpil2-lin-6-1-lin-1-3-li-lin-1-
2, generate
1, 274, 1
*Elset, elset=m_Set-1, instance=rebarpil2-lin-11-1-lin-1-2, generate
1, 274, 1
*Elset, elset=m_Set-1, instance=rebarpil2-lin-11-1, generate
1, 274, 1
*Elset, elset=m_Set-1, instance=rebarpil2-lin-12-1-lin-1-2, generate
1, 274, 1
*Elset, elset=m_Set-1, instance=rebarpil2-lin-7-1-lin-1-3-li-lin-1-
2-1, generate
1, 274, 1
*Elset, elset=m_Set-1, instance=rebarpil2-lin-4-1-lin-1-2, generate
1, 274, 1
*Elset, elset=m_Set-1, instance=rebarpil2-lin-6-1-lin-1-3-lin-1-4,
generate
1, 274, 1
*Elset, elset=m_Set-1, instance=rebarpil2-lin-4-1, generate
1, 274, 1
*Elset, elset=m_Set-1, instance=rebarpil2-lin-6-1, generate
1, 274, 1
*Elset, elset=m_Set-1, instance=rebarpil2-lin-1-3, generate
1, 274, 1
*Elset, elset=m_Set-1, instance=rebarpil2-lin-6-1-lin-1-3, generate
```

```

    1, 274, 1
*Elset, elset=m_Set-1, instance=rebarpi12-lin-7-1-lin-1-3-lin-1-4,
generate
    1, 274, 1
*Elset, elset=m_Set-1, instance=rebarpi12-lin-9-1-lin-1-3, generate
    1, 274, 1
*Elset, elset=m_Set-1, instance=rebarpi12-lin-10-1, generate
    1, 274, 1
*Elset, elset=m_Set-1, instance=rebarpi12-lin-10-1-lin-1-3, generate
    1, 274, 1
*Elset, elset=m_Set-1, instance=rebarpi12-lin-7-1-lin-1-3-li-lin-2-
1-1, generate
    1, 274, 1
*Elset, elset=m_Set-1, instance=rebarpi12-lin-3-1-lin-1-3, generate
    1, 274, 1
*Elset, elset=m_Set-1, instance=rebarpi12-lin-6-1-lin-1-3-lin-1-3,
generate
    1, 274, 1
*Elset, elset=m_Set-1, instance=rebarpi12-lin-12-1, generate
    1, 274, 1
*Elset, elset=m_Set-1, instance=rebarpi12-lin-2-1-lin-1-3, generate
    1, 274, 1
*Elset, elset=m_Set-1, instance=rebarpi12-lin-7-1-lin-1-3, generate
    1, 274, 1
*Elset, elset=m_Set-1, instance=rebarpi12-lin-7-1-lin-1-3-li-lin-1-
2, generate
    1, 274, 1
*Elset, elset=m_Set-1, instance=rebarpi12-lin-11-1-lin-1-3, generate
    1, 274, 1
*Elset, elset=m_Set-1, instance=rebarpi12-lin-4-1-lin-1-3, generate
    1, 274, 1
*Elset, elset=m_Set-1, instance=rebarpi12-lin-12-1-lin-1-3, generate
    1, 274, 1
*Elset, elset=m_Set-1, instance=rebarpi12-lin-7-1-lin-1-3-li-lin-1-
2-2, generate
    1, 274, 1
*Elset, elset=m_Set-1, instance=rebarpi12-lin-7-1-lin-1-3-lin-1-2,
generate
    1, 274, 1
*Nset, nset=rhs, instance=igirder-1
    14, 15, 72, 73, 529, 530, 531, 532, 3746, 3747, 3748,
3749, 4564, 4565
*Elset, elset=rhs, instance=igirder-1
    4515, 4516, 4517, 4518, 4519, 25295, 25296, 25297, 25298,
25299, 38555, 38556, 38557
*Elset, elset=_Surf-4_S1, internal, instance=igirder-1
    109, 110, 111, 112, 113, 114, 115, 116, 117,
118, 119, 120, 121, 122, 123, 124
    125, 126, 127, 128, 129, 130, 131, 132, 133,
134, 135, 136, 137, 138, 139, 140

*Surface, type=ELEMENT, name=Surf-6
_Surf-6_S1, S1
_Surf-6_S2, S2
*Elset, elset=_Surf-7_S6, internal, instance=igirder-1, generate
    11291, 11706, 5

```

## Appendices

---

```
*Elset, elset=_Surf-7_S4, internal, instance=igirder-1, generate
45357, 45772, 5
*Surface, type=ELEMENT, name=Surf-7
_Surf-7_S6, S6
_Surf-7_S4, S4
** Constraint: embed
*Embedded Element
m_Set-1
*End Assembly
**
** MATERIALS
**
*Material, name=concrete
*Elastic
3e+07, 0.2
*Concrete Damaged Plasticity
35., 0.1, 1.16, 0.667, 0.01
*Concrete Compression Hardening
14027.8, 0.
20416.7, 0.000250409
28611.1, 0.000648118
33055.6, 0.000927987
35694.4, 0.00123732
36527.8, 0.00150245
35416.7, 0.00185597
32083.3, 0.00222422
26111.1, 0.00271031
19583.3, 0.00324059
14305.6, 0.00377087
10000., 0.00440426
7777.78, 0.0049198
5972.22, 0.00547954
4027.78, 0.00621604
3055.56, 0.00692308
2500., 0.00739444
2222.22, 0.00777741
*Concrete Tension Stiffening
3593.27, 0.
1980.95, 0.000143108
1439.77, 0.000274589
1115.58, 0.000410666
926.887, 0.000536894
779.182, 0.000697
592.069, 0.000997701
486.444, 0.00131285
394.421, 0.00163282
356.547, 0.00194305
318.717, 0.00225811
294.315, 0.00255863
*Material, name=steel
*Elastic
2.1e+08, 0.3
*Plastic
210000.,0.
**
** BOUNDARY CONDITIONS
```

## Appendices

---

```
**
** Name: lhs Type: Displacement/Rotation
*Boundary
lhs, 1, 1
lhs, 2, 2
lhs, 3, 3
** Name: rhs Type: Displacement/Rotation
*Boundary
rhs, 2, 2
rhs, 3, 3
** -----
**
** STEP: flood
**
*Step, name=flood, nlgeom=YES, inc=10000
*Static
0.001, 1., 1e-25, 0.1
**
** LOADS
**
** Name: buoyance    Type: Pressure
*Dload
Surf-6, P, 6.867
** Name: container   Type: Pressure
*Dload
Surf-7, P, <CONTY>
** Name: flood       Type: Pressure
*Dload
Surf-5, P, <FLOODY>
** Name: gravityudl  Type: Pressure
*Dload
Surf-4, P, 21.425
**
** OUTPUT REQUESTS
**
*Restart, write, frequency=0
**
** FIELD OUTPUT: F-Output-1
**
*Output, field
*Node Output
CF, RF, RM, RT, TF, VF
*Element Output, directions=YES
ALPHA, ALPHAN, BF, CENTMAG, CENTRIFMAG, CORIOMAG, CS11, CTSHR, E,
EE, ER, ESF1, GRAV, HP, IE, LE
MISES, MISESMAX, MISESONLY, NE, NFORC, NFORCSO, P, PE, PEEQ,
PEEQMAX, PEEQT, PEMAG, PEQC, PRESSONLY, PS, ROTAMAG
S, SALPHA, SE, SEE, SEP, SEPE, SF, SPE, SSAVG, THE, TRIAX, TRNOR,
TRSHR, TSHR, VE, VEEQ
VS
**
** HISTORY OUTPUT: H-Output-7
**
*Output, history
*Element Output, elset=Set-10
INV3, PRESS, S11, S12, S13, S22, S23, S33, SP, TRES
```

## Appendices

---

```
**
** HISTORY OUTPUT: H-Output-8
**
*Element Output, elset=Set-11
INV3, PRESS, S11, S12, S13, S22, S23, S33, SP, TRES
**
** HISTORY OUTPUT: H-Output-9
**
*Element Output, elset=Set-12
INV3, PRESS, S11, S12, S13, S22, S23, S33, SP, TRES
**
** HISTORY OUTPUT: H-Output-10
**
*Element Output, elset=Set-13
INV3, PRESS, S11, S12, S13, S22, S23, S33, SP, TRES
**
** HISTORY OUTPUT: H-Output-11
**
*Element Output, elset=Set-14
INV3, PRESS, S11, S12, S13, S22, S23, S33, SP, TRES
**
** HISTORY OUTPUT: H-Output-12
**
*Element Output, elset=Set-15
INV3, PRESS, S11, S12, S13, S22, S23, S33, SP, TRES
**
** HISTORY OUTPUT: H-Output-13
**
*Element Output, elset=Set-16
INV3, PRESS, S11, S12, S13, S22, S23, S33, SP, TRES
**
** HISTORY OUTPUT: H-Output-1
**
*Element Output, elset=Set-4
INV3, PRESS, S11, S12, S13, S22, S23, S33, SP, TRES
**
** HISTORY OUTPUT: H-Output-2
**
*Element Output, elset=Set-5
INV3, PRESS, S11, S12, S13, S22, S23, S33, SP, TRES
**
** HISTORY OUTPUT: H-Output-3
**
*Element Output, elset=Set-6
INV3, PRESS, S11, S12, S13, S22, S23, S33, SP, TRES
**
** HISTORY OUTPUT: H-Output-4
**
*Element Output, elset=Set-7
INV3, PRESS, S11, S12, S13, S22, S23, S33, SP, TRES
**
** HISTORY OUTPUT: H-Output-5
**
*Element Output, elset=Set-8
INV3, PRESS, S11, S12, S13, S22, S23, S33, SP, TRES
**
```

```
** HISTORY OUTPUT: H-Output-6
**
*Element Output, elset=Set-9
INV3, PRESS, S11, S12, S13, S22, S23, S33, SP, TRES
*End Step
```

**Appendix 2:**

**Support reactions at the first end girder**

| X        | lhs1     |
|----------|----------|
| 0        | 0        |
| 1.00E-03 | 8.61E-02 |
| 2.00E-03 | 1.72E-01 |
| 3.50E-03 | 3.01E-01 |
| 5.75E-03 | 4.95E-01 |
| 9.13E-03 | 7.86E-01 |
| 1.42E-02 | 1.22187  |
| 2.18E-02 | 1.87588  |
| 3.32E-02 | 2.85689  |
| 5.03E-02 | 4.32843  |
| 7.59E-02 | 6.53579  |
| 1.14E-01 | 9.84691  |
| 1.72E-01 | 14.8299  |
| 2.58E-01 | 22.5661  |
| 2.83E-01 | 24.8138  |
| 3.21E-01 | 28.2062  |
| 3.35E-01 | 29.4935  |
| 3.56E-01 | 31.5372  |
| 3.77E-01 | 33.6439  |
| 3.98E-01 | 35.799   |
| 4.30E-01 | 39.1009  |
| 4.42E-01 | 40.3441  |
| 4.60E-01 | 42.2132  |
| 4.86E-01 | 45.0025  |
| 4.96E-01 | 46.0494  |
| 5.11E-01 | 47.6102  |
| 5.34E-01 | 49.9443  |
| 5.42E-01 | 50.8174  |
| 5.55E-01 | 52.1142  |
| 5.74E-01 | 54.0548  |
| 5.81E-01 | 54.783   |
| 5.92E-01 | 55.8769  |
| 6.08E-01 | 57.5176  |
| 6.14E-01 | 58.1309  |
| 6.23E-01 | 59.0427  |
| 6.36E-01 | 60.4072  |
| 6.42E-01 | 60.9193  |
| 6.49E-01 | 61.6884  |
| 6.61E-01 | 62.8444  |
| 6.78E-01 | 64.5881  |
| 6.84E-01 | 65.2448  |
| 6.94E-01 | 66.2363  |
| 7.08E-01 | 67.7413  |
| 7.14E-01 | 68.3092  |
| 7.22E-01 | 69.1693  |
| 7.34E-01 | 70.4831  |
| 7.38E-01 | 70.9797  |
| 7.45E-01 | 71.7332  |
| 7.56E-01 | 72.883   |
| 7.71E-01 | 74.6491  |
| 7.77E-01 | 75.3169  |
| 7.86E-01 | 76.3298  |
| 7.99E-01 | 77.8686  |
| 8.03E-01 | 78.4471  |
| 8.11E-01 | 79.3174  |
| 8.22E-01 | 80.6268  |
| 8.38E-01 | 82.595   |
| 8.44E-01 | 83.3332  |
| 8.54E-01 | 84.4417  |
| 8.68E-01 | 86.1098  |
| 8.88E-01 | 88.6199  |
| 9.09E-01 | 91.1455  |
| 9.30E-01 | 93.681   |
| 9.35E-01 | 94.3153  |
| 9.41E-01 | 94.9498  |
| 9.48E-01 | 95.9019  |
| 9.60E-01 | 97.3319  |
| 9.78E-01 | 99.4832  |
| 1        | 102.215  |

| X        | rhs1     |
|----------|----------|
| 0        | 0        |
| 1.00E-03 | 8.27E-02 |
| 2.00E-03 | 1.65E-01 |
| 3.50E-03 | 2.90E-01 |
| 5.75E-03 | 4.76E-01 |
| 9.13E-03 | 7.55E-01 |
| 1.42E-02 | 1.17362  |
| 2.18E-02 | 1.80179  |
| 3.32E-02 | 2.74406  |
| 5.03E-02 | 4.15746  |
| 7.59E-02 | 6.27759  |
| 1.14E-01 | 9.45783  |
| 1.72E-01 | 14.2452  |
| 2.58E-01 | 21.654   |
| 2.83E-01 | 23.7937  |
| 3.21E-01 | 26.9907  |
| 3.35E-01 | 28.1907  |
| 3.56E-01 | 30.0357  |
| 3.77E-01 | 31.9276  |
| 3.98E-01 | 33.8382  |
| 4.30E-01 | 36.6967  |
| 4.42E-01 | 37.7676  |
| 4.60E-01 | 39.3649  |
| 4.86E-01 | 41.7443  |
| 4.96E-01 | 42.6326  |
| 5.11E-01 | 43.9558  |
| 5.34E-01 | 45.9126  |
| 5.42E-01 | 46.6439  |
| 5.55E-01 | 47.7345  |
| 5.74E-01 | 49.3429  |
| 5.81E-01 | 49.9449  |
| 5.92E-01 | 50.8425  |
| 6.08E-01 | 52.1616  |
| 6.14E-01 | 52.653   |
| 6.23E-01 | 53.3848  |
| 6.36E-01 | 54.4727  |
| 6.42E-01 | 54.8793  |
| 6.49E-01 | 55.486   |
| 6.61E-01 | 56.3814  |
| 6.78E-01 | 57.6777  |
| 6.84E-01 | 58.1591  |
| 6.94E-01 | 58.8706  |
| 7.08E-01 | 59.913   |
| 7.14E-01 | 60.2997  |
| 7.22E-01 | 60.8697  |
| 7.34E-01 | 61.6979  |
| 7.38E-01 | 62.0041  |
| 7.45E-01 | 62.4536  |
| 7.56E-01 | 63.1058  |
| 7.71E-01 | 64.0391  |
| 7.77E-01 | 64.383   |
| 7.86E-01 | 64.8861  |
| 7.99E-01 | 65.6171  |
| 8.03E-01 | 65.8893  |
| 8.11E-01 | 66.2943  |
| 8.22E-01 | 66.8982  |
| 8.38E-01 | 67.8054  |
| 8.44E-01 | 68.1472  |
| 8.54E-01 | 68.6633  |
| 8.68E-01 | 69.4448  |
| 8.88E-01 | 70.6313  |
| 9.09E-01 | 71.8329  |
| 9.30E-01 | 73.0638  |
| 9.35E-01 | 73.3732  |
| 9.41E-01 | 73.6837  |
| 9.48E-01 | 74.152   |
| 9.60E-01 | 74.8604  |
| 9.78E-01 | 75.9294  |
| 1        | 77.3018  |

Support reactions at the first inner girder

| X        | lhs2     |
|----------|----------|
| 0        | 0        |
| 1.00E-03 | 8.08E-02 |
| 2.00E-03 | 1.62E-01 |
| 3.50E-03 | 2.83E-01 |
| 5.75E-03 | 4.65E-01 |
| 9.13E-03 | 7.38E-01 |
| 1.42E-02 | 1.14696  |
| 2.18E-02 | 1.76088  |
| 3.32E-02 | 2.68176  |
| 5.03E-02 | 4.0631   |
| 7.59E-02 | 6.13518  |
| 1.14E-01 | 9.24344  |
| 1.72E-01 | 13.9214  |
| 2.58E-01 | 21.1862  |
| 2.83E-01 | 23.2971  |
| 3.21E-01 | 26.4829  |
| 3.35E-01 | 27.6924  |
| 3.56E-01 | 29.6199  |
| 3.77E-01 | 31.6112  |
| 3.98E-01 | 33.6541  |
| 4.30E-01 | 36.8042  |
| 4.42E-01 | 37.9915  |
| 4.60E-01 | 39.7806  |
| 4.86E-01 | 42.4631  |
| 4.96E-01 | 43.4707  |
| 5.11E-01 | 44.9769  |
| 5.34E-01 | 47.2349  |
| 5.42E-01 | 48.0804  |
| 5.55E-01 | 49.3396  |
| 5.74E-01 | 51.228   |
| 5.81E-01 | 51.9371  |
| 5.92E-01 | 53.003   |
| 6.08E-01 | 54.6044  |
| 6.14E-01 | 55.2039  |
| 6.23E-01 | 56.0978  |
| 6.36E-01 | 57.4389  |
| 6.42E-01 | 57.9427  |
| 6.49E-01 | 58.7003  |
| 6.61E-01 | 59.8409  |
| 6.78E-01 | 61.5655  |
| 6.84E-01 | 62.2157  |
| 6.94E-01 | 63.1988  |
| 7.08E-01 | 64.6948  |
| 7.14E-01 | 65.2599  |
| 7.22E-01 | 66.1173  |
| 7.34E-01 | 67.4309  |
| 7.38E-01 | 67.9279  |
| 7.45E-01 | 68.6835  |
| 7.56E-01 | 69.8393  |
| 7.71E-01 | 71.6202  |
| 7.77E-01 | 72.2944  |
| 7.86E-01 | 73.3183  |
| 7.99E-01 | 74.8766  |
| 8.03E-01 | 75.4628  |
| 8.11E-01 | 76.3449  |
| 8.22E-01 | 77.6723  |
| 8.38E-01 | 79.6668  |
| 8.44E-01 | 80.4146  |
| 8.54E-01 | 81.5361  |
| 8.68E-01 | 83.2208  |
| 8.88E-01 | 85.7519  |
| 9.09E-01 | 88.2954  |
| 9.30E-01 | 90.8478  |
| 9.35E-01 | 91.4864  |
| 9.41E-01 | 92.1251  |
| 9.48E-01 | 93.0836  |
| 9.60E-01 | 94.5237  |
| 9.78E-01 | 96.6912  |
| 1        | 99.4473  |

| X        | rhs2     |
|----------|----------|
| 0        | 0        |
| 1.00E-03 | 7.82E-02 |
| 2.00E-03 | 1.56E-01 |
| 3.50E-03 | 2.74E-01 |
| 5.75E-03 | 4.49E-01 |
| 9.13E-03 | 7.13E-01 |
| 1.42E-02 | 1.109    |
| 2.18E-02 | 1.7026   |
| 3.32E-02 | 2.59299  |
| 5.03E-02 | 3.9286   |
| 7.59E-02 | 5.93206  |
| 1.14E-01 | 8.93733  |
| 1.72E-01 | 13.4583  |
| 2.58E-01 | 20.4085  |
| 2.83E-01 | 22.4151  |
| 3.21E-01 | 25.4132  |
| 3.35E-01 | 26.5387  |
| 3.56E-01 | 28.2714  |
| 3.77E-01 | 30.0537  |
| 3.98E-01 | 31.8596  |
| 4.30E-01 | 34.5766  |
| 4.42E-01 | 35.5955  |
| 4.60E-01 | 37.119   |
| 4.86E-01 | 39.3942  |
| 4.96E-01 | 40.2448  |
| 5.11E-01 | 41.5141  |
| 5.34E-01 | 43.3976  |
| 5.42E-01 | 44.102   |
| 5.55E-01 | 45.1537  |
| 5.74E-01 | 46.7098  |
| 5.81E-01 | 47.2925  |
| 5.92E-01 | 48.1623  |
| 6.08E-01 | 49.4452  |
| 6.14E-01 | 49.9236  |
| 6.23E-01 | 50.6367  |
| 6.36E-01 | 51.6985  |
| 6.42E-01 | 52.0955  |
| 6.49E-01 | 52.6885  |
| 6.61E-01 | 53.566   |
| 6.78E-01 | 54.8436  |
| 6.84E-01 | 55.3188  |
| 6.94E-01 | 56.0229  |
| 7.08E-01 | 57.0584  |
| 7.14E-01 | 57.4432  |
| 7.22E-01 | 58.0122  |
| 7.34E-01 | 58.8429  |
| 7.38E-01 | 59.1508  |
| 7.45E-01 | 59.6042  |
| 7.56E-01 | 60.2657  |
| 7.71E-01 | 61.2195  |
| 7.77E-01 | 61.572   |
| 7.86E-01 | 62.0896  |
| 7.99E-01 | 62.8457  |
| 8.03E-01 | 63.1275  |
| 8.11E-01 | 63.5475  |
| 8.22E-01 | 64.174   |
| 8.38E-01 | 65.1148  |
| 8.44E-01 | 65.4689  |
| 8.54E-01 | 66.003   |
| 8.68E-01 | 66.8103  |
| 8.88E-01 | 68.0332  |
| 9.09E-01 | 69.2685  |
| 9.30E-01 | 70.5272  |
| 9.35E-01 | 70.8433  |
| 9.41E-01 | 71.1602  |
| 9.48E-01 | 71.6377  |
| 9.60E-01 | 72.3586  |
| 9.78E-01 | 73.4452  |
| 1        | 74.8366  |

Support reactions at the second inner girder

| X        | Ih3      |
|----------|----------|
| 0        | 0        |
| 1.00E-03 | 8.27E-02 |
| 2.00E-03 | 1.65E-01 |
| 3.50E-03 | 2.90E-01 |
| 5.75E-03 | 4.76E-01 |
| 9.13E-03 | 7.55E-01 |
| 1.42E-02 | 1.17399  |
| 2.18E-02 | 1.80237  |
| 3.32E-02 | 2.74494  |
| 5.03E-02 | 4.15881  |
| 7.59E-02 | 6.27966  |
| 1.14E-01 | 9.46101  |
| 1.72E-01 | 14.2486  |
| 2.58E-01 | 21.6794  |
| 2.83E-01 | 23.8383  |
| 3.21E-01 | 27.0965  |
| 3.35E-01 | 28.332   |
| 3.56E-01 | 30.2853  |
| 3.77E-01 | 32.2943  |
| 3.98E-01 | 34.3445  |
| 4.30E-01 | 37.4706  |
| 4.42E-01 | 38.6467  |
| 4.60E-01 | 40.4122  |
| 4.86E-01 | 43.0392  |
| 4.96E-01 | 44.0245  |
| 5.11E-01 | 45.4913  |
| 5.34E-01 | 47.6814  |
| 5.42E-01 | 48.5     |
| 5.55E-01 | 49.7143  |
| 5.74E-01 | 51.5285  |
| 5.81E-01 | 52.209   |
| 5.92E-01 | 53.2307  |
| 6.08E-01 | 54.7616  |
| 6.14E-01 | 55.3336  |
| 6.23E-01 | 56.1827  |
| 6.36E-01 | 57.4521  |
| 6.42E-01 | 57.9283  |
| 6.49E-01 | 58.6433  |
| 6.61E-01 | 59.7174  |
| 6.78E-01 | 61.3363  |
| 6.84E-01 | 61.9459  |
| 6.94E-01 | 62.8659  |
| 7.08E-01 | 64.2622  |
| 7.14E-01 | 64.789   |
| 7.22E-01 | 65.5869  |
| 7.34E-01 | 66.8056  |
| 7.38E-01 | 67.2663  |
| 7.45E-01 | 67.9653  |
| 7.56E-01 | 69.032   |
| 7.71E-01 | 70.6702  |
| 7.77E-01 | 71.2897  |
| 7.86E-01 | 72.2291  |
| 7.99E-01 | 73.6559  |
| 8.03E-01 | 74.1923  |
| 8.11E-01 | 74.999   |
| 8.22E-01 | 76.2123  |
| 8.38E-01 | 78.0352  |
| 8.44E-01 | 78.7189  |
| 8.54E-01 | 79.7453  |
| 8.68E-01 | 81.2896  |
| 8.88E-01 | 83.6121  |
| 9.09E-01 | 85.9471  |
| 9.30E-01 | 88.2886  |
| 9.35E-01 | 88.8742  |
| 9.41E-01 | 89.4598  |
| 9.48E-01 | 90.338   |
| 9.60E-01 | 91.6562  |
| 9.78E-01 | 93.637   |
| 1        | 96.1481  |

| X        | rhs3     |
|----------|----------|
| 0        | 0        |
| 1.00E-03 | 7.97E-02 |
| 2.00E-03 | 1.59E-01 |
| 3.50E-03 | 2.79E-01 |
| 5.75E-03 | 4.58E-01 |
| 9.13E-03 | 7.27E-01 |
| 1.42E-02 | 1.13061  |
| 2.18E-02 | 1.73577  |
| 3.32E-02 | 2.6435   |
| 5.03E-02 | 4.0051   |
| 7.59E-02 | 6.04751  |
| 1.14E-01 | 9.11115  |
| 1.72E-01 | 13.7234  |
| 2.58E-01 | 20.8667  |
| 2.83E-01 | 22.9298  |
| 3.21E-01 | 26.0121  |
| 3.35E-01 | 27.169   |
| 3.56E-01 | 28.9438  |
| 3.77E-01 | 30.758   |
| 3.98E-01 | 32.5851  |
| 4.30E-01 | 35.3082  |
| 4.42E-01 | 36.3277  |
| 4.60E-01 | 37.8461  |
| 4.86E-01 | 40.1039  |
| 4.96E-01 | 40.9462  |
| 5.11E-01 | 42.1994  |
| 5.34E-01 | 44.0493  |
| 5.42E-01 | 44.7401  |
| 5.55E-01 | 45.7699  |
| 5.74E-01 | 47.2859  |
| 5.81E-01 | 47.8531  |
| 5.92E-01 | 48.6983  |
| 6.08E-01 | 49.9385  |
| 6.14E-01 | 50.4004  |
| 6.23E-01 | 51.0879  |
| 6.36E-01 | 52.1096  |
| 6.42E-01 | 52.4914  |
| 6.49E-01 | 53.0611  |
| 6.61E-01 | 53.9016  |
| 6.78E-01 | 55.1165  |
| 6.84E-01 | 55.5676  |
| 6.94E-01 | 56.2342  |
| 7.08E-01 | 57.2111  |
| 7.14E-01 | 57.5735  |
| 7.22E-01 | 58.1079  |
| 7.34E-01 | 58.8851  |
| 7.38E-01 | 59.1725  |
| 7.45E-01 | 59.5947  |
| 7.56E-01 | 60.208   |
| 7.71E-01 | 61.0871  |
| 7.77E-01 | 61.4113  |
| 7.86E-01 | 61.8857  |
| 7.99E-01 | 62.576   |
| 8.03E-01 | 62.833   |
| 8.11E-01 | 63.2156  |
| 8.22E-01 | 63.7859  |
| 8.38E-01 | 64.6423  |
| 8.44E-01 | 64.9647  |
| 8.54E-01 | 65.4515  |
| 8.68E-01 | 66.1881  |
| 8.88E-01 | 67.3055  |
| 9.09E-01 | 68.4363  |
| 9.30E-01 | 69.5947  |
| 9.35E-01 | 69.8858  |
| 9.41E-01 | 70.178   |
| 9.48E-01 | 70.6185  |
| 9.60E-01 | 71.2846  |
| 9.78E-01 | 72.2893  |
| 1        | 73.5788  |